CIVIL ENGINEERING STUDIES
Illinois Center for Transportation Series No. 09-044
UILU-ENG-2009-2015
ISSN: 0197-9191

COST-EFFECTIVENESS AND PERFORMANCE OF OVERLAY SYSTEMS IN ILLINOIS VOLUME 1: EFFECTIVENESS ASSESSMENT OF HMA OVERLAY INTERLAYER SYSTEMS USED TO RETARD REFLECTIVE CRACKING

Prepared By
Imad L. Al-Qadi
William G. Buttlar
Jongeun Baek
Minkyum Kim
University of Illinois at Urbana-Champaign

Research Report ICT-09-044

A report of the findings of
ICT-R58
Cost-Effectiveness and Performance of Overlay Systems in Illinois
Illinois Center for Transportation

May 2009

Technical Report Documentation Page

1. Report No.	2. Government Accession No.	3. Recipient's Catalog No.
FHWA-ICT-09-044		

4. Title and Subtitle

Cost-Effectiveness and Performance of Overlay Systems in Illinois - Volume 1: Effectiveness Assessment of HMA Overlay Interlayer Systems Used to Retard Reflective Cracking

5. Report Date
May 2009

6. Performing Organization Code

7. Author(s)
Imad L. Al-Qadi, William G. Buttlar, Jongeun Baek, and Minkyum Kim

8. Performing Organization Report N o.
ICT-09-044
UILU-ENG-2009-2015

9. Performing Organization Name and Address
Illinois Center for Transportation
Department of Civil and Environmental Engineering
University of Illinois at Urbana-Champaign
205 N. Mathews Ave., MC-250
Urbana, IL 61801

10. Work Unit (TRAIS)

11. Contract or Grant No.
ICT-R58

13. Type of Report and Period Covered

Project Report
2005-2008

12. Sponsoring Agency Name and Address
Illinois Department of Transportation
Bureau of Materials and Physical Research
126 East Ash Street
Springfield, IL 62704-4766

14. Sponsoring Agency Code

15. Supplementary Notes

16. Abstract

This project evaluated the ability of interlayer systems used in HMA overlays to retard reflective cracking. Field crack surveys and forensic investigation, including video imaging and ground penetrating radar surveys as well as laboratory testing of cored specimens, were conducted to examine the behavior of reflective cracking and reflective cracking control systems applied in Illinois. Crack extent and severity were recorded at 24 locations across Illinois. The performance evaluation focused on five types of interlayer systems: area- and strip-type non-woven fabric; two strip-type composite; and a fine, high polymer content HMA interlayer system. Two reflective cracking indices were developed to characterize the condition of HMA overlays regarding reflective cracking as well as transverse cracking. In addition, a performance benefit ratio parameter, PBR, was developed to assess the performance of treated pavements relative to control sections. The study provided a quantitative assessment for various types of reflective cracking interlayer systems. In addition, it provides a means to predict the performance of several interlayer systems under various vehicular and environmental loading conditions through a simple ESALs-T_L chart. A companion report (volume 2) provides tools for the selection of appropriate reflective crack control treatments based upon traffic, climate, and life cycle costs using a user-friendly life cycle cost analysis program (CIND – **C**ost-effective **IN**nterlayer system **D**ecision program).

17. Key Words	18. Distribution Statement
Reflective Cracking, Crack Control, Interlayer, HMA Overlay, Life cycle cost analysis, Rehabilitation	No restrictions. This document is available to the public through the National Technical Information Service, Springfield, Virginia 22161.

19. Security Classif. (of this report)	20. Security Classif. (of this page)	21. No. of Pages	22. Price
Unclassified	Unclassified	193	

ACKNOWLEDGMENT AND DISCLAIMER

This publication is based on the results of ICT-R58, **COST-EFFECTIVENESS AND PERFORMANCE OF OVERLAY SYSTEMS IN ILLINOIS***. ICT-R58 was conducted in cooperation with the Illinois Center for Transportation; the Illinois Department of Transportation, Division of Highways; and the U.S. Department of Transportation, Federal Highway Administration.*

Members of the Technical Review Panel are the following:

Joseph Vespa, IDOT
Amy Schutzbach, IDOT
David Lippert, IDOT
Jim Trepanier, IDOT
Aaron Toliver, IDOT
Patty Broers, IDOT

EXECUTIVE SUMMARY

Reflective cracking is a predominant mode of failure in hot-mix asphalt (HMA) overlays in Illinois, particularly since a vast portion of the state highway system was built with jointed concrete pavements decades ago, which have exceeded their initial design life. Reduced load transfer at joints and the presence of cracks in these pavements create high stress intensities in HMA overlays placed on them, usually resulting in rapid reflective crack development. Reflective crack control treatments, such as reinforcement and stress absorbing membrane interlayer systems, have been used in an effort to reduce the severity and rate of reflective cracking. Previous research in Illinois has shown that non-woven polypropylene (or System A) treatments are marginally cost effective in most instances; but additional research was recommended to validate these results, to evaluate other treatment systems, and to gain a better understanding of the effects of traffic and climate on treatment effectiveness.

This project evaluated the ability of interlayer systems used in HMA overlays to retard reflective cracking. Field crack surveys and forensic investigation were executed to examine the behavior of reflective cracking and reflective cracking control systems applied in Illinois. Through visual (walk-on) and video crack surveys, crack extent and severity were recorded at 24 locations across Illinois. This performance evaluation focused on five types of interlayer systems: System A (area- and strip-type) is made of non-woven fabric; System B is a self-adhesive strip-type interlayer; System D is an Interlayer Stress Absorbing Composite (ISAC); and System E, not included in the IDOT specification, is a fine, high polymer content HMA interlayer system. In addition, ground penetrating radar (GPR) was employed to look at in-depth pavement conditions in several locations.

Two reflective cracking indices were developed to characterize the condition of HMA overlays regarding reflective cracking as well as transverse cracking. A weighted reflective cracking appearance ratio was developed that represents the deterioration rate of HMA overlays caused by discontinuities such as joints and/or patches. The GPR could detect dowel bars and patches in concrete pavements; so that reflective cracking could be differentiated from other transverse cracking. A weighted transverse cracking appearance ratio was developed, which quantifies the transverse cracks developed within a unit length. In addition, a performance benefit ratio parameter, PBR, was developed to assess the performance of treated pavements relative to control sections. Prediction models based upon PBR were developed for each interlayer system as a function of annual18-kip equivalent single-axle loads (ESALs) and the lowest monthly average temperature, T_L.

A performance criterion was suggested to specify maximum allowable ESALs, $ESAL_{max}$, for each interlayer system. A simple ESALs-T_L chart was provided as a convenient tool for the selection of potential appropriate interlayer systems. Based on overall performance, it was evident that System D performed the best, followed by System E. System A (area-wide) showed marginal benefits to the overlay system. On the other hand, control sections outperformed overlays with System B or System A (strip-type).

Forensic investigation was conducted at several locations to investigate in-depth field conditions by coring and to obtain physical and mechanical material properties. Creep compliance, complex modulus, phase angle, and fracture energy were measured for HMA overlays and interlayer system E. Interface shear strength was determined to evaluate the bonding condition between interlayer systems and HMA overlay and/or

existing concrete pavement. The effectiveness of each interlayer system as a moisture barrier was assessed through permeability testing. After comparing bulk properties and fracture energy, System E was shown to have a higher fracture energy, which indicates greater crack resistance compared to conventional HMA.

A life cycle cost analysis (LCCA) was conducted to evaluate the cost-effectiveness of each interlayer system. A user-friendly life cycle cost analysis program (CIND – **C**ost-effective **IN**terlayer system **D**ecision program) was developed that allows the selection of interlayer systems. In addition, practical guidelines for interlayer system selection were developed. An accompanying project report, "Cost Effectiveness and Performance of Overlay Systems in Illinois – Volume 2: Guidelines for Interlayer System Selection Decision When Used in HMA Overlays."

Although future research and more field surveys are still needed to gain a better understanding of the role of overlay quality and thickness on overlay system performance, this study provided a quantitative assessment for various types of reflective cracking interlayer systems. It clearly showed the comparative cost effectiveness performance of various interlayer systems used in Illinois. In addition, it provides a means to predict the performance of several interlayer systems under various vehicular and environmental loading conditions, and provides tools for the selection of appropriate reflective crack control treatments based upon traffic, climate, and life cycle costs.

TABLE OF CONTENTS

1. INTRODUCTION

1.1 BACKGROUND

Hot-mix asphalt (HMA) overlays have been primarily utilized to increase the structural capacity of existing pavements or to rehabilitate distressed pavement systems. The HMA overlays, however, may experience structural weaknesses at discontinuities such as joints, patches, and cracks present in the existing pavement. These weaknesses result from stresses induced by environmental and vehicular loading, which are intensified at the vicinity of the discontinuities. When the stresses reach the tensile/shear strength of the HMA overlay, reflective cracking can be initiated. Consequently, once reflective cracking is developed, more stresses are concentrated at a crack tip and reflective cracking propagates through the overlay. Depending on interface conditions, overlay thickness, structural capacity of the pavement system, and overlay material properties, locations of crack initiation and propagation path vary.

To reduce reflective cracking, several rehabilitation methods have been commonly used. These methods include increasing overlay thickness, crack-and-seat, break-and-seat, saw-and-seal in overlay above existing joints, and the use of crack arrester granular layer or interlayer systems (Cleveland et al. 2002). An interlayer system is placed either between the overlay and the existing pavement or within the overlay. It usually is composed of a relatively thin layer of one of a variety of materials, depending on its functions. To date, no technique could provide a perfect solution to prevent reflective cracking (Lorenz 1987, Button and Lytton 2007). For example, increasing overlay thickness is only applicable for overlays thinner than nine inches (Huang 1993) and may not decrease thermal stresses significantly, while it may decrease traffic induced stresses (Jun et al. 2004). Interlayer systems have been effective in reducing the occurrence of reflective cracking (Button and Lytton 1987, Van Deuren and Esnouf 1996, Buttlar et al. 2000, Steen 2004, Al-Qadi et al. 2004). However, some applications showed little or even no success on retarding reflective cracking. This could be due to the lack of understanding about the interlayer system mechanism in reducing reflective cracking and/or inappropriate interlayer system installation (Predoehl 1989, Steinberg 1992, Epps et al. 2000). For example, Steinberg (1992) noticed, based on field experience of glass-grid interlayer, that its benefit was questionable due to improper installation.

In Illinois, three types of fabric interlayer systems have been used as reflective crack control (RCC) systems, which are placed beneath HMA overlays to retard reflective crack growth, namely: System A, System B, and System C (Schutzbach 1995). System A consists of a non-woven reinforcing fabric and is applied over a prepared pavement surface using an asphalt binder tack coat. System B consists of a woven or non-woven reinforcing fabric adhered to a waterproofing membrane and attached to the pavement via a self-adhesive bitumen material. System C is a nonproprietary asphalt-rubber waterproofing membrane interlayer topped with cover aggregate. These systems can be applied as a strip-type or area-type. By current IDOT policy, the strip-type can be placed over either rigid or flexible bases; the area-type can only be used placed over flexible bases. Prior to the installation of RCC systems, a substrate should be prepared by sealing cracks and filling depressions. Otherwise, a leveling binder should be applied.

In addition, an interlayer stress-absorbing composite (ISAC) system has been used in Illinois (Buttlar et al. 1999 and Vespa 2004). ISAC has a sandwich-like structure which consists of two geotextiles surrounding a rubberized asphalt core layer. The top layer consists of a high-stiffness, high-strength woven geotextile; the bottom layer

consists of a low-stiffness, nonwoven geotextile that is easily deformed and readily adhered to the underlying pavement with a bituminous tack coat. The middle layer—the modified rubberized asphalt—can dissipate strain energy and serves to bond the two geotextiles. ISAC is only available as a strip-type interlayer. Recently, a sand-mix interlayer system has been applied to control cracking using smaller-sized aggregates and modified asphalt binder. Sand anti-fracture (SAF) and the IL 4.75 mm mixture are classified as System E herein, although they utilize somewhat different aggregate structures and modified binder systems. Note that these mixtures are under review and are not currently defined as System E in the IDOT specification book. System E is only applicable as an area-type interlayer.

Several studies have been conducted to evaluate the effectiveness of interlayer systems to reduce reflective cracking (Buttlar et al. 1999, Titi et al. 2003, Blankenship et al. 2004, Makowski et al. 2005, Chen et al. 2006). One method to evaluate the in-situ effectiveness of interlayer systems in retarding reflective cracking is periodic field crack surveys. Buttlar et al. (1999) evaluated the cost-effectiveness of paving fabrics in delaying reflective cracking based on the performance of 52 projects in Illinois. Performance data indicated that the overlay service life would be 11.5, 14, and 10.4 years for strip-treated, area-treated, and control sections, respectively. Life cycle cost analyses indicated a marginal life cycle benefit when these fabrics were used on relatively medium to large-sized projects. The study found that the total number of reflected transverse cracks in area wide treated and untreated sections were very similar, indicating that non-woven polypropylene fabrics did not reduce the total number of reflected cracks over the long run. In addition, the project reported a lack of documentation of the control sections. Hence, the study reported herein was needed.

Field crack surveys have generally been performed visually. However, visual crack surveys are dangerous to perform, even with traffic control, can be expensive (labor and traffic control costs), and are time-consuming. Moreover, crack severity and extent are subjective and surveyor dependent. With the aid of a high-quality video camera and digital image processing methods, automated crack detection technologies have been utilized in pavement surveys. An effective and inexpensive system was developed to analyze surface distress on flexible and rigid pavements using an 8-mm video camera (Chua and Xu 1994). Al-Qadi and co-workers installed a special video camera on a GPR van to facilitate rapid and safe condition assessment (Flintsch et al. 2005). The system, which was triggered by a distance measuring instrumentation (DMI), utilized high shutter speed, low exposure time, and a high frame rate to obtain clear images at a high speed of 72 km/h. In this study, both visual and video-aided crack surveys were performed. The crack data was manually extracted from the video images.

1.2 RESEARCH OBJECTIVES AND APPROACHES

The main objective of this research was to evaluate the performance and cost-effectiveness of interlayer systems in HMA overlays in retarding reflective cracking. To accomplish this objective, an integrated method was utilized to understand the mechanism of reflective cracking and to assess the field performance of five interlayer systems used in Illinois: three reflective crack control systems of area-type System A, strip-type System A, and System B; ISAC (designated as System D); and sand mix (designated as System E). To this end, three major tasks were conducted: field survey and performance analysis, forensic investigation, and cost benefit analysis. The framework of this research approach is illustrated in Figure 1. This report is comprised of two volumes: Volume 1, “Effectiveness Assessment of HMA Overlay Interlayer Systems Used to Retard Reflective Cracking,” and Volume 2, “Guidelines for Interlayer System Selection Decision When Used in HMA Overlays.”

1.2.1 Performance Benefit Analysis

Field crack surveys were conducted to examine the performance of interlayer systems in reducing HMA overlay reflective cracking. Through visual and video surveys, the extent and severity of transverse cracks were measured. A prototype video crack surveying system was used along with visual surveys to assure operator safety, rapidity of measurements, and measurement objectivity. The cracks were also assessed by ground penetrating radar (GPR) to determine if they were truly reflective cracks. In some cases, GPR identified transverse cracks in the pavement surface as thermal cracks, which most likely developed as a result of thermal cycles, or near surface cracks. Two reflective cracking indices (RCI) are proposed in this study. In addition, a performance benefit ratio (PBR), was developed as a key parameter to evaluate in-situ interlayer system performance when compared to control sections. The effect of traffic volume and temperature are considered in the PBR parameter.

1.2.2 Forensic Investigation

Field cores were obtained from selected locations to investigate in-situ reflective cracking patterns and to obtain sufficient pavement and interlayer materials for laboratory characterization of key overlay system characteristics. Four laboratory tests were selected: creep compliance and complex modulus to characterize HMA bulk material properties; a disk-shaped compact tension (DC[T]) fracture test to measure HMA total fracture energy; a torque test for interface shear strength determination, and a permeability test to measure residual waterproofing benefit of interlayer systems in cracked HMA overlay specimens.

1.2.3 Cost Benefit Analysis

The cost-benefit of interlayer systems used in the rehabilitation of highway pavements in Illinois was evaluated using a comprehensive life-cycle cost analysis (LCCA). An LCCA program, CIND (**C**ost-effective **IN**terlayer system **D**ecision program) was developed that considers the agency cost for construction and maintenance over the life of the pavement as well as the total user cost for traffic delays. The LCCA program can also be applied to develop a decision-making procedure that can be used by designers to help select interlayer systems based upon their compatibility, effectiveness, and economy, considering the existing pavement structure capacity and condition and expected traffic volume. The results of the cost benefit analysis are presented in a companion report, “Cost Effectiveness and Performance of Overlay Systems in Illinois – Volume 2: Guidelines for Interlayer System Selection Decision When Used in HMA Overlays.”

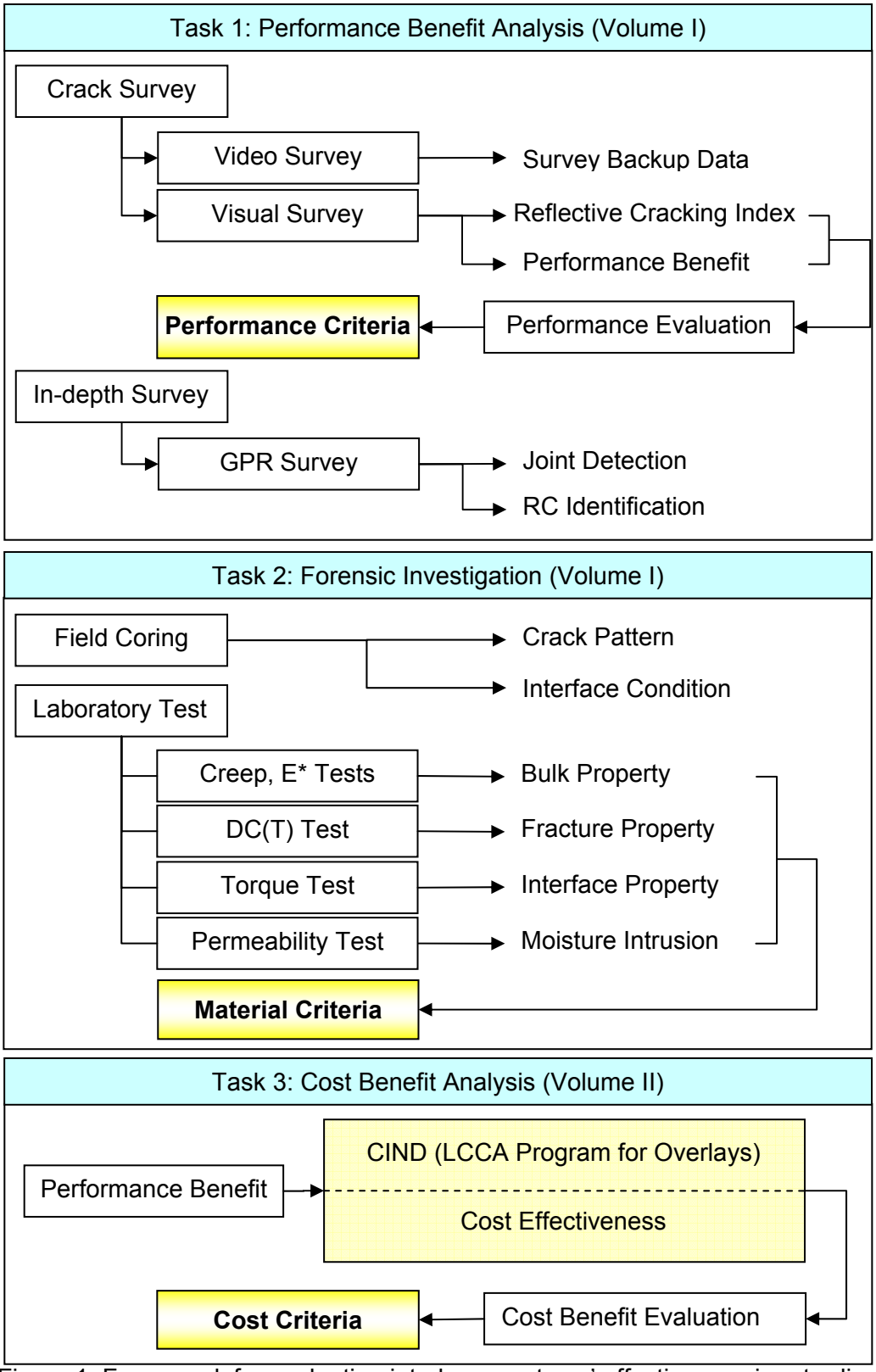

Figure 1. Framework for evaluating interlayer systems' effectiveness in retarding reflective cracking.

2. REFLECTIVE CRACKING SURVEY

2.1 INTERLAYER SYSTEMS

Several rehabilitation methods have been commonly utilized to control reflective cracking: increasing overlay thickness, crack-and-seat, break-and-seat, saw-and-seal, and installing crack arrester granular layer and interlayer systems (Mukhtar 1994, Cleveland et al. 2002). These interlayer systems have been used in an attempt to control reflective cracking for more than three decades. However, their performance and effectiveness have varied widely, and engineers and scientists do not agree on the mechanisms of reflective cracking.

A number of research studies have reported on the effectiveness of interlayer systems to reduce the occurrence of reflective cracking and have explored their cost-effectiveness (Morris and McDonald 1976, Monismith and Coetzee 1980, Button and Lytton 1987, Van Deuren and Esnouf 1996, Mukhtar and Dempsey 1996, Jenner 1996, Buttlar et al. 2000, Blomberg 2001, Dempsey 2002, Al-Qadi et al. 2003 (b), Bozkurt and Buttlar 2002, Kim et al. 2002, Kuo et al. 2003, Steen 2004, Kuo and Hsu 2003, Montestruque et al. 2004, Al-Qadi et al. 2004, Jun et al. 2004, Blankenship et al. 2004, Vespa 2005, Al-Qadi et al. 2005, Elseifi and Al-Qadi 2004). Depending on its intended function, the interlayer system can vary. The traditional interlayer system is a relatively thin fabric layer, generally a geotextile, and is installed either between the overlay and existing underlying layer or between overlay lifts. Some of the applications showed little or even no success on retarding reflective cracking due to a lack of understanding of the interlayer system mechanism and/or as a result of inappropriate installation of the interlayer (Predoehl 1989, Steinberg 1992, Donna 1993, Epps et al. 2000). For instance, Steinberg (1992) reported that the performance benefit of fiberglass/grid type interlayers could be questionable if improper installation techniques were used. Similar findings have also been reported for other interlayer materials.

According to Al-Qadi et al. (2000), interlay systems have five distinct functions, namely: 1) reinforcement; 2) stress relief; 3) separation; 4) filtration, and; 5) moisture barrier. In general, only the first two functions, e.g., reinforcement and stress relief, directly relate to reflective crack prevention in HMA overlay systems. Reinforcing interlayers are stiffer and stronger than HMA overlay materials, thereby reducing pavement deflection and overlay strain. Geogrid, made from high-density polypropylene or polyethylene with an open mesh structure, fiberglass grids, and metallic grids are examples of reinforcing layers that are sometimes used in HMA overlay systems. On the other hand, stress relief (or strain tolerant) interlayers are made of soft materials, designed to dissipate strain energy in the HMA overlay by serving as an isolation layer between the existing cracked pavement and the newly placed overlay. Nonwoven geosynthetics, stress absorbing membrane interlayers (SAMIs), and proprietary composite material systems such as interlayer stress absorbing composite “ISAC”, are good examples of stress relief interlayers. While the original SAMIs installed in the field were more akin to chip seals with a heavy tack coat application, more recently, thicker stress relief interlayer systems have gained popularity, which can be plant produced and constructed with standard HMA paving equipment (e.g. Sand Anti-Fracture (SAF), and the Illinois 4.75-mm mixture).

Interlayer system performance is most often evaluated by assessing the number of cracks per unit length, a measure sometimes referred to as crack density. However, the crack density parameter has two deficiencies. First, while the crack density represents the overall serviceability of the overlay, it does not directly evaluate the

efficiency of a given interlayer system in delaying reflective cracking. This is because all transverse cracks in a survey are counted even though some of them may not be directly related to reflective cracking. Thus, the location of joints, cracks, and or patches prior to HMA overlay is needed to positively identify reflective cracks. On the other hand, since strip interlayers are placed only on discontinuities, it is reasonable to regard all transverse cracks occurring over locations where strip interlayers were placed as reflective cracks.

The next shortcoming of the crack density parameter is the absence of a measurement of crack severity. Depending upon the mechanisms of crack relief, different interlayer systems may result in fewer, more severe cracks, or a large number of low-severity cracks, etc. High severity cracks, such as band cracking, require expensive crack repair or patching techniques to be employed, while very low severity (hairline) cracks may delay or eliminate the need for crack repair.

2.2 SURVEY LOCATIONS

In a previous study aimed at evaluating the effectiveness of various reflective crack control treatments used in Illinois, Buttlar et al. (1999) conducted a survey to identify a number of a projects around Illinois where reflective crack control treatments were used. Due to the relatively low number and lack of documentation of control sections available at the time of the study and the relatively limited number of years of field experience with area wide installation, long-term monitoring and follow-up analysis of data to evaluate cost effectiveness were recommended. Starting with the list of projects reported by Buttlar et al. (1999), 24 projects were selected for detailed study herein, based upon the type of reflective crack control used, availability of a control section, traffic level, and location within the state of Illinois.

Figure 2 illustrates the location of the selected projects. In most cases, the selected project contains a control section with a similar pavement structure as the treated section but without an interlayer. A typical HMA overlay off interstate in Illinois has a 0.75-in.-thick leveling binder and a 1.5-in.-thick wearing surface. A statistical analysis of data indicates an average overlay system thickness of 2.24 in., with a 0.38 in. standard deviation (σ) and total thickness range from 1.5 in. to 3.125 in. The HMA overlay systems selected were, in all cases, constructed on jointed concrete pavements (JCP) or on existing HMA overlays placed on JCP. Four projects are located in climate zone 1 (the coldest zone in Illinois), three projects in climate zone 3 (the warmest zone in Illinois) and the other 17 projects in climate zone 2 (central Illinois). These projects include five types and a total of 30 interlayer systems: 18 System A (13 area-wide and five strip-type), two System B, four System D, and six System E. A summary of all the sections and interlayer systems used is presented in Table 1. HMA overlays were constructed between 1988 and 2004, and the average age of the overlay systems selected was 11.3 years (σ of 4.7 years) as of 2008. Most of the sections selected were two-lane highways (one lane in each direction). In each project, a minimum 500-ft-long segment was surveyed for interlayer system evaluation.

2.3 FIELD CRACK SURVEY

Field crack surveys were conducted to collect pavement distresses, mainly transverse cracks, for all sections in 2006 and for selected sections in 2007. A visual crack survey was primarily used but supplemented with a video crack survey in several sections. Figure 3 demonstrates the visual and video crack surveys conducted. In addition, a large amount of historical crack survey data was obtained from IDOT

engineers, who have been monitoring transverse cracks on a number of the selected projects over the past several years.

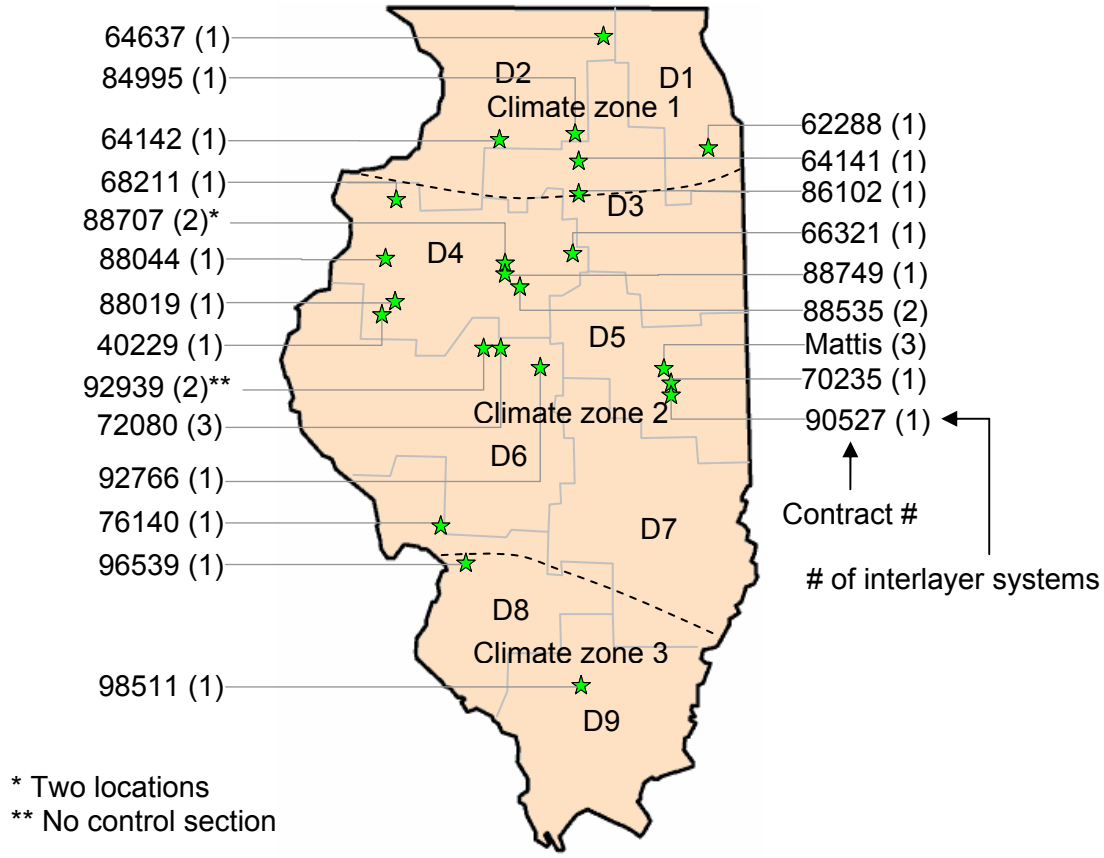

Figure 2. Survey locations.

(a) (b)

Figure 3. Field crack survey: (a) visual (walk-on) survey and (b) video surveying van.

Table 1. Survey List and Interlayer System Types

Brief Job Description							Treatment		
No	Contract#	District	Location	Const. year	Lane	Length (ft)	System	Type*	Material
1	62288	1	127th St., Chicago	2004	4	1000	A	S**	Miratac
2	64142	2	IL 40, Deer Grove	1998	2	660	A	A	Petromat
3	64637	2	IL 76, Belvidere	2003	2	6000	E	A	IL 4.75 mm
4	84995	2	IL 251, N. US30	1995	2	1000	A	A	Petromat
5	64141	3	US 34, Mendota	1997	2	1000	A	A	Petromat
6	86102	3	IL 178, Oglesby	1990	2	1000	A	S	ProGuard
7	88019	4	IL 9, East of IL41	1988	2	1000	A	A	Petromat
8	40229	4	US 136, Macomb	1988	2	1000	A	A	Petromat
9	88707	4	IL 29, Mossville	1998	2	2500	A	A	Petromat
10	88707	4	IL 29, Chillicothe	1998	2	2500	A	A	Petromat***
11	88749	4	IL 29/US24, Peoria	1997	3	800	A	A	Petromat
12	88044	4	US 34, Kirkwood	1988	2	1000	A	S	ProGuard
13	88535	4	IL 29, Creve Coeur	1997	2	1000	B D	S S	PavePrep ISAC
14	68211	4	IL 17, Aledo	2003	2	6000	E	A	IL 4.75 mm
15	66321	4	IL 117, Benson	2003	2	3000	E	A	IL 4.75 mm
16	90527	5	IL 130, Villa Grove	1995	2	1000	A	S	Petromat
17	Mattis	5	Mattis, Champaign	2000	4	4900	A B D	S S S	Fabric Roadtac ISAC
18	70235	5	IL 130, Philo	2003	2	6000	E	A	IL 4.75 mm
19	72080	6	US 136, E. San Jose	1999	2	2000	A D E	A S A	Petromat ISAC SAF
20	92766	6	US 66, Lincoln	1994	4	1000	A	A	Petromat
21	92939	6	US 136, W. San Jose	1998	2	2000	A D	A A	Petromat SAF
22	96539	8	IL 111, Pontoon Beach	1994	2	1500	A	A	Fabric
23	76140	8	IL 267, Greenfield	1998	2	8400	D	S	ISAC
24	98511	9	IL 148, Christopher	1998	2	1500	A	A	Petromat

* A: area, S: strip in a transverse direction
** Strip in a longitudinal direction
*** Petromat with modified binder asphalt for HMA overlays on IL29 at Chillicothe

2.3.1 Visual Crack Survey

The lineal amount of transverse cracking was manually recorded along with the severity of the cracks, which is classified into four levels. According to the FHWA distress manual (Miller and Bellinger 2003), joint-reflective cracking is categorized into low, medium, and high severity levels. A low-severity level crack is less than or equal to 0.25 in. wide for an unsealed crack or a sealed crack in a good condition regardless of crack width. A medium-severity level crack is 0.25 in. to 0.75 in. wide or has adjacent low-severity level random cracks. A high-severity level crack is wider than 0.75 in. or has adjacent medium to high-severity level random cracks. To accurately trace the initiation of reflective cracking, a starting severity level was added to the three aforementioned severity levels. The starting severity level crack has much smaller width than the low-severity level and its length is less than 2.0 ft. Care is required to identify starting-severity level cracks during field surveys and during the assessment of video images.

Figure 4 demonstrates crack images taken at Mattis Ave. in Champaign, IL. In this section, a starting-severity level crack (Figure 4(a)) is observed under the wheel path and at the pavement edge. A low-severity level crack shown in Figure 4(b) has been sealed (upper images) and left unsealed (lower images). After crack sealing, however, the upper crack is classified as the same severity level of the lower crack. A medium-severity level reflective crack (left image in Figure 4(c)) has adjacent cracks along the sealed main crack. One more parallel crack exists through the whole lane at 6 ft away from the medium-severity level crack, which is likely the reflection of the edge of a concrete joint patch. Finally, the high-severity level crack shown in Figure 4(d) represents a typical band crack. It is hypothesized that band cracking results from local debonding of the overlay or interlayer system in the vicinity of the joint, from concrete joint spall, and as a manifestation of shearing type crack propagation. Since the accuracy of determining severity levels is relevant to environmental conditions, primarily the direction of sun light and moisture on the surface of the pavement, crack surveys were conducted in both directions. Field crack survey maps for all of the sections are provided in Appendix B.

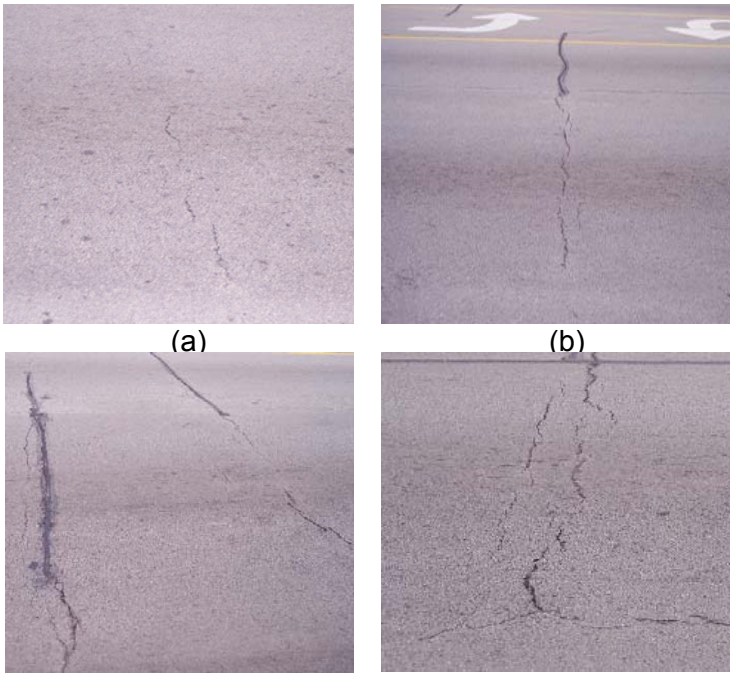

Figure 4. Typical reflective cracking severity: (a) starting-severity level, (b) sealed and unsealed low-severity level; (c) medium-severity level (left), and (d) high-severity level.

2.3.2 Video Crack Surveying

To create a more efficient and safer crack surveying environment, video crack surveys were performed at several locations. Video crack survey equipment was mounted on a van with ground penetrating radar (GPR) and a video integration system. The system, GaVIS, Figure 5, developed by Al-Qadi and co-workers consists of four measurement systems: GPR antennae, a digital video camera, a distance measurement instrument (DMI), and a data acquisition system (Baek et al. 2008). A 640 by 480 pixel digital video camera was mounted at the end of an extension bar, which can capture 10-ft-long by 12-ft-wide video images at highway speeds. The video image covers a whole lane and one pixel of the image spans across a 0.25 in. by 0.25 in. area, which is enough to distinguish a low-severity level crack. Because sunlight greatly affects the determination of a crack's severity level, care is required to adjust image brightness, which can be accomplished using the iris diaphragm on the video camera and though software-level image processing. In-house video image acquisition software, Camera Grabber, was used to collect video image data. By changing exposure time, brightness, and gain, high quality video images could be achieved. Due to differences in lighting conditions, different settings were required for the various pavements investigated.

The distorted raw video image captured by the wide-angle camera lens (the left image in Figure 6(a)) was corrected using a simple geometric correction function (the right image in Figure 6(b)) using the Camera Viewer software. From the captured video images, crack length and severity were determined following a procedure analogous to that used in the visual surveys. Although outside of the scope of the current study, more advanced automated crack detection techniques can be utilized in the future to reduce analysis time (Lee and Kim 2005, Y. Huang and B. Xu 2006).

Figure 6(b) demonstrates the four severity levels of cracks observed in the video images. For example, the extent of the sealed crack labeled L is 0.8 (crack length to lane width) and of low-severity level while the crack labeled H is a high-severity band

reflective crack with 1.0 extent due to partially broken crack sealant and adjacent cracks. Ten consecutive video crack images are compared with a visual crack survey map to evaluate the video crack data. As shown in Figure 6(c), for instance, the crack surveys were conducted in one, 100-ft-long lane on IL 130 Philo southbound. All sealed cracks are very clearly visible in both crack maps. Additionally, an unsealed longitudinal crack at 75 ft to 95 ft was detectable on the large-scale image.

Figure 5. The video integration system (GaVIS) setup.

The applicability of the video crack survey is examined by comparing detected cracks from visual and video crack surveys. The number of detected transverse cracks and their corresponding crack severities are listed in Table 2. The total number of cracks identified from the video crack survey is 15.2 % less than that of the visual crack survey. The missing cracks would belong to the starting- and low-severity level crack categories since the medium- and high-severity cracks are very easily differentiable from background noise and/or pavement surface. So, under the assumption that no missing cracks are in the medium- and high-severity levels, the missing starting- and low-severity level cracks become 20.9 % (=31/148x100). On the other hand, regarding the severity distributions, the largest population is the low-severity level (67.3 % for the visual survey and 81.2 % for the video survey). This suggests that the visual crack survey is currently more accurate than the video crack survey in identifying crack severity. From the video crack data, it is difficult to identify the severity level of sealed cracks. Sealed cracks are too dark to recognize inside deterioration. As a result, crack severities are under predicted. In general, the video method can provide safe, rapid, and simple crack surveys. The relatively low detectability of crack extent can be improved by using a lighting system and a higher resolution video camera.

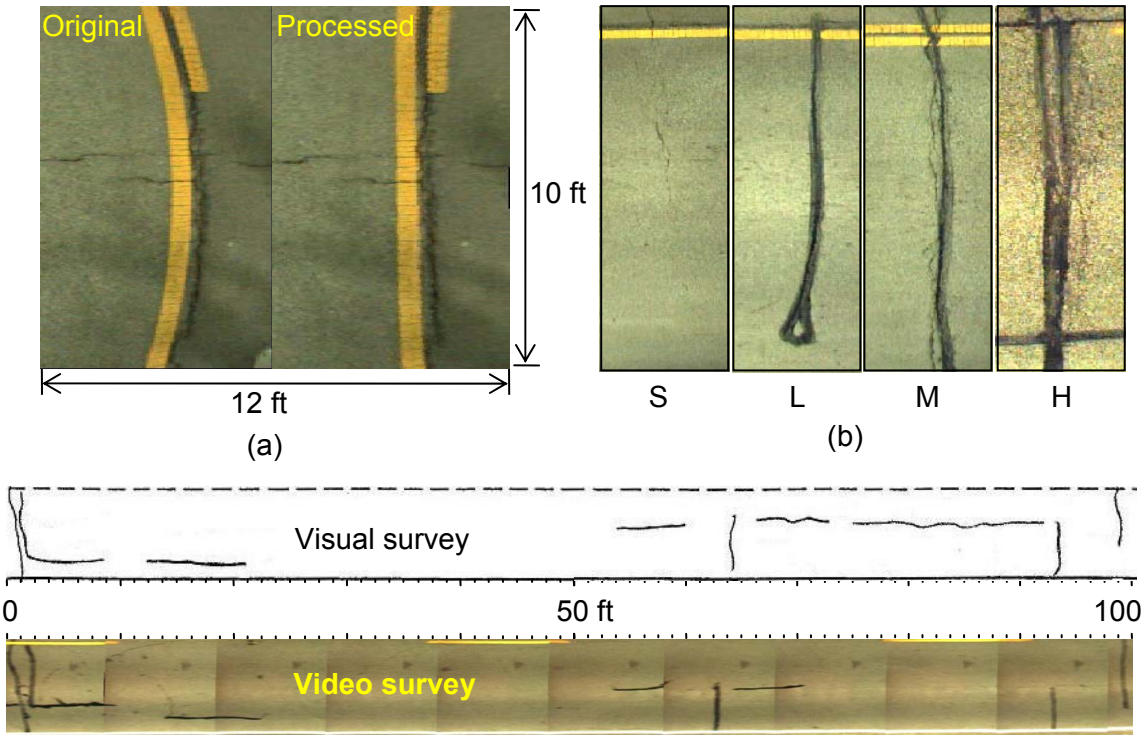

Figure 6. Video crack survey: (a) original distorted (left) and processed (right) images, (b) severity levels on video images, and (c) comparison of visual survey crack map and video images at IL 130 southbound section 4.

Table 2. Comparison of Number of Cracks from Visual and Video Crack Surveys at Philo IL 130

Severity	Number of Cracks (%)		Difference
	Visual	Video	
Starting	16 (8.2)	3 (1.8)	-13 (-6.4)
Low	132 (67.3)	134 (81.2)	+2 (+13.9)
Medium	40 (20.4)	25 (15.2)	-15 (-5.2)
High	8 (3.1)	3 (1.8)	-5 (-1.3)
Sum	196 (100)	165 (100)	-31(-15.2)

2.4 GROUND PENETRATING RADAR SURVEY

2.4.1 Ground Penetrating Radar Application to Pavements

The ground penetrating radar (GPR) technique has been utilized to assess pavement conditions as well as to predict pavement layer thicknesses (Al-Qadi et al. 2005). It is a nondestructive method using electromagnetic (EM) waves. A transmitter antenna sends EM waves into the ground and a receiver collects the EM waves reflected from material interfaces or scattered from inhomogeneities when the materials have different dielectric properties. Regarding the GPR antenna's position, two types of GPR antennae are used: air-coupled (horn) antenna positioned at 0.5 ft to 3.5 ft above the ground; and a ground-coupled antenna, which is in full contact with the pavement

surface during the surveys. The air-coupled antenna is used to collect data at highway speeds. Due to surface reflection, the penetration depth may be affected. On the other hand, ground-coupled antenna provides a relatively higher penetration depth when compared to air-coupled at the same frequency. However, data collection speed is limited to 10mph. Based on travel time and amplitude of received EM waves, layer thicknesses, material densities, moisture contents, and internal flaws can be estimated. The accuracy of the GPR to estimate pavement layer thicknesses was presented by several researchers (Maser and Scullion 1992, Lahouar et al. 2002, Al-Qadi et al. 2003). Moreover, GPR was successfully utilized to detect interlayer systems in pavements (Al-Qadi et al. 2004).

To complement the video crack survey, a GPR survey was conducted mainly to locate joints and patches in existing pavements. Joint and patch locations are needed to identify reflective cracking that is related to discontinuities. A 1.0 GHz air-coupled antenna was used to locate joints and patches; while a 1.5 GHz ground-coupled antenna was used to detect interlayer systems.

2.4.2 Joint and Patch Detection

Figure 7 shows GPR data collected from a 350-ft-long section at Philo IL 130 using the 1GHz air-coupled antenna. The horizontal and vertical axes represent distance and travel time, respectively. The travel time is relevant to pavement depth, but not linearly because various pavement layers have different material dielectric constants. A white thick line in the upper part represents strong signals reflected from HMA overlay surface. Another continuous thick line, thinner than the first one, represents the interface between the HMA overlay and the existing concrete surface. Knowing the distance between the two lines (travel time), HMA overlay thickness is predicted as 4.0 in. This prediction is confirmed by a measured field core, Figure 7(b). In addition, though it is not apparent in some locations, a weak reflection line exists within HMA overlay. The weak reflection is roughly at half the HMA overlay thickness. In this case, cores show the overlay consists of two layers constructed at two different periods. This reflection suggests that bonding condition at the interface is of poor quality.

Four discontinuities are found in the second line at a uniform spacing of 100 ft, which coincide with pavement joint spacing. In addition, two distinct patterns are found at discontinuities. Multiple reflections with a finite width are found through the concrete pavement. These reflections result from a scattering effect when an EM wave encountered an object having a different dielectric property such as steel, water, or air. In this case, the scattering is caused by a dowel bar in the middle of the concrete pavement as shown in Figure 7(c). The data was further confirmed using a ground-coupled antenna. Hence, the location is identified as a joint location. The second pattern type has a small width in the middle of the concrete pavement or within the HMA overlay. This represents patches used to repair existing pavement. An example of a section with PCC and HMA patches is demonstrated in Figure 7(d). In the first, a strip is located within the HMA overlay. This suggests a reflection from the top of a PCC patch that was used to repair the old HMA overlay and PCC pavement. The second strip's reflection occurs within the PCC slab without any reflection through the whole HMA overlay. In this case, the existing PCC pavement was repaired with a HMA patch. Such conclusions are made because the dielectric constant of concrete is significantly greater than that of HMA.

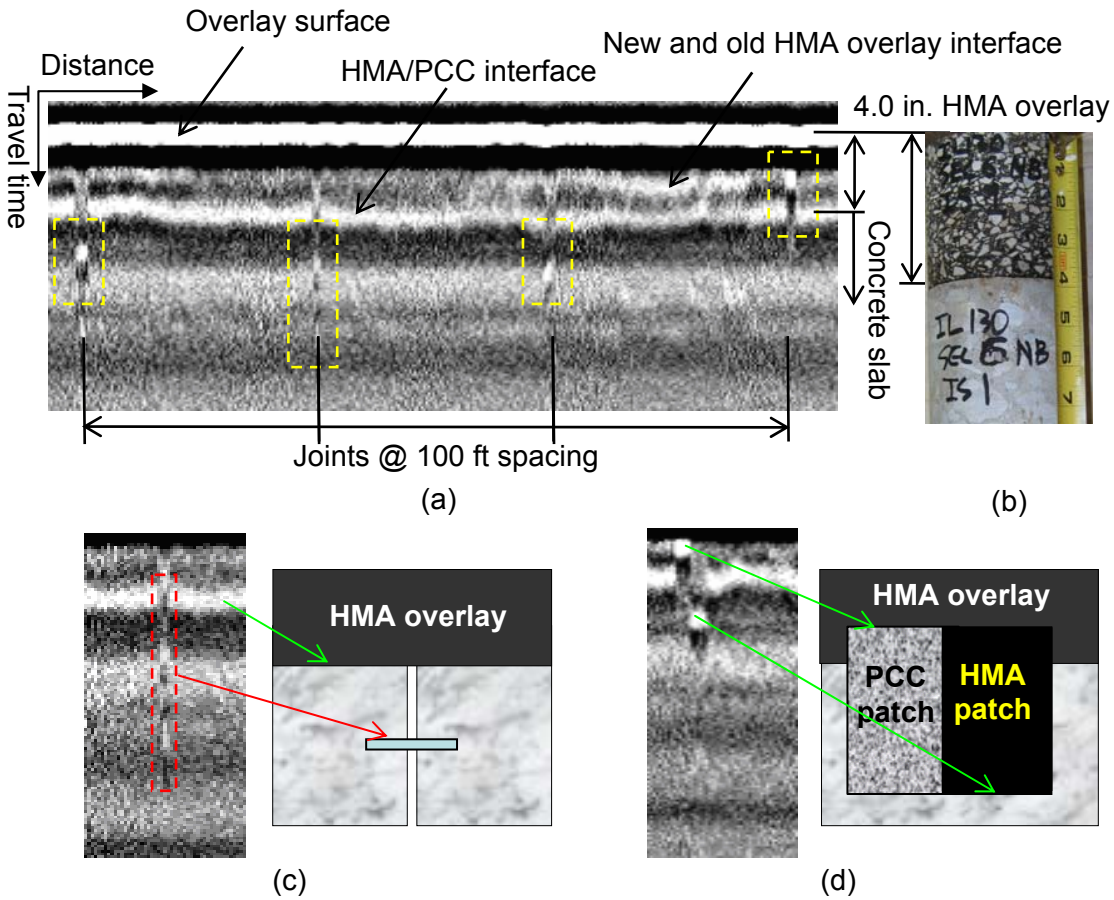

Figure 7. 1.0 GHz air-coupled GPR data (IL 130, Philo): (a) joint and patch detection; (b) field core; typical GPR data and corresponding pavement profiles for (c) a dowel bar and (d) patches.

2.4.3 Interlayer System Detection

One of the difficulties in assessing interlayer system performance arises when incomplete or inaccurate documentation of interlayer system locations exists, particularly in the case of strip-type interlayers installed at irregular intervals. Compared to other fabric interlayer systems evaluated in this research, ISAC is relatively thick. This suggests the possibility of using the 1.5 GHz ground-coupled antenna to verify field installation locations. The GPR survey was conducted on US 136 westbound east of San Jose during field coring; traffic control was used to facilitate the ground-coupled GPR survey at five mph. Figure 8 illustrates a GPR data collected on a 30-ft-long section with ISAC and having a similar structure as the overlay in the IL 130 section. The data was collected at 12 scans per foot.

Figure 8(b) provides a detailed view of two strong parabolic-shaped reflections located at 30-ft-long uniform intervals. The parabolic scattering of the EM waves indicates the presence of dowel bars. Directly above the dowel bar, a 3-ft-long strip-shaped reflection was detected, which is characteristically different than a reflection associated with a pavement patch. According to the construction report, this section contains ISAC strips along transverse joints, which were installed on an old HMA overlay. The GPR data and ability to identify ISAC locations was confirmed by field coring.

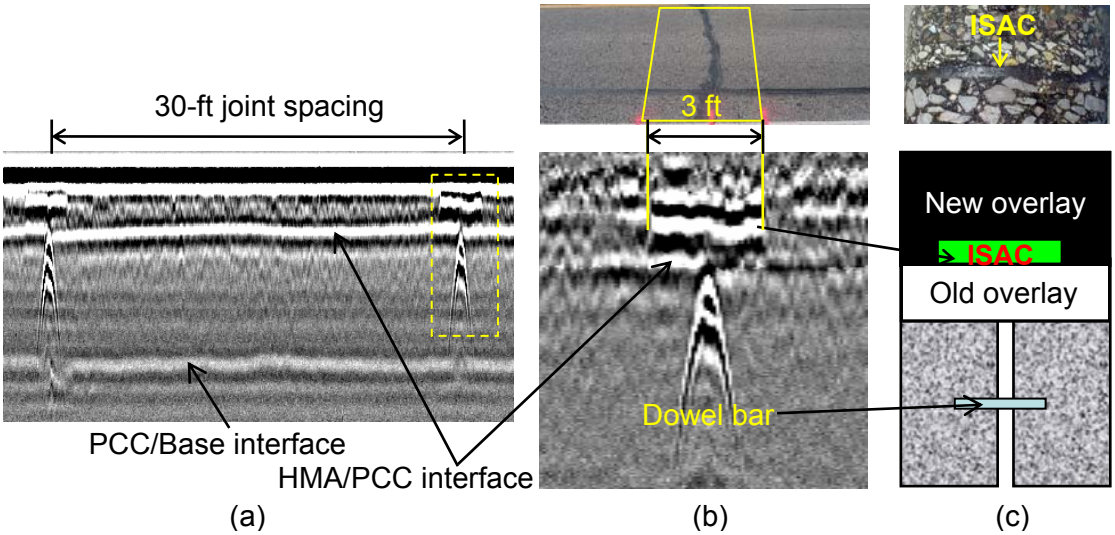

Figure 8. 1.5 GHz ground-coupled GPR data (IL 136, East of San Jose): (a) ISAC and dowel bar detection; (b) detail in vicinity of PCC joint, and; (c) pavement profile.

2.5 REFLECTIVE CRACKING IDENTIFICATION

The main objective of utilizing GPR in this study was to identify joint-associated reflective cracking with other forms of overlay cracking. This was accomplished by combining visual crack data with GPR survey data. A distance measurement instrumentation (DMI) was used to synchronize the location of transverse cracks from video crack surveys and GPR surveys.

Figure 9 illustrates the GPR data collected using 1.0 GHz air-coupled antenna and crack patterns observed in section 1 (STA. 135+00 to 140+00) of the IL 130 northbound project near Philo. Based on typical reflection patterns in the GPR data, one joint, three HMA patches, and two PCC patches were detected in the 500-ft-long section. Compared to a pre-construction crack map, shown in Figure 9(b), the presence of a PCC patch was confirmed. In addition, from IDOT maintenance reports, it was confirmed that three HMA patches were placed as partial-depth repairs at STA: 135+02, 136+02, and 138+01. No treatment had been applied to the joint at STA. 137+00. In 2006, the three-year-old overlay exhibited four transverse cracks, as shown in Figure 9(c). Cracks A and C were associated with HMA patches; while crack D is with a PCC patch. These cracks are classified as patch-associated reflective cracks. On the other hand, crack B was classified as joint-associated reflective cracking. Therefore, all transverse cracks in this section could be identified as reflective cracks. On the other hand, while 1.0 and 2.0 GHz air-coupled antennae could not identify joints at US 136 eastbound east of San Jose, IL, due possibly to missing the location of the dowels, the ground-coupled 1.5 GHz system successfully identified the joints. Hence, further research is needed prior to developing guidelines on the use of GPR for identifying reflective cracking.

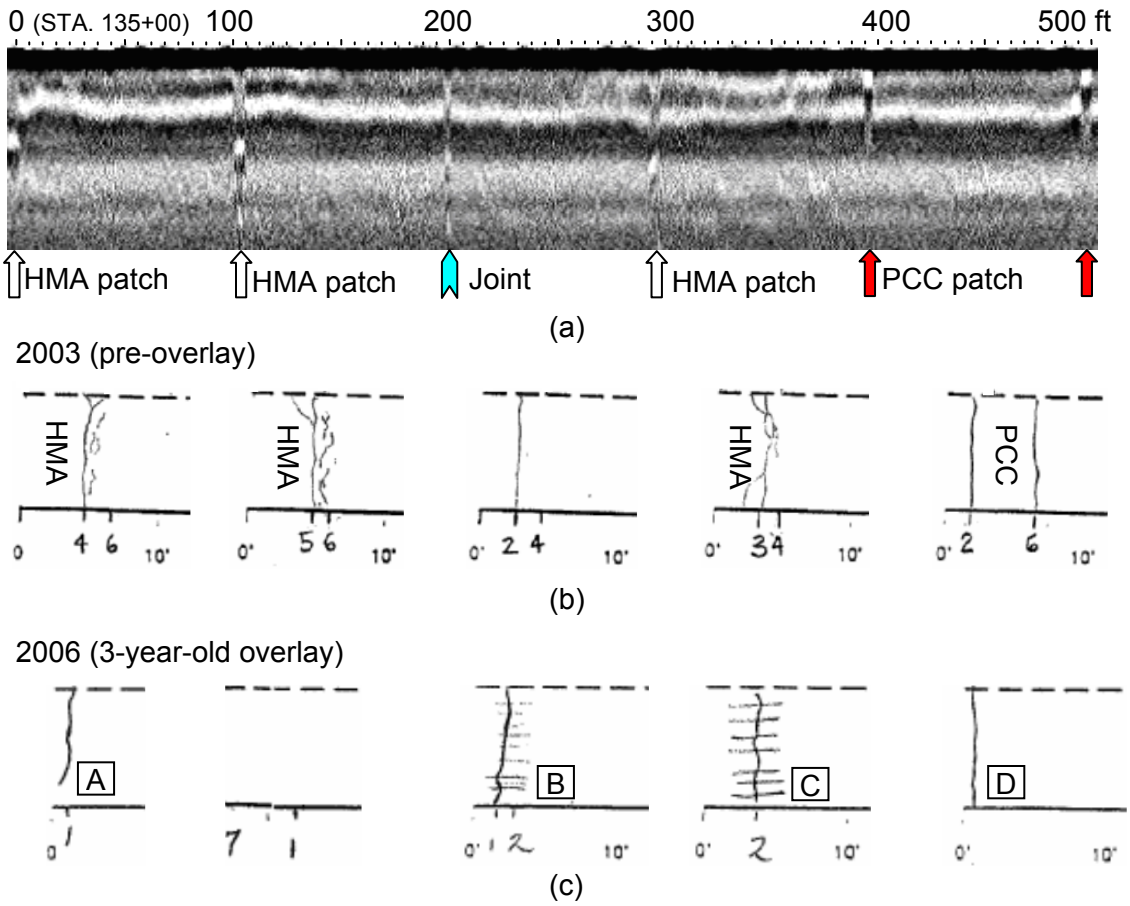

Figure 9. Reflective cracking identification (IL 130 northbound section 1): (a) GPR survey, (b) 2003 pre-construction crack map, and (c) 2006 crack survey map.

3. REFLECTIVE CRACKING INDEX

To predict the performance of interlayer systems, the HMA overlay condition needs to be evaluated with regards to reflective cracking. Using the extent and severity of reflective cracking or transverse cracking obtained from a field crack survey, an index is developed to quantify the status of HMA overlays. Two approaches are used to develop the index, depending on the available crack data. In many pavement sections in this study, reflective cracking could not be confirmed, especially when area-type interlayer systems are used. In this case, all transverse cracks are considered in the index, using the transverse cracking appearance ratio (R_{TCA}). However, when joint- and patch-associated reflective cracking is identified, the index is computed using the reflective cracking appearance ratio (R_{RCA}).

3.1 TRANSVERSE CRACKING APPEARANCE RATIO

Because identifying actual reflective cracking is difficult, a typical crack survey considers total crack length or number of cracks. The transverse cracking appearance ratio, R_{TCA}, is used to account for all transverse cracks. The R_{TCA} is defined as the number of transverse cracks per a unit length of 100 ft as follows:

$$R_{TCA} = \frac{N_{TC}}{L_T / 100} \quad (1)$$

where, R_{TCA} is transverse cracking appearance ratio,
N_{TC} is total number of transverse cracks, and
L_T is total survey length (ft), which is divided by 100 to represent the unit length.

No variable is included in the calculation of R_{TCA} to consider joint characteristics such as joint spacing or joint location. For overlays having various joint intervals, different R_{TCA}s will result in spite of similar performance. Under the same conditions and behavior, it is expected that lower R_{TCA} can be achieved when existing concrete pavement joint spacing is longer because reflective cracking development potential per unit length is less. Because of that, R_{TCA} is not an appropriate index to evaluate interlayer systems. In addition, as HMA overlays deteriorate, other distresses besides reflective cracking could appear, such as fatigue, thermal, and block cracking. Since all these cracks are considered in R_{TCA}, the R_{TCA} is unsuitable for evaluating long-term HMA overlay performance. Therefore, R_{TCA} may be applicable for short-term performance evaluation of interlayer systems installed on jointed concrete pavement having the same joint spacing.

3.2 REFLECTIVE CRACKING APPEARANCE RATIO

When the reflective cracking location is known, accurate analysis can be conducted using the reflective cracking appearance ratio, R_{RCA}. Only reflective cracking is included to compute the R_{RCA} (Equation 2). The R_{RCA} ranges from 0.0 (no reflective cracking) to 1.0 (reflective cracking is present at all joints/cracks/patches). If double reflective cracking or adjacent cracks occur, these are considered as one equivalent instance of reflective cracking. The number of discontinuities is set to two for a patch.

$$R_{RCA} = \frac{N_{RC}}{N_J} \quad (2)$$

where, R_{RCA} is reflective cracking appearance ratio;
N_{RC} is total number of reflective cracking; and
N_J is total number of discontinuities underneath overlay.

The R_{RCA} is easy to use to evaluate strip-type interlayer systems since reflective cracking locations are specified in most cases. It is, however, difficult to determine the R_{RCA} for area-type interlayer systems. In this case, either R_{TCA} or R_{RCA} may be used depending on field data availability. Given that the behavior of reflective cracking is affected by external conditions such as traffic volume and environmental conditions, the aforementioned indices should be carefully used and the outcome cautiously interpreted.

3.3 WEIGHT FACTOR

With time, reflective crack condition usually worsens. Both R_{TCA} and R_{RCA} consider crack extent only; crack severity is not included. To better explain this effect, an example is shown in Figure 10. In this example, R_{RCA} increases rapidly during early HMA overlay early service life; it reaches 0.88 at 2.8 years old. After that, the value levels off and reaches 1.0 at 4.7 years old. The value 1.0 suggests that all reflective cracking has occurred. The data is compared to that at 6.0 years, R_{RCA} = 1.0. At 4.7 years, 25 reflective cracks are present; but all cracks are at low-severity level. However, at 6.0 years, 13 low-severity level and 12 medium-severity level cracks exist. This suggests that 12 out of 25 reflective cracks further deteriorated over the 1.3 years to the medium-severity level. Hence, R_{RCA} could not capture the change in crack severity.

To account for crack severity, a weight factor is included in the indices. The method used in a condition rating system (CRS) was adopted. A CRS value is determined for individual distresses observed at the pavement surface. Based on the CRS value, a road condition can be ranked from 9.0 (excellent) to 1.0 (poor). The procedure to compute the weight factor is addressed in Table 3. Of the original CRS value (column A), a part is reduced by other distresses except reflective cracking (column B). Hence, the net reduction of the CRS value due to reflective cracking is computed by subtracting the net reduction from the maximum CRS value of 9.0 (column C). Using a trial-and-error method, the determined weight factors are based on minimized sum of square error (SSE) between the net reduction and weighted R_{RCA}. The SSE is 1.41 when the uniform weight factors are used in the R_{RCA}; the SSE becomes 0.13 when linear weight factors of 0.75, 1.5, 2.25, and 3.0 are used for starting, low, medium, and high severity levels, respectively. Hence, these values are used in this study.

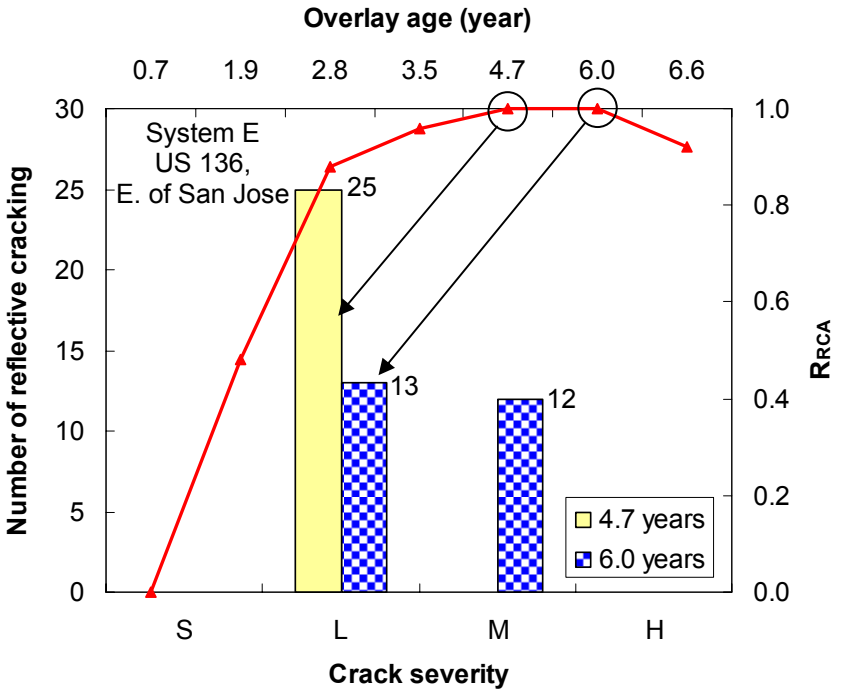

Figure 10. Number of reflective cracking at 4.7 and 6.0 years old and R_{RCA} variations over overlay age (US 136, E. of San Jose)

Table 3. CRS Values to Determine Weight Factors

Year	Original CRS "A"	CRS loss by other distress** "B"	CRS loss by RC Only (9 – A – B) "C"	Weight factor		
				Severity	Uniform	Linear
				Starting	1	0.75
				Low	1	1.50
				Medium	1	2.25
				High	1	3.00
1999	9.00	0.00	0.00		0.00	0.00
2000*	8.50	0.00	0.50		0.00	0.00
2001	8.00	0.00	1.00		0.48	0.69
2002*	7.80	0.15	1.05	Weighted R_{RCA}	0.80	1.08
2003	7.60	0.30	1.10		0.88	1.29
2004*	6.90	0.65	1.45		0.92	1.38
2005	6.20	1.00	1.80		0.92	1.71
				SSE	1.41	0.13

* Average value of the previous and next year

** Sum of CRS loss caused by distresses other than reflective cracking

Using the weight factors, weighted R_{RCA} is calculated as follows:

$$R_{RCAW} = \frac{\sum_{i=1}^{4}\left[W_i \times (N_{RC})_i\right]}{N_J} \quad (3)$$

where, R_{RCAW} is weighted reflective cracking appearance ratio;
W_i is weighted factors for i^{th} crack severity (from 1 for starting to 4 for high-severity);
$(N_{RC})_i$ is total number of reflective cracking with i^{th} crack severity; and
N_J is number of discontinuities.

Similarly, R_{TCAW} is calculated as follows:

$$R_{TCAW} = \frac{\sum_{i=1}^{4}\left[W_i \times (N_{TC})_i\right]}{L_T/100} \quad (4)$$

where, R_{TCAW} is weighted transverse cracking appearance ratio;
$(N_{TC})_i$ is total number of transverse cracking with i^{th} crack severity; and
L_T is total surveyed length in ft.

It is possible to characterize the behavior of reflective cracking and to evaluate the performance of interlayer systems using the uniform and weighted R_{RCA}. As demonstrated in Figure 11, for a control section, a constant R_{RCA} of 1.0 is obtained starting at 2.8 years; while R_{RCAW} ranges from 1.4 to 1.8. The results can be interpreted as reflective cracking occurred over all joints in the control section at 2.8 years after overlay placement; all were low-level severity reflective cracks, and no noticeable deterioration occurred until 8.0 years after the overlay placement since R_{RCAW} does not increase. Hence, appropriate maintenance, such as crack sealing, could be applied. On the other hand, for the section with System D, R_{RCA} and R_{RCAW} have similar trends: They rapidly increase until year six and then stabilize when R_{RCA} reaches 0.9 or R_{RCAW} reaches 1.3. This shows clearly that an increase in the number of reflective cracks leads to an increase in R_{RCAW}. In addition, for an R_{RCAW} to R_{RCA} ratio around 1.5, the reflective cracking is regarded as low-severity. Hence, the appearance of reflective cracking is retarded when System D is used. The System D worked efficiently in retarding reflective cracking in the first 4.9 years. However, after 6.0 years, its performance diminished.

The aforementioned reflective cracking analysis can be validated using field crack survey data at IL 267 Greenfield (Figure 12). For the control section at 4.9 years after the placement of HMA overlay, 76% (38/50) of the reflective cracks were low-severity level and 16% (8/50) and 8% (4/50) were medium- and high-severity levels, respectively. On the other hand, only 10% (10/101) starting-severity level and 30% (30/101) low-severity level reflective cracking occurred in the section with System D. System D retards 49% of the total reflective cracking (100% in the control section and 41% in the System D section); most of the retarded reflective cracking was medium- and high-severity level. Hence, System D is effective in alleviating the number and severity of reflective cracks. However, at 8.3 years, the majority of reflective cracking (86% (43/50) for control section and 88% (89/101) for System D) is low-severity level; only 10% medium-severity level reflective cracking is diminished by System D (14% in the control

section and 4% in the System D section). Again, System D demonstrated the ability to retard reflective cracking; especially at early service life.

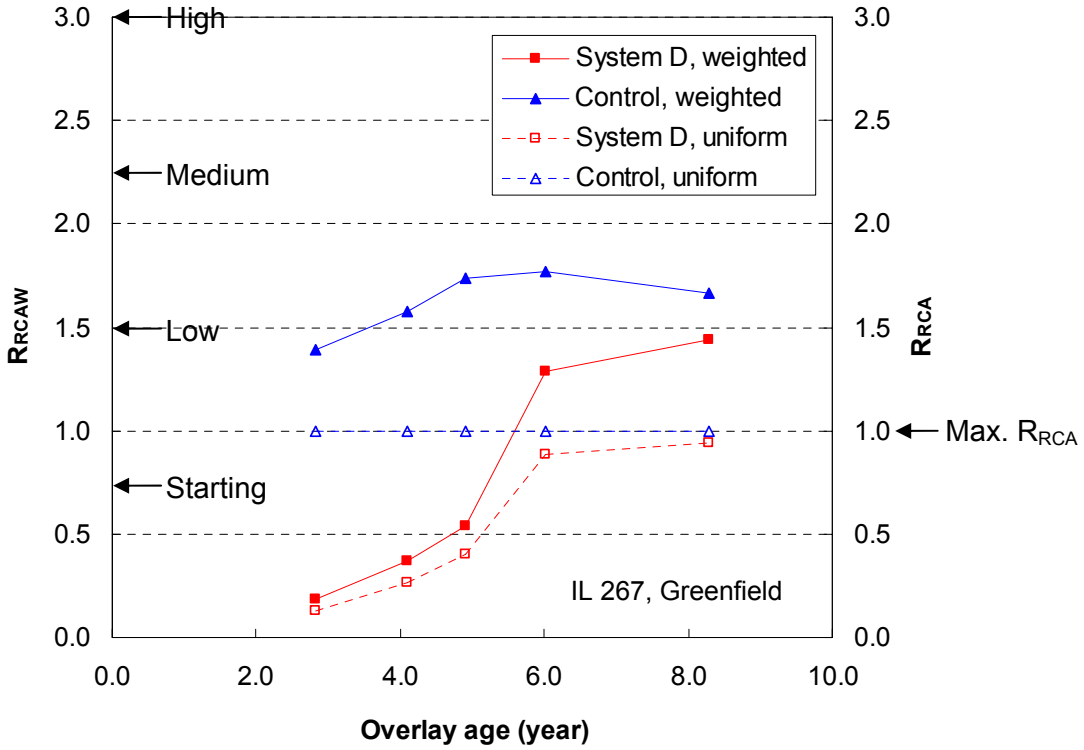

Figure 11. Comparisons of uniform and weighted R_{RCA} for System D and control section (IL 267 at Greenfield).

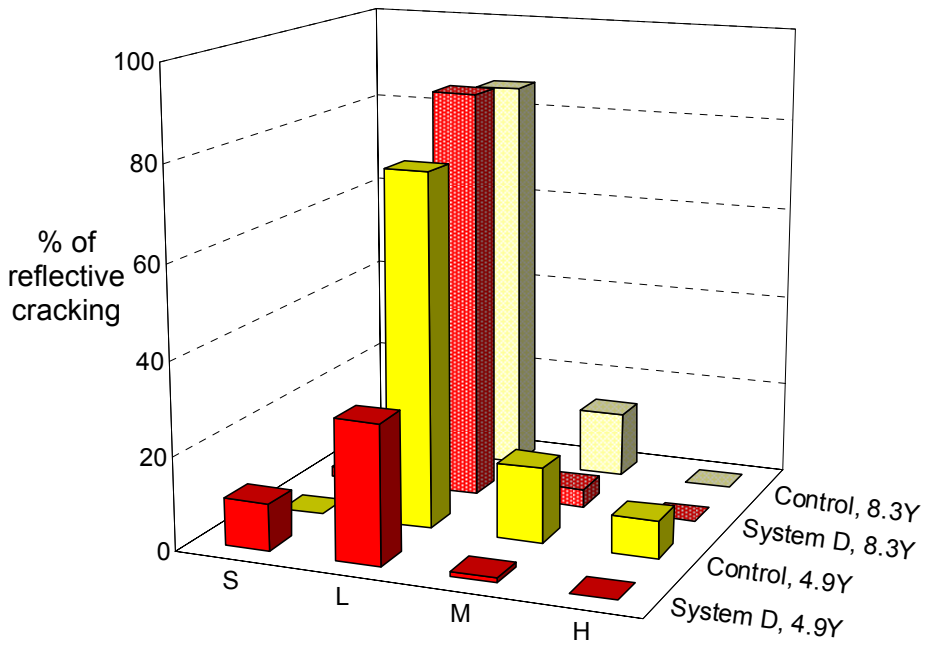

Figure 12. Comparisons of % of reflective cracking corresponding to severity level for control and System D sections at 4.9 and 8.3 years (IL 267 at Greenfield).

The applicability of the R_{TCAW} was evaluated at various locations (IL 178 at Oglesby and IL 148 at Christopher) where area-type system A is installed. Oglesby is located in District 3 (climate zone 2) and two-way average annual daily traffic (AADT) is 2650 in 2008; Christopher is located in District 9 (climate zone 3) and has 5800 two-way AADT in 2008. The two sections have different characteristics regarding traffic volume and climate zone. As shown in Figure 13, the R_{TCAW} varies from 2.7 to 6.1 for the control section at Christopher; while it varies from 7.4 to 12.3 at Oglesby. Although it is difficult to compare the behavior of the two sections directly because of the aforementioned variations as well as the overlay age, it can be simply concluded from the R_{TCAW} values that System A at IL 148 has performed better than the control section as well as the interlayer system A at IL 178. This clearly suggests that the performance of interlayer systems at various locations can be appropriately quantified.

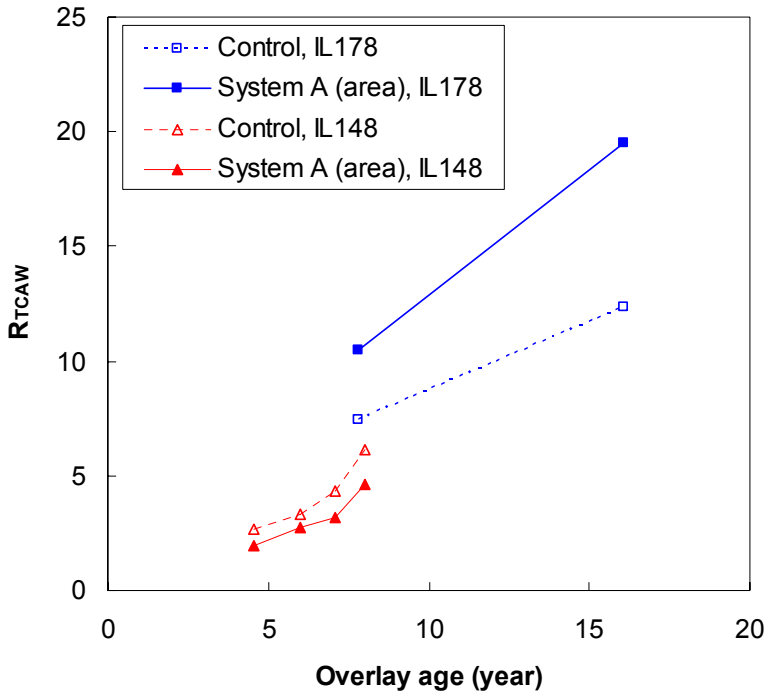

Figure 13. R_{TCAW} variations over overlay age at different locations (IL 178 at Oglesby and IL 148 at Christopher).

In summary, weighted reflective and transverse cracking appearance ratios can be effectively used to evaluate interlayer system performance. The indices are relevant to local characteristics of HMA overlay pavements so they may not be used directly for the evaluation of interlayer systems applied at different locations. To address location differences, parameters such as climate, traffic, and overlay thickness must be included.

4. EVALUATION OF INTERLAYER SYSTEMS

4.1 DETERIORATION RATE

In the previous chapter, new reflective cracking indices (RCI) were proposed to quantify overlay performance. Almost invariably, as a pavement ages, the RCI increases, while the overall serviceability of the pavement decreases. A deterioration rate can be computed as an indicator of HMA overlay status using the RCI parameters developed herein regarding reflective cracks and unclassified transverse cracks. Originally, the deterioration rate developed by Schutzbach (1995) and Buttlar et al. (1999) used the condition rating system (CRS) to estimate the service life of HMA overlays. In their research, the deterioration rate was computed as loss of CRS rating points per year. Using a trigger CRS value and the deterioration rate, the service life of HMA overlays could be obtained. In this study, two RCIs are used to compute the deterioration rate: reflective cracking appearance rate for strip-type interlayer systems and transverse cracking appearance rate for area-type interlayer systems. Detailed information on RCIs versus overlay age for all sections can be found in Appendix A. A typical example of weighted reflective cracking appearance rate, R_{RCAW}, and transverse cracking appearance rate, R_{TCAW}, as a function of overlay age is presented in Figure 14. Despite the mismatch at early overlay age which can be observed in Figure 14(a), the three fitted linear regression curves show a good agreement with the R_{RCAW} values for the three interlayer systems investigated at the Mattis Ave. section. In Figure 14(b), the R_{TCAW} values of the control and area-type System A are in agreement with the linear regression curves. In fact, as more traffic and environmental loadings are applied, reflective cracking becomes more severe, along with other types of distresses.

Using linear regression curves for each section, RCIs are estimated and compared with the RCIs obtained from field crack data. Figure 15 shows the comparison of obtained and estimated RCIs for all sections. The data set shows that a good correlation exists when using the linear deterioration model: R^2 of 0.95 and a P-value of 0.90 were obtained though statistical analysis of variation (ANOVA). In other words, the linear regression curves appear to be a valid method for estimating the RCI curves regardless of the interlayer system used in this study. However, the deterioration rate provides insufficient information for interlayer system performance evaluation because it depends on pavement structure, traffic volume, interlayer system, and environmental conditions. In the following section, control sections are used to ensure accurate, quantitative evaluation of reflective crack control systems.

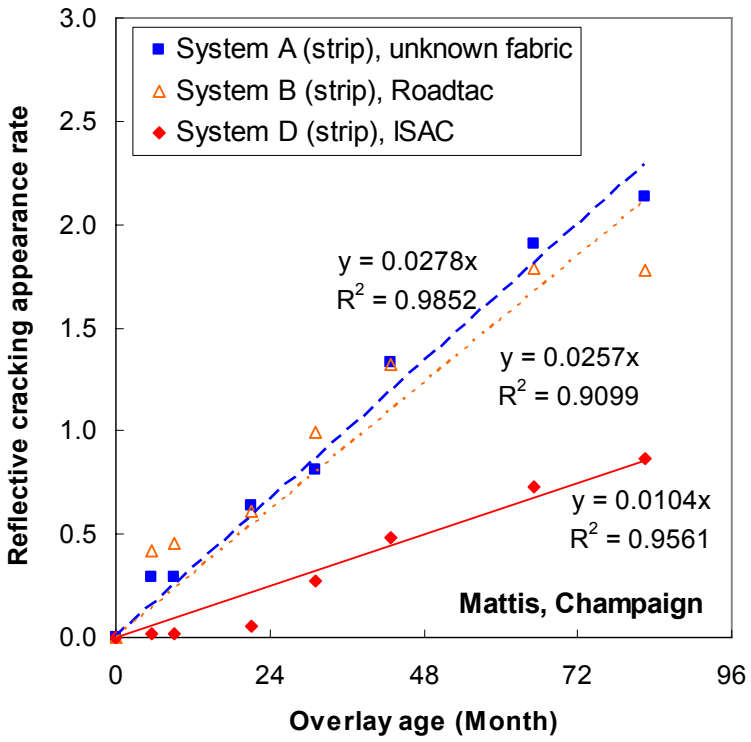

(a)

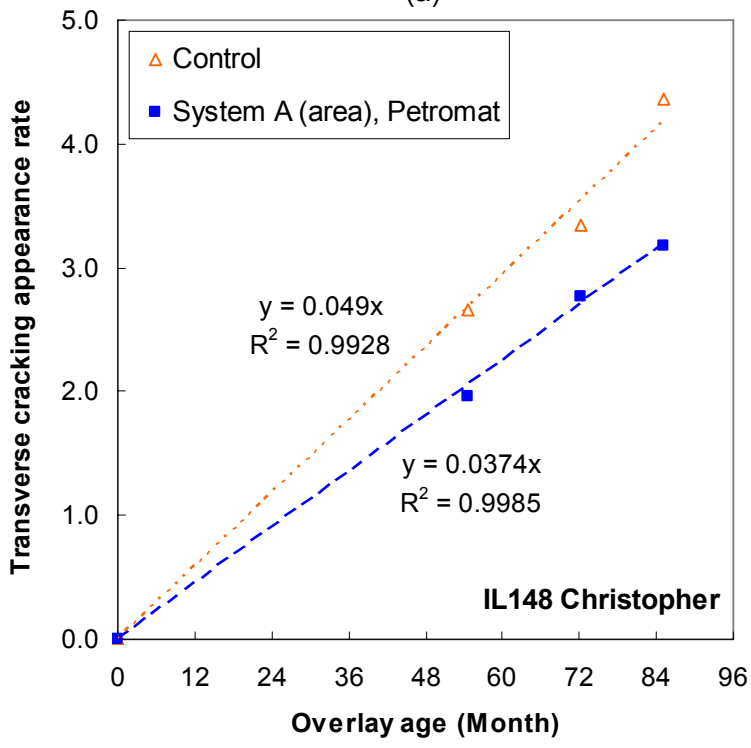

(b)

Figure 14. Reflective cracking index variations over overlay age: (a) R_{RCAW} at Mattis and (b) R_{TCAW} at IL 130 Philo.

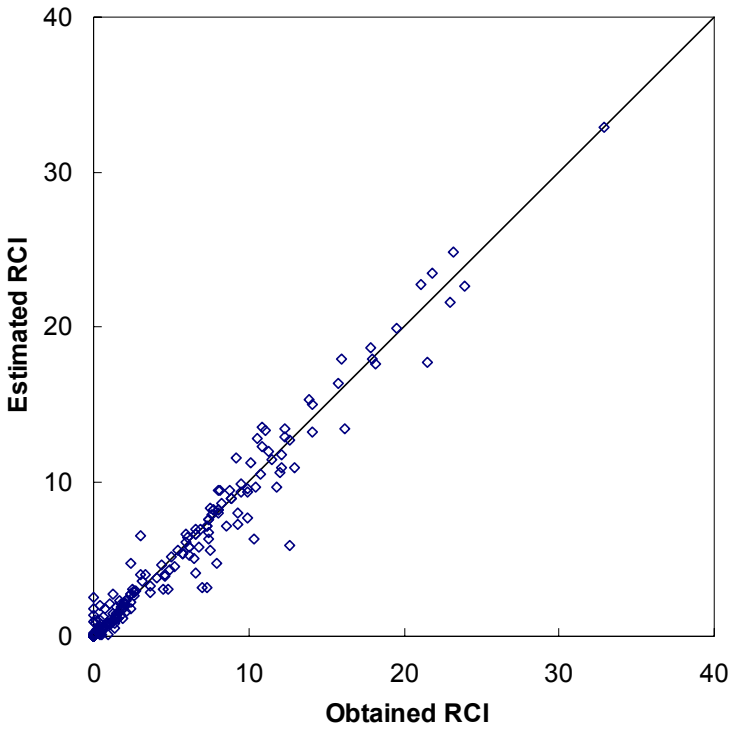

Figure 15. Relationship between estimated and obtained reflective cracking index.

4.2 PERFORMANCE BENEFIT RATIO

To quantify the relative extension of overlay service life of an interlayer treated pavement relative to an untreated control section, a performance benefit ratio, PBR is introduced. Figure 16 demonstrates two RCI versus overlay age curves for a typical treated and untreated overlays. From the RCI curve, the service life of an overlay is determined when a RCI reaches a certain trigger value. The PBR is defined as the ratio of a treated overlay life span, L_{target} , to an untreated overlay, L_{base}. The trigger value may be needed to determine the service life and consequently, the PBR. However, since the deterioration rate decreases linearly, the PBR is calculated with RCI curve slopes, S_{target} and S_{base}. Naturally, the ratio of L_{target} to L_{base} is geometrically the same as the ratio of the inverse of the slopes of the RCI curves as shown in Equation 5. Stated otherwise, regardless of the rehabilitation trigger level selected, a unique PBR can be computed under the assumption of linearity, which was validated in the previous section. In addition, when no control section is available, a combined PBR can be calculated using two single PBRs. In this case, the two PBRs should have a common target interlayer system ($S_{com.target}$) and similar conditions (traffic volume and climate).

$$PBR = \frac{L_{target}}{L_{base}}$$

$$= \frac{S_{base}}{S_{target}} \qquad (single\ PBR) \qquad (5)$$

$$= \frac{S_{base}}{S_{com.target}} \frac{S_{com,target}}{S_{target}} \qquad (combined\ PBR)$$

where, PBR is a performance benefit ratio;
L_{base} and L_{target} are base (control) and target (treated) service life spans; and
S_{base} and S_{target} are base and target slopes of RCI curves.

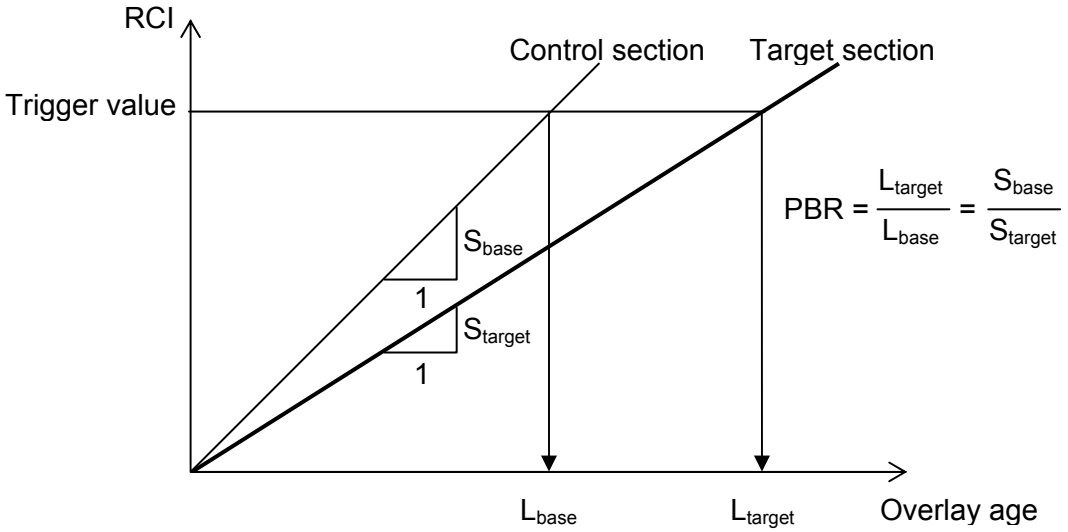

Figure 16. Schematic of performance benefit ratio and service life of HMA overlays.

Figure 17 shows the performance benefit ratios obtained from 25 interlayer systems used in HMA overlays across Illinois: 9 System A (area), 4 System A (strip), 2 System B, 4 System D, and 6 System E. Single PBRs of the interlayer systems were obtained from each control section except two sections which have no control section. In the US 136 east section, a single PBR of 1.29 is calculated from a System E section and then the combined PBR becomes 2.40 (= 1.29 x 1.85) where 1.85 is the PBR of the System E section obtained from a control section. In the US 136 west section, the single PBR of System E is 0.92 and the combined PBR turns out to be 1.28 by multiplying 1.39 that is obtained in the US 136 east section similar to the US 136 west section. Out of the total matrix, a few sections were excluded in this analysis because crack history was not available. Detailed calculations of the PBR and section descriptions are listed in Table 4; in addition, brief evaluation reports are included in Appendix A. For each interlayer system, the PBRs are not consistent even though similar overlay designs and interlayer products are considered. As shown in Table 4, the evaluated sections have different traffic volumes and environmental conditions. For example, for two System E projects, PBR of the IL 76 section is 1.17 under AADT of 7200, annual 18-kip equivalent single-axle loads (ESALs) of 1088, and lowest monthly average temperature, T_L of 12.4 ^oF; PBR of the IL 117 section is 1.88 under 800 AADT, 15 ESALs, and T_L of 14.0 ^oF. This suggests that the performance of interlayer systems is influenced by other factors. This

variation in performance can be observed in all interlayer systems. So, the PBR of interlayer systems can be affected by traffic volume as well as environmental conditions. The effect of those variables on PBR for each interlayer system will be discussed in the following chapter.

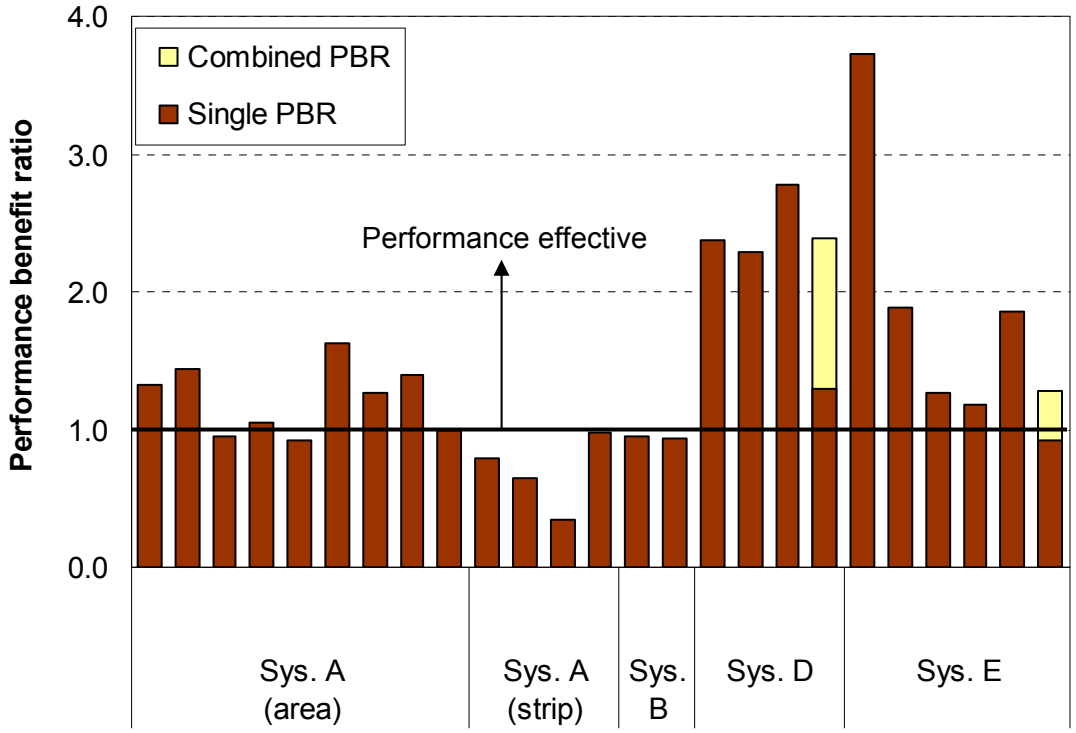

Figure 17. Performance benefit ratios for all sections (25 interlayer systems).

Table 4. Summary of the Benefit Ratio and Traffic Volume

Location	District	Base	Target	S_{base}	S_{target}	PBR*	AADT**	Annual ESALs**	T_L*** (°F)
IL 251, N. US30	2	Control	Sys. A, Area, Petromat	0.0873	0.0606	1.44	1200	0.047	10.9
IL 40, Deer Grove	2	Control	Sys. A, Area, Petromat	0.1684	0.1034	1.63	2400	0.124	12.1
US 34, Mendota	2	Control	Sys. A, Area, Petromat	0.1423	0.1125	1.26	2300	0.034	15.0
IL 29, Chillicothe	4	Control	Sys. A, Area, Petromat	0.0696	0.0729	0.95	16400	0.194	16.2
IL 9, E. IL 41	4	Control	Sys. A, Area, Petromat	0.0918	0.0879	1.04	950	0.021	15.1
IL 29, Mossville	4	Control	Sys. A, Area, Petromat	0.0864	0.0937	0.92	16400	0.194	16.2
US 136, E. San Jose	6	Control	Sys. A, Area, Petromat	0.3145	0.2265	1.39	2450	0.177	16.9
IL 148, Christopher	9	Control	Sys. A, Area, Petromat	0.0546	0.0413	1.32	5800	0.090	23.4
IL 111, Pontoon Beach	8	Control	Sys. A, Area, unknown	0.0642	0.0643	1.00	13800	0.233	23.7
IL 178, Oglesby	3	Control	Sys. A, Strip, ProGuard	0.0669	0.1032	0.65	2650	0.093	15.0
US 34, Kirkwood	4	Control	Sys. A, Strip, ProGuard	0.0518	0.1485	0.35	4250	0.304	15.0
IL 130, Villa Grove	5	Control	Sys. A, Strip, Petromat	0.1395	0.1752	0.80	3250	0.033	17.2
Mattis, Champaign	5	Control	Sys. A, Strip, Unknown	0.0283	0.0288	0.98	20800	0.054	17.2

* Performance benefit ratio
** Average annual daily traffic (AADT) and annual 18-kip equivalent single-axle loads (ESALs) in a design lane obtained in 2008
*** Lowest monthly average temperature

Table 4 (Continued). Summary of the Benefit Ratio and Traffic Volume

Location	District	Base	Target	S_{base}	S_{target}	PBR	AADT	Annual ESALs	T_L (^oF)
IL 29, Creve Coeur	4	Control	Sys. B, Strip, PavePrep	0.0619	0.0655	1.02	33600	0.308	16.2
Mattis, Champaign	5	Control	Sys. B, Strip, Roadtac	0.0283	0.0303	0.93	20800	0.054	17.2
IL 29, Creve Coeur	4	Control	Sys. D, Strip, ISAC	0.0619	0.0270	1.44	33600	0.308	16.2
Mattis, Champaign	5	Control	Sys. D, Strip, ISAC	0.0283	0.0102	2.77	20800	0.054	17.2
IL 267, Greenfield	8	Control	Sys. D, Strip, ISAC	0.0290	0.0122	2.38	2150	0.099	20.3
IL 76, Belvidere	2	Control	Sys. E, Area, IL4.75	0.1029	0.0877	1.17	7200	0.194	12.4
IL 17, Aledo	4	Control	Sys. E, Area, IL4.75	0.0764	0.0205	3.73	4800	0.073	13.2
IL 117, Benson	4	Control	Sys. E, Area, IL4.75	0.0743	0.0395	1.88	800	0.026	14.0
IL 130, Philo	5	Control	Sys. E, Area, IL4.75	0.0727	0.0574	1.27	7400	0.067	17.2
US 136, E. San Jose	6	Control	Sys. E, Area, SAF	0.3145	0.1700	1.85	2450	0.177	16.9
US 136, E. San Jose	6	Sys. E, Area, SAF	Sys. D, Strip, ISAC	0.0268	0.0207	1.29 (2.40)[+]	2450	0.177	16.9
US 136, W. San Jose	6	Sys. A, Area, Petromat	Sys. E, Area, SAF	0.0864	0.0937	0.92 (1.28)[+]	1650	0.165	16.9

[+] Parenthesis value is combined PBR.

The PBR for each interlayer system is summarized in Table 5. The PBR varies in different ranges: 0.92 to 1.63 for System A (area); 0.35 to 0.98 for System A (strip); 0.93 to 1.02 for System B; 1.44 to 2.77 for System D; and 1.17 to 1.88 for System E. Based on the average PBR, System D shows the best performance (average PBR of 2.25). One data point of System E locations can be excluded since its PBR of 3.73 is too high compared to other locations. Despite this, System E with average PBR of 1.49 ranks second. For System A (area), the average PBR is 1.22 while it is less than 1.0 in some locations. On the other hand, System A (strip) and System B whose average PBRs are not greater than 1.0 are not beneficial to control reflective cracking. The outcome should be used cautiously since the PBRs are determined from a limited amount of data.

Table 5. Summary of Performance Benefit Ratio for Interlayer Systems

Interlayer system		Performance benefit ratio			# Data
System	Type	Ave.	Max.	Min.	
A	Area	1.22	1.63	0.92	9
	Strip	0.69	0.98	0.35	4
B	Strip	0.98	1.02	0.93	2
D	Strip	2.25	2.77	1.44	4
E	Area	1.86 (1.49)	3.73 (1.88)	1.17	6 (5)*

* One data point is excluded at IL 17 Aledo.

4.3 SENSITIVITY ANALYSIS FOR THE PERFORMANCE BENEFIT RATIO

4.3.1 Potential Variables

To identify variables that may influence the performance benefit ratio, a sensitivity analysis was conducted. Since the vast majority of overlay systems evaluated in this study had similar HMA overlay thickness and existing pavement structure, thickness and pavement structure were not included as variables in the sensitivity analysis. Only traffic volume, environment, and joint spacing were considered as potential variables. As shown in Table 4, traffic volume was represented in 2008 by two-way AADT in whole lanes and total number of annual ESALs to a design lane for mixed traffic loads; environment was roughly characterized by a climate zone and more specifically by a single temperature to indicate the lowest monthly average temperature. Joint spacing (JS) of the evaluated sections is 30 ft, 50 ft, or 100 ft.

Current AADT data was collected through traffic maps provided by the Illinois Department of Transportation (IDOT 2008). Due to a lack of historical traffic data, current traffic data was utilized in this study. An assumption of zero traffic growth over the past several years was made in the estimation of traffic level for past years. The ESALs quantities used in this study included vehicle mix and loading effects, which is a better indicator of reflective cracking progress because ESALs are a measure of actual pavement loading. According to IDOT's pavement design manual (2002), the ESALs are calculated using traffic factor (Equation 6). The traffic combines number of vehicles in each category and its corresponding equivalent factor.

Roads in Illinois are classified into four classes: class I, class II, class III, and class IV. Roads and streets in class I are designed as a facility, or as part of a future facility, with four or more lanes; the pavement is designed for greater than 3500 AADT. Class II includes roads and streets designed as a two-lane facility with structural design traffic between 2000 and 3500 AADT. Roads and streets with structural design traffic between 750 AADT and 2000 AADT belong to class III and the other roads and streets are classified as class IV. Vehicles are categorized into three levels: Passenger vehicles (PV), single-unit trucks (SU), and multiple-unit trucks (MU). Depending on the number of lanes in the facility and facility location, either rural or urban, percent of total vehicular class volume (P, S, and M for PV, SU, and MU, respectively) in a design lane is determined. In order to consider pavement damage by traffic, a constant to represent equivalent factor to 18-kip single-axle load is used. Since HMA overlay pavement design is based on rigid pavement design, the traffic factor is calculated as follows:

$$TF = DP \times \left[a_k \times P \times PV + b_k \times S \times SU + c_k \times M \times MU\right] \quad (6)$$

where, TF is traffic factor ;

DP is design period, usually 20 years for rigid pavements, but this study uses annual TF so DP becomes one year;

PV, SU, and MU are total number of passenger vehicles, single-unit trucks, and multiple-unit trucks, respectively; and

a, b, and c are constants for each vehicle category according to the road's class of k: for class I, $a_1 = 0.15$, $b_1 = 143.81$, and $c_1 = 696.42$; for class II, $a_2 = 0.15$, $b_2 = 135.78$, and $c_2 = 567.21$; for class III, $a_3 = 0.15$, $b_3 = 129.58$, and $c_3 = 562.47$; for class IV, $a_4 = 0.15$, $b_4 = 127.75$, and $c_4 = 555.90$.

Illinois spans across three climate zones: zone 1 (northern Illinois, Districts 1 and 2), zone 2 (central Illinois, Districts 3 to 7), and zone 3 (southern Illinois, Districts 8 and 9). The evaluation sections are distributed across Illinois as shown in Figure 2; based upon the aforementioned definitions, 5, 16, and 3 sections are located in climatic zones 1, 2, and 3, respectively. A representative low temperature, T_L, is introduced instead of relying upon these broad climate categorizations since the climate zones are too broad to characterize climate variation of each location, T_L is defined as the lowest monthly average temperature that is obtained based on monthly average temperature data since 1990 (The Illinois State Climatologist 2008).

A sensitivity analysis was performed to examine the correlation of PBRs to ESALs, T_L, and joint spacing (JS). Figure 18 shows correlation coefficients (CC) between PBR and the potential variables. The CC indicates a degree of linearity and direction of two random variables, ranging from -1.0 to +1.0. According to Cohen (1998), when the coefficient is above 0.5, the correlation is regarded as "high" generally. The CCs were obtained for each interlayer system to examine each potential variable. System B was not included in this analysis because it had only two data points. As shown in Figure 18, not surprisingly, ESALs and JS are negatively correlated with the PBR for each interlayer system. This suggests that the relative benefit of interlayer treated sections relative to the control section is diminished with increasing ESALs and/or joint spacing. As to the environmental variables, it shows a trend towards negative for System A (area) and positive for the other interlayer systems. The positive CC for T_L means that as the climate becomes more severe, less difference is observed between treated and untreated sections. Given that the data available is limited, more samples are needed for each interlayer system with respect to the ESALs and representative temperatures to conduct more robust statistical analysis.

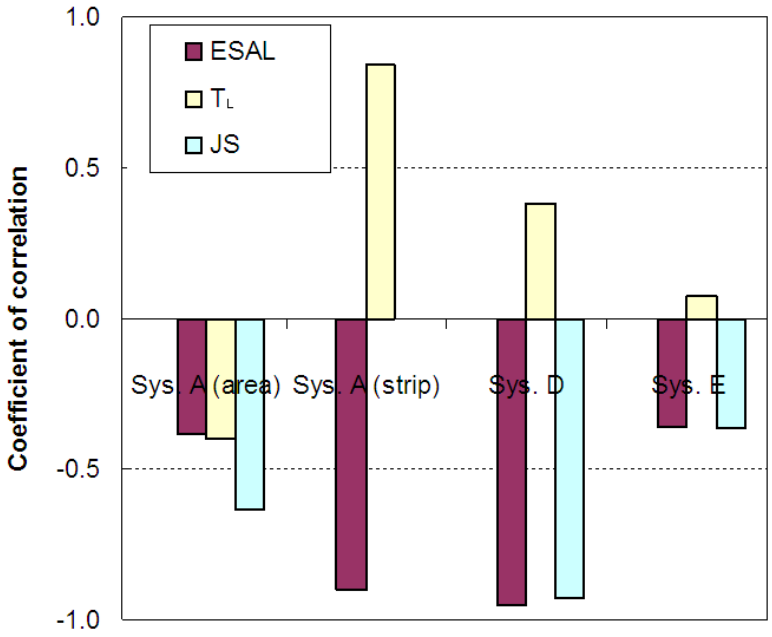

Figure 18. Correlation between performance benefit ratio and traffic and environmental variables.

4.3.2 Effect of ESALs on PBR

The effect of ESALs on the PBR is examined. The variations of PBR with respect to ESALs are shown in Figure 19. In general, the PBRs gradually decrease as the ESALs increase. This trend is more apparent in the strip-type interlayer systems. System D has the strongest correlation (R^2 of 0.908) and the greatest negative PBR change with respect to ESALs (PBR/ESALs of -4.85). On the other hand, its correlation is not strong for the area-type interlayer systems: R^2 of System A (area) and System E are 0.148 and 0.129, respectively. This implies that the performance benefit of System D is very sensitive to traffic volume compared to the other interlayer systems. For each interlayer system, the following results were obtained:

- For low volume roads (less than 0.2 million ESALs per year), System A (area) can provide a positive benefit (average PBR of 1.22); but at somewhat higher traffic volumes (over 0.3 million ESALs annually), it is expected that System A (area) is ineffective in retarding reflective cracking (PBR less than unity).
- For the strip-type System A, a strong correlation (R^2=0.815) between the PBR and ESALs was found. All PBRs were less than 1.0 regardless of traffic loading level. For example, PBR is 0.35 at a high traffic levels (0.3 million ESALs).
- For the strip-type System B, two PBRs of 0.93 and 1.02 were obtained at traffic levels of 53,000 and 308,000 ESALs, respectively.
- In general, for System D, the PBR (2.77 at Mattis Avenue) at the low level traffic volume (0.05 million ESALs annually) was 1.9 times greater than that (1.44 at IL 29 Creve Coeur) at high traffic volumes (0.3 million ESALs annually).
- For System E, IL4.75-mm “sand mix” and sand anti-fracture mixture (SAF), the same trend was observed after excluding one data point that was a very high outlier.

- Comparing the regression curves for interlayer systems with positive PBRs at the given traffic volume level, System D and System E showed superior performance relative to area-wide System A.

Coefficient and p-value of intercept and ESALs in the linear regression are listed in Table 6. The p-value is an indicator for possibility that the null hypothesis is true. When a p-value is equal to or smaller than a significant level such as 0.05, i.e., 5.0%, the null hypothesis is rejected. In other word, ESALs in this linear regression can be statistically significant at the level of 0.05 when its p-value is equal to or less than 0.05. Therefore, ESALs are only statistically significant for System D at the 5.0% level; therefore, the PBR for System D can be estimated as a function of annual ESALs per design lane. For the other systems, the PBR may not be a function of ESALs.

Table 6. Regression Analysis Results for PBR with ESALs

Interlayer system	Intercept		ESALs		R^2	# Data
	Coefficient	P-value	Coefficient	P-value		
System A (area)	1.37	**5.52E-05***	-1.21	0.307	0.148	9
System A (strip)	0.93	**0.013**	-1.95	0.097	0.815	4
System D	3.02	**0.004**	-4.85	**0.049**	0.908	4
System E	1.70	**0.017**	-1.66	0.553	0.129	5

* Bold indicates the p-value is less than 0.05.

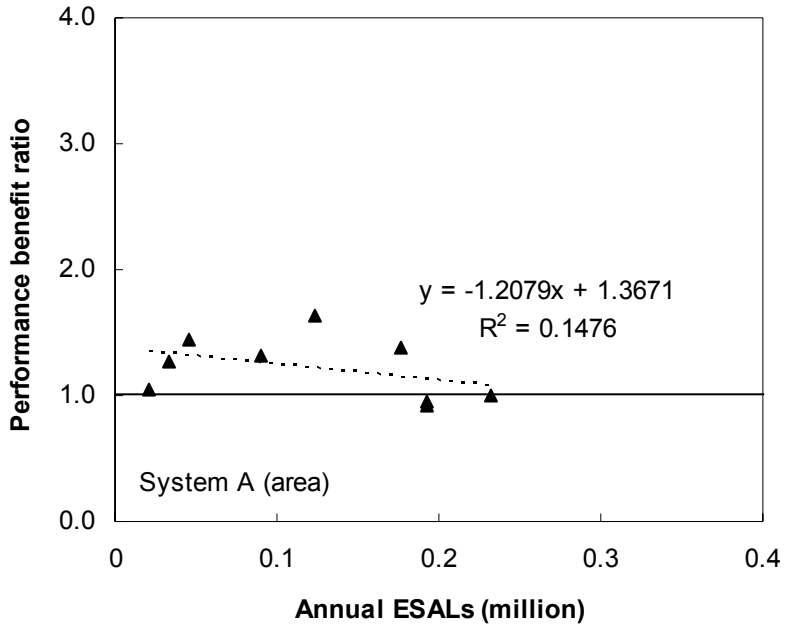

(a)

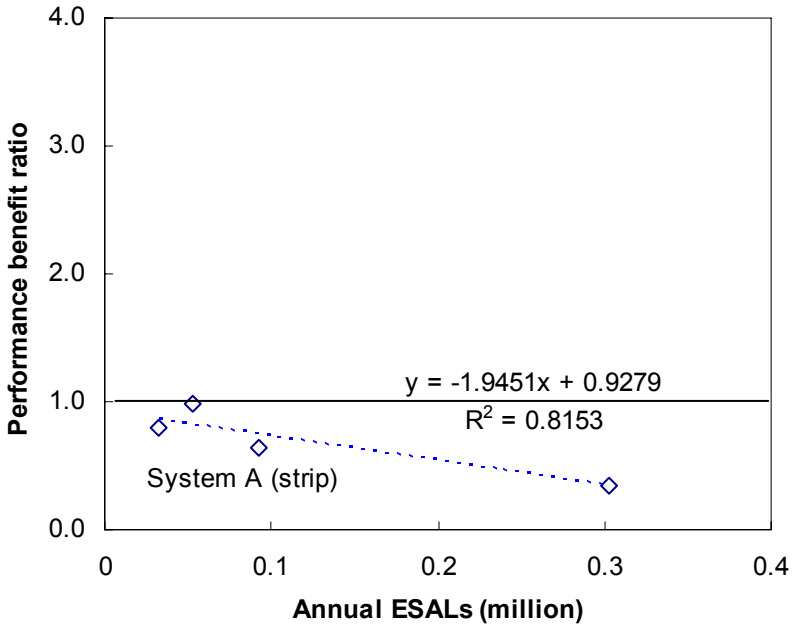

(b)

Figure 19. Performance benefit ratio variation with annual ESALs: (a) System A (area), (b) System A (strip), (c) System B, (d) System D, and (e) System E.

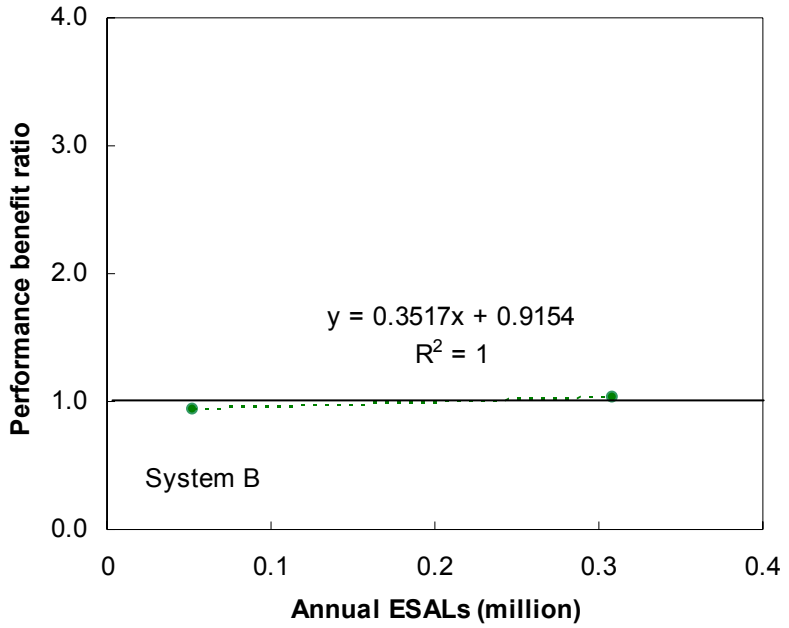

(c)

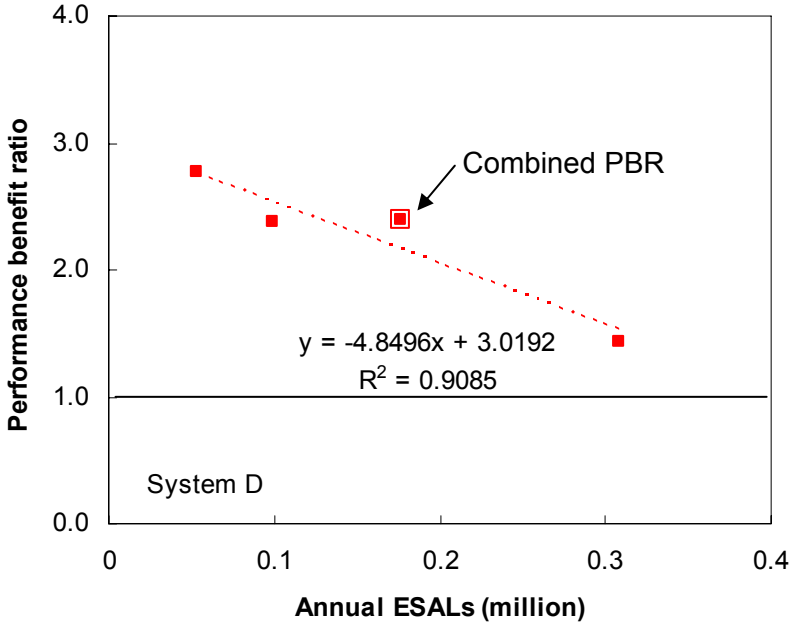

(d)

Figure 19 (continued). Performance benefit ratio variation with annual ESALs: (a) System A (area), (b) System A (strip), (c) System B, (d) System D, and (e) System E.

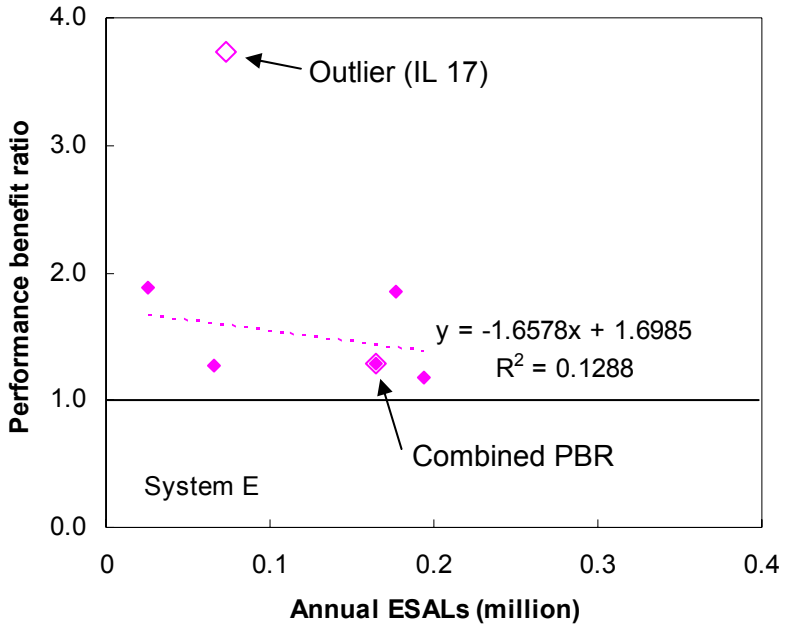

(e)

Figure 19 (continued). Performance benefit ratio variation with annual ESALs: (a) System A (area), (b) System A (strip), (c) System B, (d) System D, and (e) System E.

4.3.3 Effect of Temperature on PBR

Next, the performance benefit ratio was examined with respect to representative low temperature, T_L. A simple linear regression was used to characterize the relationship between PBR and T_L. As shown in Figure 20, the correlation was not as good as that for ESALs. However, the strip-type interlayer systems, System A (strip) and System D, showed relatively steep positive slopes, i.e., PBR decreases when strip-type interlayer systems were utilized in a cold region. This phenomenon can be explained as reflective cracking frequently initiated at the edge of a strip due to debonding and/or slippage between strip and surrounding layers. Severe temperature drops in winter can accelerate debonding and consequently induce edge reflective cracking. On the other hand, area-type interlayer systems showed less sensitivity to temperature changes.

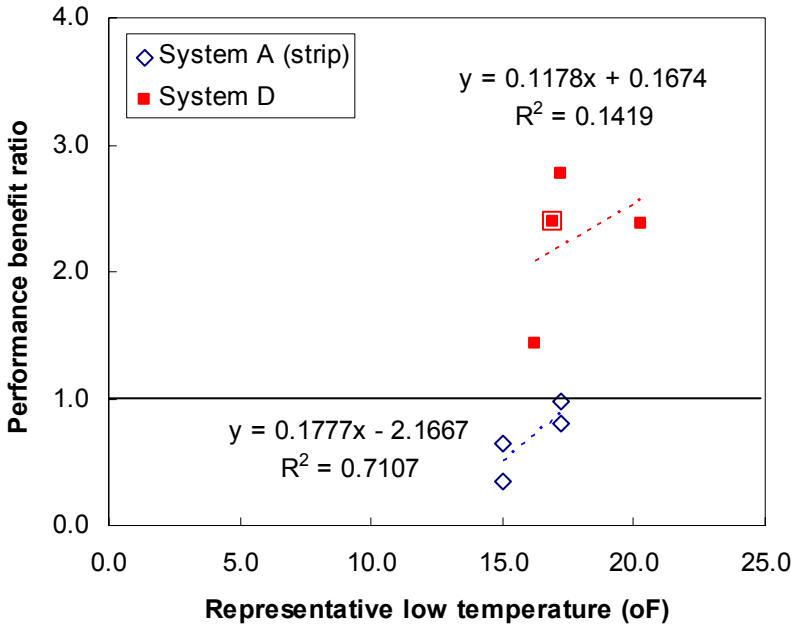

(a)

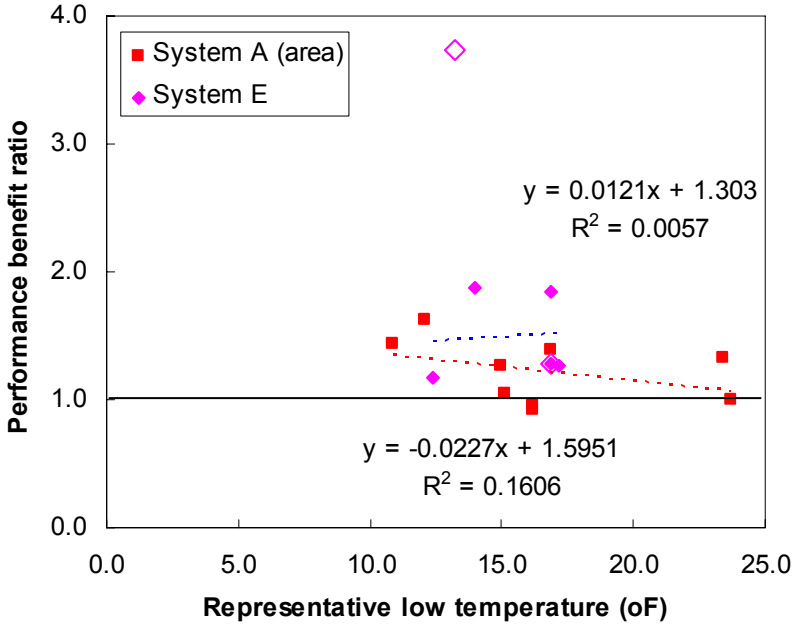

(b)

Figure 20. Performance benefit ratio variations with representative low temperature: (a) strip-type interlayer systems and (b) area-type interlayer systems.

4.3.4 Effect of Joint Spacing on PBR

Finally, the performance of the interlayer systems was investigated with respect to joint spacing. As shown in Figure 21, System D shows a strong correlation between PBR and JS (R^2 of 0.865). Another strip-type System A (strip) was excluded in this analysis because all sections had the same JS of 30 ft. Two area-wide interlayer systems of System A and System E have less sensitivity to JS than System D. Regardless of their sensitivity levels, interlayer system performance tends to decrease

with the increase of joint spacing as mentioned earlier. It may result from higher stress at the vicinity of the joint that can be induced due to thermal stress when underlying concrete pavements have a longer span. Consequently, interlayer systems may not work efficiently in severe conditions. For example, the IL 29 at Creve Coeur section has the lowest PBR of 1.44 among the System D sections. Its joint spacing is 50 ft while the others have JS of 30 ft. In addition, PBR of strip-type interlayer systems is based on R_{RCAW} which counts for only reflective cracking at joints/patches, but does not include transverse cracking in the middle of slabs. So, PBR of the strip-type interlayer systems is more sensitive to JS than that for the area-type interlayer systems.

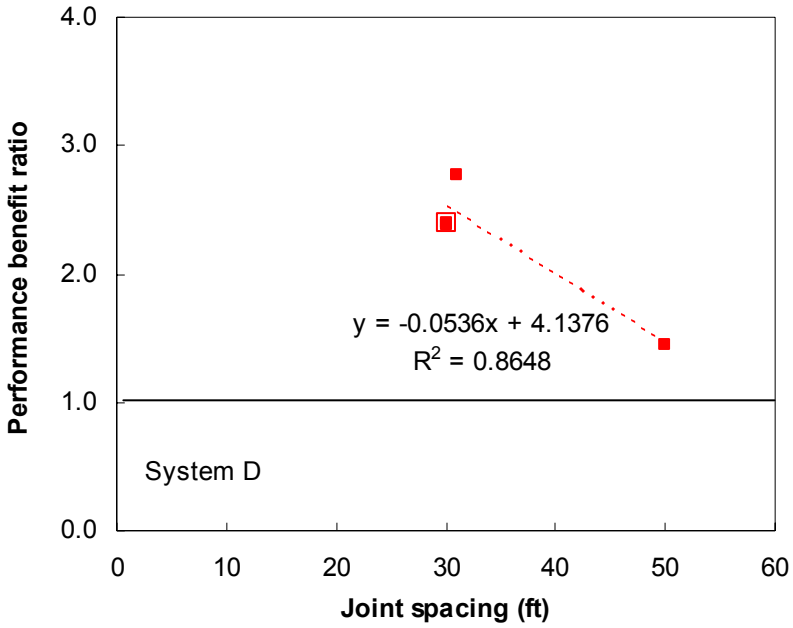

(a)

Figure 21. Performance benefit ratio variations with joint spacing: (a) System D and (b) the other interlayer systems.

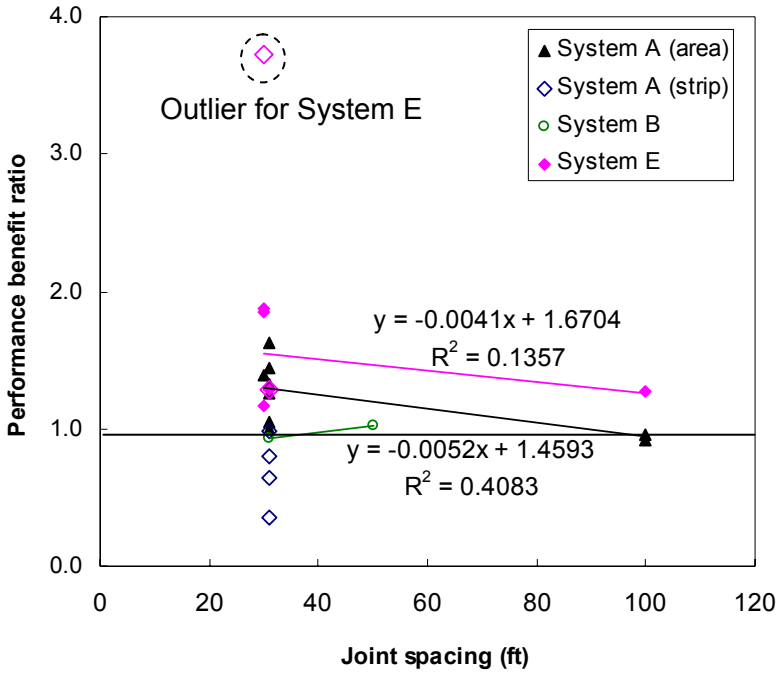

(b)

Figure 21 (continued). Performance benefit ratio variations with joint spacing: (a) System D and (b) the other interlayer systems.

4.3.5 Performance Benefit Ratio Prediction Model

As shown earlier, the PBR is dependent mainly on interlayer system type; the PBR is somewhat sensitive to ESALs and to a lesser degree to representative low temperature and joint spacing, depending on interlayer systems. Thus, the three variables are combined in a linear regression equation to estimate the PBR of each interlayer system. Table 7 shows an intercept and three coefficients for ESALs, T_L, and JS for each interlayer system. Among several combinations of ESALs, T_L, and JS, one combination with the highest R^2 was selected.

Table 7. Regression Analysis Results for Performance Benefit Ratio with ESALs, Representative Low Temperature, and Joint Spacing

Interlayer system	Intercept		ESALs (10^6)		T_L (^oF)		JS (ft)		R^2
	Coefficient	P-value	Coefficient	P-value	Coefficient	P-value	Coefficient	P-value	
Sys. A (area)	1.94	0.001	0.82	0.513	-0.0317	0.144	-0.0065	0.062	0.634
Sys. A (strip)	-0.51	0.812	-1.32	0.415	0.0847	0.548	-	-	0.894
Sys. D	5.29	0.000	-3.49	0.000	-0.0854	0.000	-0.0279	0.000	1.000
Sys. E	1.27	0.576	-3.36	0.487	0.0695	0.647	-0.0098	0.460	0.621

For System D, all p-values for ESALs, T_L, and JS are zero. Hence, it is appropriate to include the three variables into the regression as follows:

$$PBR_D = 5.29 - 3.49 \times 10^{-6} (ESALs) - 0.0854 (T_L) - 0.0279 (JS) \quad (8)$$

where, PBR_D is performance benefit ratio for System D;
ESALs are annual 18-kip equivalent single-axle loads in millions;
T_L is representative low temperature in ^oF; and
JS is joint spacing of existing concrete pavement in ft.

On the other hand, for the other interlayer systems, the p-values are greater than 0.05 for ESALs, T_L, and JS, which means the variables are insignificant in the linear regression. Thus, no variable needs to be considered for PBR prediction. While the R^2 of the regressions shown in Table 7 are statistically accurate, they can be possibly misleading due to the small population of data used. Thus, until more data are collected to develop a more reliable PBR prediction model, it is appropriate to use average PBR values listed in Table 5 to represent the PBR of each interlayer system as follows:

System A (area): average PBR = 1.22; standard deviation = 0.23;
System A (strip): average PBR = 0.69; standard deviation = 0.23;
System B: average PBR = 0.98; standard deviation = 0.04, and;
System E: average PBR = 1.49; standard deviation = 0.31.

The performance benefit ratios for the 25 interlayer systems were calculated using Equation 8 for System D and using the average values for the other interlayer systems. Figure 22 illustrates the comparison of obtained and estimated PBRs. With the exception of a single identified outlier, good agreement was obtained (R^2 of 0.844). This outlier is associated with System E and was also excluded in earlier regression analysis.

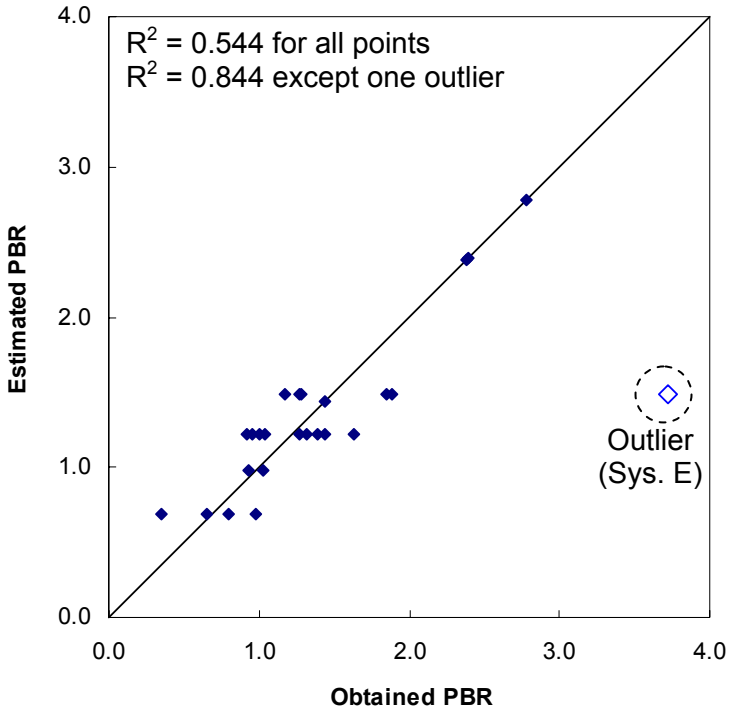

Figure 22. Comparisons of obtained and estimated PBR.

4.4 EVALUATION OF INTERLAYER SYSTEMS

4.4.1 The Performance Benefit Ratio Application in Illinois Districts

The State of Illinois has nine des for all systems except System D are insensitive to traffic volume, temperature, and joint spacing; System A (area), System A (strip), System B, and System E have similar PBR values. Figure 23 presents the average PBRs attained in field observations for each interlayer system. As shown in the figure, System A (area) and System E may achieve positive performance state wide while System A (strip) and System B may not be effective to control reflective cracking.

Table 8. Representative Low Temperature, T_L, of Illinois Districts

District	1	2	3	4	5	6	7	8	9
T_L (^oF)	11.6	12.6	15.0	15.3	17.2	16.9	19.5	22.0	23.4

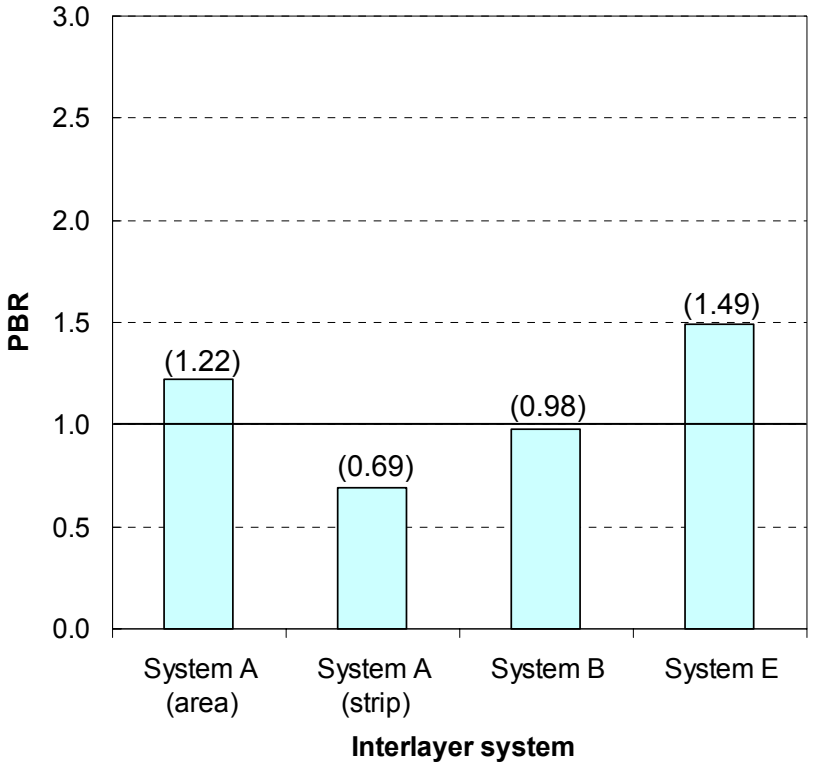

Figure 23. Average performance benefit ratio for System A (area), System A (strip), System B, and System E.

For System D, the PBR values were estimated from the Equation 8. Figure 24 demonstrates the PBR variations for System D with respect to traffic loading, districts, and joint spacing. If the PBR is above 1.0, System D is considered effective in controlling reflective cracking in that district. In most districts, System D shows positive performance. However, System D was ineffective for high-volume roads (greater than 0.3 million ESALs) in the southern districts, climate zone III when joint spacing is 50 ft.

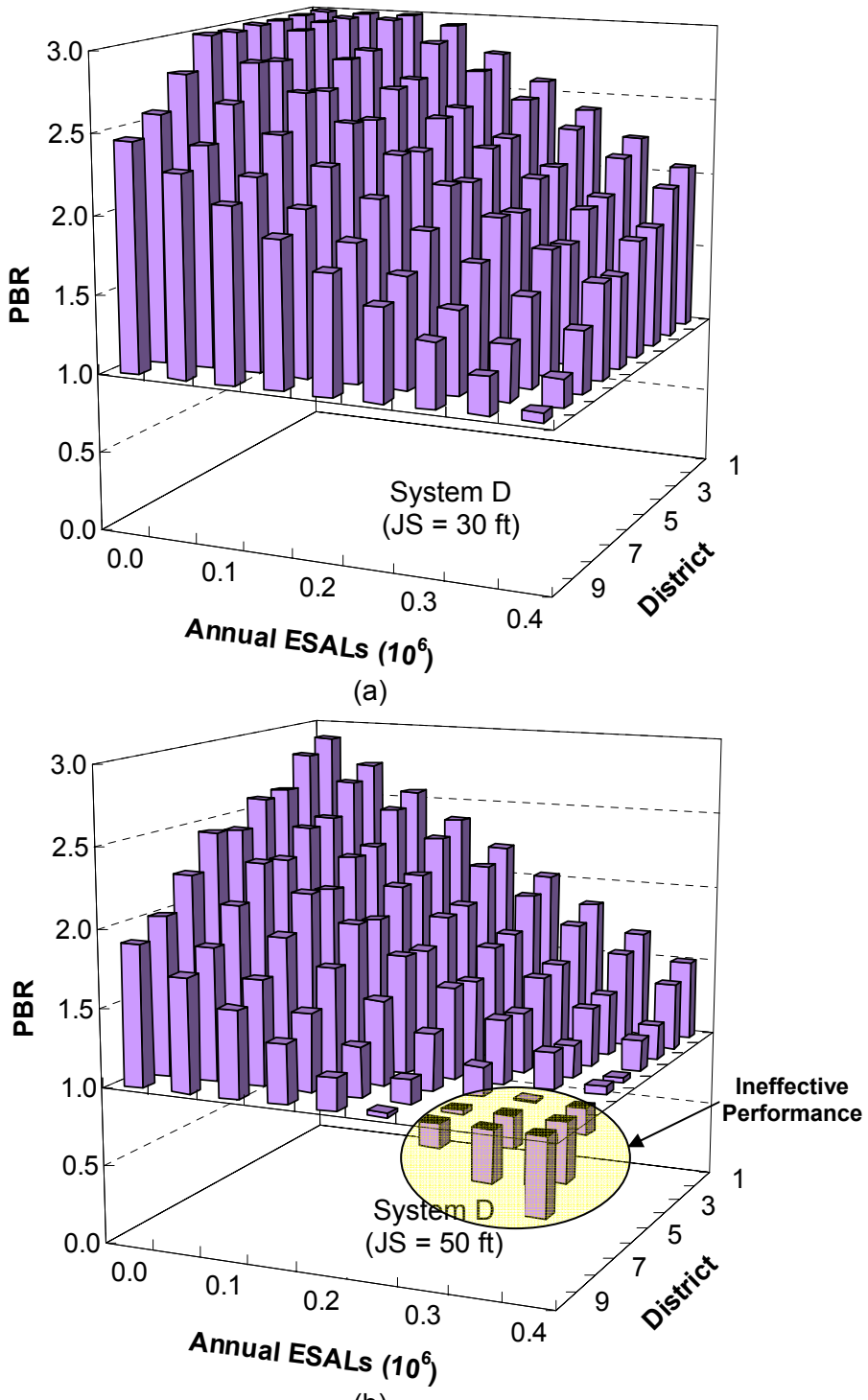

Figure 24. Performance benefit ratio versus ESALs and districts for various interlayer systems: (a) System D with JS of 30 ft, and (b) System D with JS of 50 ft.

4.4.2 Maximum Allowable ESALs

A variation of the performance benefit ratio of System A (area), System D, and System E is compared with respect to the ESALs. Figure 25 shows all data points of PBRs and fitted curves with ESALs; temperature variation and joint spacing were not

considered. It is clear that the PBR of System D decreases as ESALs increase. The PBRs of System E and System A (area) appear to decrease with an increase in ESALs from an engineering point of view even though the PBR was not shown to be a function of ESALs based on the results of the statistical analysis. The maximum allowable ESALs at PBR=1.0, was calculated using the fitted curves. As shown in Figure 25, the maximum allowable ESALs are approximately 0.4 million ESALs for System D and System E and 0.3 million ESALs for System A (area). The maximum allowable ESALs for System D with respect to climate condition and joint spacing can be determined using the PBR prediction model (Equation 8). For example, the maximum allowable ESALs becomes 0.26 million ESALs for District 9 with joint spacing of 50 ft instead of 0.4 million ESALs. Beyond these maximum allowable ESALs, it is not desirable to select an interlayer system which will result in a PBR of less than 1.0, as the system will perform worse than an untreated section while carrying a higher initial cost.

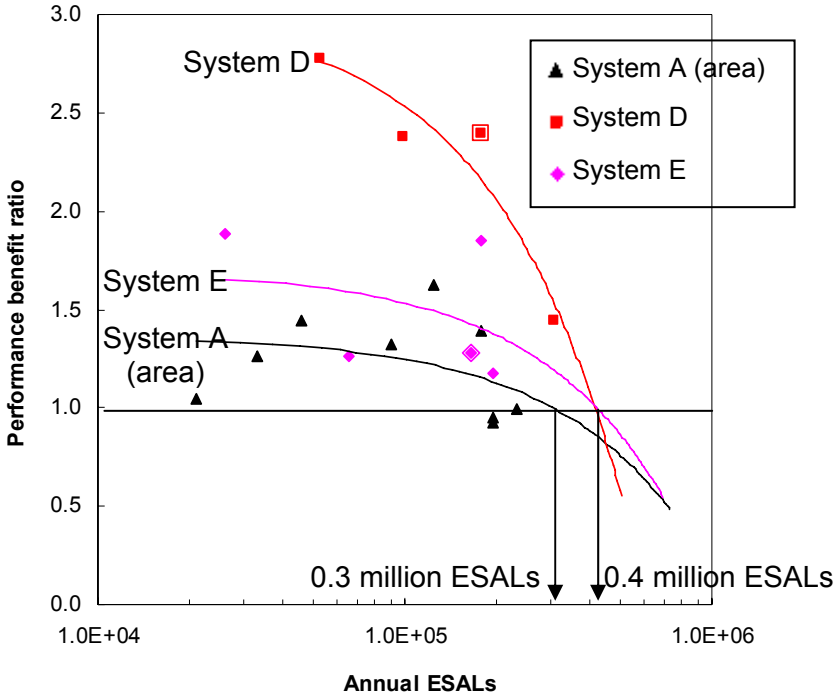

Figure 25. Performance benefit ratio variations over ESALs.

An interlayer system application map was constructed to aid the designer in the selection of the most effective interlayer system as a function of maximum allowable ESALs, location (Illinois district), and underlying PCC joint spacing. The application area is specified with upper and lower limits. Figure 26 illustrates the application limit of each interlayer system at joint spacings of 30 ft and 50 ft, respectively. The upper limits of System E and System A (area) are constant at 0.4 million ESALs and 0.3 million ESALs, respectively. For System D, the upper limit is dependent on district and joint spacing as shown in Equation 8. Under the upper limit, it is effective to apply interlayer systems to retard reflective cracking. The lower the ESALs are from the upper value, the more effective the interlayer is. On the other hand, the lower limit needs to be specified when two or more interlayer systems are compared. The lower limit of System E shown in Figure 26 (a) is determined when the PBR of System D is equal to 1.49 which is the average PBR of System E. So, System E is more efficient than System D in an area

above the lower limit of System E. Hence, in this case, the upper limit of System D at PBR_D of 1.0 is shifted to the lower limit of System E at $PBR_{D\&E}$ of 1.49. As a particular case for System A (area) shown in Figure 26 (d), its upper limit of 0.3 million ESALs is even lower than its lower limit. Thus, there is no applicable region for System A (area). Based on those four application maps shown in Figure 26, System D was found to be the most effective treatment over most ESALs and temperature ranges. Especially, in cold regions (Districts 1 and 2), System D was the most effective method regardless of traffic volume and joint spacing. However, the performance of System D is not as good as that of System E and/or System A (area) in warm regions with high traffic volume because System D performs less efficiently than the other systems whose performances are not affected by traffic and environmental conditions. So, System E was the best interlayer system in Districts 8 and 9 with higher traffic volume (150,000 annual ESALs). In other regions, the selection of an interlayer system depends on traffic volume and joint spacing.

To examine the applicability of the application map, two examples are presented. The first one is IL 267 at Greenfield, which is located in District 8 (climate zone 3), has a low traffic volume (0.1 million ESALs) and a joint spacing of 30 ft. The section was treated with System D. Based on the map for System D marked in Figure 26 (d) and the section traffic and climate conditions, it is expected to provide a significantly high performance benefit ratio. As given in Table 4, the PBR of System D is 2.38, which is the highest single PBR among similar interlayer systems. Another example is US 136 east at San Jose, District 6 (climate zone 2): 0.18 million ESALs, joint spacing of 30 ft, and interlayer systems A (area), D, and E were used. As marked in Figure 26 (c), it is in the middle of System D application area and also far from the lower limit of System E. Hence, the PBR of System D is expected to be much higher than 1.49 of PBR for System E. Also, the location is much lower than the two upper limits for System A (area) and System E. Thus, their PBRs may be slightly greater than the average PBR. The obtained PBRs are 2.40, 1.85, and 1.39 for System D, System E, System A (area), which agrees with the prediction. Therefore, this chart can be used to readily identify an appropriate interlayer system for a given region, expected traffic level, and joint spacing of existing concrete pavement.

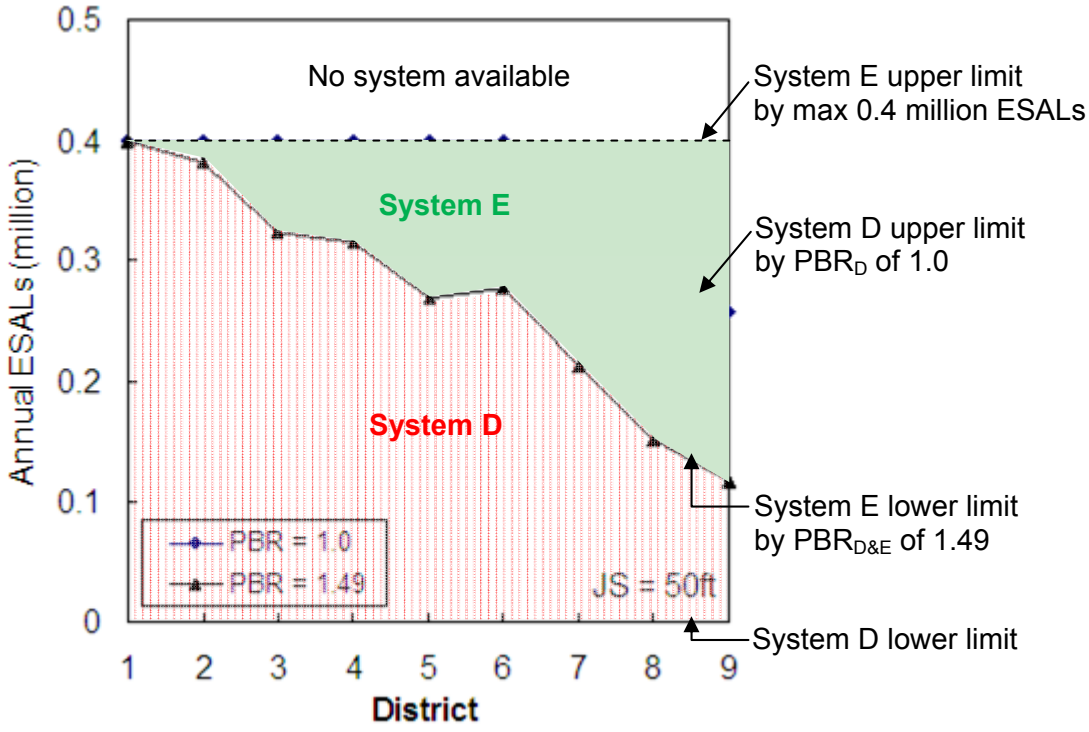

(a)

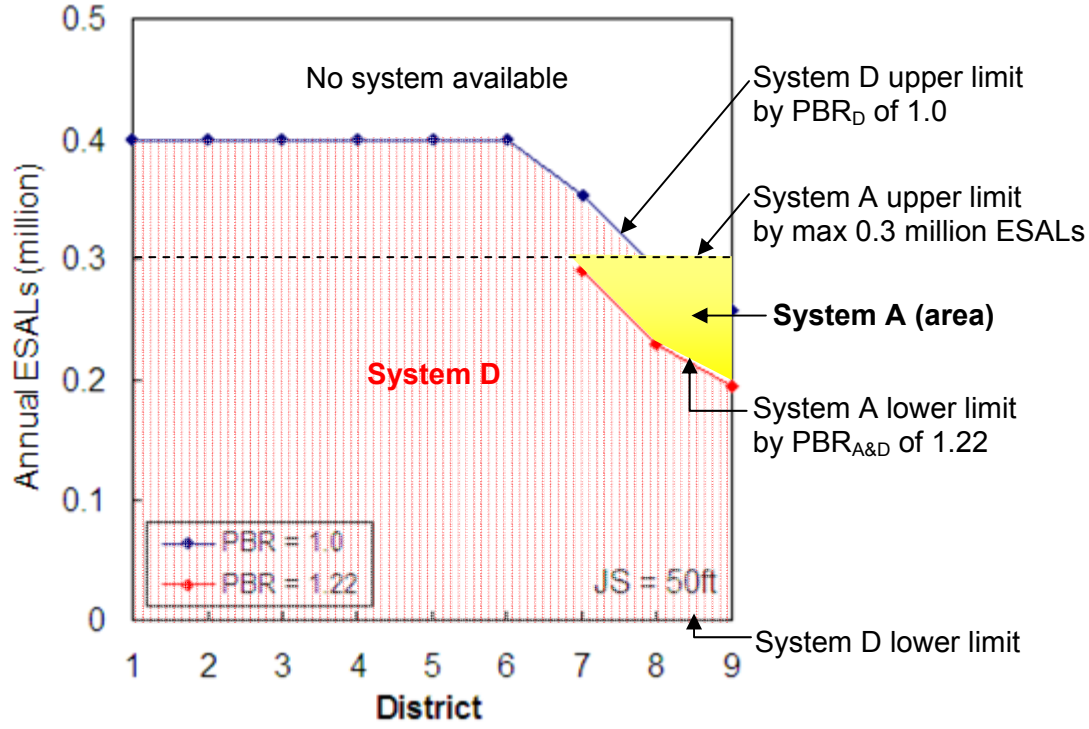

(b)

Figure 26. Interlayer system application map regarding ESALs and district: (a) for System D and System E at JS of 50 ft; (b) for System D and System A (area) at JS of 50 ft; (c) for System D and System E at JS of 50 ft; and (d) for System D and System A (area) at JS of 50 ft.

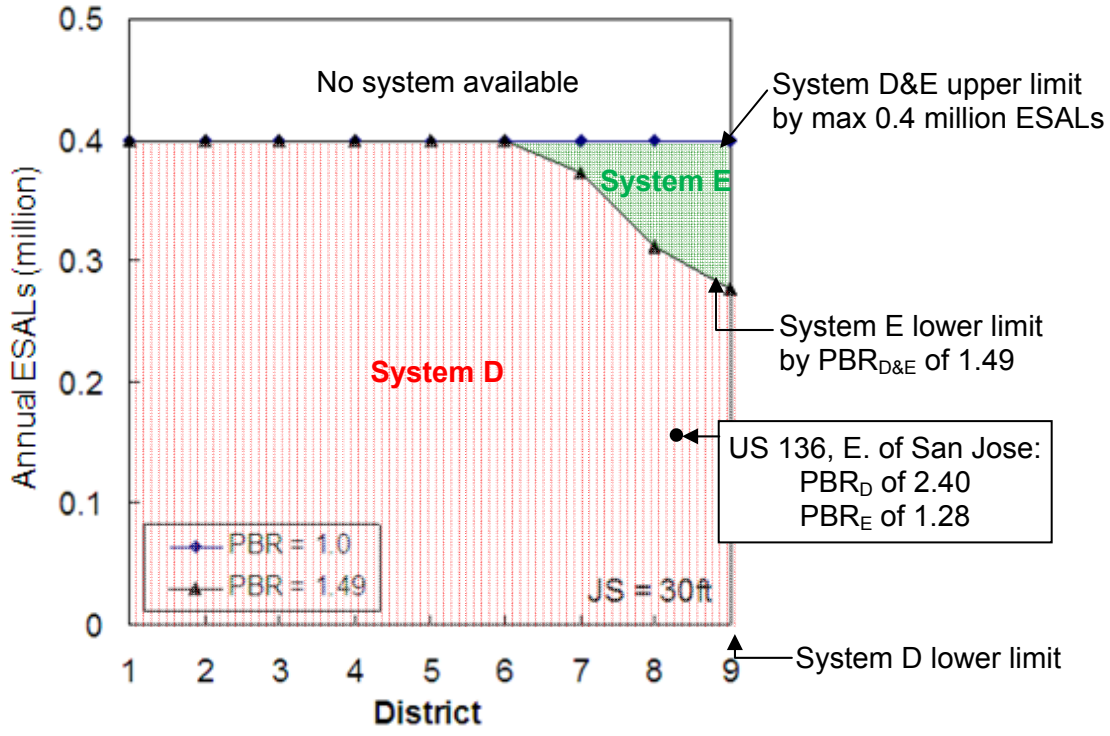

(c)

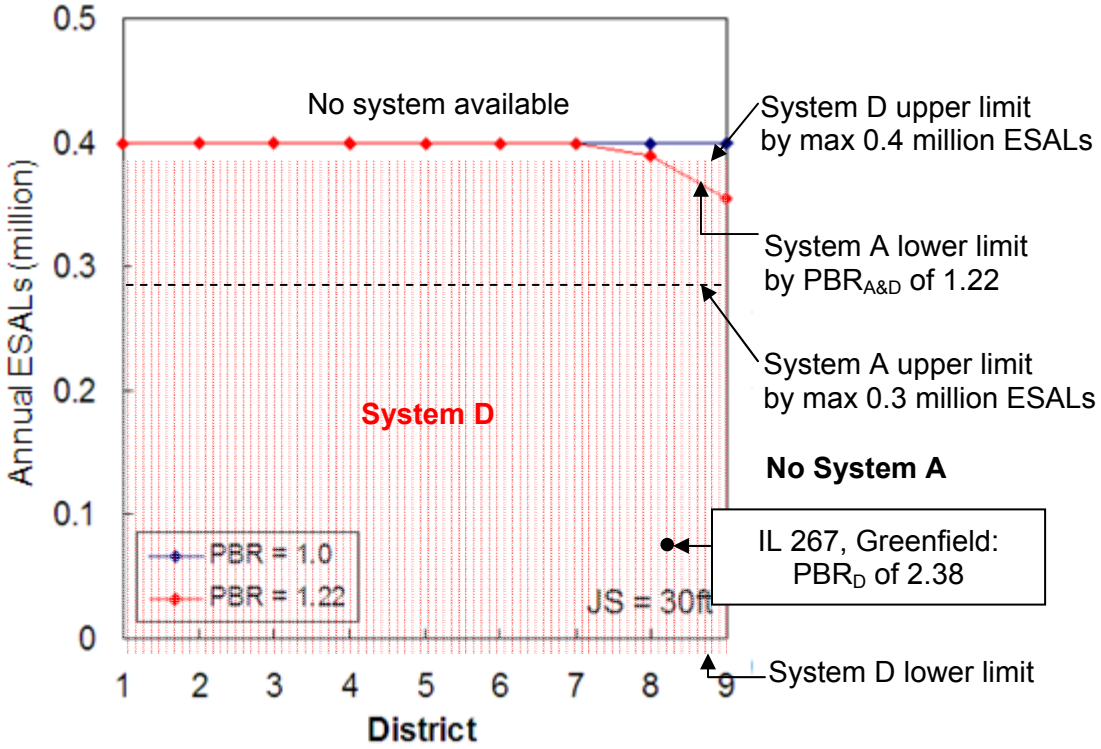

(d)

Figure 26 (continued). Interlayer system application map regarding ESALs and district: (a) for System D and System E at JS of 50 ft; (b) for System D and System A (area) at JS of 50 ft; (c) for System D and System E at JS of 30 ft; and (d) for System D and System A (area) at JS of 30 ft.

5. FORENSIC INVESTIGATION

Forensic investigations were conducted at five selected locations through field coring and laboratory tests. The main objectives of the coring were: 1) to observe and document the field conditions at selected projects and reflective cracking patterns in the overlay lift; 2) to identify the current condition of interlayer fabric installed in the overlay system and to examine bonding between layers, and; 3) to obtain field samples of overlay mixtures and interlayers for further laboratory testing. A series of laboratory tests were conducted on the samples obtained from field cores. The main objectives of the lab tests were: 1) characterizing the physical/mechanical properties of overlay mixtures and the mixture-type interlayers (System E); 2) evaluating the fracture properties of overlay mixtures and System E interlayers; 3) determining the overlay and PCC interface shear strength; 4) characterizing the permeability of cracked cores with intact interlayers; and 5) providing in-depth information for the further analyses of reflective cracking control systems.

5.1 FIELD CORING

5.1.1 Location

Five locations around central Illinois were selected for forensic investigation in 2006. After a series of site visits to several candidate sites, five locations were selected for detailed investigation, considering factors such as reflective crack control treatment used, overlay age, and reflective cracking severity. Details on the field coring and materials used are listed in Table 9.

Table 9. Selected Coring Projects

No.	Location	District	Completion Year	Interlayer System	Overlay Mixture
1	IL 29 Creve Coeur	4	1997	System B & D (Strip)	IL 12.5-mm NM D* AC20
2	IL 29 Mossville-Chilicothe	4	1998	System A (Area)	IL 9.5-mm NM D AC20, MAC-10
3	IL 130 Philo	5	2003	System E (IL 4.75 mm)	IL 9.5-mm NM D PG64-22
4	US 136 East of San Jose	6	1999	System A (Area) System D (Strip) System E (SAF)	IL 9.5-mm NM D AC20
5	Mattis Ave. Champaign	5	2000	System A, B, and D (Strip)	Unknown

*NM D: Nominal Maximum aggregate size, Dense graded

As summarized in Table 9, the rehabilitation treatments ranged in overlay age from three to nine years. Various types of reflective cracking control treatments, i.e., Systems A, B, D, and E were included. System E is a mixture-type interlayer system: IL

4.75-mm Superpave and sand anti-fracture (SAF) mixture, both of which use a highly modified binder in conjunction with a blend of manufactured and natural sand along with fines. Various binders have been used with the IL 4.75-mm mixture; but, a PG 76-28 SBS modified binder was utilized in the interlayer system at southbound IL 130. The overlay mixtures were found to have relatively similar aggregate structures, as most are designated as IL 9.5-mm nominal maximum (NM) D mixtures. However, the IL 29 Creve Coeur mixture was found to have a nominal maximum aggregate size (NMAS) of 12.5 mm. Although no specific information regarding Mattis Avenue mixtures was available, cores obtained from Mattis Ave. appear to have very similar aggregate composition to the other mixtures. In the IL 29 Mossville-Chillicothe and US 136 San Jose projects, 10% to15% of reclaimed asphalt pavement (RAP) was present.

5.1.2 Types of Cores

Figure 27 schematically illustrates three different types of field cores taken and their corresponding locations across the pavement lane. A set of 6-inch diameter bulk testing cores were taken between the wheel path to produce laboratory specimens for bulk material property testing (creep, fracture). Another set of 6-inch cores were taken over transverse cracks. These cores were expected to provide information on interlayer system condition, crack propagation pattern, condition of underlying structure, etc. Also, cores with intact interlayers were used for permeability testing. To assess the interface condition of interlayer/AC overlay and the existing PCC surface, a set of 4-inch cores were taken in crack-free areas as indicated in Figure 27. Precise coring locations were field selected to ensure that cores were taken over the interlayer fabric installed underneath. Interface shearing cores were full depth (HMA overlay/interlayer/PCC slab), while other cores were taken only down to the PCC layer.

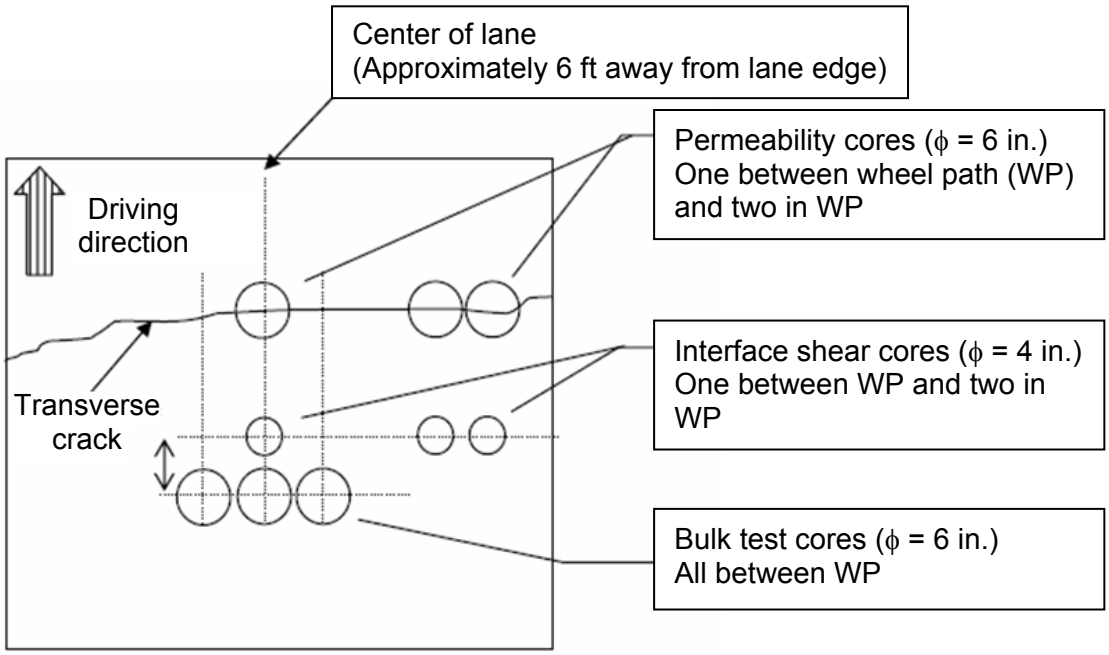

Figure 27. Types of cores and locations.

Table 10 summarizes the number and type of field cores obtained from each project and the number of samples produced from these cores. A total of 101 cores were taken from the five projects. Many of the 4-inch cores were not acceptable for the purpose of interface shearing testing due to their inability to stay intact during the coring

process. Five interface shearing (IS) cores from the IL 29 Mossville project were the only acceptable cores for the testing. Some of the 6-inch cores taken over the transverse cracks for permeability testing were also badly damaged during coring operations. A total of 14 permeability (P) cores from three locations were deemed acceptable and subsequently tested. A total of 32 bulk (B) property and 31 fracture (F) testing specimens were produced from 23 6-inch cores. This number includes six leveling binder course (LBC) mixtures and three SAF mixtures taken from the IL 130 and US 136 projects.

Table 10. Obtained Field Cores and Number of Lab Testing Samples Produced

Location	Field Cores		Lab Testing Samples			
	4-inch	6-inch	B*	F*	IS*	P*
IL 29 Creve Coeur	5	8	3	3	0	0
IL 29 Mossville-Chillicothe	6	10	6	5	5	3
IL 130 Urbana-Philo	12	11	7	7	0	0
US 136 San Jose	7	18	10	10	0	3
Mattis, Champaign	9	15	6	6	0	8
Total	39	62	32	31	5	14

* B: 6-inch bulk property testing sample F: 6-inch fracture testing sample IS: 4-inch interface shearing test sample P: 6-inch permeability testing sample

5.1.3 Findings

Findings from the forensic investigation of field cored projects are summarized below. A discussion of the forensic data collected is presented, which provides insight towards the causes of reflective cracking in each of project. More details are provided in Appendix B.

5.1.3.1 Position of Interlayers/ Interface Debonding

- IL 29 Creve Coeur

Three-foot wide, System B and System D strips were placed directly onto bare PCC, as a means to retard reflective cracking over transverse joints. All five 4-inch IS cores appeared to be debonded from the underlying PCC layer. This may be an indication of either poor bonding of the fabrics to the relatively smooth existing PCC surface; possibly an insufficient amount of tack coat; or excessive stress transmitted from a core barrel during coring. Figure 28 shows an example of debonded surfaces, where the PCC surface appears to be free of tack coat material and the interlayer fabric surface shows evidence of complete separation and free rotation during the coring operation.

Figure 28. Debonded surface of interlayer fabric (IL 29 Creve Coeur).

- IL 29 Mossville-Chillicothe

Area-wide System A fabric was placed in between 0.75 in. of LBC and 1.5 in. of HMA overlay lift, which was all placed over a lift of existing HMA overlay. The fabric layer appeared to be intact and showed no debonding even in the case of cracked permeability cores. Figure 29 shows a 4-inch IS core with full bonding between all layers.

Figure 29. Intact interface shear core from IL 29 Mossville.

- US 136 San Jose

System D strips and area-wide System A fabrics were reportedly placed on an existing HMA overlay surface and under 0.75 in. of conventional LBC. Cores taken on the System D verified locations of fabric strips as reported on plans. Moderate to severe moisture damage (stripping) was found in the HMA overlay materials; possibly resulting from combined effects of a moisture susceptible mixture placed adjacent to an impermeable fabric interlayer. When coring in locations thought to contain the System A reflective crack control treatment, i.e., just west of the System D in the westbound lane, the recovered cores did not show evidence of the interlayer fabric. In a follow up site visit by IDOT researchers, the presence of fabric was detected just west of the last coring site. Fabric was detected by examining the edge of pavement in areas where the overlay had become dislodged.

- Mattis Avenue, Urbana

Systems A, B, and D were placed directly onto an existing PCC pavement. Similar to the IL 29 Creve Coeur project, all of the 4-inch IS cores taken from the three interlayer systems were found to be debonded from the underlying PCC layer.

From this relatively limited number of observations, it could be recognized that fabric layers placed directly onto PCC surfaces may often become debonded during service life, while fabrics sandwiched between asphalt layers seemed to maintain better bonding throughout the life of the overlay. A hypothesized reflective cracking mechanism related to interlayer debonding is discussed in the following section.

5.1.3.2 Crack Patterns: Offset, Detour, and Jump

Through inspection of pavement cores, associated core holes, and pre-construction surveys, the presence and extent of reflective crack 'offset' could be observed. Typical crack offset distances from the existing, underlying joint or crack location ranged from almost zero to over one foot, depending on a number of factors, such as: type of treatment, aggregate composition, vertical position of reflective cracking control treatment, thickness of overlay lift(s), loading conditions, etc. Table 11 presents pictures of selected cores and core holes, showing crack patterns and approximate crack offset distances. Reflective cracks observed in IL 29 Mossville, US 136 San Jose (WB), and Mattis Ave. were found to have 'jumped over' the interlayers (the majority of interlayer lifts were found to be intact).

On the other hand, cracks in US 136 San Jose (EB) and IL 130 Philo, where SAF and IL 4.75-mm sand mix were used, were found to have propagated through the interlayer lifts. Unlike the majority of cores, which show a finite extent of crack offset, cores taken from the IL 29 Creve Coeur project were found to have more than 18 in of crack offset away from the existing joint. In other words, the reflective cracks were found through coring to be located at the edge of fabric strips. This was clearly evidenced by the fact that fabric was only present on one side of the core sample and because the joint was not visible when inspecting the bottom of the core hole. This phenomenon is hereafter referred to as 'reflective crack detouring,' and a hypothesized mechanism of this type of reflective crack is illustrated in Figure 30. It should also be noted that cores revealed a nominally triangular shaped void along the edge of the fabric treatments at IL 29 Creve Coeur, possibly due to asphalt mixture segregation caused by a sudden elevation change and sharp geometrical discontinuity, resulting in low density in the asphalt mixture in this location. This could also explain why cracks were found to have reflected from the edge of these strip treatments. Thus, in summary, the reflective cracking that appears on the edges of strip treated fabrics can be explained as a result of fabric debonding or poor compaction, or both.

Table 11. Selected Pictures of Cores over Reflective Cracks

Location	P-core 1	P-core 2	P-core 3	Offset Extent
IL 29 Creve Coeur (Sys. B)				< 18”
IL 29 Mossville (Sys. A)			---	< 1”
US 136 San Jose (Sys. A, D, and E)				< 2”
Mattis (Sys. D)				< 2”
Mattis (Sys. B)				< 2”
Mattis (Sys. A)			---	< 1”
IL 130 Philo (Sys. E)				< 2”

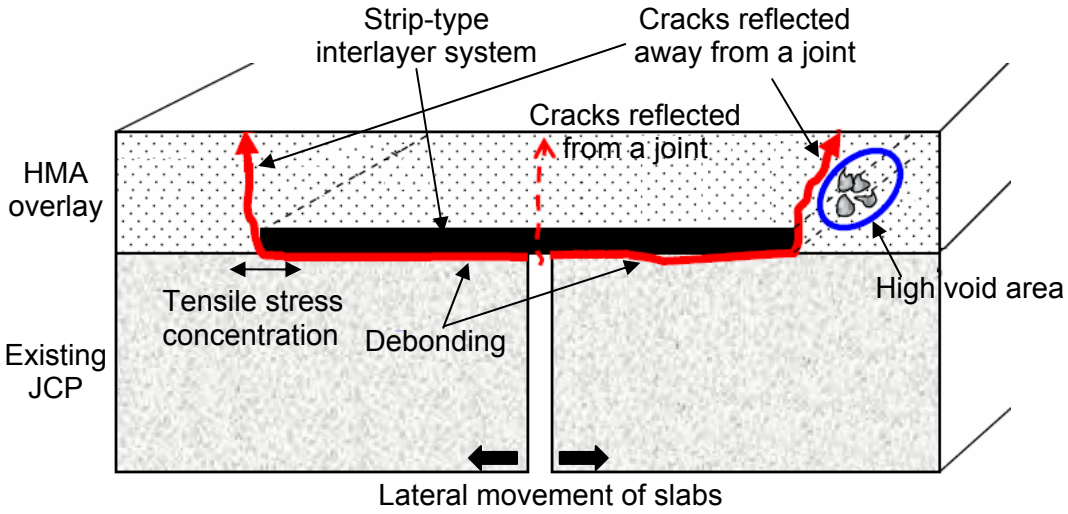

Figure 30. Reflective crack detouring mechanism.

5.2 LABORATORY TEST

Figure 31 schematically summarizes the general material properties or other quantities which were sought through laboratory characterization of core samples. The stiffness of an HMA pavement is logically related to the formation of cracks, i.e., stiffer materials generally tends to be more brittle. Another more direct index of reflective cracking resistance is the fracture energy of HMA or interlayer materials, which is the energy required to completely separate (fracture) the material per unit area of crack surface (Wagoner 2006). The interface bond strength is also a critically important component to the reflective crack control system, as demonstrated in previous sections. Waterproofing of existing PCC joints or cracks by an impermeable fabric interlayer system even after reflective cracks appear is also a quantity of interest. A laboratory testing suite, which involves five distinct test methods, was developed and conducted to gather this information from field cored samples.

The five laboratory tests were conducted on field-cored samples from the five aforementioned coring projects. Three tests are utilized for HMA (overlays and/or mixture-type interlayers): Indirect tension (IDT) creep compliance/stiffness, indirect tension complex modulus (E*) of asphalt concrete materials, and fracture energy by disc-shaped compact tension (DC[T]). The other tests are employed to characterize an interaction between HMA overlay and surrounding layers such as PCC and interlayer systems: water permeability of interlayer fabric and torsional interface shear strength of PCC and bituminous material. Table 12 summarizes the five test setups.

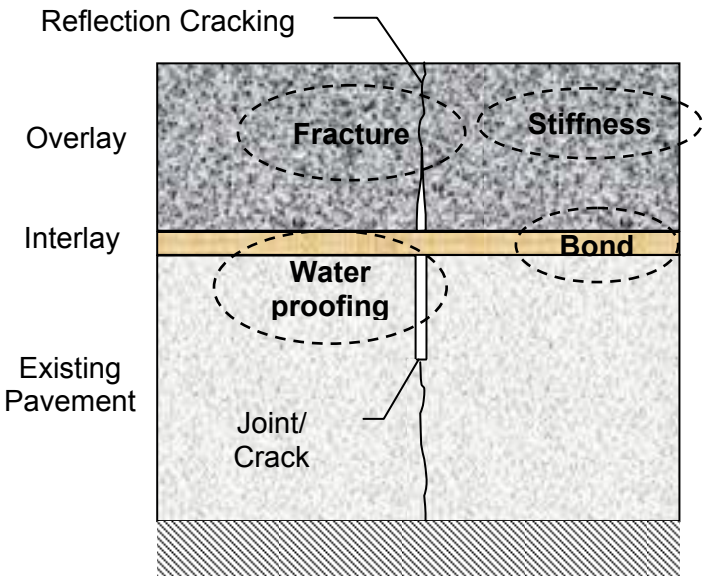

Figure 31. Information sought through laboratory testing.

Table 12. Laboratory Testing Suite Overview

Tests	Temp. (°F)	Time or Frequency	Excitation	Measure-ment	Resulting Value
IDT - Creep	-4/14/ 32	100 s	Constant load	Creep strain	D(t)/S(t)
IDT - E*	-4/14/ 32	10, 1, 0.1, 0.01 Hz	Sinusoidal load	Sinusoidal strain	E*
DC(T) Fracture	14	50 ~ 150 s	Constant CMOD	Load	G_f
Permeability	59 ~ 66	Varying	Gravity	Time of falling water head	k
Interface Shearing	14	N/A	Torque	Max torque	τ

From the cored samples from five projects, 11 different types of HMA materials were identified and coded as shown in Table 13 which summarizes the composition and age of the mixtures based on the available mix design information provided by IDOT. According to the information, these mixtures can be roughly categorized into three different groups, i.e. IL 12.5-mm, IL 9.5-mm, and IL 4.75-mm NMAS. Since the same wearing surfaces were used in eastbound and westbound, samples from US 136ES and US 136WS were deemed to be identical, and therefore lumped together and renamed as US 136EW, reducing total number of mixtures into ten. The two IL 4.75-mm mixtures, i.e. IL 130SI and US 136EI, are basically used as LBC mixtures, but they were tested to assess potential benefits as reflective crack relief interlayers. Approximately 10% to 15% of RAP material was used in the IL 29 Mossville-Chillicothe section and the US 136 San Jose section. Other mixture and binder properties are also provided in Table 13.

Table 13. Description of the 11 Mixtures Tested

Material Code	Description	NMA Size	% Natural Sand	% RAP	AC Grade	% AC	Mix Age (Yr)
IL 29CC	IL 29 Creve Coeur Conventional surface mixture	12.5 mm	11.0	0.0	AC20	4.7	9
IL 29MO	IL 29 Mossville Polymer modified surface mixture	9.5 mm	26.5	15.0	MAC10	5.6	8
IL 29CH	IL 29 Chilicothe Conventional surface mixture	9.5 mm	31.0	15.0	AC20	5.6	8
IL 130SN	IL 130 Philo southbound Conventional surface mixture	9.5 mm	23.0	0.0	PG64-22	5.6	3
IL 130SI	IL 130 Philo southbound System E (IL4.75mm)	4.75 mm	18.1	0.0	PG76-28	8.6	3
IL 130NI	IL 130 Philo northbound Conventional leveling binder (IL9.5mm)	9.5 mm	-	-	-	-	3
US 136EW	US 136 San Jose eastbound Conventional surface mix	9.5 mm	23.0	10.0	AC20	5.4	7
US 136EI	US 136 San Jose eastbound System E (SAF)	4.75 mm	34.0	0.0	-	8.5	8
US 136WI	US 136 San Jose westbound Conventional leveling binder (IL9.5mm)	9.5 mm	-	-	-	-	8
MatBD	Mattis Ave. Champaign Conventional surface mix	9.5 mm	-	-	-	-	6

5.2.1 Creep Compliance and Dynamic Modulus Test

AASHTO T322 was referenced for the IDT creep testing. The E* testing was conducted in the IDT setup to utilize field core samples whose thickness varies between 1.0 in and 2.0 in.

5.2.2 Fracture Test: Disk-Shaped Compact Tension

ASTM D7313-07 or the 'DC(T)' was to obtain the fracture energy (G_f [J/m^2]) of overlay materials and thicker interlayer treatments, such as the IL 4.75-mm mixture and SAF (Wagoner 2006), as shown in Figure 32. In this test, fracture energy is calculated as a function of the area under the load versus crack mouth opening displacement (CMOD) curve (and divided by fracture area), as shown in Figure 33.

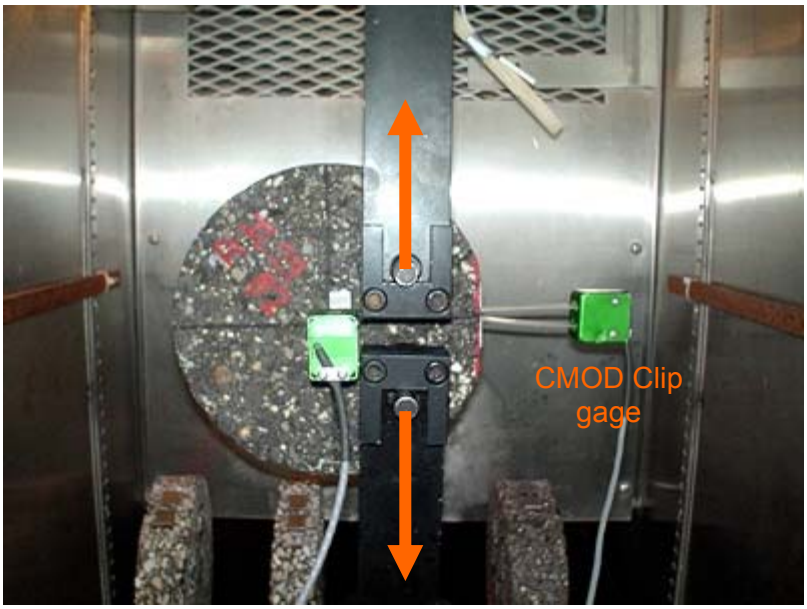

Figure 32. DC(T) fixture with specimen in test position.

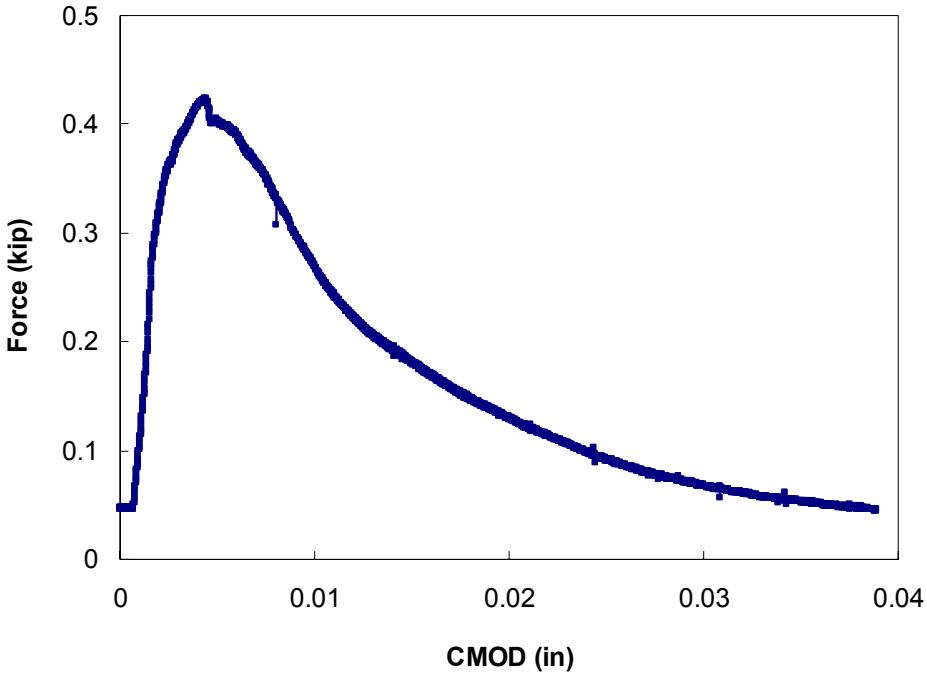

Figure 33. An example plot of load-CMOD curve from DC(T) testing

5.2.3 Interface Bond Test

To determine bond (shear) strength at the interface between an interlayer and adjacent layers, a laboratory torque bond test was conducted with field cores although it is also directly applicable in the field. The test apparatus and procedures were followed in accordance with an UK guideline (Wheat 2007) as shown in Figure 34. A 4-in.-diameter field core is trimmed such that the interface is located 0.8 ± 0.4 in. above the mounting rim. In the original test procedure, a target temperature of 68 ^{O}F is used. However, for the purposes of the reflective cracking study at low temperature, a target temperature was 14 ^{O}F which is the same temperature of the fracture test. A torque is applied and the maximum torque is recorded and used in the calculation of bond strength.

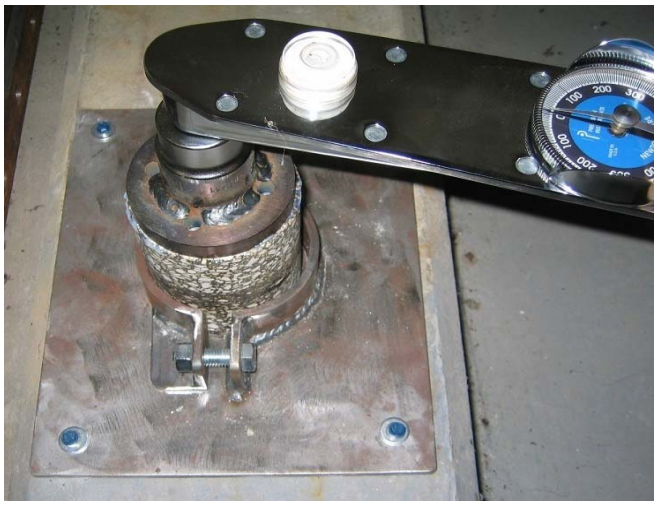

Figure 34. Torque bond test apparatus.

5.2.4 Permeability Test

A falling head permeameter was used to measure the permeability constant (k) in accordance to the ASTM PS 129-01. A difference in the testing protocol used was the thickness of the specimen, as the main objective of this testing was to determine the permeability of the fabric interlayers after a number of years of service in the field, as opposed to the permeability of the overlay mixture itself. Samples with varying thickness were tested. Crack sealant above the fabric interlayers was removed prior to testing, if present. However, any sealant present under the fabric (originally applied to the existing PCC joints or cracks) could not be completely removed and was therefore left intact when present.

5.3 LABORATORY TEST RESULTS

5.3.1 Creep Stiffness and Dynamic Modulus

In the interest of brevity, a selection of typical test results is now presented. Detailed results of tests conducted from pavement cores obtained in this study can be found in Appendix B. Figure 35 and Figure 36 allow a relative comparison of the stiffness of the overlay and interlayer materials tested in this study. As expected, large differences exist between traditional surface overlay materials and specially designed interlayers, as the latter contain higher asphalt content, a softer, polymerized binder, and a finer aggregate gradation. For example, SAF used in US 136 eastbound at San Jose has the lowest stiffness as well as softest dynamic modulus in most time domains.

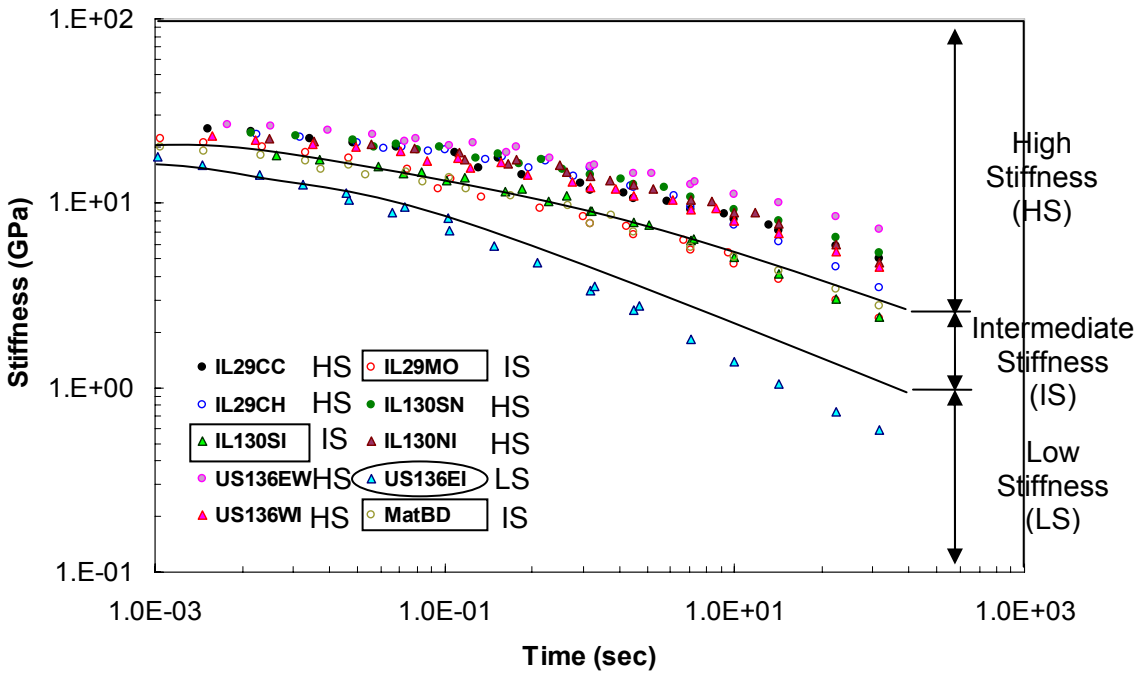

Figure 35. Measured creep stiffness grouped in three stiffness categories.

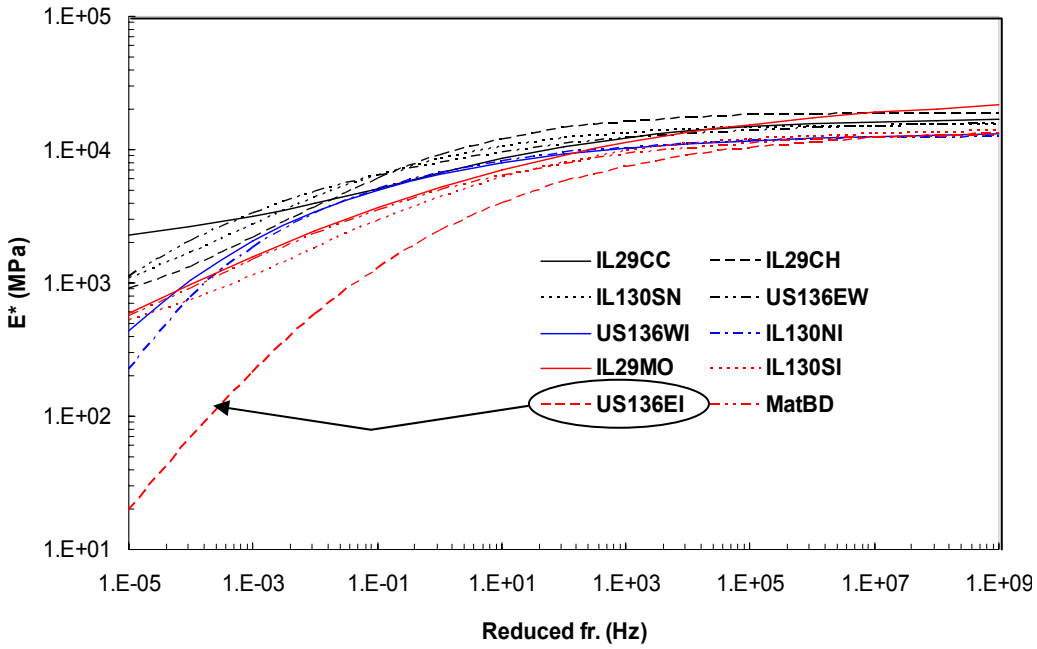

Figure 36. Sigmoid E* master curves of all mixtures.

Table 14 summarizes the calculated fracture energy at 14 ^{O}F, normalized peak load, and the number of replicates tested, ranked in the order of descending fracture energy (high fracture energy indicates more crack resistance). As observed from the creep and E* test result, US 136EI (SAF) exhibits the highest fracture energy, while the IL 130NI ranked as the lowest. The normalized peak load tracked relatively well with fracture energy, as shown in Figure 37.

Table 14. Measured Fracture Energy (G_f) and Normalized Peak Load

Material code	Fracture energy G_f (J/m^2)		Normalized Peak Load (kN/m)	Replicates
US 136EI	1,884		59.7	3
IL 130SI	594		65.3	3
IL 29CH	387		61.4	3
MatBD	385		54.3	6
IL 29MO	304	Moderately brittle	51.0	2
IL 130SN	292		56.8	3
US 136WI	282		46.1	2
IL 29CC	275		47.8	3
US 136EW	257		51.3	5
IL 130NI	151	Extremely brittle	36.9	1

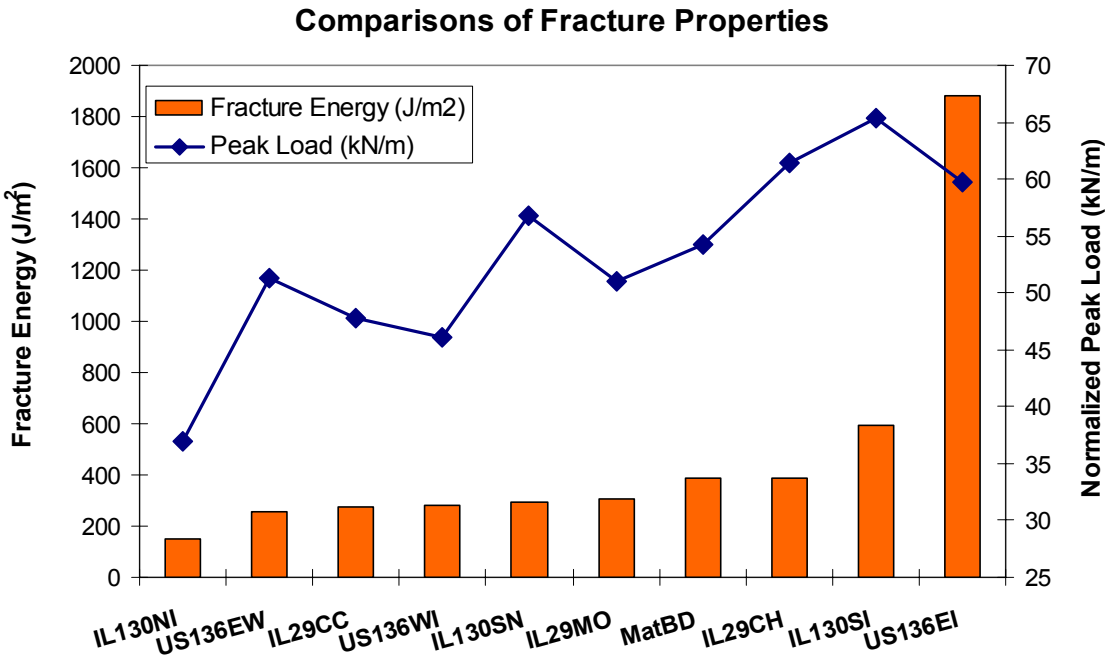

Figure 37. Measured fracture energy and normalized peak load.

5.3.2 Performance Ranking of Overlay and Interlayer Mixtures

Table 15 provides an overall ranking of the ten HMA overlays and interlayer mixtures tested based upon the bulk material properties measured at 32 ^{O}F. Also, the rough stiffness category discussed earlier and a ranking by fracture energy, as discussed, are presented for a comparison to the simplified ranking system results. In general, lower stiffness, lower phase angle, and higher fracture energy resulted in a lower (better) ranking. Individual and average rankings considering both bulk and fracture properties are provided in the center of the table. The left-hand side of the table provides an overall composite ranking, where projects with identical average ranking scores were given an identical overall ranking order. Interestingly, the overall ranking provided by the bulk material tests were in direct agreement with the ranking of mixtures via the DC(T) fracture tests. This indicates that the stiffer mixtures were also found to be the most brittle mixtures in this study. This also indicates that the DC(T) fracture test, which is much simpler to perform than the IDT creep or E* test, may be a useful test for material design specifications, quality control or assurance testing, and/or for forensic evaluation of asphalt overlay mixtures and interlayers used where reflective cracking is of concern.

In terms of the magnitude of DC(T) fracture energies, experience has shown (Wagoner et al. 2006) that values below a threshold of about 400 J/m^2 can be considered to be marginally brittle, while values below 200 J/m^2 can be considered to be extremely brittle. As shown in Figure 37, the overlay mixtures found on most of the projects evaluated in this study were in the very brittle to marginally brittle range. It is hypothesized that better overlay performance (slower cracking rate, less crack severity) would be obtained by using overlay mixtures with increased fracture energy. This can typically be achieved by using polymer modified binder, higher effective asphalt content, use of RAP with softer base binder, and/or stronger aggregates, although it is acknowledged that significant changes in aggregate selection may be practically limited.

Table 15. Comparison of Ranking for Overall Bulk and Fracture Material Property.

Mixture type	Overall Ranking	Material Code	Individual Ranking			Average Ranking	Fracture
			S(t)	E*	δ		
System E	1	US 136EI	1	1	1	1.0	1
	3	IL 130SI	3	4	5	4.0	2
leveling binder	5	US 136WI	6	5	4	5.0	7
	7	IL 130NI	8	7	8	7.7	10
Wearing surface	2	IL 29MO	2	3	3	2.7	5
	4	MatBD	4	2	7	4.3	4
	5	IL 29CH	5	8	2	5.0	3
	7	IL 29CC	7	6	10	7.7	8
	9	IL 130SN	9	10	6	8.3	6
	10	US 136EW	10	9	9	9.3	9

5.3.3 Interface Bond (Shear) Strength

From the five project locations, 45 field cores were taken for the bond strength test. A variety of interface failures occurred in approximately half of the cores. Interface failure ratio is listed in Table 16 regarding interlayer type and failure location. Among the failure types, the major interface failure occurs when interlayer is placed between HMA overlay and PCC surface: 94% (16/17) failure for fabric interlayer and 100% (4/4) failure for mixture type interlayer. Those failure percentages are three times higher than interface failure (33%) between HMA overlay and bare PCC layer. The least interface failure (8%) is observed when fabric interlayer is located between HMA overlays. Based on the limited number of coring results, it is not possible to acknowledge the reason and moment the interfaces are broken. Nonetheless, the coring results suggest that a weaker interface bonding condition exists when interlayer systems are placed directly on the PCC pavement surface and that relatively better interface conditions can be achieved when interlayer systems are installed between HMA layers.

To evaluate the interface bonding condition more quantitatively, the torque bond strength test was performed with available field cores. Since most of interface field cores were broken, only 21 specimens were tested at various temperatures. While the target temperature of the test was 14 ^{O}F, actual test temperatures varied from 12 ^{O}F to 86 ^{O}F because no environmental chamber was used. Bond strength at an interface as described by the maximum torque achieved in a failure test is calculated as follows:

$$\tau = \frac{12M \times 10^6}{\pi D^3} \times 145.1 \qquad (9)$$

Where, τ is the inter-layer bond strength (ksi);
M is the maximum applied torque (lbs-ft); and
D is the specimen diameter (in.).

Table 16. Interface failure ratio and types.

Interlayer type		Interface type		
		HMA / PCC	HMA/ Interlayer / PCC	Between HMA overlays
Fabric	Sys. A	1/3	6/6	0.5*/6
	Sys. B	-	3.5/4	-
	Sys. D	-	6.5*/7	-
	Sub (%)	33	94	8
Mix.	IL-4.75	-	3/3	0/6
	IL-9.5	1/3	-	2/6
	SAF	-	1/1	0/1
	Sub (%)	33	100	15

* 0.5 means partially broken interface

Table 17 shows the interface bond strength obtained for different interlayer types, substrates, and temperatures. As a reference, the bond strength at the interface between the HMA overlay and PCC (without interlayer) for samples taken from IL29 at Mossville is 102 psi at 12 ^{O}F. When ISAC is installed on top of PCC pavement, the bond strength is 89 psi at 18 ^{O}F. Due to maximum torque of 369 lbs-ft, the upper limit of the bond strength which can be measured is 261 psi. For the mixture type of interlayer including conventional levelling binder, the bond strength is calculated as the maximum of 261 psi since the interface was not broken until the maximum torque was applied at 14 ^{O}F. Thus, it is not possible to differentiate the interface strength at 14 ^{O}F for the mixture-type interlayers using this test. On the other hand, the bond strength of the same interface is reduced to 97 psi at 86 ^{O}F, which is close to the bond strength at the HMA/PCC interface and the HMA/ISAC/PCC interface.

Since test temperatures were not constant, a correction factor is needed to adjust the bond strength to the target temperature of 14 ^{O}F. According to Leng et al. (2008), bond strength at PCC/HMA interface increases with the increase of temperature. By using a logarithmic function as shown in Figure 38, experimental bond strengths have been fitted with good results for temperatures ranging from 50 ^{O}F to 86 ^{O}F. Correction factors are calculated using the ratio of bond strength at the target temperature to the reference temperature (14 ^{O}F).

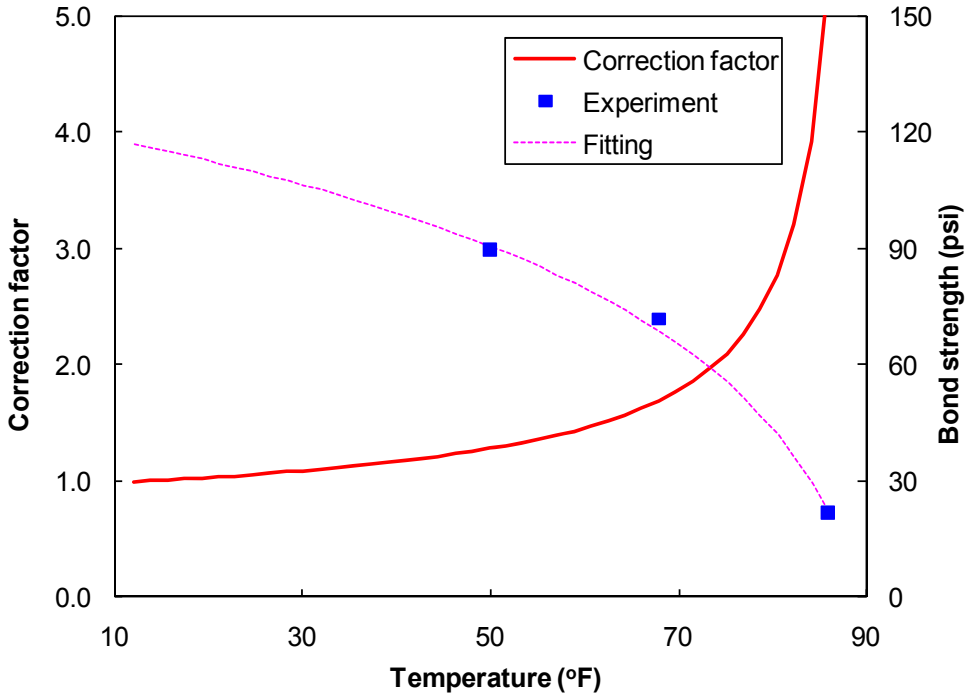

Figure 38. Temperature correction factor for bond strength at 14 °F.

Figure 39 shows average bond strength corrected at 14 °F and interface coring failure ratio at various interface conditions. When interlayer systems are installed between the HMA overlay and PCC slab, bond strength is lower than that that of the bare HMA/PCC interface. Relatively strong bond strength is achieved when both mixture- and fabric-type interlayers are located at the interface between two HMA overlays. By combining the two results of field coring observations and torque tests, bonding conditions at interfaces can be categorized as follows:

- High level: mixture type and fabric interlayer between HMA layers ($\tau \geq 200$ psi);
- Medium level: bare HMA and PCC (100 psi $\leq \tau <$ 200 psi) ; and
- Low level: interlayer between HMA and PCC ($\tau <$ 100 psi).

Table 17. Interface Shear Strength at Various Interface Conditions

Interface			Bond strength (psi)		Torque (lbs-ft)	Temp. (^{o}F)
			Measured	Normalized		
HMA PCC	IL 29 MO	H // P1*	102	101	144	12
		H // P2	162	207	229	50
	IL 130 S6 NB+	H // P1	-	-	-	-
		H // P2	224	228	317	18
HMA Interlayer PCC	IL 29 CC	H / SB // P	10	12	15	39
		H / IC // P	89	90	125	18
HMA Interlayer HMA	IL 29 MO	H / SA // H1	240	240	339	14
		H / SA // H2	224	224	317	14
		H / SA // H3	10	13	15	50
	IL 29 CH	H / SA // H4	261	282	369**	28
		H / SA // H5	261	259	369	12
		H / SA // H6	214	274	303	50
	IL 130 S6 SB	H / IL4.75 // H1	97	513	137	86
		H / IL4.75 // H2	261	261	369	14
		H / IL4.75 // H3	261	261	369	14
	IL 130 S6 NB	H / IL9.5 // H1	261	263	369	16
		H / IL9.5 // H2	261	261	369	14
		H / IL9.5 // H3	261	261	369	14
	IL 130 S11 SB+	H / IL4.75 // H4	261	261	369	14
		H / IL4.75 // H5	261	261	369	14
		H / IL4.75 // H6	261	261	369	14
	IL130 S11 NB	H / IL9.5 // H4	261	261	369	14

+ S6 NB: Section 6 in northbound and S11 SB: Section 11 in southbound
* H: HMA, P: PCC, SA: system A, IC: ISAC
** Maximum torque

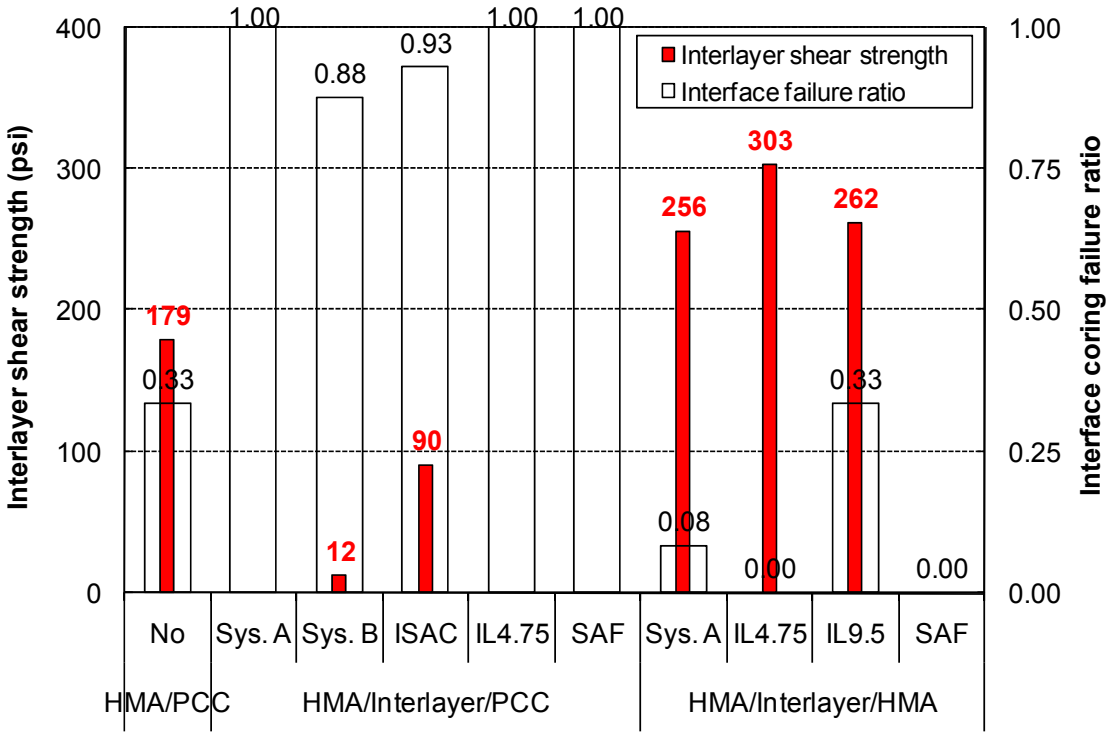

Figure 39. Comparisons of interlayer bond strength at -10°C and interface coring failure ratio at various interface conditions.

5.3.4 Permeability

Permeability cores were obtained and tested from the following projects: IL 29 Mossville-Chillicothe (area-wide System A); US 136 East San Jose (system D, system E (SAF)), and; Mattis (Systems A, B, and D). Table 18 summarizes the permeability testing measurements. The permeability constant, k, is calculated by using the following equation:

$$k = \frac{al}{A(t_2 - t_1)} \ln \frac{h_1}{h_2} \cdot \frac{1}{2.54} \qquad (10)$$

where, k is coefficient of water permeability, in./s;
A and a are cross-sectional area of specimen and inlet standpipe, in.^{2}, respectively;
h_1 and h_2 are water head (in.) at time t_1 and t_2 (s), respectively; and
l is the thickness of the test specimen (in.).

In this equation, the test specimen thickness is interlayer thickness, while 0.1 in was used as the average fabric thickness. The two SAF specimens' thickness was 1.0 in. The inner diameter of the inlet standpipe was 1.25 in. The values of k obtained from Equation 10 do not consider the difference in water viscosity at different testing temperatures. This value therefore requires a correction, which involves multiplying a viscosity correction factor, R_T, by k to get the final value of k_{68}, which is the water permeability coefficient at 68 °F. To qualitatively summarize the results in Table 18, permeability categorization criteria developed in Arkansas (Westerman 1998) were referenced in Table 19.

Table 18. Permeability Testing Measurements

Core ID	Elapsed time (sec)	T (^{O}F)	K (10^{-5} in./s)	R_T	k_{68} (10^{-5} in./s)
IL 29MO-P1	6	63	110	1.077	1200
IL 29MO-P2	10015	63	0.075	1.077	0.081
IL 29MO-P3	66	64	10	1.051	11
US 136ISAC-P2[1)]	∞				
US 136SAF-P1	1066	62	5.2	1.092	5.7
US 136SAF-P2	2908	59	2.0	1.135	2.3
MatD-P1[1)]	∞				
MatD-P2[1)]	672500[3)]	63	0.0010	1.077	0.0011
MatD-P3[1)]	70111	63	0.0095	1.077	0.01
MatB-P1[2)]	93	66	7.1	1.025	7.3
MatB-P2	524	66	1.3	1.025	1.3
MatB-P3[1)]	37118	64	0.018	1.051	0.019
MatA-P1	436	64	1.6	1.051	1.7
MatA-P3[2)]	197	64	3.4	1.051	3.5

1) More than heavy amount of sealant
2) Punching hole is present
3) Estimated time based on a shorter observation overnight

Table 19. Permeability categories

Category*	*k* (10^{-5} in./s)
High permeability	4.0×10^{5} ~ 4.0
Low permeability	4.0 ~ 0.4
Practically impermeable	0.4 or slower

According to the Arkansas criteria, qualitative permeability ratings for the samples tested in this study are presented in Table 20. System D appears to be impermeable in spite of the presence of reflective cracking. The System A strip-fabric used in the Mattis section was found to have low permeability, while area-type

application of System A in the IL29 Mossville section ranged from low to high permeability. System B strip-fabric in the Mattis section was found to vary across all three permeability categories, i.e. highly permeable to impermeable. The SAF layer in the US136 eastbound section was categorized across low to high permeability categories.

Table 20. Permeability ratings of selected interlayers

Generic Type	Interlayer Type	Permeability Rating
Fabric	IL 29 – System A, Area	Low to high
	US 136 – System D, Strip	Impermeable
	Mattis Avenue – System D, Strip	Impermeable
	Mattis Avenue – System B, Strip	Impermeable to high
	Mattis Avenue – System A, Strip	Low
Mixture	US 136 – System E (SAF)	Low to high

6. SUMMARY AND RECOMMENDATIONS

6.1 SUMMARY

Reflective crack interlayer systems, such as reinforcement and stress absorbing membrane, have been used in an effort to reduce the severity and rate of reflective cracking in Illinois. Previous research in Illinois has shown that non-woven polypropylene (or System A) interlayer systems are marginally cost effective in most instances, but additional research was recommended to validate these results, to evaluate other interlayer systems, and to gain a better understanding of the effects of traffic and climate on interlayer system effectiveness.

The aforementioned research needs were addressed through a field and laboratory investigation of selected composite pavements in Illinois. Five interlayer systems were investigated: System A – non-woven polypropylene geotextile fabric, applied either in strips or "area wide;" System B – self-adhesive membrane interlayer systems ("peel and stick" strip treatments); System C – conventional stress absorbing membrane interlayer which has been rarely used in Illinois, or SAMI (not commonly used in Illinois); System D – an interlayer stress absorbing composite (ISAC) strip treatment, developed in a project sponsored by the Illinois Cooperative Highway Research Program in the 1990s; and System E – a sand-sized aggregate gradation with high polymer-modified binder.

The research tasks involved: visual surveys of overlay cracking; digital video imaging and ground penetrating radar (GPR) measurement evaluation; field coring and visual inspection of cored pavement; laboratory testing of cored specimens; development of reflective cracking indices; and in a companion report, development of user-friendly life-cycle cost analysis (LCCA) software; and development of practice guidelines. Based upon the research conducted, the following findings have been drawn:

- Ground penetrating radar (GPR) testing was found to be an effective tool for rapid, non-destructive evaluation of rehabilitated pavement systems, particularly allowing the analyst to differentiate between reflective cracks and other transverse cracks in HMA overlays, by locating pavement joints, dowel bars, and patches. It was successfully employed as a tool to detect one of the strip reflective crack interlayer systems and used for pavement HMA overlay thickness estimation.
- Field coring on selected projects provided very useful insight towards reflective cracking mechanisms; for instance, debonding, crack offsetting, and crack trajectory were evident through inspection of field cores and core holes.
- Mechanical properties of overlay and interlayer system materials, obtained through laboratory testing, were found to be highly correlated with field performance.
- Permeability testing showed that while reflective cracks would eventually propagate above the stress absorbing interlayer systems (System D), waterproofing benefits would continue for some time.
- Field performance data showed a clear trend of reduction of interlayer system effectiveness as traffic loading increases.
- Two reflective cracking indices were developed to quantify reflective cracking distress: a reflective cracking appearance ratio, R_{RCA}, and a transverse cracking appearance ratio, R_{TCA}. The R_{RCA} and R_{TCA} indices represent the total amount of

transverse cracking per joint and transverse crack length in proportion to underlying joint length, respectively. The two indices were modified to include crack severity using weighing factors (R_{RCAW} and R_{TCAW}).

- Using the deterioration rate, a performance benefit ratio, PBR, was proposed to represent the extension of service life of HMA overlays compared with an untreated HMA overlay. For System D, the PBR was shown to be a function of annual 18-kip equivalent single-axle loads (ESALs), lowest monthly average temperature, T_L, and joint spacing (JS). However, the PBR of System A (area) and System E is insensitive to traffic volume and climate. Accordingly, PBR prediction models were developed for System D.
- Based on the PBR parameter, System D was shown to outperform the other systems investigated regardless of traffic volume, followed by System E. System A (area-type) was found to have a marginal performance benefit. On the other hand, control sections outperformed overlays with System B or System A (strip-type).
- For simplicity, a performance criterion was suggested to specify maximum allowable ESALs for System A (area), System D, and System E. An ESALs-T_L (district) chart was provided as a convenient tool for the selection of candidate interlayer systems.

6.2 EXPECTED BENEFITS

This study provided a quantitative assessment for various types of reflective cracking interlayer systems. Results are presented in two volumes: “Cost Effectiveness and Performance of Overlay Systems in Illinois-Volume 1: Effectiveness Assessment of HMA Overlay Interlayer Systems Used to Retard Reflective Cracking”; and “Cost Effectiveness and Performance of Overlay Systems in Illinois-Volume 2: Guidelines for Interlayer System Selection Decision When Used in HMA Overlays.” This study clearly showed the performance of interlayers systems and their comparative cost effectiveness in the field. In addition, it provides a means to predict the performance of several interlayer systems under various vehicular and environmental loading conditions. Significant cost savings is expected when using the simplified ESALs-T_L chart for selecting the appropriate interlayer system outlined in volume 1 or using the developed CIND (**C**ost-effective **IN**terlayer system **D**ecision program), which provides a systematic approach for cost effective evaluation of reflective cracking interlayer systems outlined in volume 2.

6.3 RECOMMENDATIONS

- This study recommends the use of the simplified ESALs-T_L chart to select the appropriate interlayer system to retard reflective cracking (volume 1) and CIND program for detailed and cost effectiveness analysis (volume 2).
- More data can be used to fine-tune the CIND program. This can be accomplished by surveying additional sections and/or by obtaining more data from the previously surveyed sections.
- A better understanding of the mechanisms of reflective crack offset and the role of pre-existing concrete condition on interlayer selection and overlay design are still needed.

7. REFERENCES

AASHTO T322, "Standard Test Method for Determining the Creep Compliance and Strength of Hot-Mix Asphalt (HMA) Using the Indirect Tensile Test Device." *Standard Specifications for Transportation Materials and Methods of Sampling and Testing*, 24th Edition. AASHTO Provisional Standards. 2004.

Al-Qadi, I. L., M. Elseifi, and A. Loulizi, "Geocomposite Membrane Effectiveness in Flexible Pavements." *Final Report Project TRA-00-002*, The Roadway Infrastructure Group, Virginia Tech Transportation Institute, Blacksburg, VA. 2000.

Al-Qadi, I. L., S. Lahouar, and A. Loulizi, "Successful Application of GPR for Quality Assurance/Quality Control of New Pavements." *In Transportation Research Record: Journal of the Transportation Research Board*, No 1861, Transportation Research Board, National Research Council, Washington, D.C., 2003, pp. 86 – 97.

Al-Qadi, I. L., M. A. Elseifi, and D. Leonard, "Development of an overlay design model for reflective cracking with and without steel reinforcement," Journal of the Association of Asphalt Pavement Technologists, Vol. 72, 388-423, 2003 (b).

Al-Qadi, I. L., S. Lahouar, A. Loulizi, M. A. Elseifi, and J. A. Wikes, "Effective Approach to Improve Pavement Drainage Layers." *Journal of Transportation Engineering*, Vol. 130, Issue 5, 2004. pp. 658 – 664.

Al-Qadi, I. L., S. Lahouar, K. Jiang, M. McGhee, and D. Mokarem, "Accuracy of Ground Penetration Radar for Estimating Rigid and Flexible Pavement Layer Thickness." *In Transportation Research Record: Journal of the Transportation Research Board*, No. 1940, Transportation Research Board, National Research Council, Washington, D.C., 2005, pp. 69 – 78.

ASTM D7313-07A, "Standard Test Method for Determining Fracture Energy of Asphalt-Aggregate Mixtures Using the Disk-Shaped Compact Tension Geometry." *Annual Book of ASTM Standards*, Vol. 04.03. ASTM International, 2007.

ASTM PS 129-01, "Standard Test Method for Measurement of Permeability of Bituminous Paving Mixtures Using a Flexible Wall Permeameter." *Annual Book of ASTM Standards*, Vol. 04.03. ASTM International, 2003.

Baek, J., I. L. Al-Qadi, W. Xie, and W. G. Buttlar, "In-Situ Assessment of Interlayer Systems to Abate Reflective Cracking in Hot-Mix Asphalt Overlays." *In Transportation Research Record: Journal of the Transportation Research Board*, TRB, National Research Council, Washington, D.C., 2008. (in press)

Blankenship, P., N. Iker, and J. Drbohlav, "Interlayer and Design Considerations to Retard Reflective Cracking", *In Transportation Research Record: Journal of the Transportation Research Board*, No. 1896, Transportation Research Board, Washington, D.C. 2004, pp.177 – 186.

Blomberg, J. M., Application of Sand Anti-Fracture Layer for Pavement Rehabilitation, Research Investigation 97-045 and 99-042, Missouri Department of Transportation, Jefferson City, Missouri, http://168.166.124.22/RDT/reports/Ri97045/ Brf2001.htm on June 13, 2007, 2001.

Bozkurt, D. and W. G. Buttlar, “Tree-Dimensional Finite Element Modeling to Evaluate Benefits of Interlayer Stress Absorbing Composite for Reflective Crack Mitigation.” *Presented for the 2002 Federal Aviation Administration Airport Technology Transfer Conference*, 2002.

Buttlar, W. G., D. Bozkurt, and B. J. Dempsey, “Evaluation of Reflective Crack Control Policy.” *Final Report, Project1A-H1*, Illinois Transportation Research Center, Illinois Department of Transportation, 1999.

Buttlar, W. G., D. Bozkurt, and B. J. Dempsey, “Cost-Effectiveness of Paving Fabrics Used to Control Reflective Cracking.” *In Transportation Research Record: Journal of the Transportation Research Board*, No. 1730, Transportation Research Board, National Research Council, Washington, D.C., 2000, pp. 139 – 149.

Button, J. W. and R. L. Lytton, “Evaluation of Fabrics, Fibers, and Grids in Overlays.” *Proceedings of 6th International Conference on Structural Design of Asphalt Pavements*, Vol. 1, Ann Arbor, MI, 1987, pp. 925 – 934.

Button, J. W. and R. L. Lytton, “Guidelines for Using Geosynthetics with Hot Mix Asphalt Overlays to Reduce Reflective Cracking.” *Presented at the 86th Transportation Research Board Annual Meeting*, CD-ROM, Transportation Research Board, Washington D.C. 2007.

Chen, D. H., T. Scullion, and J. Bilyeu, “Lessons Learned on Jointed Concrete Pavement Rehabilitation Strategies in Texas.” *Journal of Transportation Engineering*, Vol. 132, No. 3, 2006, pp. 257 – 265.

Chua, K. M. and L. Xu, “Simple Procedure for Identifying Pavement Distresses from Video Images.” *Journal of Transportation Engineering*, Vol. 120, No. 3, 1994, pp. 412 – 431.

Cleveland, G. S., J. W. Button, and R. L. Lytton, “Geosynthetics in Flexible and Rigid Pavement Overlay Systems to Reduce Reflection Cracking.” *Publication FHWA/TX-02/1777-1*, FHWA, U.S. Department of Pavement, 2002.

Cohen, J., *Statistical Power Analysis for the Behavioral Sciences* (2nd Ed.) Hillsdale, NJ: Lawrence Erlbaum Associates. ISBN 0-8058-0283-5, 1998.

Dempsey, B. J., “Development and Performance of Interlayer Stress Absorbing Composite in Asphalt Concrete Overlays.” *In Transportation Research Record: Journal of the Transportation Research Board*, No. 1809, Transportation Research Board, National Research Council, Washington, D.C., 2002, pp. 175 – 183.

Donna, H. S., “Crack-Reduction Pavement-Reinforcement GlassGrid.” Prepared in cooperation with the U.S. Department of Transportation, Colorado Department of Transportation, Federal Highway Administration, 1993.

Elseifi, M. A., and I. L. Al-Qadi, “A Simplified Overlay Design Model against Reflective Cracking Utilizing Service Life Prediction,” *International Journal on Road Materials and Pavement Design*, Vol. 5, No. 2, 169-191, 2004.

Epps, A., J. T. Harvey, Y. R. Kim, and R. Roque, “Structural Requirements of Bituminous Paving Mixtures.” *Transportation in the New Millennium*, Transportation Research Board, Washington, D. C. 2000.

Flintsch, G. W., I. L. Al-Qadi, A. Loulizi, S. Lahouar, K. McGhee, and T. Clark, “Field Investigation of High Performance Pavements in Virginia.” *Publication VTRC 05-CR9*, Virginia Department of Transportation, 2005.

Huang, Y. H., *Pavement Analysis and Design*, Prentice Hall, Englewood Cliffs, New Jersey, 1993.

Huang, Y. and B. Xu, "Automatic Inspection of Pavement Cracking Distress." *Journal of Electric Imaging*, Vol. 15(1), 2006.

Illinois Department of Transportation, "Average Annual Daily Traffic Map." visited on May 1st 2008 via http://www.gettingaroundillinois.com/default.aspx?ql=aadt

Illinois State Climatologist Data, "Monthly Climate Data for Sites across the State." visited on May 1st 2008 via http://www.sws.uiuc.edu/data/climatedb/

Jenner, C. G., "Polymer Geogrid Reinforcement Construction," *Proceeding of International Symposium on Geosynthetics*, Shanghai, China, pp. 139 – 144, 1996.

Jun, Y., F. Guanhua, L. Qing, C. Rongsheng, and D. Xuejun, "Deep Analysis on Interlayer Restraining Reflective Cracks in Asphalt Overlay Old Concrete Pavement." *Proceedings pro37: Cracking in Pavements: Mitigation, Risk Assessment and Prevention*, C. Petit, I. L. Al-Qadi, and A. Millien, Eds., Limoges, France, May 5-7, 2004, pp. 223 – 230.

Kim, J. and W. G. Buttlar, "Analysis of Reflective Crack Control System Involving Reinforcing Grid over Base-Isolating Interlayer Mixture." *Journal of Transportation Engineering*, Vol. 128 No. 4, 2002, pp. 375 – 384.

Kuo, C.-M. and T.-R. Hsu, "Traffic Induced Reflective Cracking on Pavements with Geogrid-Reinforced Asphalt Concrete Overlay." *Presented at the 82nd Annual Meeting of the Transportation Research Board*, CD-ROM, Transportation Research Board, Washington, D.C. 2003.

Lahouar, S., I. L. Al-Qadi, A. Loulizi, T. M. Clark, and D. T. Lee, "Approach to Determining In-Situ Dielectric Constant of Pavements: Development and Implementation at Interstate 81." *In Transportation Research Record: Journal of the Transportation Research Board*, No 1806, Transportation Research Board, National Research Council, Washington, D.C., 2002, pp. 81 – 87.

Leng, Z., H. Ozer, I. L. Al-Qadi, S. H. Carpenter, "Interface Bonding between HMA and Various PCC Surfaces: Laboratory Assessment," *Presented in the 87th Annual Meeting of the Transportation Research Board,* CD-ROM, Washington D.C. 2008.

Lee, H. and J. Kim, "Quantification and Automated Crack Measurement System." *Report TR-457*, Iowa Department of Transportation, 2005.

Lorenz, V. M., "New Mexico Study of Interlayers Used in Reflective Crack Control." *In Transportation Research Record: Journal of the Transportation Research Board*, No. 1117, Transportation Research Board, National Research Council, Washington, D.C., 1987, pp. 94 – 103.

Makowski, L., D. L. Bischoff, P. Blankenship, D. Sobczak, and F. Haulter. Wisconsin Experiences with Reflective Crack Relief Projects. *In Transportation Research Record: Journal of the Transportation Research Board, No. 1905*, TRB, National Research Council, Washington, D.C., 2005, pp. 44 – 55.

Maser, K. R., and T. Scullion, "Automated Pavement Subsurface Profiling Using Radar: Case Studies of Four Experimental Field Sites." *In Transportation Research Record: Journal of the Transportation Research Board*, No. 1344, Transportation Research Board, National Research Council, Washington, D.C., 1992, pp. 148 – 154.

Miller, J. S. and W. Y. Bellinger, “Distress Identification Manual for the Long-term Pavement Performance Program (4th Revised Ed.).” *Publication FHWA-RD-03-031*, FHWA, U.S. Department of Transportation, 2003.

Monismith, C. L. and N. F. Coetzee, “Reflection Cracking: Analysis, Laboratory Studies and Design Consideration.” *Journal of the Association of Asphalt Paving Technologists*, Vol. 49, 1980, pp.268 – 313.

Montestruque, G., R. Rodrigues, M. Nods, and A. Elsing, “Stop of Reflective Crack Propagation with the Use of Pet Geogrid as Asphalt Overlay Reinforcement.” *Proceedings pro37: Cracking in Pavements: Mitigation, Risk Assessment and Prevention*, C. Petit, I. L. Al-Qadi, and A. Millien, Eds., Limoges, France, May 5-7, 2004, pp. 231 – 239.

Morris, G. R. and C. H. McDonald, “Asphalt-Rubber Stress-Absorbing Membranes: Field Performance and State of the Art.” *In Transportation Research Record: Journal of the Transportation Research Board*, No. 595, Transportation Research Board, Washington, D. C., 1976, pp. 52 – 58.

Mukhtar, M. T., “Interlayer Stress Absorbing Composite (ISAC) for Mitigating Reflection Cracking in Asphalt Concrete Overlays.” Ph.D. Dissertation, University of Illinois at Urbana-Champaign, Urbana, IL, 1994.

Mukhtar, M. T. and B. J. Dempsey, "Interlayer Stress Absorbing Composite (ISAC) for Mitigating Reflective Cracking in Asphalt Concrete Overlays." *Final Report, Transportation Engineering Series No. 94, Cooperative Highway and Transportation Series No. 260*, University of Illinois at Urbana-Champaign, Urbana-Champaign, IL, 1996.

Predoehl, N. H., “Evaluation of Paving Fabric Test Installation in California.” *Final Report*, Draft Report, California Department of Transportation, Translab. 1989.

Schutzbach, A. M., “Bituminous Overlay Policy – A Performance Evaluation.” *Physical Research No. 116*, Illinois Department of Transportation, Bureau of Materials and Physical Research, Springfield, Illinois, 1995, pp. 43.

Steen, E. R., “Stress Relieving Function of Paving Fabrics when Used in New Road Construction.” *Proceedings of the 5th International RILEM Conference, Cracking in Pavements – Mitigation, Risk Assessment, and Prevention*, C. Petit, I. L. Al-Qadi, and A. Millien, Eds., Limoges, France. 2004.

Steinberg, M. L., “Geogrid as a Rehabilitation Remedy for Asphaltic Concrete Pavements.” *In Transportation Research Record: Journal of the Transportation Research Board*, No. 1369, Transportation Research Board, Washington, D. C., 1992, pp. 54 – 62.

Titi, H., M. Rasoulian, M. Martinez, B. Becnel, and G. Keel, “Long-Term Performance of Stone Interlayer Pavement.” *Journal of Transportation Engineering*, Vol. 129. Issue 2, 2003, pp. 118 – 126.

Van Deuren, H. and J. Esnouf, “Geotextile Reinforced Bituminous Surfacing.” Proceedings of 3rd International RILEM Conference - Reflective Cracking in Pavements: Design and Performance of Overlays, Eds. L. Francken, E. Beuving, A. A. A. Molenaar, 1996.

Vespa, J. W., “An Evaluation of Interlayer Stress Absorbing Composite (ISAC) Reflective Crack Relief System.” *Report No. FHWA/IL/PRR 150*, Illinois Department of Transportation, Springfield, Illinois, 2005.

Wagoner, M. P., “Fracture Tests for Bituminous-Aggregate Mixtures: Laboratory and Field Investigations.” *Ph. D. Dissertation*, University of Illinois at Urbana-Champaign, Urbana, 2006

Westerman, J. R., “AHTD’s Experience with Superpave Pavement Permeability.” Presented at Arkansas Superpave Symposium, January 21, 1998.

Wheat, M., “Evaluation of Bond Strength at Asphalt Interfaces,” *M.S Thesis*, Kansas State University, Manhattan, KS, 2007.

APPENDIX A FIELD BRIEF EVALUATION REPORTS

A.1 RTE 344 CHICAGO; CONTRACT NO. 62288

A.1.1 SECTION DESCRIPTION

This project, RTE 344 (127th St.) Calumet Part at Chicago (Contract No. 62288), was completed in June 2004. The project is located south of Chicago (Cook County, District 1), Illinois, as shown in Figure A.1.1. The evaluated section is located just east of I-57 (STA. 11+58 and STA. 22+25.5). It has two lanes in each direction: eastbound and westbound (Figure A.1.2). Existing pavements consist of jointed concrete pavement (JCP) with hot-mix asphalt (HMA) overlay. The thickness and joint spacing of the existing JCP is unknown. After milling existing HMA overlay, new overlay was resurfaced with 2.5 in. HMA (1.75 in. wearing surface, Polymer Superpave N90 Mix F and 0.75 in. binder level, Superpave N70). The treatments used in this project are the following: Strip-type System A made of TC Mirafi was treated all longitudinal lanes and shoulder joints. This evaluation considered two lanes in both directions except one middle turning lane. The control section is located between Ashland Ave. and Justine St. (STA. 15+00 to 18+00). Traffic volume in 2008 was reported as 22700 AADT according to traffic map on IDOT.

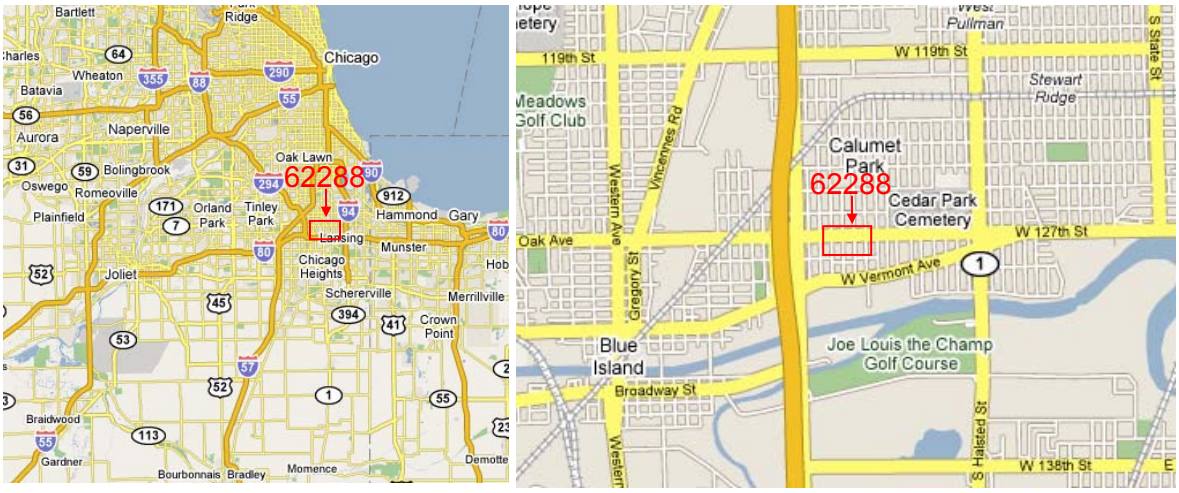

Figure A.1.1. Section location.

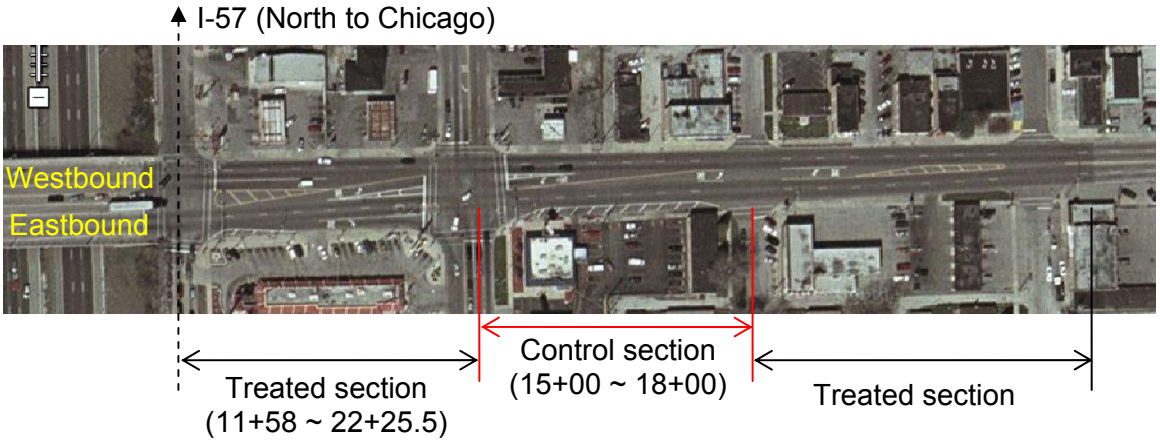

Figure A.1.2. Section layout.

A.1.2 FIELD EVALUATION

A.1.2.1 Survey

The UIUC research team conducted only visual survey on Oct. 7, 2006 to quantify surface cracking in transverse direction. A 4400-ft-long section was surveyed (1100-ft-long in each lane). The crack severity of this section had been monitored since 2004 by IDOT. The same surveying criteria were used in this reflective cracking evaluation. The severity and extent of transverse cracks were reported. Figure A.1.3 shows typical cracks and unique distress found in this section. Longitudinal reflective cracking was developed along shoulder joints (Figure A.1.3(a)) . As a unique type, a crack was developed around a manhole or initiated from an edge of a manhole (Figure A.1.3(b)).

(a) (b)

Figure A.1.3. (a) Longitudinal reflective cracking and (b) cracks around a manhole.

A.1.3 DATA ANALYSIS

A.1.3.1 Crack Analysis

For data analysis of this section, extent and severity of reflective cracking is utilized to compute uniform, R_{TCA}, and weight, R_{TCAW}, transverse cracking appearance rates. All transverse cracking are examined regardless the strip locations. Table A.1.1 summarizes the crack survey results for the control and treated sections for the past three years. According to the pre-survey prior to the new overlay, more cracks existed in the control section than the treated section. Of the all cracks regardless crack severity, 86% and 61% of transverse cracks are developed two years after the new overlay in the control and treated section. However, since the treatment was installed in a longitudinal direction, the surveyed transverse cracks are not able to represent a capacity of the interlayer system on retarding reflective cracking. Thus, this section is excluded from overall interlayer system evaluation.

Table A.1.1. Summary of Crack Survey

	Control section (821ft)			
Severity	6/14/04	6/15/04	10/25/05	10/7/06
S	1	0	2	19
L	71	0	9	43
M	1	0	2	8
H	8	0	0	0
# Crack	81	0	13	70
R_{TCA}	2.47	0.00	0.40	2.13
R_{TCAW}	2.44	0.00	0.33	1.54
	Treated section (300ft)			
Severity	6/14/04	6/14/04	6/14/04	6/14/04
S	0	0	0	0
L	26	26	26	26
M	7	7	7	7
H	0	0	0	0
# Crack	34	34	34	34
R_{TCA}	1.00	1.00	1.00	1.00
R_{TCAW}	1.01	1.01	1.01	1.01

A.1.4 SUMMARY OF SECTION EVALUATION

One task was performed in 2006 at RTE 344 (127th St.) Calumet Park in Chicago. Table A.1.2 summarizes the conducted survey and analysis.

Table A.1.2. Summary for RTE 344 (127th St.) Calumet Park, Chicago

Year	2006
Survey	Visual crack survey
Forensic investigation Analysis	Crack

From the RTE 344 Chicago section, the interlayer system evaluations and findings are presented as follows:

- Compared to the control section, more than 60% of transverse cracks were developed within two years of overlay age.
- The performance benefit ratio is not available for this section. While strip-type interlayer systems were applied in a longitudinal direction, only transverse crack data is available for the performance evaluation.

A.2 IL 40 DEER GROVE; CONTRACT NO. 64142

A.2.1 SECTION DESCRIPTION

This project, IL 40 at Deer Grove (Contract No. 64142), was completed in February 1998. The project is located north of Deer Grove (Whiteside County, District 2), Illinois, as shown in Figure A.2.1. The evaluated section is close to Rock Falls across I-88 (STA. 17+700 and STA. 17+893, metric). It has one lane in each direction: northbound and southbound (Figure A.2.2). Existing pavement system consists of 30 ft JCP with 1.5 in. HMA overlay where strip reflective crack treatments were placed. The thickness of the existing JCP is unknown. Without milling, 2.4 in. new overlay was directly on existing HMA overlay (1.6 in. wearing surface and 0.8 in. binder level). The treatment used in this project was system A, Amoco non-woven polypropylene, in the northbound and southbound lanes except a control section. The control section is located at 17+825.350 to 17+892.670 in northbound. This evaluation considered two lanes in both directions. Traffic volume in 2008 was reported as 2400 AADT (395 MU and 180 SU) according to traffic map on IDOT.

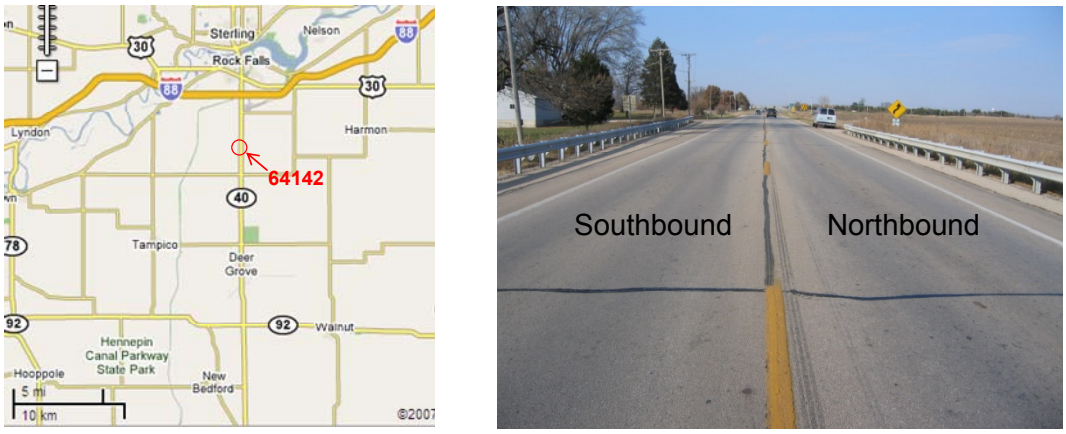

Figure A.2.1 Section location.

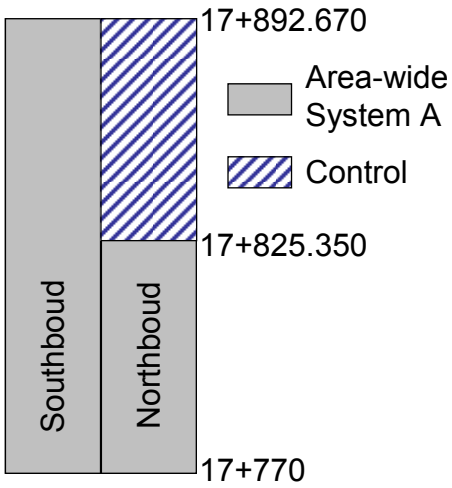

Figure A.2.2. Section layout.

A.2.2 FIELD EVALUATION

A.2.2.1 Survey

The UIUC research team conducted only visual survey to quantify surface cracking on Nov. 5, 2006. A 1280-ft-long section was surveyed (640 ft in each lane). The crack severity of this section has been monitored since 2003 by IDOT. The same surveying criteria were used in this evaluation. The severity and extent of transverse cracks were reported. Most transverse cracks were sealed (Figure A.2.3 (a)); longitudinal cracks appeared in widening joints were not sealed (Figure A.2.3 (b) bottom). Construction joints were observed at both starting and ending points and seriously deteriorated PCC pavements at joints existed at north of the surveyed section (Figure A.2.3 (c) and (d)).

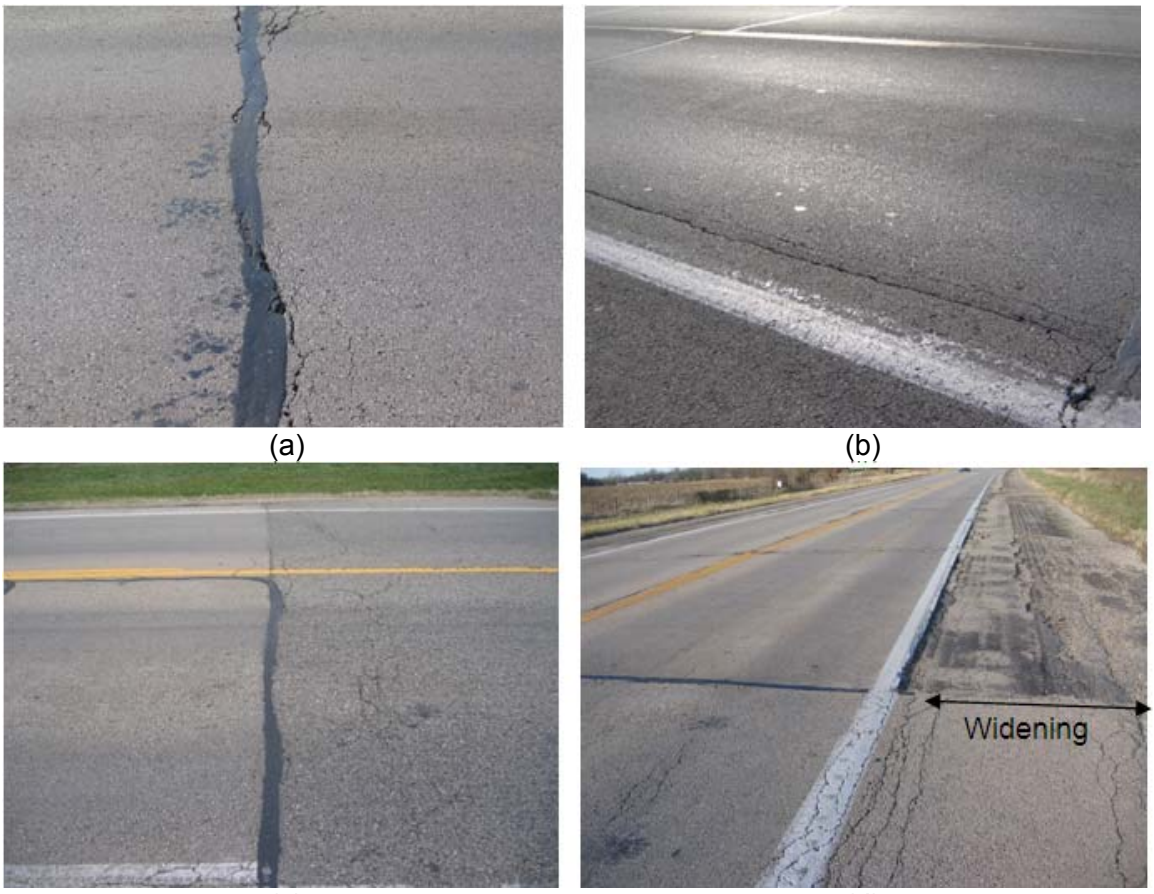

Figure A.2.3. Sealed transverse cracking in northbound: (a) treated and (b) control section; construction joint: (c) at a starting and (e) ending point.

A.2.3 DATA ANALYSIS

A.2.3.1 Crack Analysis

For data analysis of this section, extent and severity of reflective cracking is utilized to compute uniform, R_{RCA}, and weight, R_{RCAW}, reflective cracking appearance rates. All transverse cracks are included for the evaluation. Table A.2.1 summarizes the crack survey results for the control and treated sections for the past nine years. In both sections, low-severity-level cracks appear at the beginning until 2004. After that, those

cracks deteriorate to the medium-severity level. Of the all cracks regardless crack severity, more transverse cracks are developed in the control section than in the treated section.

Table A.2.1. Summary of Crack Survey

	Control section (221 ft)			
Severity	8/14/03	9/30/04	8/31/05	11/5/06
S	5	6	4	1
L	8	7	5	6
M	3	4	9	14
H	0	0	0	2
# Crack	16	17	18	23
R_{TCA}	7.2	7.7	8.1	10.4
R_{TCAW}	10.2	10.9	13.9	21.5
	Treated section (106 1ft)			
Severity	8/14/03	9/30/04	8/31/05	11/5/06
S	9	9	12	2
L	39	40	35	46
M	2	6	14	20
H	0	0	0	3
# Crack	50	55	61	71
R_{TCA}	4.7	5.2	5.7	6.7
R_{TCAW}	6.6	7.6	8.8	12.2

In order to investigate the effect of the interlayer system on crack severity as well as extent, R_{RCA} and R_{RCAW} are compared with respect to overlay age in Figure A.13.4. For System A section, both R_{RCA} and R_{RCAW} increase approximately linearly until eight years at 12.2 of R_{RCAW} and at 6.7 of R_{RCA}. This indicates that new cracks are being developed and the severity of all cracks becomes also deteriorated. Similarly, both of the R_{RCA} and R_{RCAW} of the control section increase linearly up to 10.4 and 21.5, respectively. Compared with the control section, the treated section shows better performance to delay the occurrence of reflective cracking. Using the slopes of the curves, the performance benefit ratio of the System A becomes 1.6, i.e., the service life of the treated overlay is extended by a factor of 1.6.

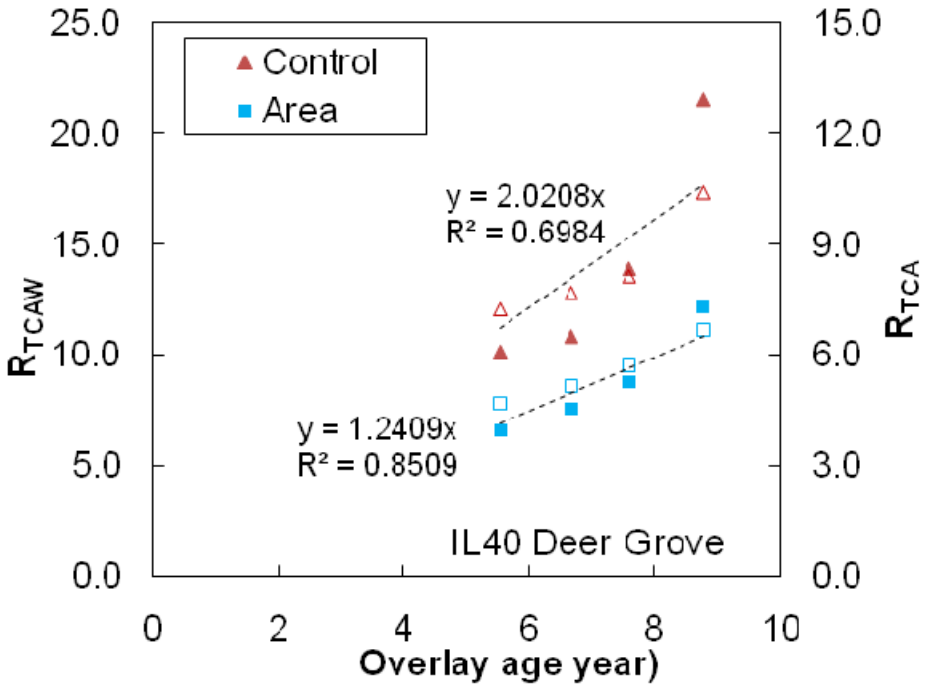

Figure A.13.4. Comparisons of the R_{TCA} and R_{TCAW} on the control and treated section with area-type System A.

A.2.4 SUMMARY OF SECTION EVALUATION

One task was performed in 2006 at IL 40 near Deer Grove. Table A.2.2 summarizes the conducted survey and analysis.

Table A.2.2. Summary for IL 40, Deer Grove

Year	2006
Survey	Visual crack survey
Forensic investigation Analysis	Crack

From the IL 40 Deer Grove section, the interlayer system evaluation and findings are presented as follows:

- Compared to the control section, the area-type System A performs better to abate reflective cracking and extend the service life of the HMA overlay.
- The performance benefit ratio of the area-type System A to the control section is 1.6.

A.3 IL 76 BELVIDERE; CONTRACT NO. 64637

A.3.1 SECTION DESCRIPTION

This project, IL 76 at Belvidere (Contract No. 64637), was completed in October 2003. The project is located at Belvidere (Boone County, District 2), Illinois, as shown in Figure A.3.1. Total 6.7-mile-long section is from US 20 north of Belvidere to the Wisconsin State line (STA. 180+00 to STA. 300+00). It has two lanes in each direction: northbound and southbound (Figure A.3.2). Existing pavement system consists of 30 ft jointed reinforced concrete pavement (JRCP) constructed in early 1930's and multiple HMA overlays followed until 1994. The existing JRCP had a 9-6-9 varied thickness. 2.25 in. new overlay was directly on existing HMA overlay (1.5 in. wearing surface with N50 and N70 Mix D and 0.75 in. binder level with IL-9.5 N50 and N70 Mix D). The treatment used in this project was system E, "Sand mix" which is IL-4.75 N50 level binder with N50 Mix D. There are four segments which have three 500-ft-long sections each. This evaluation considered two lanes in both directions. Traffic volume in 2003 was reported as 3050 AADT on section 1 – 6 and 7800 AADT on section 7 – 12. In 2008, the section 7 – 12 has 7200 AADT (616 MU and 264 SU) according to traffic map on IDOT.

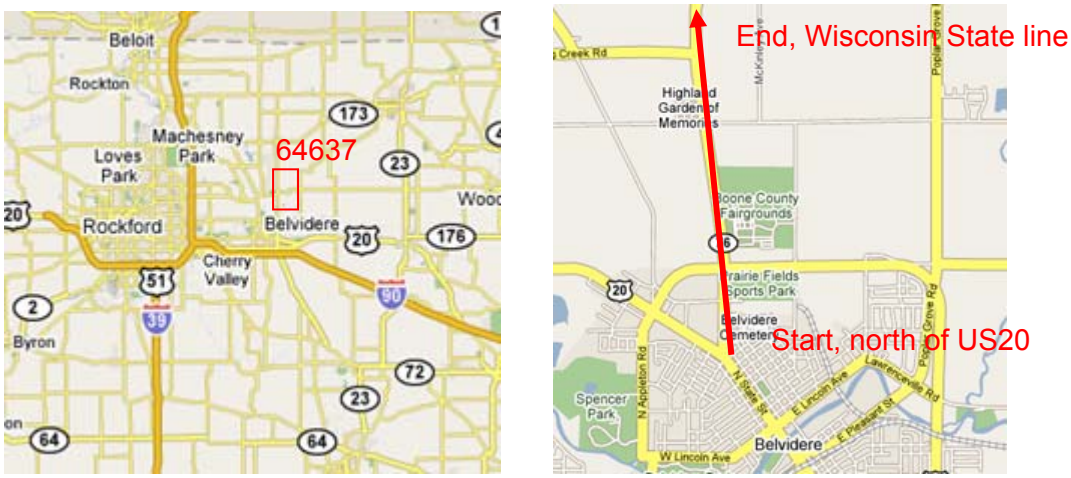

(a)

(b)

Figure A.3.1 Section location.

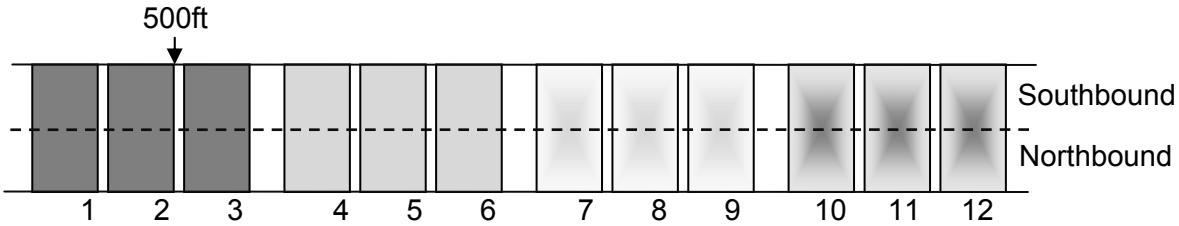

Section 1 – 3 (Control 1): Mix D surface, N50 + IL9.5 level binder, N50
Section 4 – 6 (System E1): Mix D surface, N50 + IL4.75 level binder, N50
Section 7 – 9 (System E2): Mix D surface, N70 + IL4.75 level binder, N50
Section 10 –12 (Control 2): Mix D surface, N70 + IL9.5 level binder, N70

Figure A.3.2. Section layout.

A.3.2 FIELD EVALUATION

A.3.2.1 Survey

The UIUC research team conducted visual and video survey to quantify surface cracking on June 20, 2006. A 12000-ft-long section was surveyed (12 x 500ft in both lanes). The crack severity of this section has been monitored since 2003 by IDOT. The same surveying criteria were used in this evaluation. The severity and extent of transverse cracks were reported. Most of transverse cracks were not sealed (Figure A.3.3 (a)); some of longitudinal or centerline cracks were sealed (Figure A.3.3 (b)).

(a) (b)

Figure A.3.3. (a) Unsealed transverse cracks and (b) sealed center and edge longitudinal cracks.

A.3.3 DATA ANALYSIS

A.3.3.1 Crack Analysis

For data analysis of this section, extent and severity of reflective cracking is utilized to compute uniform, R_{TCA}, and weight, R_{TCAW}, transverse cracking appearance rates. All transverse cracks are included for the evaluation. Table A.3.1 summarizes the crack survey results for the control and treated sections for the past three years. In both sections, low-severity-level cracks appear at the beginning until 2005. After that, those cracks deteriorate to the medium-severity level. Of the all cracks regardless crack

severity, more transverse cracks are developed in the control section than in the treated section.

Table A.3.1. Summary of Crack Survey

	Control1 section (3000 ft)			
Severity	6/1/03	8/13/04	8/17/05	6/20/06
S	0	0	0	4
L	0	27	37	28
M	0	0	4	20
H	0	0	0	0
# Crack	0	27	41	52
R_{TCA}	0.00	0.90	1.37	1.73
R_{TCAW}	0.00	1.35	2.15	3.10
	System E1 section (3000 ft)			
Severity	6/1/03	8/13/04	8/17/05	6/20/06
S	0	0	2	14
L	0	7	13	29
M	0	0	0	3
H	0	0	0	0
# Crack	0	7	15	46
R_{TCA}	0.00	0.23	0.50	1.53
R_{TCAW}	0.00	0.35	0.70	2.03
	Control2 section (3000 ft)			
Severity	6/1/03	8/13/04	8/17/05	6/20/06
S	0	9	2	11
L	0	12	68	63
M	0	0	0	25
H	0	0	0	0
# Crack	0	21	70	99
R_{TCA}	0.00	0.70	2.33	3.30
R_{TCAW}	0.00	0.83	3.45	5.31
	System E2 section (3000 ft)			
Severity	6/1/03	8/13/04	8/17/05	6/20/06
S	0	5	3	16
L	0	22	45	45
M	0	0	5	31
H	0	0	0	0
# Crack	0	27	53	92
R_{TCA}	0.00	0.90	1.77	3.07
R_{TCAW}	0.00	1.24	2.73	5.03

Based on the R_{TCAW} of the four segments, a deterioration rate was obtained. The deterioration rate is defined as the increase of R_{TCAW} per overlay age. Since the deterioration rate is linear regarding the overlay age, the slope of the four segments is compared to examine the performance of the interlayer system on retard reflective cracking. Less amount of deterioration is achieved when the System E is utilized for the level binder regardless surface mixture type. For the systems E1 and E2, the deterioration rate increase 2.8 times when N70 surface mixture is accompanied with. Since the two segments have different traffic level that the System E1 had 3050 AADT

and the System E2 had 7800 AADT, the increase might be also affected by traffic volume. In order to minimize the effect of traffic volume effect on the deterioration rate, it is normalized by AADT, not ESALs, under an assumption that the two locations have the same fraction of truck traffic volume. When the deterioration rates of the control1 and System E1 segments are normalized by the AADT, the difference becomes less than 10%. Therefore, the effect of surface mixture on reflective cracking may be not significant for this case. On the other hand, for the control segments, the deterioration rate difference is larger than that for the treated sections. After the normalization, the control1 segment shows 1.6 times higher degradation rate than the control2 segment. It can indicate that N70 mixture has higher crack resistance than N50 mixture.

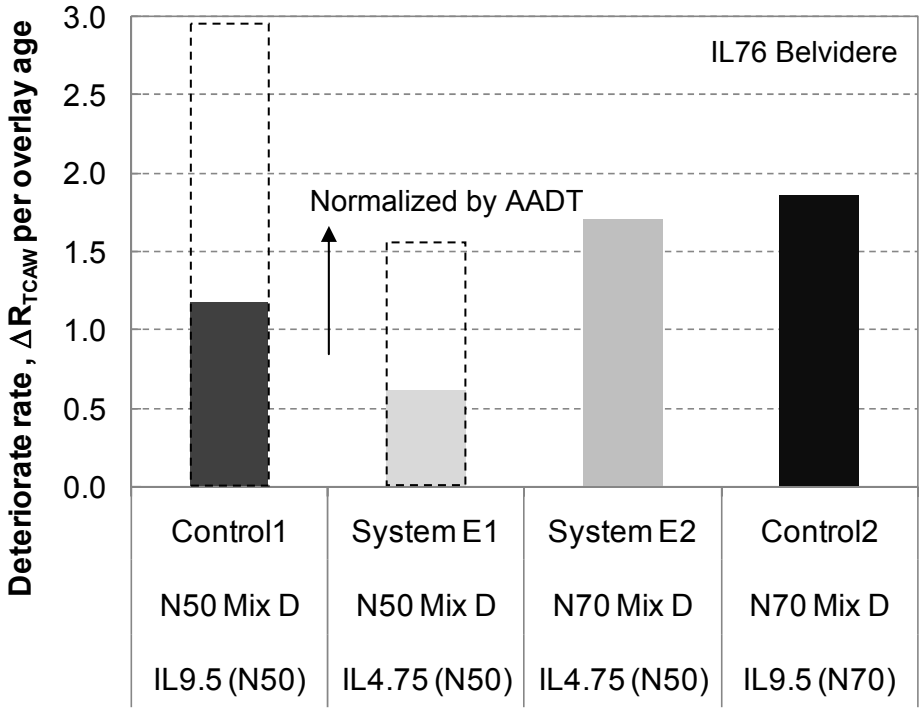

Figure A.3.4. Comparisons of deterioration rate, ΔR_{TCAW} per year on the control and treated sections with System E.

In order to investigate the effect of the interlayer system on crack severity as well as extent, performance benefit ratio of the System E is compared at two AADT levels (Figure A.13.5). The performance benefit ratio at relatively lower AADT level is 1.9 times higher than that at the higher AADT level. It is, herein, noticed that the control2 segment has N70 mixture in the level binder and the System E2 segment has N50 mixture for the IL 4.75 mixture. So, the performance benefit ratio was affected by the compaction level. If the same compaction level of level binder is used, somehow less performance benefit ratio could be obtained. In spite of this dissimilarity, it is clear that the performance of the System E depends upon traffic volume and can be better at lower volume road.

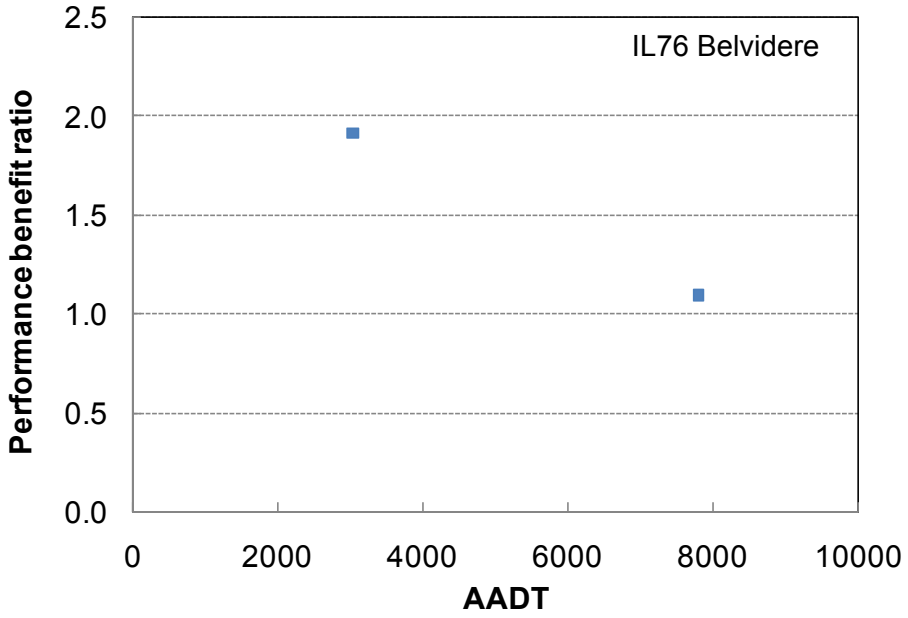

Figure A.3.5. Performance benefit ratio of the System E to the control section at different AADT levels.

A.3.4 SUMMARY OF SECTION EVALUATION

One task was performed in 2006 at IL76 Belvidere. Table A.3.2 summarizes the conducted survey and analysis.

Table A.3.2. Summary for IL76, Belvidere

Year	2006	2007
Survey	Visual crack survey Video crack survey	N/A
Forensic investigation Analysis	Crack	

From the IL76 Belvidere section, the interlayer system evaluation and findings are presented as follows:

- Regarding reflective cracking, mixture type of level binder affects more than that of surface mixture.
- Compared to the control section, the System E performs better to abate reflective cracking than the control section.
- The performance benefit ratio of the System E is dependent on traffic volume: the better performance the System E can achieve, the lower traffic volume HMA overlay has.
- The performance benefit ratio of the System E to the control section is 1.09 at 7800 AADT and 1.90 at 3050 AADT.

A.4 IL 251 NORTH OF US 30; CONTRACT NO. 84995

A.4.1 SECTION DESCRIPTION

This project, IL251 north of US 30 (Contract No. 84995), was completed in November1995. The project is located at Bureau County, District 2, Illinois, as shown in Figure A.4.1. It has one lane in each direction: northbound and southbound (Figure A.4.2). Existing pavement system consists of JCP and 4 in. HMA overlays. The thickness and joint spacing of the existing JCP is unknown. 3.0 in. new MHA overlay was placed on existing HMA overlay (3.0 in. wearing surface with AC-10 binder). The treatment used in this project was area-type System A made of AmoPave. There are two 500-ft-long sections for a control (STA.1597+50 to STA. 1592+50) and for a treated control (STA.1432+50 to STA. 1427+50). This evaluation considered two lanes in both directions. Traffic volume in 1998 was reported as 1200 AADT (100 MU and 50 SU). Also, in 2008, AADT is the same as 1200 but MU and SU are 154 and 51, respectively, according to traffic map on IDOT.

Figure A.4.1 Section location.

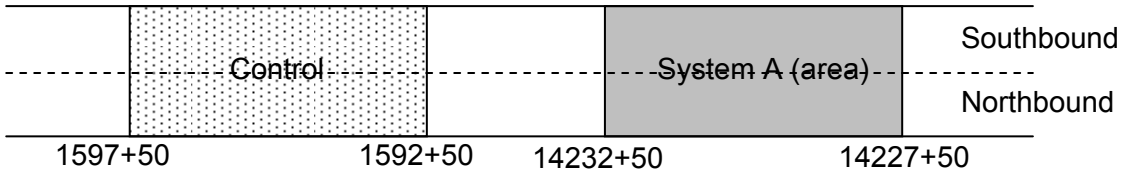

Figure A.4.2. Section layout.

A.4.2 FIELD EVALUATION

A.4.2.1 Survey

The UIUC research team conducted visual and video survey to quantify surface cracking on Sep. 17, 2006. A 1000-ft-long section was surveyed (2 x 500 ft in both lanes). The crack severity of this section was monitored in 1998. The same surveying criteria were used in this evaluation. The severity and extent of transverse cracks were reported. Most of transverse cracks belonged to low- and medium-severity levels. For transverse cracks, maintenance such as crack sealing has not been done well. Thus, highly deteriorated reflective cracking was observed (Figure A.4.3.3 (a)). As Figure A.4.3.3 (b) shows, an

additional crack (upper) was developed after a half-length crack was sealed. Along a wheel path, either sealed or not longitudinal cracks were also found in both directions (Figure A.4.3 (c)). It might be guessed as either fatigue cracks or longitudinal reflective cracks at shoulder joints. Right after visual crack survey, a GPR and video survey was scheduled, but they were stopped by raining (Figure A.4.3.3 (d)).

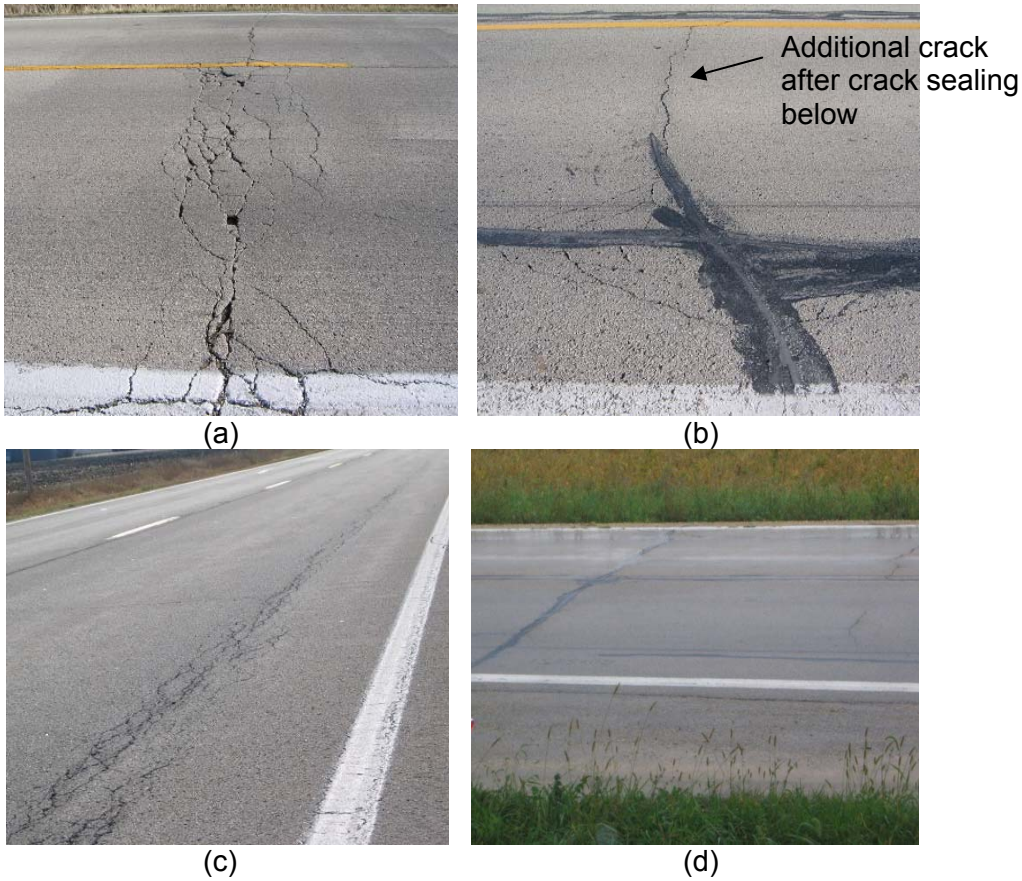

Figure A.4.3. (a) Unsealed transverse cracks and (b) Sealed center and edge longitudinal cracks.

A.4.3. DATA ANALYSIS

A.4.3.1 Crack Analysis

For data analysis of this section, extent and severity of reflective cracking is utilized to compute uniform, R_{TCA}, and weight, R_{TCAW}, transverse cracking appearance rates. All transverse cracks are included for the evaluation. Table A.4.1 summarizes the crack survey results for the control and treated sections. In both sections, a quite large number of low-and medium-severity-level cracks were developed during the past eight years. Of the all cracks regardless crack severity, 50% more transverse cracks occurred in the control section than in the treated section.

In order to investigate the effect of the interlayers on crack severity as well as extent, R_{TCA} and R_{TCAW} are compared with respect to overlay age in Figure A.4.4. For both sections, R_{TCA} and R_{TCAW} increase linearly. This indicates that while new cracks were developed, existing cracks were further deteriorated. Using R_{TCWA}, a constant deterioration rate is obtained: 1.047 and $0.726R_{TCWA}$ per overlay age. Therefore, the area-type System A shows better performance to delay the occurrence of reflective

cracking as well as to mitigate the deterioration of the reflective cracking. Based on the deterioration rates, the performance benefit ratio of the area-type System A becomes 1.44.

Table A.4.1. Summary of Crack Survey

	Control section (1000 ft)		System A (area) section (1000 ft)	
Severity	6/25/98	9/17/06	6/25/98	9/17/06
S	0	4	0	2
L	6	38	2	17
M	7	22	5	19
H	0	0	0	3
# Crack	13	64	7	41
R_{TCA}	1.3	6.4	0.7	4.1
R_{TCAW}	2.6	11.4	1.5	8.0

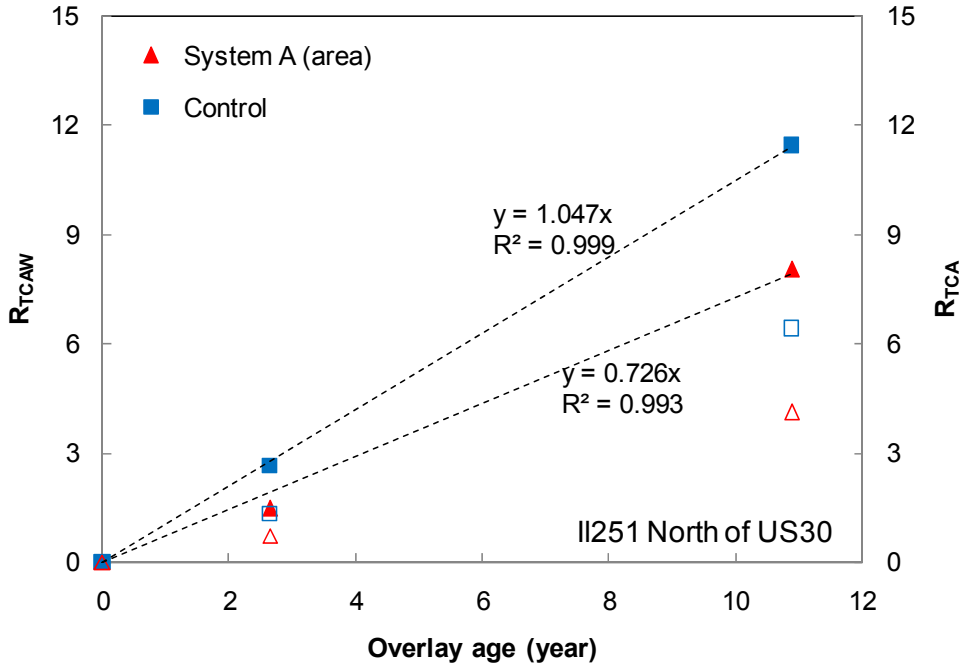

Figure A.4.4. Comparisons of the number of reflective cracks on the system B and system D interlayer systems.

A.4.4 SUMMARY OF SECTION EVALUATION

One task was performed in 2006 at IL 271 north of US 30. Table A.4.2 summarizes the conducted survey and analysis.

Table A.4.2. Summary for IL 251 north of US 30

Year	2006	2007
Survey	Visual crack survey	N/A
Forensic investigation Analysis	Transverse crack	

From the IL 251 section, the interlayer system evaluation and finding are presented as follows:

- Compared to the control section, the area-type System A performs better to abate reflective cracking.
- The performance benefit ratio of the area-type System is 1.44.

A.5 US 34 MENDOTA; CONTRACT NO. 64141

A.5.1 SECTION DESCRIPTION

This project, US 34 Mendota (Contract No. 64141), was completed in September 1997. The project is located at Bureau and La Salle County, District 2, Illinois, as shown in Figure A.5.1. The evaluated section is 7.7-mile-long between La Moille and Mendota (STA. 66+421 to 75+623 and 0+000 to 3.217, metric). It has one lane in each direction: westbound and eastbound. The pavement system consists of JCP with HMA overlay. The thickness and joint spacing of the existing JCP is unknown. After 1.5 in. milling, 2.0 in. new MHA overlay was placed on existing HMA overlay (1.25 in. wearing surface and 0.75 in. leveling binder with AC-10). The treatment used in this project was area-type System A made of Petromat. The fabric was installed right on the level binder in both directions. Two consecutive 500-ft-long sections for a control (STA.72+400 to 72+550) and for a treated control (STA.72+550 to 72+700) were evaluated (Figure A.5.2). This evaluation considered two lanes in both directions. Traffic volume in 2008 was reported as 2300 AADT (95 MU and 95 SU) according to traffic map on IDOT.

(a)

La Moille

Mendota

Figure A.5.1 Section location.

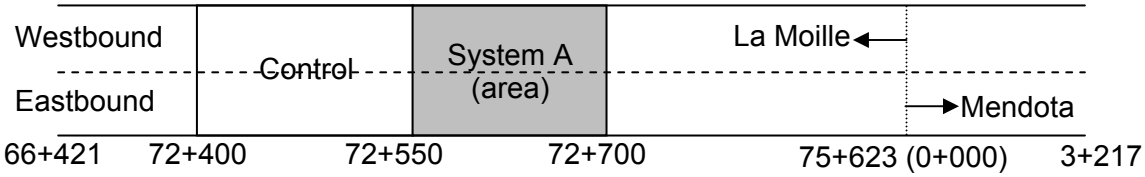

Figure A.5.2. Section layout.

A.5.2 FIELD EVALUATION

A.5.2.1 Survey

The UIUC research team conducted visual and video survey to quantify surface cracking on Sep. 16, 2006. A 1000-ft-long section was surveyed (2 x 500 ft in both lanes). The crack severity of this section has been monitored since 2003. The same surveying criteria were used in this evaluation. The severity and extent of transverse cracks were reported. Most of transverse cracks belonged to low- and medium-severity levels and were not sealed (Figure A.5.3.3). A typical double reflective cracking was found under a wheel path; single reflective cracking occurred out of the wheel path (Figure A.5.3.3 (b)).

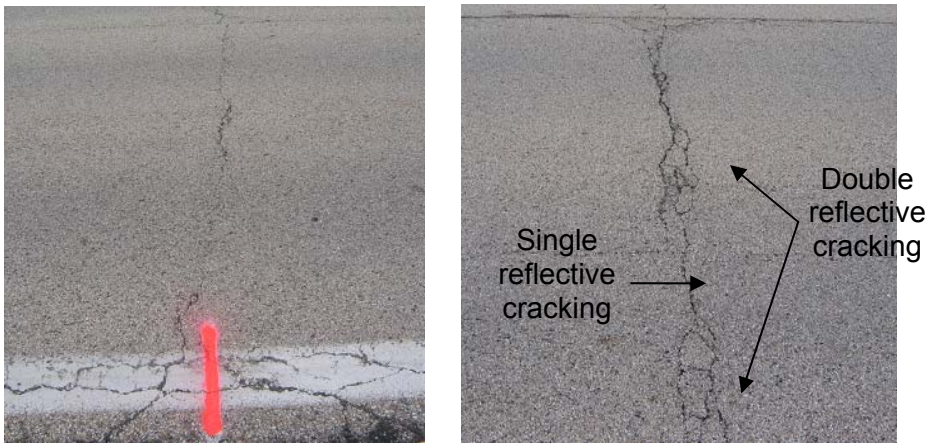

(a) (b)

Figure A.5.3. (a) Low-severity-level cracking and (b) medium-severity-level of single and double reflective cracking.

A.5.3 DATA ANALYSIS

A.5.3.1 Crack Analysis

For data analysis of this section, extent and severity of reflective cracking is utilized to compute uniform, R_{TCA}, and weight, R_{TCAW}, transverse cracking appearance rates. All transverse cracks are included for the evaluation. Table A.5.1 summarizes the crack survey results for the control and treated sections. In both sections, a quite large number of low-and medium-severity-level cracks were developed during the past nine years. Of the all cracks regardless crack severity, 20% less transverse cracks occurred in the treated section than in the control section.

Table A.5.1. Summary of Crack Survey

	Control section (1000 ft)			
Severity	6/1/03	8/13/04	8/17/05	6/20/06
S	7	7	7	2
L	37	19	15	44
M	7	29	33	20
H	0	0	2	0
# Crack	51	55	57	66
R_{TCA}	5.1	5.5	5.7	6.6
R_{TCAW}	7.7	9.9	10.8	11.3
	System A (area) section (1000 ft)			
Severity	8/14/03	9/30/04	8/30/05	9/16/06
S	13	15	11	5
L	51	32	29	49
M	4	25	33	27
H	0	2	5	1
# Crack	68	74	78	82
R_{TCA}	6.8	7.4	7.8	8.2
R_{TCAW}	9.5	12.2	14.1	14.1

In order to investigate the effect of the interlayers on crack severity as well as extent, R_{TCA} and R_{TCAW} are compared with respect to overlay age in Figure A.5.4. For both sections, R_{TCA} and R_{TCAW} increase linearly. Using R_{TCWA}, a constant deterioration rate is obtained: 1.655 and 1.314R_{TCWA} per overlay age for the control and treated section, respectively. Therefore, the area-type System A shows better performance to delay the occurrence of reflective cracking as well as to mitigate the deterioration of the reflective cracking. Based on the deterioration rates, the performance benefit ratio of the area-type System A becomes 1.26.

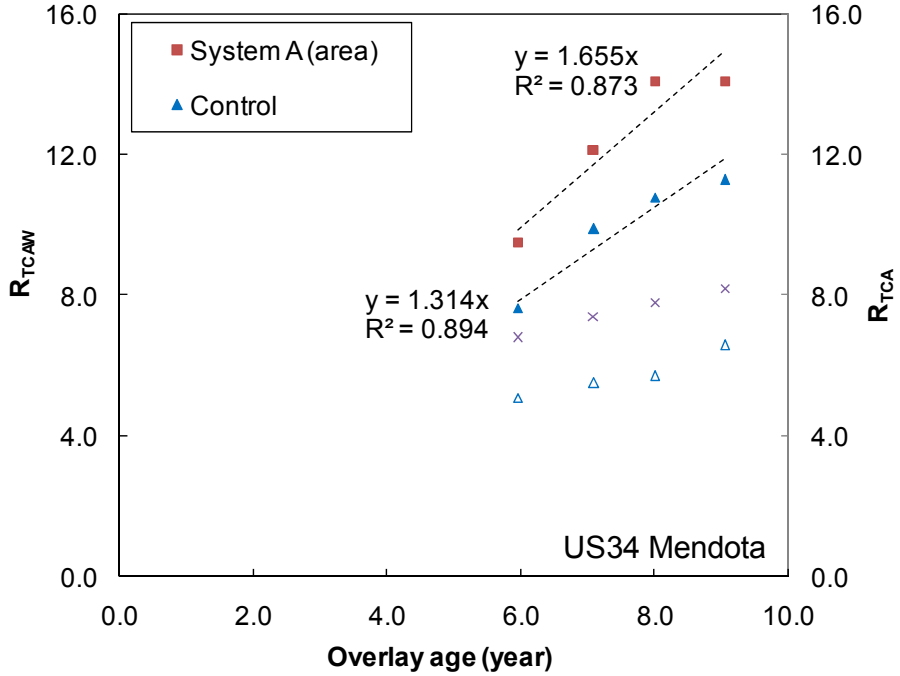

Figure A.5.4. Comparisons of the R_{TCAW} and R_{TCA} on the area-type System A and control sections.

A.5.4 SUMMARY OF SECTION EVALUATION

One task was performed in 2006 at US 34 Mendota. Table A.5.2 summarizes the conducted survey and analysis.

Table A.5.2. Summary for US 34 Mendota

Year	2006	2007
Survey	Visual crack survey	N/A
Forensic investigation Analysis	Transverse crack	

From the US 34 Mendota section, the interlayer system evaluation and finding are presented as follows:

- Compared to the control section, the area-type System A performs better to abate reflective cracking.
- The performance benefit ratio of the area-type System is 1.26.

A.6 IL 178 OGLESBY; CONTRACT NO. 86102

A.6.1 SECTION DESCRIPTION

This project, IL 178 Oglesby (Contract No. 86102), was completed in September 1990. The project is located southeast of Oglesby and south to Lowell at La Salle County, District 3, Illinois, as shown in Figure A.6.1. It has one lane in each direction: northbound and southbound. The pavement system consists of JCP with HMA overlay. The existing JCP has varied thickness (9-6-9). Joint spacing was unknown. 2.5 in. new MHA overlay was placed on existing HMA overlay (1.5 in. wearing surface and 1.0 in. leveling binder). The treatment used in this project was strip-type System A made of Phillips Fiber same as ProGuard. The fabric was installed right on the existing overlay in both directions. The locations of the strips were not identified. The evaluated section has a 500-ft-long treated section (STA. 20+00 to 25+00) and a 425-ft-long control section in southbound (STA. 7+00 to 11+26). Traffic volume in 1998 was reported as 3850 AADT (325 MU and 175 SU). In 2008, traffic volume decreased in that the section had 2650 AADT (273 MU and 227 SU) according to traffic map on IDOT.

(a)

(b)

Figure A.6.1 Section location.

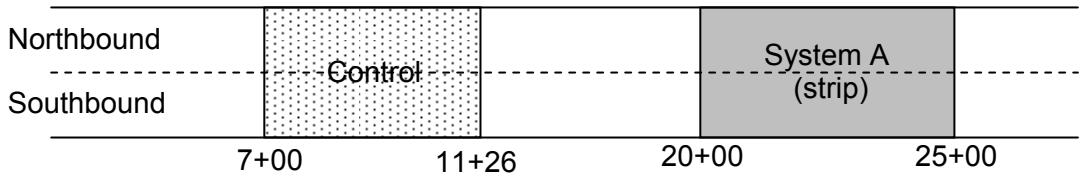

Figure A.6.2. Section layout.

A.6.2 FIELD EVALUATION

A.6.2.1 Survey

The UIUC research team conducted visual and video survey to quantify surface cracking on Sep. 16, 2006. An 1850-ft-long section was surveyed (2 x 500 ft for the treated section and 2 x 425 ft for the control section). The crack severity of this section was measured in 1998. The same surveying criteria were used in this evaluation. The severity and extent of transverse cracks were reported. Majority of transverse cracks belongs to the medium-severity level. Highly deteriorated cracks were also observed in transverse direction and they were channelized to longitudinal cracks (Figure A.6.3.3 (a)). However, most of cracks observed were unsealed. Block cracking was often observed in the treated section (Figure A.6.3.3 (b)).

(a) (b)

Figure A.6.3. (a) High-severity-level cracking and (b) block cracking.

A.6.3 DATA ANALYSIS

A.6.3.1 Crack Analysis

For data analysis of this section, extent and severity of reflective cracking is utilized to compute uniform, R_{TCA}, and weight, R_{TCAW}, transverse cracking appearance rates. While the use of R_{RCA} or R_{RCAW} is preferred for the strip-type interlayer evaluation, all transverse cracks were included in this analysis since the application locations of the strips were not identified. Table A.6.1 summarizes the crack survey results for the control and treated sections. A quite large number of cracks were developed and also the severity of the cracks became worse during the past eight years. As not expected, 50% more transverse cracks occurred in the treated section than in the control section.

Table A.6.1. Summary of Crack Survey

	Control section (850 ft)		System A (strip) section (1000 ft)	
Severity	6/25/98	9/16/06	6/25/98	9/16/06
S	0	1	0	2
L	1	21	6	25
M	20	25	16	51
H	5	4	0	14
# Crack	27	53	54	92
R_{TCA}	3.2	6.2	5.4	9.2
R_{TCAW}	7.4	12.3	10.5	19.5

In order to investigate the effect of the interlayers on crack severity as well as extent, R_{TCA} and R_{TCAW} are compared with respect to overlay age in Figure A.6.4. For both sections, R_{TCA} and R_{TCAW} increase linearly. Using R_{TCWA}, a constant deterioration rate is obtained: 0.802 and 1.238R_{TCWA} per overlay age for the control and treated section, respectively. Therefore, the strip-type System A shows worse performance to delay the occurrence of reflective cracking as well as to mitigate the deterioration of the reflective cracking. Based on the deterioration rates, the performance benefit ratio of the strip-type System A becomes 0.65 which is less than 1.0. Thus, the strip-type System A does not have any performance benefit on retarding reflective cracking.

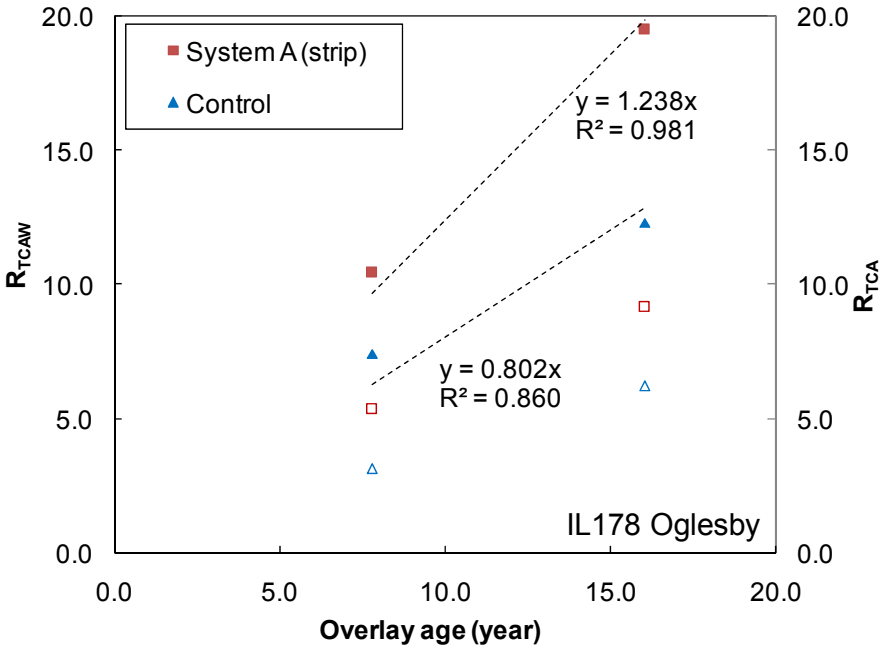

Figure A.6.4. Comparisons of the R_{TCAW} and R_{TCA} on the strip-type System A and control sections.

A.6.4 SUMMARY OF SECTION EVALUATION

One task was performed in 2006 at IL 178 Oglesby. Table A.6.2 summarizes the conducted survey and analysis.

Table A.6.2. Summary for IL 178 Oglesby

Year	2006	2007
Survey	Visual crack survey Video crack survey	N/A
Forensic investigation Analysis	Transverse crack	

From the IL 178 Oglesby section, the interlayer system evaluation and finding are presented as follows:

- Compared to the control section, the strip-type System A performs worse to abate reflective cracking.
- The performance benefit ratio of the strip-type System is 0.65.

A.7 IL 9 PRAIRIE CITY; CONTRACT NO. 88019

A.7.1 SECTION DESCRIPTION

This project, IL 9 Prairie City (Contract No. 88019), was completed in 1988. The project is located at east of IL 41 close to Macomb, McDonough County, District 4, Illinois, as shown in Figure A.7.1. It has one lane in each direction: westbound and eastbound. Existing pavement system consists of JCP and 3 in. HMA overlays. The thickness of the existing JCP is 9-6-9. 2.0 in. new MHA overlay was placed on existing HMA overlay (1.25 in. wearing surface and 0.75 in. level binder with AC-10 binder). The treatment used in this project was area-type System A made of Petromat. There are two 500-ft-long sections for a control (STA.519+00 to 524+00) and for a treated control (STA.573+00 to 578+00) as shown in Figure A.7.2. This evaluation considered two lanes in both directions. Traffic volume in 2003 was reported as 875 AADT (125 MU and 60 SU). Also, in 2008, AADT is 950 (54 MU and 96 SU) according to traffic map on IDOT.

(a)

(b)

Figure A.7.1 Section location.

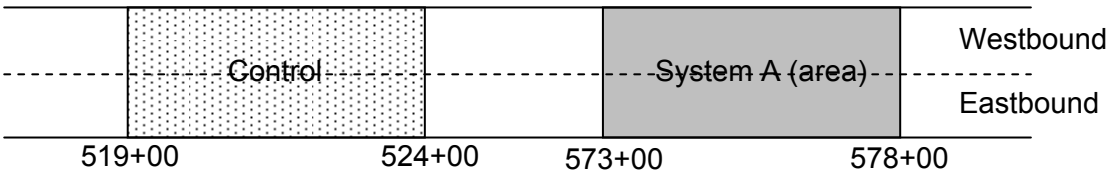

Figure A.7.2. Section layout.

A.7.2 FIELD EVALUATION

A.7.2.1 Survey

The UIUC research team conducted visual survey to quantify surface cracking on Nov. 26, 2006. A 1000-ft-long section was surveyed (2 x 500 ft in both lanes). The crack severity of this section was monitored in 1998. The same surveying criteria were used in this evaluation. The severity and extent of transverse cracks were reported. Most of transverse cracks belonged to medium- and high-severity levels. All cracks did not receive crack sealing though highly deteriorated reflective cracking was observed (Figure A.7.3.3 (a)). Those highly deteriorate transverse and longitudinal cracks were linked and so looked like block cracking. Since too many cracks were observed in this section, it was hard to distinguish reflective cracking from those transverse cracks.

(a) (b)

Figure A.7.3. (a) Unsealed high-severity-level transverse cracking and (b) unsealed middle and edge longitudinal cracks.

A.7.3 DATA ANALYSIS

A.7.3.1 Crack Analysis

For data analysis of this section, extent and severity of reflective cracking is utilized to compute uniform, R_{TCA}, and weight, R_{TCAW}, transverse cracking appearance rates. All transverse cracks are included for the evaluation. Table A.7.1 summarizes the crack survey results for the control and treated sections. In both sections, a quite large number of cracks were developed and highly deteriorated during the past eight years. Of the all cracks regardless crack severity, 10% less transverse cracks occurred in the treated section than in the control section.

In order to investigate the effect of the interlayers on crack severity as well as extent, R_{TCA} and R_{TCAW} are compared with respect to overlay age in Figure A.7.4. For both sections, R_{TCA} and R_{TCAW} increase linearly. Herein, the slope of those R_{TCA} curves is

much higher than R_{TCAW}. It indicates that existing cracks were further deteriorated rather instead new cracks were created. Using R_{TCAW}, a constant deterioration rate is obtained: 1.248 and 1.196R_{TCWA} per overlay age from the control and treated section, respectively. Consequently, the performance benefit ratio of the area-type System A becomes 1.04.

Table A.7.1. Summary of Crack Survey

	Control section (1000 ft)		System A (area) section (1000 ft)	
Severity	6/22/98	11/26/06	6/22/98	11/26/06
S	15	0	28	0
L	66	23	56	10
M	0	46	0	45
H	0	31	0	36
# Crack	81	104	84	93
R_{TCA}	8.1	10.4	8.4	9.3
R_{TCAW}	11.0	23.9	10.5	23.0

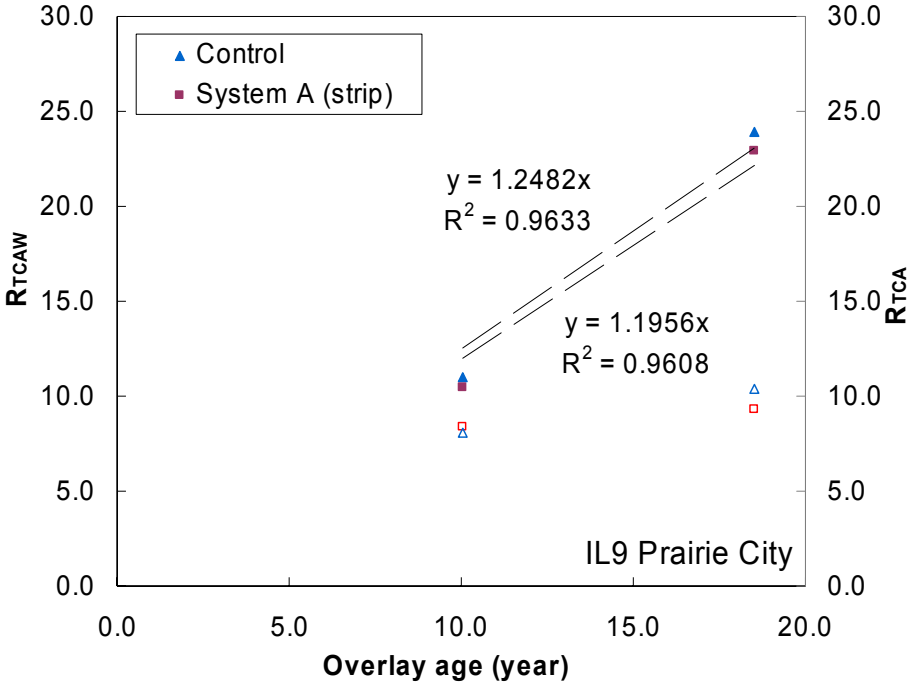

Figure A.7.4. Comparisons of the number of reflective cracks on the system B and system D interlayer systems.

A.7.4 SUMMARY OF SECTION EVALUATION

One task was performed in 2006 at IL 9 Prairie City, east of IL 41. Table A.7.2 summarizes the conducted survey and analysis.

Table A.7.2. Summary for IL 9 Prairie City

Year	2006	2007
Survey	Visual crack survey	N/A
Forensic investigation Analysis	Transverse crack	

From the IL 9 Prairie City section, the interlayer system evaluation and finding are presented as follows:

- Compared to the control section, the area-type System A does not have performance benefit to abate reflective cracking.
- The performance benefit ratio of the area-type System is 1.04.

A.8 US 136 MACOMB; CONTRACT NO. 40229

A.8.1 SECTION DESCRIPTION

This project, US 136 Macomb (Contract No.40229), was completed in 1988. The project is located at east of IL 41 close to Macomb, McDonough County, District 4, Illinois, as shown in Figure A.8.1. It has one lane in each direction: westbound and eastbound. Existing pavement system consists of JCP and HMA overlays. The thickness of the existing JCP is 9-6-9. 2.0in new MHA overlay was placed on existing HMA overlay (1.25 in. wearing surface and 0.75 in. level binder). The treatment used in this project was area-type System A made of Petromat. There are two 500-ft-long sections as shown in Figure A.8.2. A control starts at roadside sign “136 McDonough 22” which is approximately 0.5 mile west of IL 41 junction; a treated control starts at roadside sign “Macomb 6 Carthage 34 which is 600 ft west of IL 41 junction. This evaluation considered two lanes in both directions. Traffic volume in 2003 was reported as 4450 AADT. Also, in 2008, AADT is 4200 (381 MU and 119 SU) according to traffic map on IDOT.

Figure A.8.1 Section location.

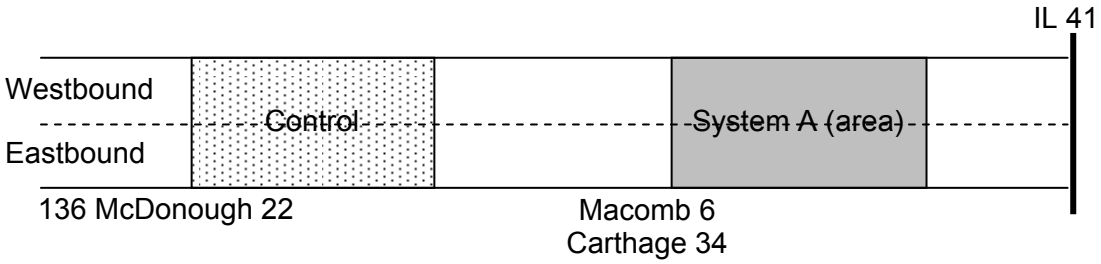

Figure A.8.2. Section layout.

A.8.2 FIELD EVALUATION

A.8.2.1 Survey

The UIUC research team conducted visual survey to quantify surface cracking on Oct. 29, 2006. A 1000-ft-long section was surveyed (2 x 500 ft in both lanes). The crack severity of this section was monitored in 1998. The same surveying criteria were used in this evaluation. The severity and extent of transverse cracks were reported. Most of transverse cracks belonged to low- and medium- -severity levels. All cracks did not receive crack sealing though intermediately deteriorated cracks were observed (Figure A.8.3.3 (a)). Transverse and longitudinal cracks were linked and so looked like block cracking. Since too many cracks were observed in this section, it was hard to distinguish reflective cracking from those transverse cracks. Moreover, it was not able to account for those linked cracks correctly in the crack index in that only transverse cracks are included but block cracks are excluded.

(a) (b)

Figure A.8.3. (a) Unsealed longitudinal and transverse cracking and (b) block cracking.

A.8.3 DATA ANALYSIS

A.8.3.1 Crack Analysis

For data analysis of this section, extent and severity of reflective cracking is utilized to compute uniform, R_{TCA}, and weight, R_{TCAW}, transverse cracking appearance rates. All transverse cracks are included for the evaluation. Table A.8.1 summarizes the crack survey results for the control and treated sections. In both sections, a quite large number of cracks were developed and linked each other. Of the all cracks regardless crack severity, 20% more transverse cracks occurred in the treated section than in the control section. However, it might not represent field crack conditions very well since the linked cracks were excluded in crack counting.

Table A.8.1. Summary of Crack Survey

	Control section (1000 ft)		System A (area) section (1000 ft)	
Severity	6/19/98	10/29/06	6/19/98	10/29/06
S	7	7	13	15
L	37	19	51	32
M	7	29	4	25
H	0	0	0	2
# Crack	51	55	68	74
R_{TCA}	5.1	5.5	6.8	7.4
R_{TCAW}	7.7	9.9	9.5	12.2

In order to investigate the effect of the interlayer systems on crack severity as well as extent, R_{TCA} and R_{TCAW} are compared with respect to overlay age in Figure A.8.4. For both sections, R_{TCA} and R_{TCAW} increase linearly. The intercept of the linear regression curves is not zero. It means that they have a different trend compared with other locations. It might result from that cracks were developed in other places such as between two parallel cracks or cross linked each other rather than the cracks were further deteriorated. It implies that this overlay materials are more sensitive to block cracking which is related to environmental conditions. So, typical approach used could not be applied for this section evaluation. Therefore, this section is excluded from the interlayer system evaluation.

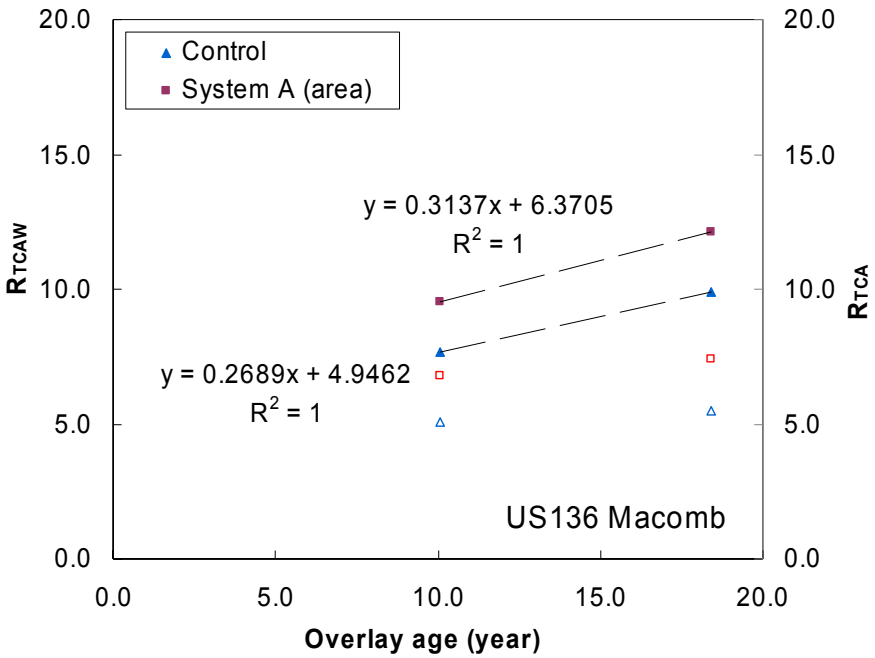

Figure A.8.4. Comparisons of the number of R_{TCAW} and R_{TCA} on the area-type System A and control sections.

A.8.4 SUMMARY OF SECTION EVALUATION

One task was performed in 2006 at US 136 Macomb, west of IL41. Table A.8.2 summarizes the conducted survey and analysis.

Table A.8.2. Summary for US 136 Macomb

Year	2006	2007
Survey	Visual crack survey	N/A
Forensic investigation Analysis	Transverse crack	

From the US 136 Macomb section, the interlayer system evaluation and finding are presented as follows:

- In the control and treated sections, transverse and longitudinal cracks were cross-linked like block cracking 18 years after the HMA overlay construction. Consequently, transverse cracking was not identified from block cracking
- Compared to the control section, the area-type System A does not show better performance benefit.

A.9 IL 29 MOSSVILLE-CHILLICOTHE; CONTRACT NO. 88707

A.9.1 SECTION DESCRIPTION

This project, IL 29 Mossville-Chillicothe (contract No. 88707), was completed in July, 1998. The section is located northeast of Peoria, Mossville to Chillicothe, Peoria County, District 4, Illinois, as shown in Figure A.9.1. 7.2-mile-long evaluated sections are between Mossville and Chillicothe (STA. 15+345 to 26+975, metric). It has two lanes in each direction: northbound and southbound (Figure A.9.2). The pavement system consists of JRCP. The thickness and joint spacing of the existing JRCP is 10 in. and 100 ft. 2.25 in. new MHA overlay was placed directly on existing JRCP (1.5 in. wearing surface and 0.75 in. level binder). Two types of materials were used for the level binder: conventional AC-20 and polymer modified MAC-10. The treatment used in this project was area-type System A made of Petromat. So, total 500-ft-long four segments are evaluated in only northbound. Traffic volume in 2003 was reported as 15800 AADT. Also, in 2008, AADT is 16400 (528 MU and 422 SU) according to traffic map on IDOT.

Figure A.9.1 Section location

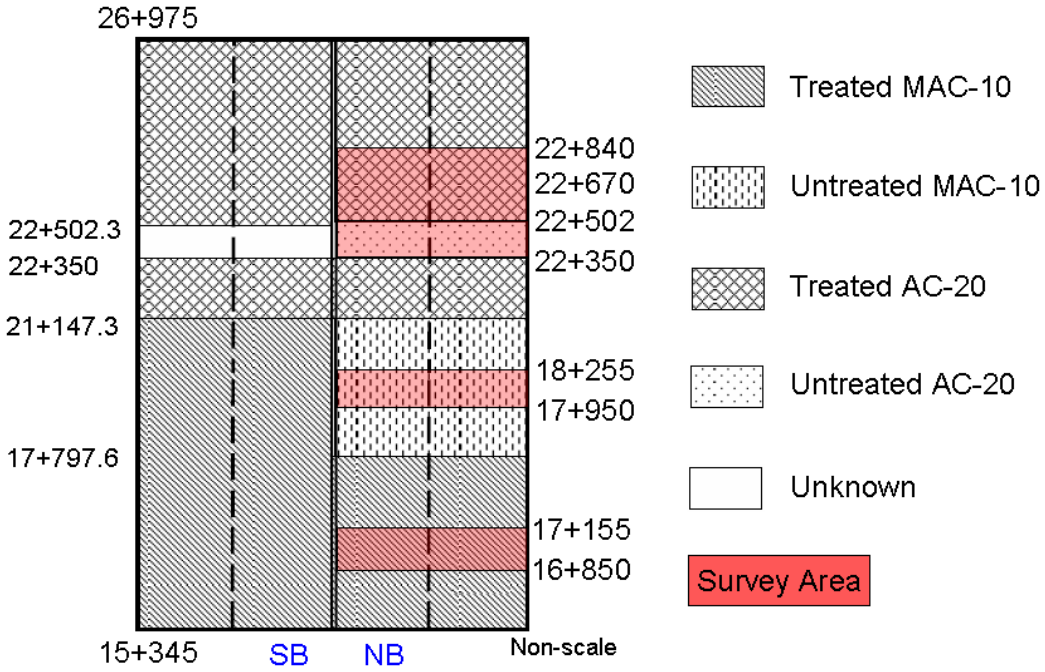

Figure A.9.2 Section Layout.

A.9.2 FIELD EVALUATION

The UIUC research team conducted a visual, video, and GPR surveys. The visual and video surveys to quantify surface cracking; while the GPR survey is to predict pavement layer thicknesses and locate interface systems. Video and GPR surveys were conducted at highway speed. Specimens were obtained through coring from the field for further testing. This task was conducted on May 22 and 23, 2006 and coordinated with IDOT researchers and District 4 (traffic control and coring crews). Additional visual crack survey was conducted on May 23, 2007.

A.9.2.1 Visual Survey

A 2500-ft-long section was surveyed (3 x 500 ft and 1 x 1000 ft in two northbound lanes). The crack severity of this section has been monitored since 2003 by IDOT. The same surveying criteria were used in this evaluation. The severity and extent of transverse cracks were reported. Figure A.9.3 shows typical reflective cracks found in this section. Joint-associated (Figure A.9.3 (a)) and patch-associated (Figure A.9.3 (b)) reflective cracking were observed. As Figure A.9.3 (a) shows, first, the sealed crack occurred under a wheel path and then the unsealed crack out of the wheel path was developed later. Other distress types were also reported.

(a) (b)

Figure A.9.3 Transverse cracking: (a) Medium and (b) High severity

A.9.2.2 Coring

Cores with 4-in and 6-in diameter were obtained from the evaluated sections (Figure A.9.4). Construction information, crack mapping, and GPR survey results were used to locate pavement joints and treatment locations. Table A.9.1 presents the number of cores and locations. Cores on top of reflective crack, in both wheel-path (WP) and between wheel-paths (BWP) were obtained. Cores for bulk testing were obtained from WP intact surface; while cores for interface shear testing were obtained from both WP and BWP over treated locations.

(a) (b)

Figure 4 Field coring work: (a) Coring locations (b) Coring samples.

Table A.9.1. Coring Details

Project	Section	Core Type	Diameter (in)	# of cores
IL 29	Mossville (MAC-10)	Permeability	6	3
		Bulk	6	3
		Interface Shear	4	3
	Chillicothe (AC-20)	Permeability	6	1
		Bulk	6	3
		Interface Shear	4	3

A.9.3 DATA ANALYSIS

A.9.3.1 Crack Analysis

For data analysis of this section, extent and severity of reflective cracking is utilized to compute uniform, R_{TCA}, and weight, R_{TCAW}, transverse cracking appearance rates. All transverse cracks are included for the evaluation. Table A.9.2 and Table A.9.3 summarize the crack survey results for the control and treated sections. In both sections, various severity levels of cracks were developed. For all levels of transverse cracks, little more transverse cracks occurred in the treated section than in the control section in both locations. Especially, 34% more cracks were developed in the Mossville sections where MAC-10 was used for overlay mixture than the Chillicothe sections where AC-20 was used.

In order to investigate the effect of the interlayer systems on crack severity as well as extent, R_{TCA} and R_{TCAW} are compared with respect to overlay age in Figure A.9.4. For both sections, R_{TCA} and R_{TCAW} increase linearly. Two curves for the control and treated sections are very close, i.e., the deterioration rates are similar each other: 1.037 and 1.124 for the control and treated section, respectively, in the Mossville and 0.8358 and 0.8754 in the Chillicothe. Thus, the performance benefit ratio of the area-type System A is 0.92 and 0.95 in the Mossville and Chillicothe section, respectively.

The deterioration rate of MAC-10 is 26% higher than that of AC-20 as shown in Figure A.9.5. binder type used in HMA overlay mixture is more sensitive than the interlayer system regarding reflective cracking.

Table A.9.2. Summary of Crack Survey for the Mossville Section

	Control section (500 ft)			
Severity	8/15/03	11/10/04	10/5/05	5/22/06
S	5	5	6	9
L	72	76	79	67
M	1	5	10	20
H	0	1	1	2
# Crack	78	87	96	99
R_{TCA}	3.9	4.4	4.8	5.0
R_{TCAW}	5.7	6.6	7.4	8.0
	System A (area) section (500 ft)			
Severity	8/15/03	11/10/04	10/5/05	5/22/06
S	2	3	1	18
L	51	49	51	38
M	7	10	12	18
H	10	16	17	22
# Crack	70	78	81	96
R_{TCA}	3.5	3.9	4.1	4.8
R_{TCAW}	6.2	7.3	7.8	8.9

Table A.9.3. Summary of Crack Survey for the Chillicothe Section

	Control section (500 ft)			
Severity	8/15/03	11/10/04	10/5/05	5/22/06
S	2	3	3	1
L	32	32	29	32
M	0	3	6	5
H	0	0	0	0
# Crack	34	38	38	38
R_{TCA}	3.4	3.8	3.8	3.8
R_{TCAW}	5.0	5.7	5.9	6.0
	System A (area) section (500 ft)			
Severity	8/15/03	11/10/04	10/5/05	5/22/06
S	3	2	5	7
L	41	45	41	24
M	7	6	6	21
H	8	9	14	16
# Crack	59	62	66	68
R_{TCA}	3.0	3.1	3.3	3.4
R_{TCAW}	5.2	5.5	6.0	6.8

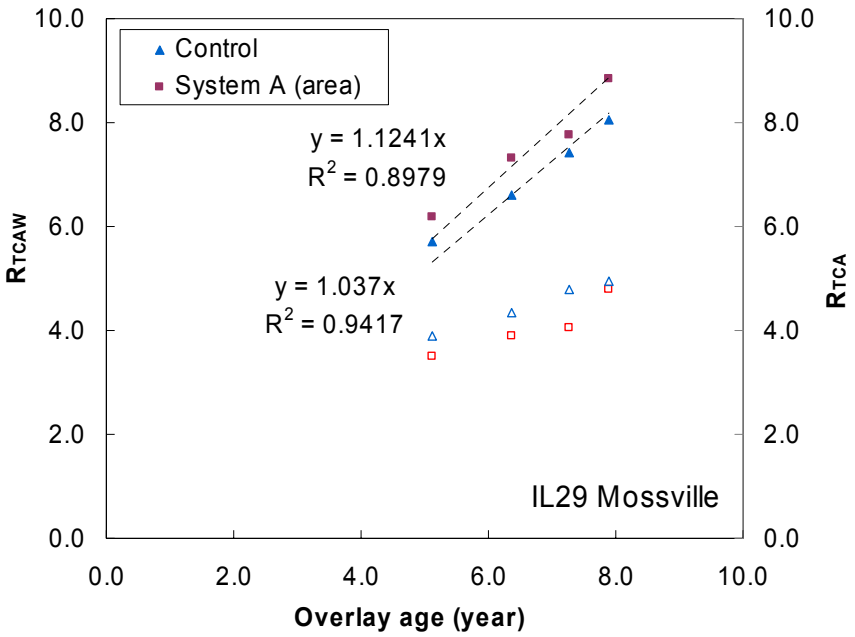

(a)

Figure A.9.4. Comparisons of the number of R_{TCAW} and R_{TCA} on the area-type System A and control sections: (a) Mossville and (b) Chillicothe.

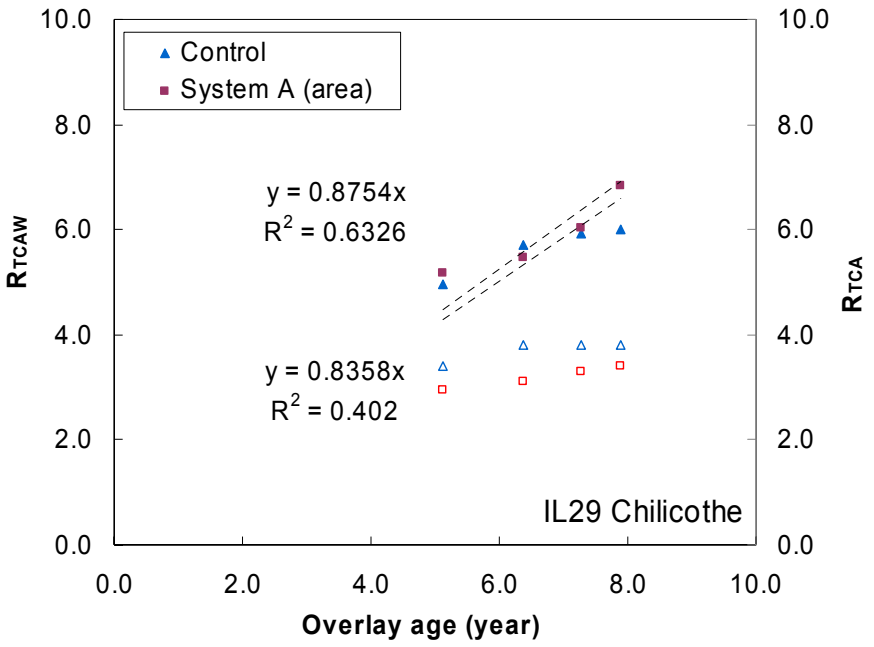

(b)

Figure A.9.4 (continued). Comparisons of the number of R_{TCAW} and R_{TCA} on the area-type System A and control sections: (a) Mossville and (b) Chillicothe.

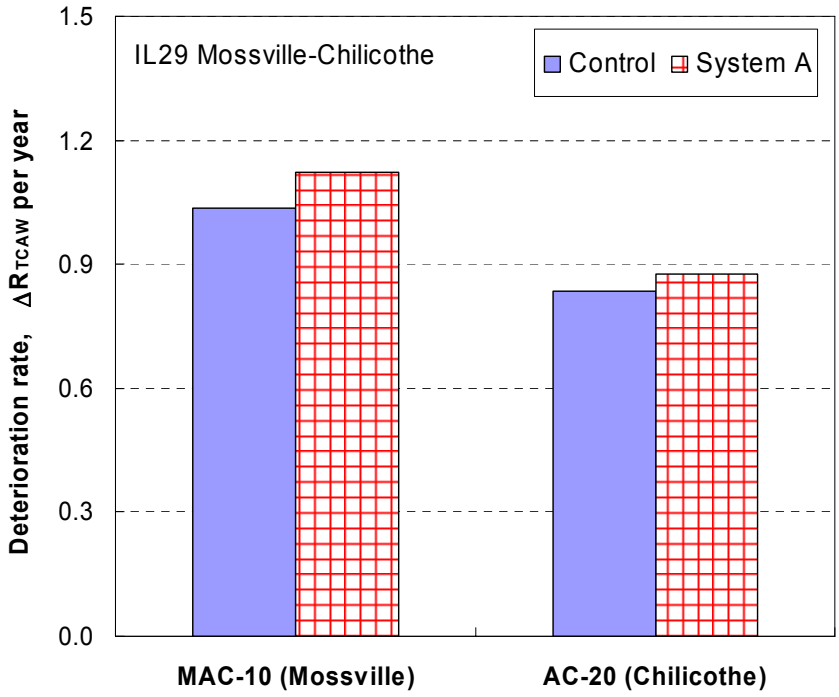

Figure A.9.5 Comparisons of deterioration rates in MAC-10 and AC-20 binder on the control and treated sections.

A.9.4. SUMMARY OF SECTION EVALUATION

One task was performed in 2006 and 2007 at IL 29 Mossville-Chillicothe. Table A.9.3 summarizes the conducted survey and analysis.

Table A.9.3. Summary for IL 29 Mossville-Chillicothe

Year	2006	2007
Survey	Visual crack survey Video crack survey GPR survey	Visual crack survey
Forensic investigation	Coring	
Analysis	Transverse crack	Transverse crack

From the IL 29 Mossville-Chillicothe section, the interlayer system evaluation and finding are presented as follows:

- Compared to the control section, the area-type System A does not show better performance benefit in both locations.
- The performance benefit ratio of the area-type System A in Mossville and Chillicothe sections is 0.92 and 0.95, respectively.
- Compared to the MAC-10 binder used in HMA overlay mixture (Mossville), AC-20 binder used in Chillicothe enhanced reflective crack resistance by a factor of 1.26.

A.10 IL 29 CHILLICOTHE; CONTRACT NO. 88707

THIS SECTION EVALUATION IS INCLUDED IN APPENDIX A.9.

A.11 IL 29/US24 PEORIA; CONTRACT NO. 88749

A.11.1 SECTION DESCRIPTION

This project, IL 29/US 24 Peoria (contract No. 88749), was completed in October, 1997. The section is located at Jefferson St., Peoria, Peoria County, District 4, Illinois, as shown in Figure A.11.1. The evaluated sections are between STA. 33+352 and 35+910 (metric). It is one-way road which has five lanes of three lanes for traffic and two outer lanes for parking. 1.5 in. new HMA overlay was constructed on existing HMA overlaid brick pavement. No level binder was used. The treatment used in this project was area-type System A made of Petromat. Prior to the overlay construction, variable depth roto-milling was executed to make crown and patching. Then, the fabric was installed on milled surface in center and west lanes between STA. 35+475 and 35+225 and all lanes between STA. 33+352 to 25+225, and 35+475 to 35+910 (Figure A.11.2). Chip seal was added by Peoria City in 2004. So, total three 830-ft-long lanes were evaluated in only southbound. Traffic volume in 2003 was reported as 13000 AADT. Also, in 2008, AADT is 10000 (440 MU and 410 SU) according to traffic map on IDOT.

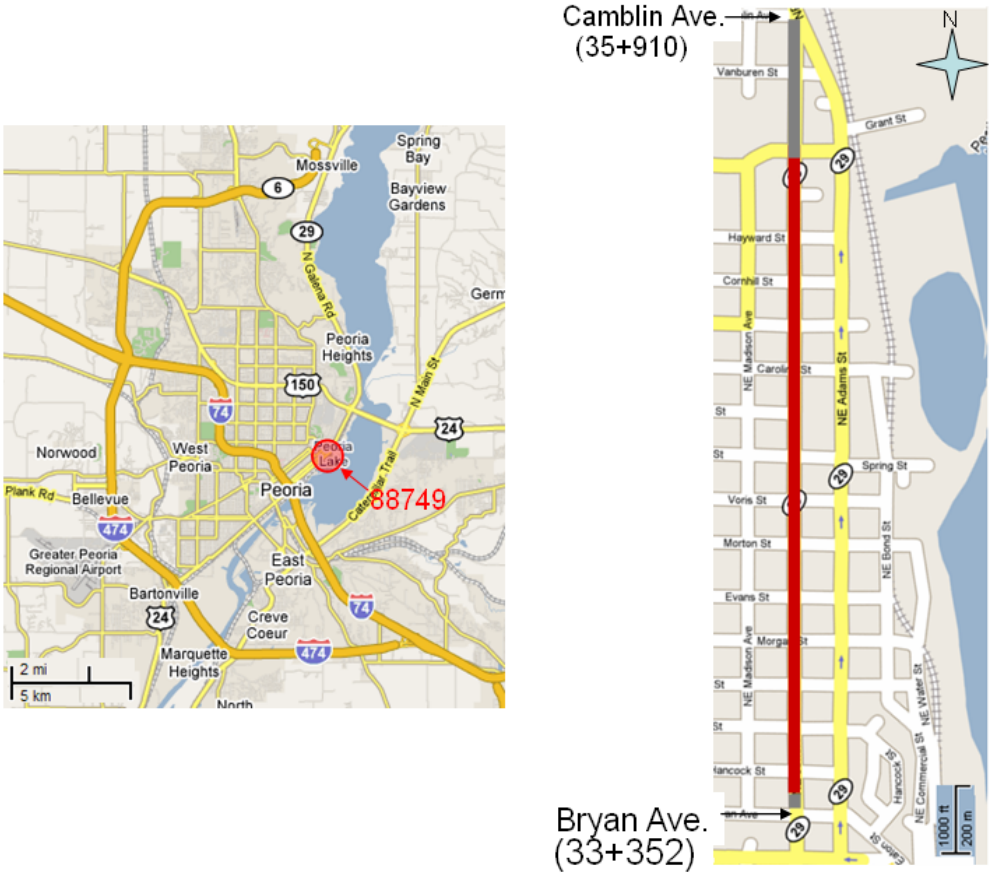

Figure A.11.1 Section location.

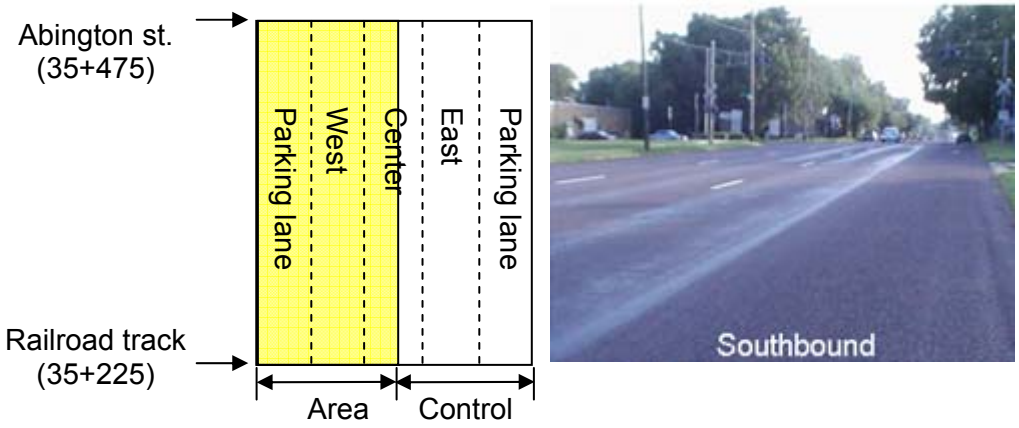

Figure A.11.2 Section layout.

A.11.2 FIELD EVALUATION

The UIUC research team conducted a visual, video, and GPR surveys. The visual and video surveys to quantify surface cracking; while the GPR survey is to predict pavement layer thicknesses and locate interface systems. Video and GPR surveys were conducted at highway speed. This task was conducted on August 5, 2006.

A.11.2.1 Survey

A 2490-ft-long section was surveyed (3 x 830 ft in center, east, and west lanes). While crack severity of this section has been monitored since 2003 by IDOT, it was no longer useful due to the application of chip seal in 2004. The same surveying criteria were used in this evaluation. The severity and extent of transverse cracks were reported. Figure A.11.3 shows typical surface conditions in this section. At the end of the evaluation section, the use of chip seal was confirmed (Figure A.11.3 (a)). Blooding was often observed in many places (Figure A.11.3 (b)). The video and GPR survey was conducted on August 6, 2006 at highway speed without moving traffic control. The survey was conducted in a weekend.

(a) (b)

Figure A.11.3 Surface conditions: (a) Chip seal and (b) bleeding.

A.11.3 DATA ANALYSIS

A.11.3.1 GPR Survey

GPR was utilized to obtain pavement thickness and joint locations. In this survey, HMA overlay and brick thickness are calculated and the condition of existing pavement are analyzed (Figure A.11.4). Based on the GPR data analysis, the average thickness of the HMA overlays and brick surface is 2.3 in. and 4 in., respectively. Also, existed full-depth repair was detected.

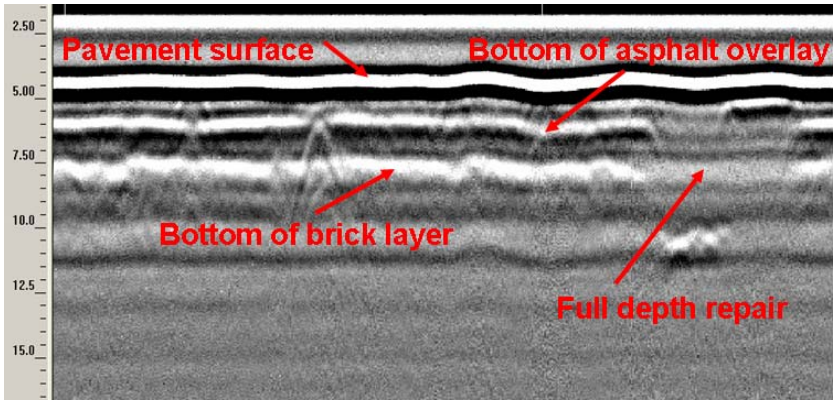

(a)

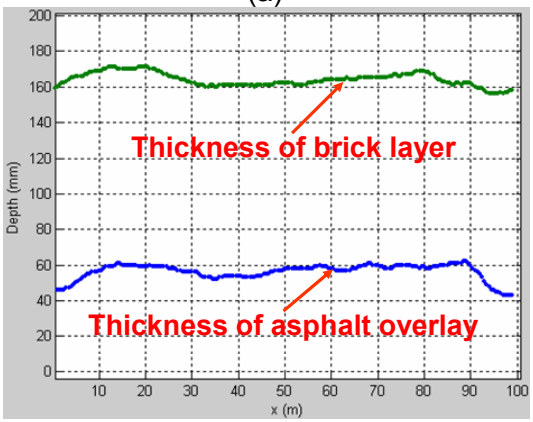

(b)

Figure A.11.4 GPR data analysis: (a) Layer configuration in depth and (b) Thickness of overlay and brick layer over section

A.11.3.2 Crack Analysis

Table A.11.1 shows crack length measured in this section. All of transverse cracks in this section excluding only two cracks are low-severity levels. Total transverse crack length is compared for each lane regardless of crack severity. The west lane has the lowest crack length, in that, the most excellent pavement condition. However, since the volume of traffic on each lane is not equivalent, i.e., the center lane has higher traffic than others, it is not reasonable to compare the results directly. It is necessary to compensate the effect of high traffic on developing cracks in the center lane if traffic data is given. Also, the half of the center lane was not treated and there is no exact information. As a simple analysis without considering traffic variable, the west lane with treatment shows 23.3% better performance of retarding reflective cracking than the east, untreated lane.

Table A.11.1 Comparison of Total Crack length for Each Lane

	Untreated	Treated	
Lane	East	Center*	West
Total transverse crack length, lane	22.7	27.4	16.2
(% to untreated section)	(100)	(131)	(76.7)
Traffic	lower	Higher	lower

* Half part of the lane was not treated.

A.11.4 SUMMARY OF SECTION EVALUATION

One task was performed in 2006 at IL 29/US 24 downtown Peoria. Table A.11.2 summarizes the conducted survey and analysis.

Table A.11.2. Summary for IL 29/US 24 Peoria

Year	2006	2007
Survey	Visual crack survey Video crack survey GPR survey	
Forensic investigation		
Analysis	Transverse crack	

From the IL 29/US 24 Peoria section, the interlayer system evaluation and finding are presented as follows:

- Compared to the control section, the area-type System A provides better performance to delay reflective cracking in lower traffic volume, but worse performance in higher traffic volume.
- Due to unexpected chip sealing in 2004, this section evaluation is excluded from global performance analysis.

A.12 US 34 KIRKWOOD; CONTRACT NO. 88044

A.12.1 SECTION DESCRIPTION

This project, US 34 Kirkwood (Contract No. 88044), was completed in 1988. The project is located south of Gladstone to south of Kirkwood, Warren County, District 4, Illinois, as shown in Figure A.12.1. It has one lane in each direction: westbound and eastbound. The pavement system consists of JCP with 3.0 in. HMA overlay. The thickness and joint spacing of the existing JCP is unknown, 2.0 in. new MHA overlay was placed on existing HMA overlay (1.25in wearing surface and 2.0 in. leveling binder). The treatment used in this project was strip-type System A made of ProGuard. The locations of the strips were not identified. The evaluated section has one 500-ft-long control and treated section (Figure A.12.2). Traffic volume in 1998 was reported as 4200 AADT. In 2008, AADT was 4250 (1020 MU and 204 SU) according to traffic map on IDOT.

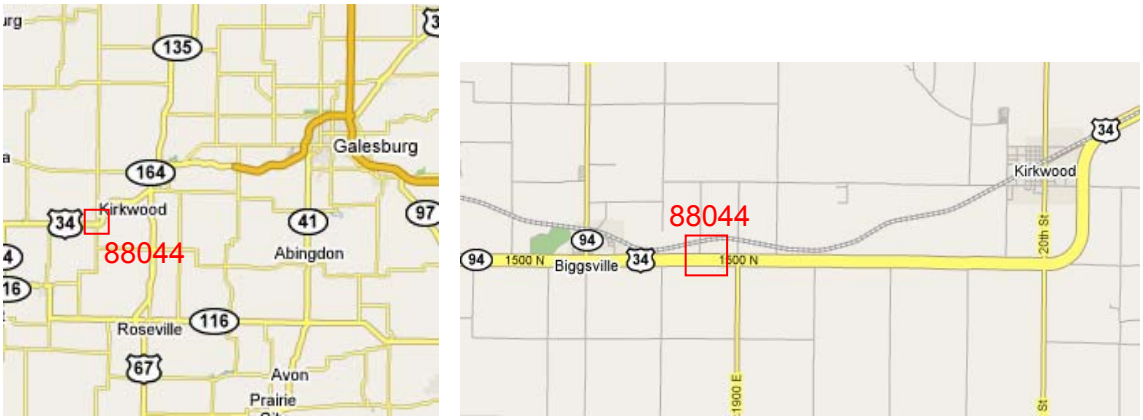

(a)

(b)

Figure A.12.1. Section location.

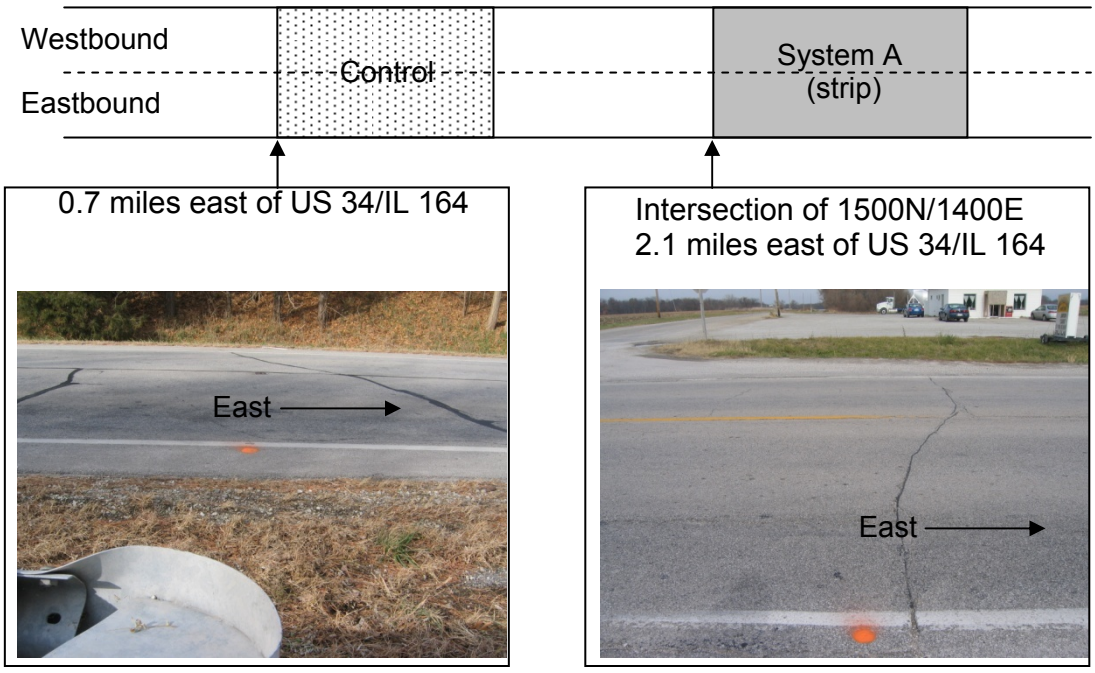

Figure A.12.2. Section layout.

A.12.2 FIELD EVALUATION

A.12.2.1 Survey

The UIUC research team conducted visual survey to quantify surface cracking on Nov. 12, 2006. A1000-ft-long section was surveyed (2 x 500 ft for the control and treated section in both directions). The crack severity of this section was measured in 1998. The same surveying criteria were used in this evaluation. The severity and extent of transverse cracks were reported. Figure A.12.3 shows typical reflective cracks found in this section: unsealed and sealed transverse crack. Other distress types were also reported.

(a) (b)

Figure A.12.3. Medium-severity-level transverse crack: (a) unsealed and (b) sealed one.

A.12.3 DATA ANALYSIS

A.12.3.1 Crack Analysis

For data analysis of this section, extent and severity of reflective cracking is utilized to compute uniform, R_{TCA}, and weight, R_{TCAW}, transverse cracking appearance rates. While the use of R_{RCA} or R_{RCAW} is preferred for the strip-type interlayer evaluation, all transverse cracks were included in this analysis since the application locations of the strips were not identified. Table A.12.1 summarizes the crack survey results for the control and treated sections. In the treated section, total number of transverse cracks increased as well as the severity of the cracks became worse. However, in the control section, majority of transverse cracks was the medium-severity level in 1998; the number of cracks did not increase during the past eight years. Moreover, one third of the medium-severity-level cracks became downgraded to the low-severity level. Those trends might result in crack sealing which could improve the crack severity. Thus, depending on maintenance procedure, the crack severity could be affected. Nonetheless, crack sealing may not affect the number of cracks. Finally, two times more transverse cracks occurred in the treated section than in the control section.

Table A.12.1. Summary of Crack Survey

	Control section (1000 ft)		System A (strip) section (1000 ft)	
Severity	6/22/98	11/12/06	6/22/98	11/12/06
S	0	0	0	3
L	7	26	99	24
M	40	21	2	38
H	0	0	0	67
# Crack	47	47	101	132
R_{TCA}	4.7	4.7	10.1	13.2
R_{TCAW}	10.4	9.2	18.0	32.9

In order to investigate the effect of the interlayers on crack severity as well as extent, R_{TCA} and R_{TCAW} are compared with respect to overlay age in Figure A.12.4. In the treated section, R_{TCA} and R_{TCAW} increase linearly while in the control section, R_{TCA} and R_{TCAW} do not increase ten years after the HMA overlay construction. Regardless, using R_{TCWA}, a constant deterioration rate is obtained: 0.6247 and $1.7911R_{TCWA}$ per overlay age for the control and treated section, respectively. Therefore, the strip-type System A shows worse performance to delay the occurrence of reflective cracking as well as to mitigate the deterioration of the reflective cracking. Based on the deterioration rates, the performance benefit ratio of the strip-type System A becomes 0.35. Thus, the strip-type System A does not have any performance benefit on retarding reflective cracking. Herein, it needs to notice that this approach to obtain the performance benefit ratio is not accurate since the R_{TCAW} does not show a good linearity in the control section. However, the trend that the treatment is not working well is valid unless there were significant rehabilitations and/or maintenances in the control section.

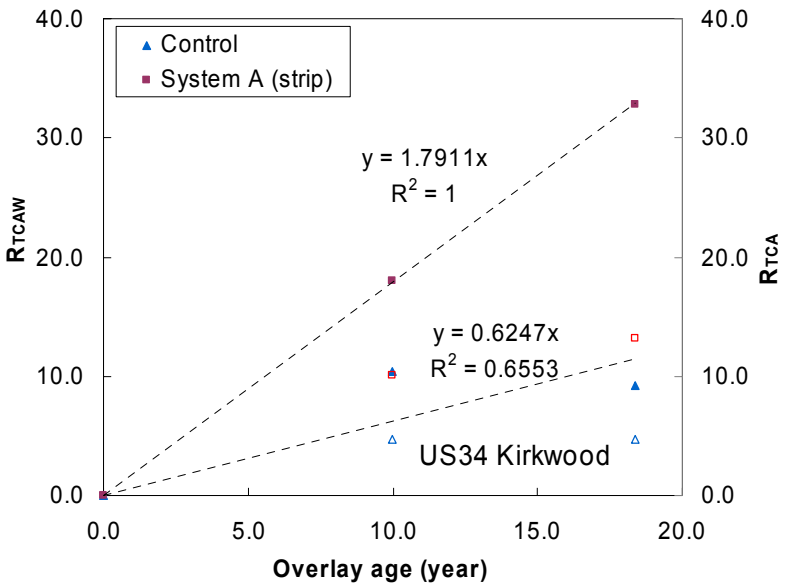

Figure A.12.4. Comparisons of the R_{TCAW} and R_{TCA} on the strip-type System A and control sections.

A.12.4 SUMMARY OF SECTION EVALUATION

One task was performed in 2006 at US 34 Kirkwood. Table A.12.2 summarizes the conducted survey and analysis.

Table A.12.2. Summary for US 34 Kirkwood

Year	2006	2007
Survey	Visual crack survey	N/A
Forensic investigation Analysis	Transverse crack	

From the US 34 Kirkwood section, the interlayer system evaluation and finding are presented as follows:

- Compared to the control section, the strip-type System A performs worse to abate reflective cracking.
- The performance benefit ratio of the strip-type System is 0.35.

A.13 IL 29 CREVE COEUR; CONTRACT NO. 88535

A.13.1 SECTION DESCRIPTION

This project, IL29 Creve Coeur (Contract No. 88535), was completed in October 1997. The project is located south of Peoria (Tazewell County, District 4), Illinois, as shown in Figure A.13.1. The evaluated section is under I-474 between on/off ramps (STA. 7+474 to 7+800, metric). It has three lanes in each direction: northbound and southbound (Figure A.13.2). The pavement system consists of JRCP with HMA overlay. The existing JRCP is 10-in. thick. The joints are spaced at 50 ft. The overlay is 2.25 in. HMA: 1.0 in. wearing surface and 1.25 in. binder level. The treatments used in this project are the following: 11 System D (ISAC) strips and 13 System B strips (PavePrep) strips in the northbound and southbound inner lanes; area-wide fabric treatments were used in the middle and outer lanes. This evaluation only considered the inner lanes. The control measurements were conducted at selected cracks/ joints without treatment. Traffic volume at the time of overlay construction in 1998 was reported as 28900 AADT (850 ADTT and 750 MU) in the previous report and in 2008 was reported as 33600 AADT (1750 ADTT and 1050 MU) according to traffic map on IDOT.

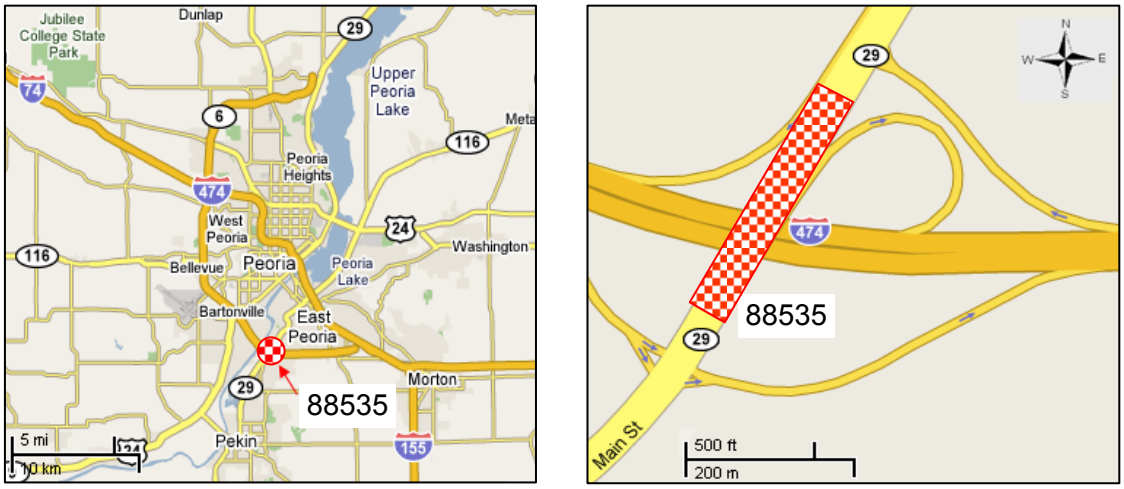

(a)

(b)

Figure A.13.2. Section location.

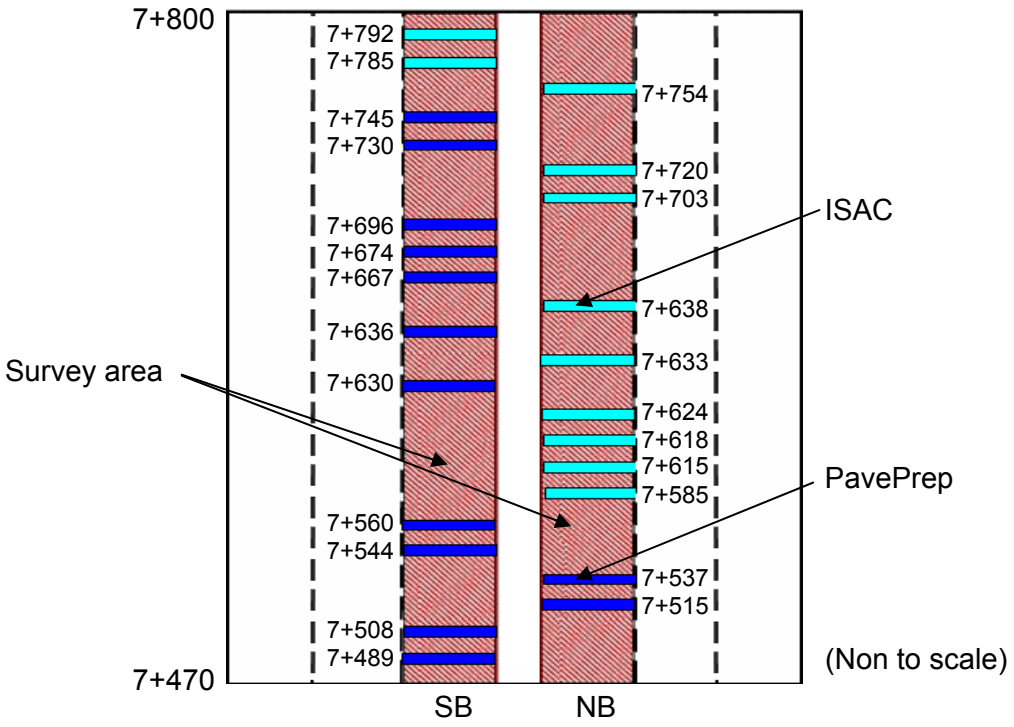

Figure A.13.2. Section layout.

A.13.2 FIELD EVALUATION

The UIUC research team conducted visual, video, and GPR surveys. The visual and video surveys quantified surface cracking; while the GPR surveys predicted pavement layer thicknesses and located interface systems. The video and GPR surveys were conducted at highway speed. Specimens were obtained through coring from the field for forensic investigation as well as laboratory testing. This task was conducted on May 22, 2006, and coordinated with IDOT researchers and District 4 (traffic control and coring crews). The survey was repeated on August 6, 2006, at highway speed without moving traffic control. The survey was conducted on a weekend. In addition, the second visual crack survey was conducted on September 23, 2007.

A.13.2.1 Visual Survey

A 2000-ft-long section was surveyed (1000-ft-long in each direction). The crack severity of this section had been monitored since 2000 by IDOT. The same surveying criteria were used in this reflective cracking evaluation. The severity and extent of transverse cracks were reported. Figure A.13.3 shows typical reflective cracks found in this section. Single (Figure A.13.3(a)) and double (Figure A.13.3(b)) reflective cracks were observed right over a joint or a-couple-of-inch shift from a joint. Reflective cracking exists along two edges of a strip and patch. Other distress types, such as block cracking, were also reported. During coring work, a video crack survey and GPR survey were conducted with a moving traffic control as shown in Figure A.13.4.

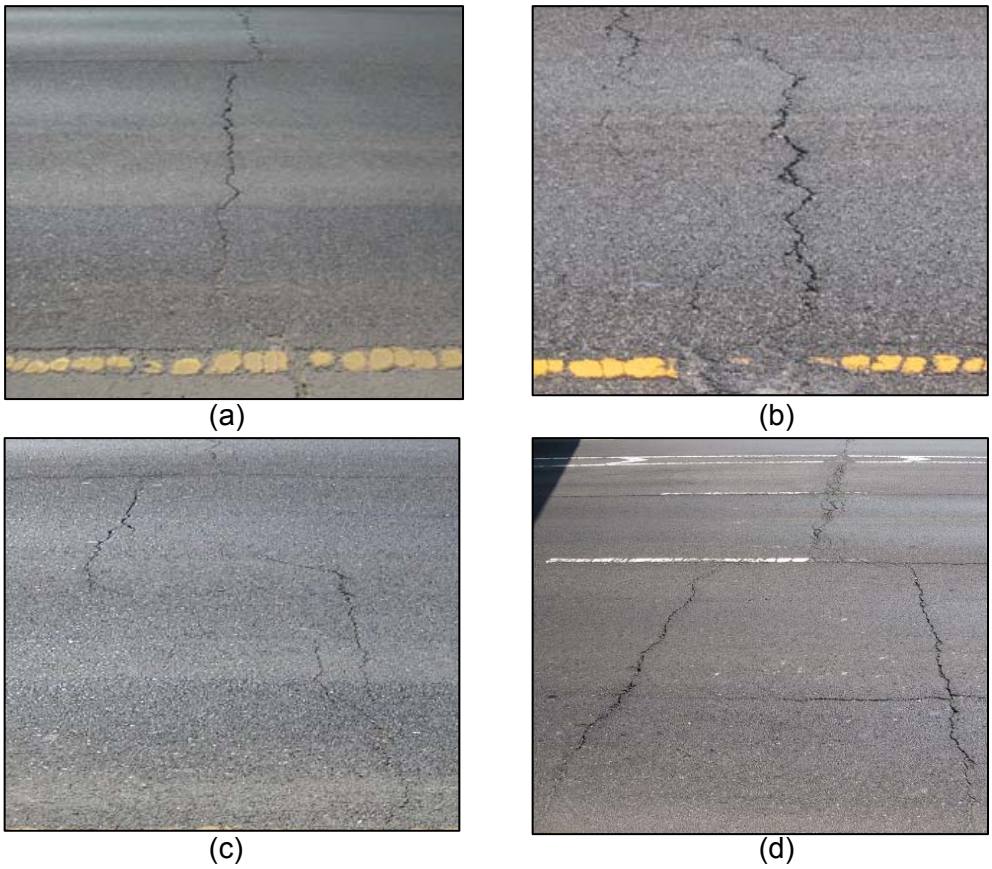

Figure A.13.3. Transverse reflective cracking: (a) a single crack; (b) double cracks; and cracks along the edge of (c) an ISAC strip and of (d) a patch.

Figure A.13.4. Video and GPR surveys with a moving traffic control.

A.13.2.2 Coring

Cores with 4-in and 6-in diameter were obtained from the evaluated sections (Figure A.13.5). Construction information, crack mapping, and GPR survey results were used to locate pavement joints and treatment locations. Table A.13.1 presents the number of cores and locations. Cores on top of reflective crack, in both wheel-path (WP) and between wheel-paths (BWP) were obtained. Cores for bulk testing were obtained from WP intact surface; while cores for interface shear testing were obtained from both WP and BWP over treated locations.

(a)

(b)

Figure A.13.5. Field coring work: (a) coring truck (b) coring locations on a transverse crack.

Table A.13.1. Coring Details

Project	Section	Core Type	# of cores
IL 29 Creve Coeur	System B (PavePrep)	Permeability Bulk Interface Shear	2 4 3
	System D (ISAC)	Permeability Bulk Interface Shear	2 0 2

A.7.2 DATA ANALYSIS

A.13.3.1 Video Survey

The quality of the video image recorded on May 22, 2006, was not good enough to use for data analysis because the video recorder was not set correctly to receive fast images at highway speed. Therefore, another trial was performed on August 6, 2006, after fine-tuning. The second video data were good enough to count the number of transverse cracks and distinguish crack severity as shown in Figure A.13.6. The captured video image is clear enough to differentiate crack extent and severity compared to the photo image. The severity is a low to medium level and coincides with the field visual survey classification.

Figure A.13.6. Comparison of video-captured and photo images at STA. 7+638.

A.13.3.2 GPR Survey

The possibility of GPR testing was examined to detect interlayer systems and joints. A 1.0 GHz air-couple antenna was selected to collect data at highway speed while video crack surveys were being conducted. Figure A.13.7 shows the GPR setup 1.0 GHz antenna running over a joint and the GPR data obtained. A scan rate of 1scan/ft of the GPR data is too fast to detect joints (or dowel bars), and the interlayer systems are too thin to be detected. However, it was possible to estimate the thickness of HMA overlay as 2.34 in. and the design overlay thickness as 2.25 in.

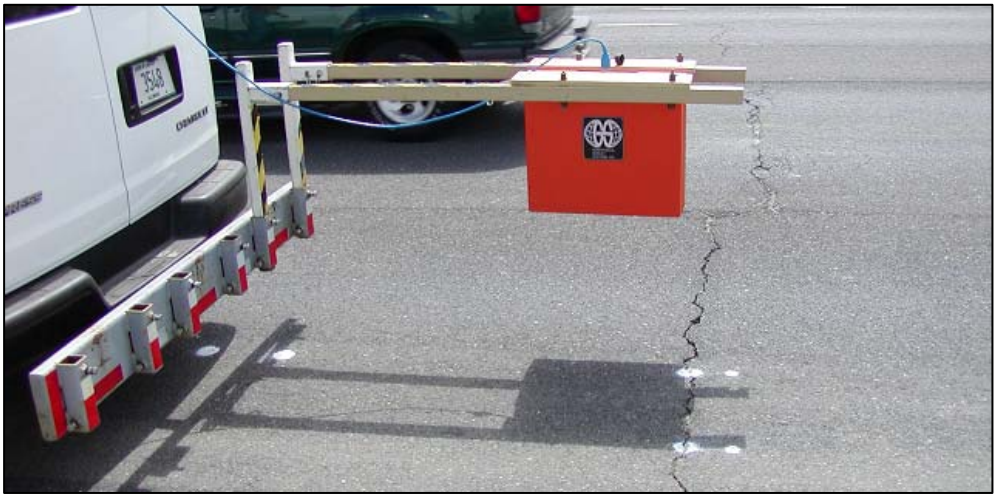

(a)

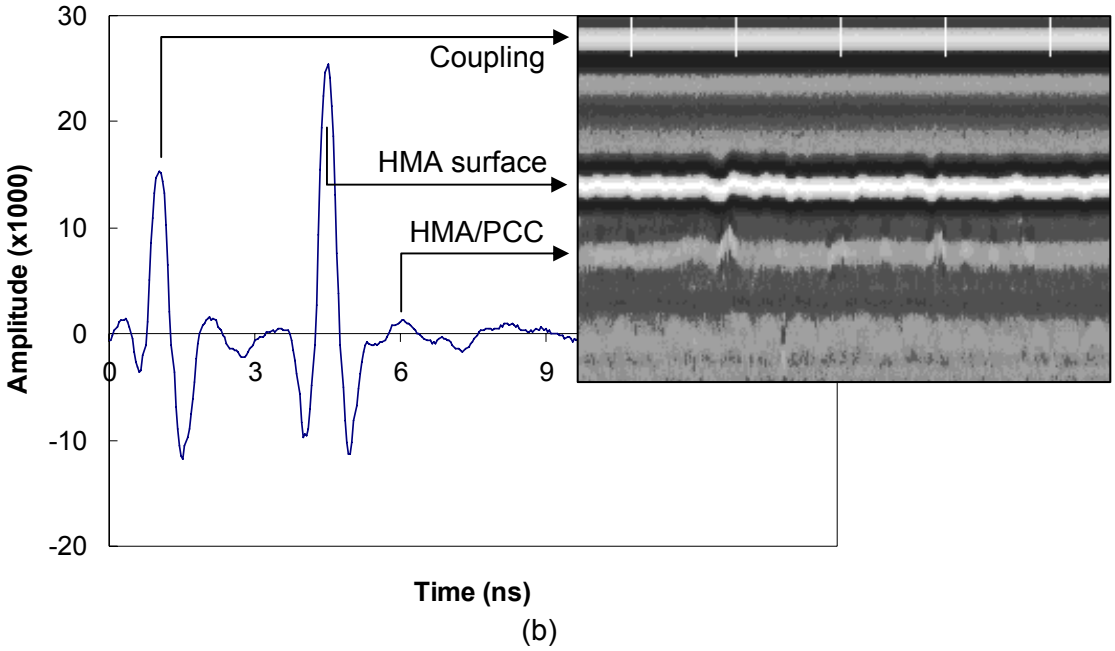

(b)

Figure A.13.7. GPR test (a) 1.0 GHz air-couple antenna setup and (b) typical GPR data.

A.13.3.3 Crack Analysis

For data analysis of this section, extent and severity of reflective cracking is utilized to compute uniform, R_{RCA}, and weight, R_{RCAW}, reflective cracking appearance rates. Excluding other unidentified transverse cracking, only reflective cracking is examined

accordingly to strip locations (11 ISAC strips and 13 PavePrep strips). Table A.13.2 summarizes the crack survey results for the ISAC and PavePrep sections for the past eight years. In both sections, low-severity-level cracks appear at the beginning as a new crack and are the majority until 2002 in the ISAC section and 2001 in the PavePrep section. After that, those cracks deteriorate to the medium-severity level in a couple of years and then to the high-severity level. During the same period, new low-severity-level cracks appear in other joints. Of the all cracks regardless crack severity, 50% of reflective cracks are developed within three years for the PavePrep section and five years for the ISAC section; 90% of reflective cracks are developed within six years for the PavePrep section and nine years for the ISAC section.

Table A.13.2. Summary of Crack Survey

System D (ISAC), 11 strips								
Severity	6/1/00	3/26/01	7/24/02	10/8/03	8/10/04	10/26/05	5/22/06	9/23/07
S	0	0	1	0	0	0	2	0
L	3	4	4	4	4	5	5	5
M	0	0	1	3	3	0	0	1
H	0	0	0	1	1	4	4	4
# Crack	3	4	6	8	8	9	11	10
R_{RCA}	0.27	0.36	0.55	0.73	0.73	0.82	1.00	0.91
R_{RCAW}	0.41	0.55	0.82	1.47	1.47	1.81	1.94	2.01
System B (PavePrep), 13 strips								
Severity	6/1/00	3/26/01	7/24/02	10/8/03	8/10/04	10/26/05	5/22/06	9/23/07
S	0	0	0	0	0	0	0	0
L	8	7	0	2	2	2	2	3
M	0	3	8	3	3	3	1	1
H	0	0	2	7	7	7	9	9
# Crack	8	10	10	12	12	12	12	13
R_{RCA}	0.62	0.77	0.77	0.92	0.92	0.92	0.92	1.00
R_{RCAW}	0.92	1.33	1.85	2.37	2.37	2.37	2.48	2.60

In order to investigate the effect of the interlayers on crack severity as well as extent, R_{RCA} and R_{RCAW} are compared with respect to overlay age in Figure A.13.8. For the PavePrep section, both R_{RCA} and R_{RCAW} increase linearly until six years at 2.37 of R_{RCAW} and until four years at 0.92 of R_{RCA} and then become level-down. At the beginning, the increase rate of the R_{RCA} is relatively higher than that of the R_{RCAW}. This indicates that new cracks are being developed rather than existing cracks becoming further deteriorated. At the next stage, the slope of the R_{RCAW} is higher than that of the R_{RCA}, meaning that the existing cracks severed instead of showing up as new reflective cracks. On the other hand, both of the R_{RCA} and R_{RCAW} of the ISAC section increase linearly until the survey year (over ten years). The R_{RCA} reaches close to 1.0, but the R_{RCAW} is only 2.0. Reflective cracking occurs at most of the joints the ISAC installed, but still averages as medium-severity level. Compared to the PavePrep, the ISAC shows better performance to delay the occurrence of reflective cracking at early overlay age as well as to mitigate the deterioration of the reflective cracking at later service life. Using a trigger value of 2.0 of R_{RCAW}, the service life of the overlay with PavePrep and with the ISAC is 5.2 years and 9.5 years, respectively, i.e., the performance benefit ratio of the ISAC to the PavePrep becomes 1.82. In the same way, the performance benefit ratio becomes 1.31 at 2.0 of R_{RCAW}. Therefore, the performance of the ISAC is relatively

higher than that of the PavePrep, especially at the beginning as a factor of 1.82 which lessens to 1.31 when medium-severity-level reflective cracking occurs.

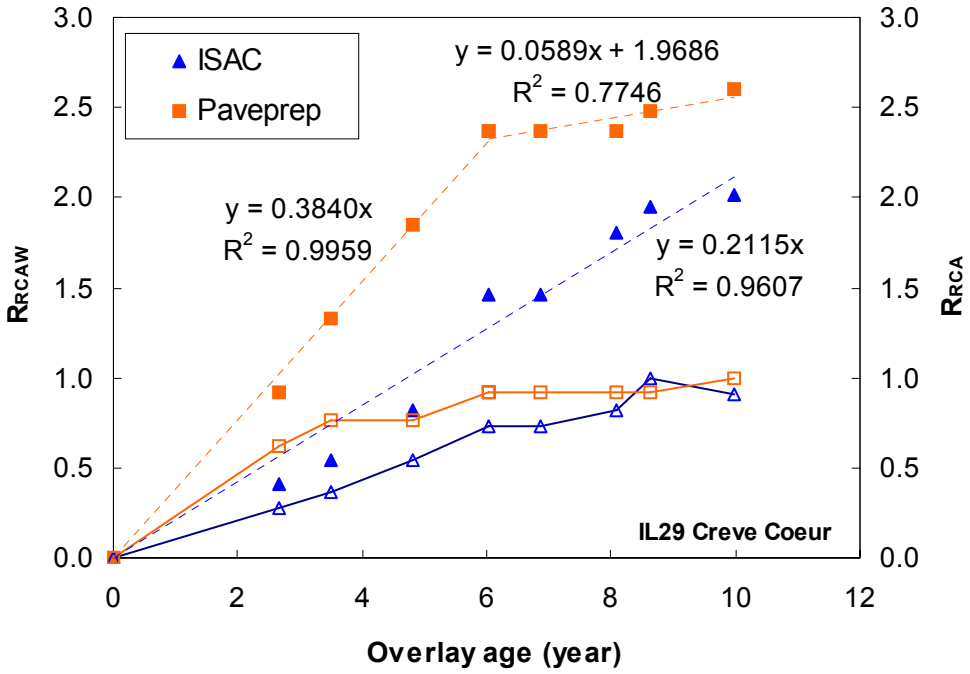

Figure A.13.8. Comparisons of the R_{RCAW} and R_{RCA} of the systems B and D section.

A.13.4 SUMMARY OF SECTION EVALUATION

Several tasks were performed in 2006 and 2007 at IL 29 Creve Coeur. Table A.13.3 summarizes the conducted survey, forensic investigation, and analysis.

Table A.13.3. Summary for IL 29 Creve Coeur

Year	2006	2007
Survey	Visual crack survey Video crack survey GPR survey	Visual crack survey
Forensic investigation	Coring Laboratory tests	
Analysis	Crack GPR	Crack

From the IL 29 Creve Coeur section, the interlayer system evaluations and findings are presented as follows:

- Compared to the PavePrep (strip-type system B), the ISAC (strip-type system D) performs better to abate reflective cracking and extend the service life of the HMA overlay.
- The performance benefit ratio of the ISAC to the PavePrep is 1.82 for medium or lower-severity-level reflective cracking and 1.31 for medium or higher-severity-level reflective cracking.
- Video crack surveys were fine-tuned enough to detect low-severity-level cracks.
- From the GPR survey, the thickness of HMA overlay was accurately estimated, but dowel bars or joints were not detected.

A.14 IL 17 ALEDO; CONTRACT NO. 68211

A.14.1 SECTION DESCRIPTION

This project, IL 17 Aledo (Contract No. 68211), was completed in 2003. The project is located west edge of Aledo to 3.35 mi east of Aledo (Mercer County, District 4), Illinois, as shown in Figure A.14.1 Total 3.35-mile-long section is from STA. 827+18 to 1004+00. It has one lane in each direction: westbound and eastbound. The pavement system consists of 30 ft JCP and multiple HMA overlays. The existing JCP had a 9-6-9 varied thickness. 2.25 in. new HMA overlay was directly on existing HMA overlay (1.5 in. wearing surface and 0.75 in. binder level with IL-9.5 mix). The treatment used in this project was system E, “Sand mix”. There are two sections which have three 500-ft-long sections each (Figure A.14.2). This evaluation considered two lanes in both directions. Traffic volume in 2003 was reported as 4800 AADT. In 2008, the section has the same of 4800 AADT (600 ADTT and 150 MU) according to traffic map on IDOT.

Figure A.14.1. Section location.

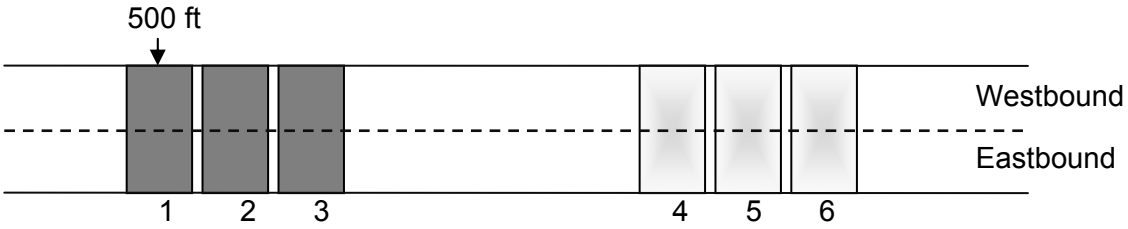

Control (IL9.5) System E (IL4.75)

1. STA. 855+00 to 860+00
2. STA. 880+00 to 885+00
3. STA. 900+00 to 905+00
4. STA. 935+00 to 935+00
5. STA. 960+00 to 965+00
6. STA. 980+00 to 985+00

Figure A.14.2. Section layout.

A.14.2 FIELD EVALUATION

A.14.2.1 Survey

The UIUC research team conducted visual survey to quantify surface cracking on November 12, 2006. A 6000-ft-long section was surveyed (6 x 500 ft in both lanes). The crack severity of this section has been monitored since 2003 by IDOT. The same surveying criteria were used in this evaluation. The severity and extent of transverse cracks were reported. Figure A.14.3 shows reflective cracks found in this section. Most of transverse cracks were single cracks (Figure A.14.3 (a)); a double crack was rarely observed (Figure A.14.3 (b)). Some locations, longitudinal cracks were observed at shoulder and center of a lane. There were no sealed cracks.

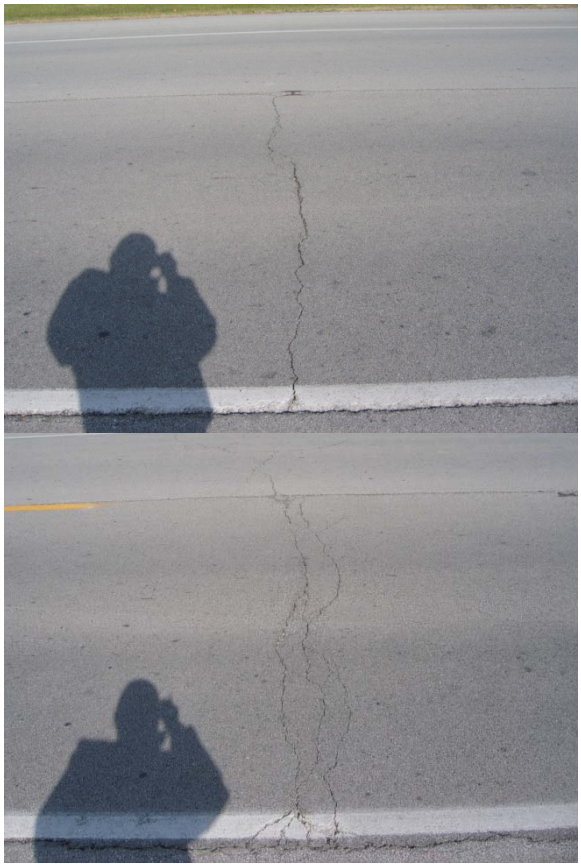

(a) (b)

Figure A.14.3. (a) single (b) double reflective cracking.

A.14.3 DATA ANALYSIS

A.14.3.1 Crack Analysis

For data analysis of this section, extent and severity of reflective cracking is utilized to compute uniform, R_{TCA}, and weight, R_{TCAW}, transverse cracking appearance rates. All transverse cracks are included for the evaluation. Table A.14.1 summarizes the crack survey results for the control and treated sections for the past three years. In both sections, relatively small number of cracks occurred until 2005. In 2006, the number of cracks increases suddenly from 18 to 65 in the control section and from 7 to 18 in the

treated section; medium- and high-severity-level cracks occur newly. Compared to the control section, 72% of cracks decrease in the treated section.

In order to investigate the effect of the interlayers on crack severity as well as extent, R_{TCA} and R_{TCAW} are compared with respect to overlay age in Figure A.14.4. For the both section, R_{RCA} and R_{RCAW} increase exponentially during this period of 3.5 years. Compared to the control section, the treated section shows better performance over the whole evaluation years. Using a linear regression, the performance benefit ratio of the System E to the control section becomes 3.73 meaning that the performance of the System E is much higher than that of the control section. However, it needs to monitor long-term performance of this crack behavior since it is not sure that the crack behavior will follow either the linear or exponential curve.

Table A.14.1. Summary of Crack Survey

Control section (3000 ft)				
Severity	6/1/03	8/30/04	8/30/05	11/12/06
S	0	0	5	10
L	0	2	13	37
M	0	0	0	13
H	0	0	0	5
# Crack	0	2	18	65
R_{RCA}	0	0.1	0.6	2.2
R_{RCAW}	0.0	0.1	0.8	3.7
System E section (3000 ft)				
Severity	6/1/03	8/30/04	8/30/05	11/12/06
S	0	0	6	2
L	0	0	1	12
M	0	0	0	3
H	0	0	0	1
# Crack	0	0	7	18
R_{RCA}	0.0	0.0	0.2	0.6
R_{RCAW}	0.0	0.0	0.2	1.0

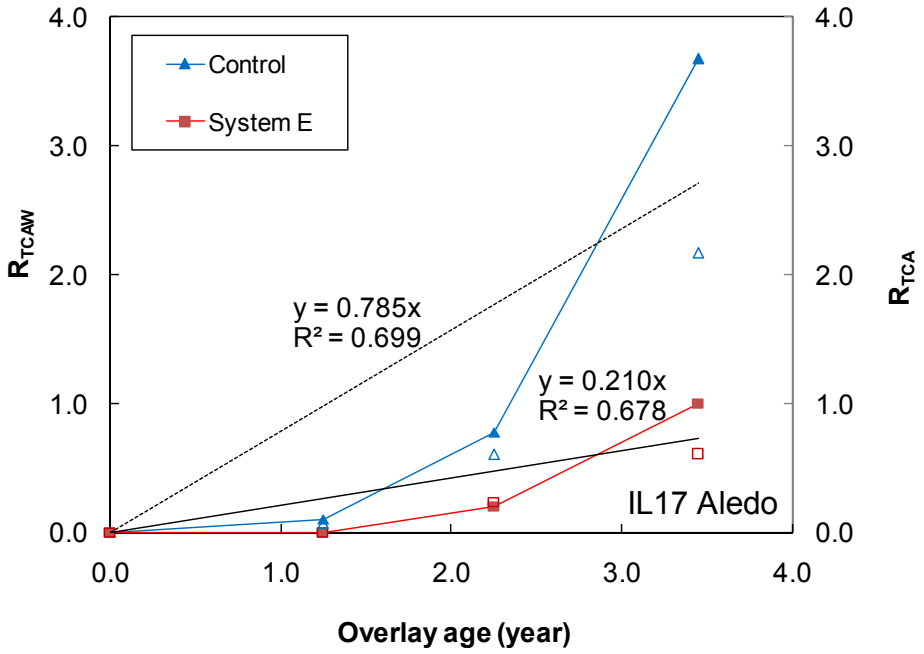

Figure A.14.4. Comparisons of the R_{TCAW} and R_{TCA} on the control and treated section with System E.

A.14.4 SUMMARY OF SECTION EVALUATION

One task was performed in 2006 at IL 17 Aledo. Table A.14.2 summarizes the conducted survey and analysis.

Table A.14.2. Summary for IL 17 Aledo

Year	2006	2007
Survey	Visual crack survey	N/A
Forensic investigation		
Analysis	Transverse Crack	

From the IL 17 Aledo section, the interlayer system evaluation and findings are presented as follows:

- Abrupt change of crack extent and severity was observed three years after the overlay construction. Compared to the control section, the performance of the System E becomes better three years after the overlay construction.
- The performance benefit ratio of the System E to the control section is 3.73.

A.15 IL 117 BENSON; CONTRACT NO. 66321

A.15.1 SECTION DESCRIPTION

This project, IL 117 at Benson (Contract No. 66321), was completed in 2003. The project is located between Benson (Woodford County, District 4) and Toluca (Marshall County, District 3), Illinois, as shown in Figure A.15.1 Total 9.0-mile-long section is from STA. 6+28 (Woodford County) to 483+28 (Marshall County). It has one lane in each direction: northbound and southbound. Existing pavement system consists of 30 ft JCP and multiple HMA overlays. The existing JCP had a 9-6-9 varied thickness. 2.25 in. new HMA overlay was directly on existing HMA overlay (1.5 in. wearing surface and 0.75 in. binder level with IL-9.5 mix). The treatment used in this project was system E, “Sand mix”. There are two sections which have six 500-ft-long segments each (Figure A.15.2). This evaluation considered two lanes in both directions. Traffic volume in 2003 was reported as 750 AADT. In 2008, the section has 800 AADT (84 MU and 36 SU) according to traffic map on IDOT. There were no sealed cracks.

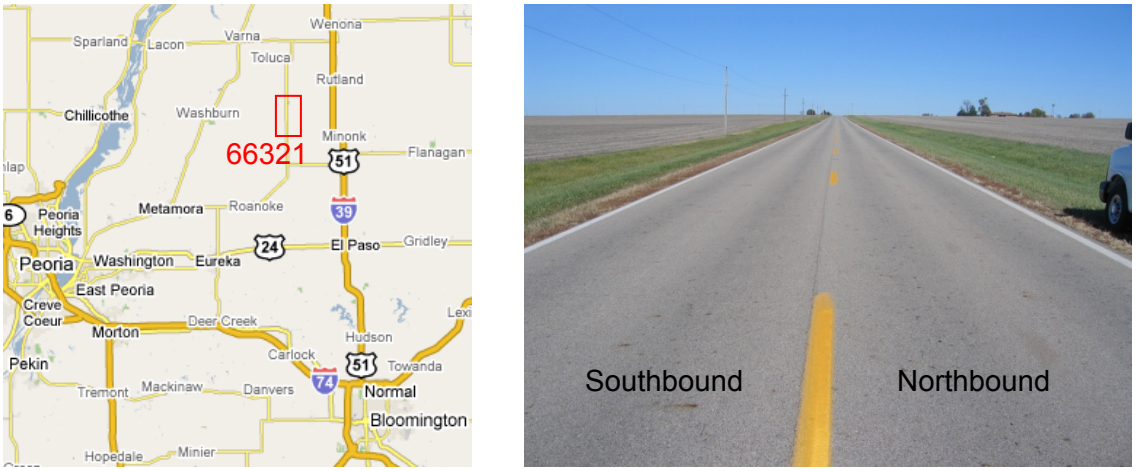

Figure A.15.1. Section location.

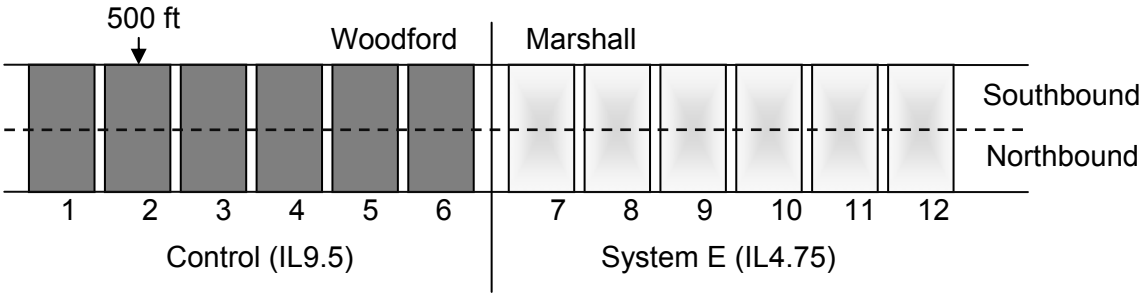

1. STA. 35+00 to 40+00
2. STA. 75+00 to 80+00
3. STA. 115+00 to 120+00
4. STA. 150+00 to 155+00
5. STA. 190+00 to 195+00
6. STA. 230+00 to 235+00
7. STA. 300+00 to 305+00
8. STA. 330+00 to 335+00
9. STA. 360+00 to 365+00
10. STA. 390+00 to 395+00
11. STA. 420+00 to 425+00
12. STA. 450+00 to 455+00

Figure A.15.2. Section layout.

A.15.3 FIELD EVALUATION

A.15.2.1 Survey

The UIUC research team conducted visual survey to quantify surface cracking on October 29, 2006. A 12000-ft-long section was surveyed (12 x 500ft in both lanes). The crack severity of this section has been monitored since 2003 by IDOT. The same surveying criteria were used in this evaluation. The severity and extent of transverse cracks were reported. Figure A.15.3 shows typical reflective cracks found in this section. Most of transverse cracks were single cracks, not double cracks. Some locations, longitudinal cracks were observed in the middle of a lane. No sealed crack was found.

(a) (b)

Figure A.15.3. (a) Unsealed transverse cracks and (b) unsealed longitudinal cracks.

A.15.3 DATA ANALYSIS

A.15.3.1 Crack Analysis

For data analysis of this section, extent and severity of reflective cracking is utilized to compute uniform, R_{TCA}, and weight, R_{TCAW}, transverse cracking appearance rates. All transverse cracks are included for the evaluation. Table A.15.1 summarizes the crack survey results for the control and treated sections for the past three years. In both sections, relatively small number of cracks occurred until 2005. In 2006, the number of cracks increases suddenly from 22 to 188 in the control section and from 24 to 79 in the treated section; medium- and high-severity-level cracks occur newly. Compared to the control section, 58% of cracks decrease in the treated section.

Table A.15.1. Summary of Crack Survey

Control section (3000 ft)				
Severity	6/1/03	8/15/04	8/30/05	10/29/06
S	0	5	7	67
L	0	11	15	91
M	0	0	0	27
H	0	0	0	3
# Crack	0	16	22	188
R_{RCA}	0.0	0.3	0.4	3.1
R_{RCAW}	0.0	0.3	0.5	4.5
System E section (3000 ft)				
Severity	6/1/03	8/15/04	8/30/05	10/29/06
S	0	1	16	17
L	0	2	8	43
M	0	0	0	17
H	0	0	0	2
# Crack	0	3	24	79
R_{RCA}	0.0	0.1	0.4	1.3
R_{RCAW}	0.0	0.1	0.4	2.1

In order to investigate the effect of the interlayers on crack severity as well as extent, R_{TCA} and R_{TCAW} are compared with respect to overlay age in Figure A.15.4. For the both section, R_{RCA} and R_{RCAW} increase exponentially during this period of 3.5 years. Compared to the control section, the treated section shows worse performance at the first year, but better performance at the third year. Using a linear regression, the performance benefit ratio of the System E to the control section becomes 1.88. Therefore, the performance of the System E is relatively higher than that of the control section. However, it needs to monitor long-term performance of this crack behavior since it is not sure that the crack behavior will follow either the linear or exponential curve.

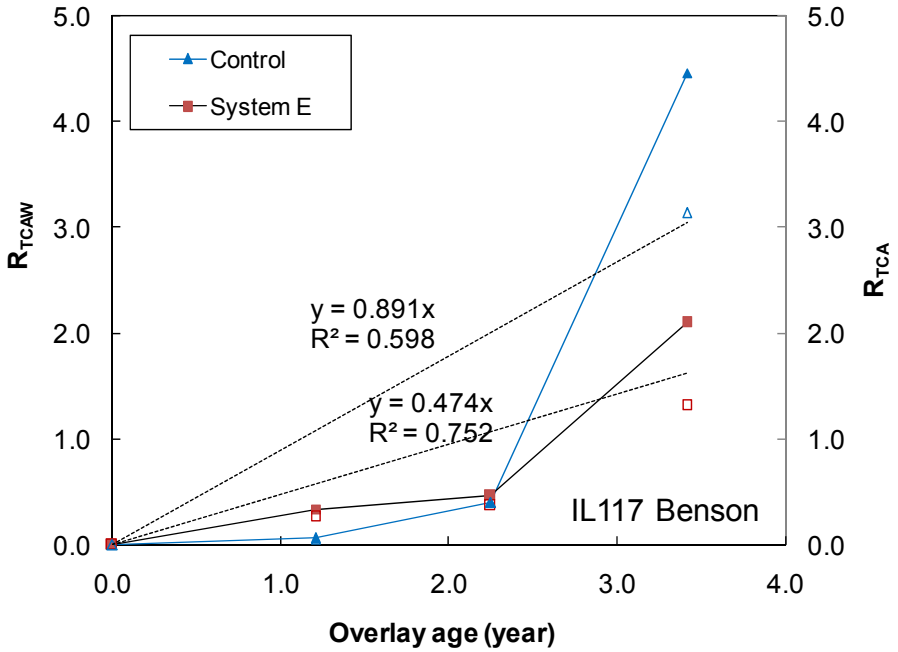

Figure A.15.4. Comparisons of the R_{TCAW} and R_{TCA} on the control and treated section with System E.

A.15.4 SUMMARY OF SECTION EVALUATION

One task was performed in 2006 at IL 117 Benson. Table A.15.2 summarizes the conducted survey and analysis.

Table A.15.2. Summary for IL 117 Benson

Year	2006	2007
Survey	Visual crack survey	N/A
Forensic investigation Analysis	Transverse Crack	

From the IL 117 Benson section, the interlayer system evaluation and findings are presented as follows:

- Abrupt change of crack extent and severity was observed three years after the overlay construction. Compared to the control section, the performance of the System E becomes better three years after the overlay construction.
- The performance benefit ratio of the System E to the control section is 1.88.

A.16 IL 130 VILLA GROVE; CONTRACT NO. 90527

A.16.1 SECTION DESCRIPTION

This project, IL 130 Villa Grove (Contract No. 90527), was completed in September 1995. The project is located from Camargo to Philo (Champaign County, District 5), Illinois, as shown in Figure A.16.1. It has one lane in each direction: northbound and southbound. The pavement system consists of JCP with existing HMA overlay. The thickness and joint spacing of the existing JCP is unknown, 2.25 in. new MHA overlay was placed on the existing HMA overlay (1.25 in. wearing surface and 0.75 in. leveling binder). The treatment used in this project was strip-type System A made of Petromat. The strips were placed on top of the level binder. The locations of the strips were not identified. The evaluated section has one 500-ft-long control (STA. 2044+00 to 2049+00) and treated section (STA. 162+90 to 167+90). Traffic volume in 1998 was reported as 4000 AADT. In 2008, AADT was 3250 (99 MU and 71 SU) according to traffic map on IDOT.

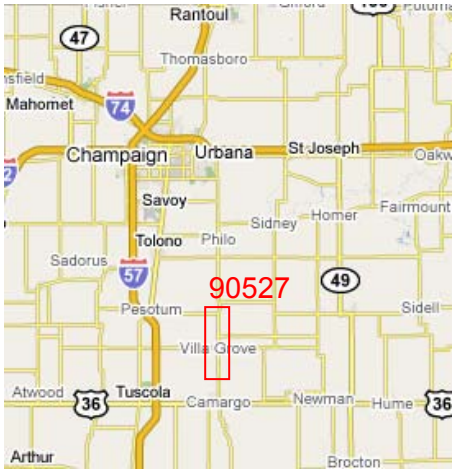

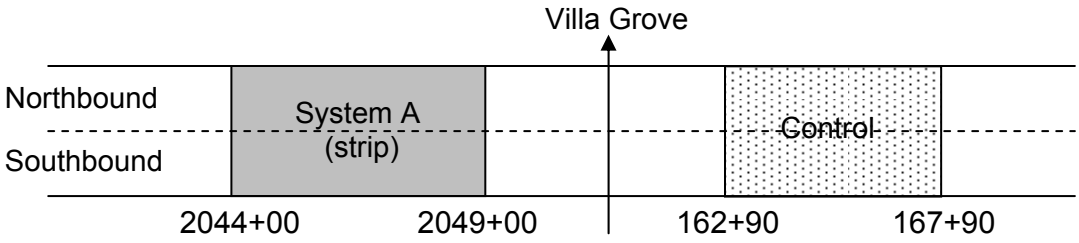

Figure A.16.1 Section location and layout.

A.16.2 FIELD EVALUATION

A.16.2.1 Survey

The UIUC research team conducted visual survey to quantify surface cracking on Oct. 29, 2006. A1000-ft-long section was surveyed (2 x 500 ft for the control and treated section in both directions). The crack severity of this section was measured in 1998. The same surveying criteria were used in this evaluation. The severity and extent of transverse cracks were reported. Other distress types were also reported.

A.16.3 DATA ANALYSIS

A.16.3.1 Crack Analysis

For data analysis of this section, extent and severity of reflective cracking is utilized to compute uniform, R_{TCA}, and weight, R_{TCAW}, transverse cracking appearance rates. While the use of R_{RCA} or R_{RCAW} is preferred for the strip-type interlayer evaluation, all transverse cracks were included in this analysis since the application locations of the strips were not identified. Table A.16.1 summarizes the crack survey results for the control and treated sections. In both sections, total number of transverse cracks increased and also, majority of crack severity moved from low level to medium level. Compared to the control section, 20% and 68% more cracks were developed in the treated section in 1998 and 2006, respectively.

Table A.16.1. Summary of Crack Survey

	Control section (1000 ft)		System A (strip) section (1000 ft)	
Severity	6/22/98	10/29/06	6/22/98	10/29/06
S	13	0	16	0
L	30	24	70	27
M	10	59	3	71
H	0	2	0	4
# Crack	53	85	89	102
R_{TCA}	5.3	8.5	8.9	10.2
R_{TCAW}	7.9	17.9	12.6	21.8

In order to investigate the effect of the interlayers on crack severity as well as extent, R_{TCA} and R_{TCAW} are compared with respect to overlay age in Figure A.16.2. In both sections, R_{TCA} and R_{TCAW} increase bi-linearly. The first slope of those indices is much higher than the second one. Thus, it is not suitable to obtain the average deterioration rate of those sections simply from the slope as did in other projects. Nonetheless, it is clear that the treatment was not efficient to delay reflective cracking since R_{TCAW} of the treated section is always higher than that of the control section. Despite of this shortcoming, the performance benefit ratio can be calculated as 0.80 using the linear deterioration rates as shown in Figure A.16.4. Also, the obtained performance benefit ratio of 0.8 is enough to imply that the strip-type System A has no performance benefit.

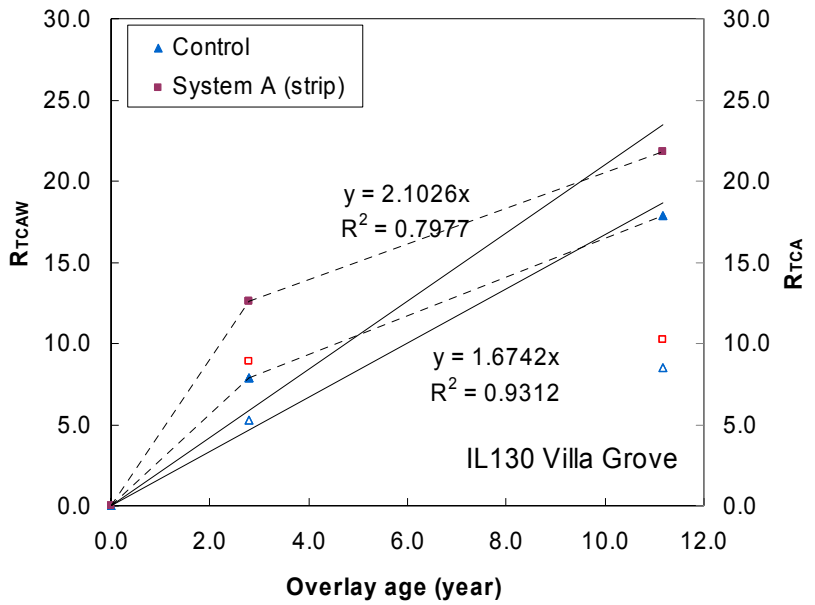

Figure A.16.2. Comparisons of the R_{TCAW} and R_{TCA} on the strip-type System A and control sections.

A.16.4 SUMMARY OF SECTION EVALUATION

One task was performed in 2006 at IL 130 Villa Grove. Table A.16.2 summarizes the conducted survey and analysis.

Table A.16.2. Summary for IL 130 Villa Grove

Year	2006	2007
Survey	Visual crack survey	N/A
Forensic investigation		
Analysis	Transverse crack	

From the IL 130 Villa Grove section, the interlayer system evaluation and finding are presented as follows:

- Compared to the control section, the strip-type System A showed worse performance to abate reflective cracking.
- The performance benefit ratio of the strip-type System is 0.35.

A.17 MATTIS AVE.; CONTRACT NO. N/A

A.17.1 SECTION DESCRIPTION

This project, Mattis Ave., was completed in 2000. The project is located at Champaign downtown (Champaign County, District 5), Illinois, as shown in Figure A.17.1. The evaluated section is between Kirby Ave. and Springfield Ave. (STA. 5+00 to 53+83). It has two lanes in each direction: northbound and southbound with a bi-directional center turn lane. The pavement system consists of JCP with HMA overlay. The thickness and joint spacing of the existing JCP is unknown. The overlay is 3.125 in. HMA: 1.625 in. wearing surface and 1.5 in. binder level. The treatments used in this project are the following: 10 System A, 485 System B, and 102 System D (ISAC) strips (Figure A.17.2). 39 untreated joints were selected as a control section. Traffic volume at the time of overlay construction in 2000 was reported as 15000 AADT (200 ADTT) in the previous report and in 2008 was reported as 20800 AADT (280 ADTT and 140 MU) according to traffic map on IDOT.

(a)

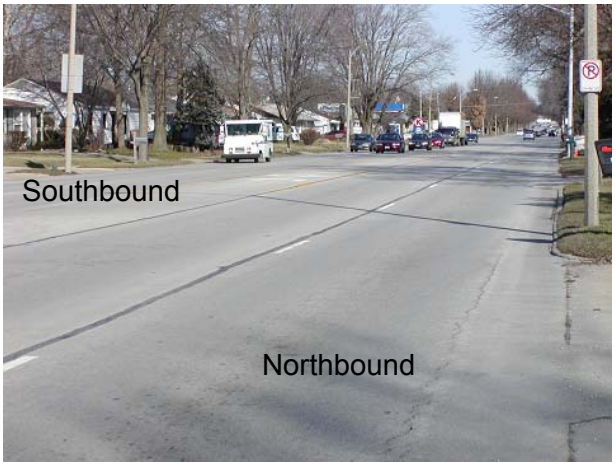

(b)

Figure A.17.3. Section location.

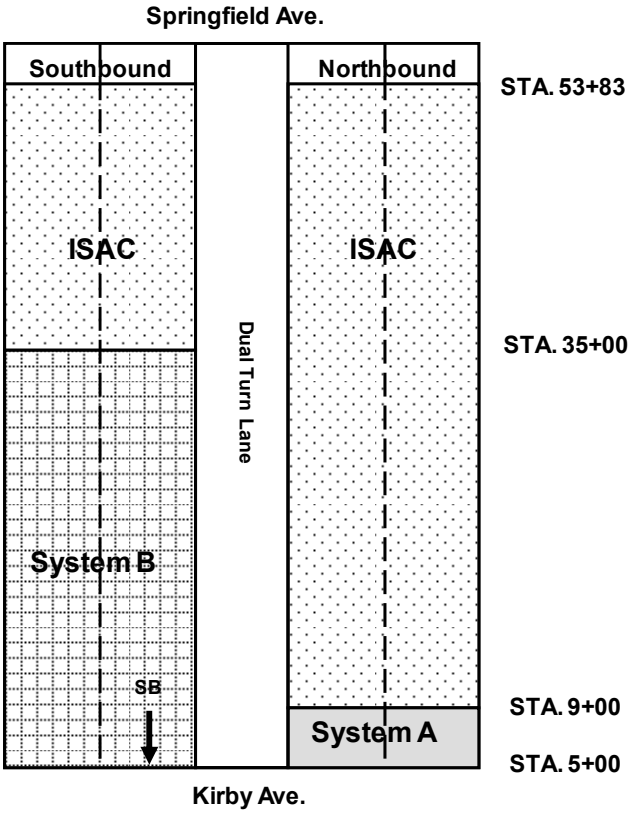

Figure A.17.2. Section layout.

A.17.2 FIELD EVALUATION

The UIUC research team conducted visual, video, and GPR surveys. The visual and video surveys quantified surface cracking; while the GPR surveys predicted pavement layer thicknesses and located interface systems. The video and GPR surveys were conducted at highway speed. Specimens were obtained through coring from the field for forensic investigation as well as laboratory testing. This task was conducted on March 2, 2006, and coordinated with IDOT researchers and District 5 (traffic control and coring crews). In addition, the second visual crack survey was conducted on August 11, 2007.

A.17.2.1 Survey

A 19200-ft-long section was surveyed (4800-ft-long in four lanes). The crack severity of this section had been monitored since 2000 by IDOT. The same surveying criteria were used in this reflective cracking evaluation. The severity and extent of transverse cracks were reported. Figure A.17.3 shows typical reflective cracks found in this section. Sealed and unsealed crack have the same low severity level (Figure A.17.3(a)). Sealed medium-severity-level crack with medium-severity-level cracks becomes high level (Figure A.17.3(b)). Two parallel reflective cracks were developed at the edge of an underlying patch (Figure A.17.3.(c)). Also, longitudinal cracks were observed at outer lane shoulder. Besides, other distress types, such as block cracking, were also reported.

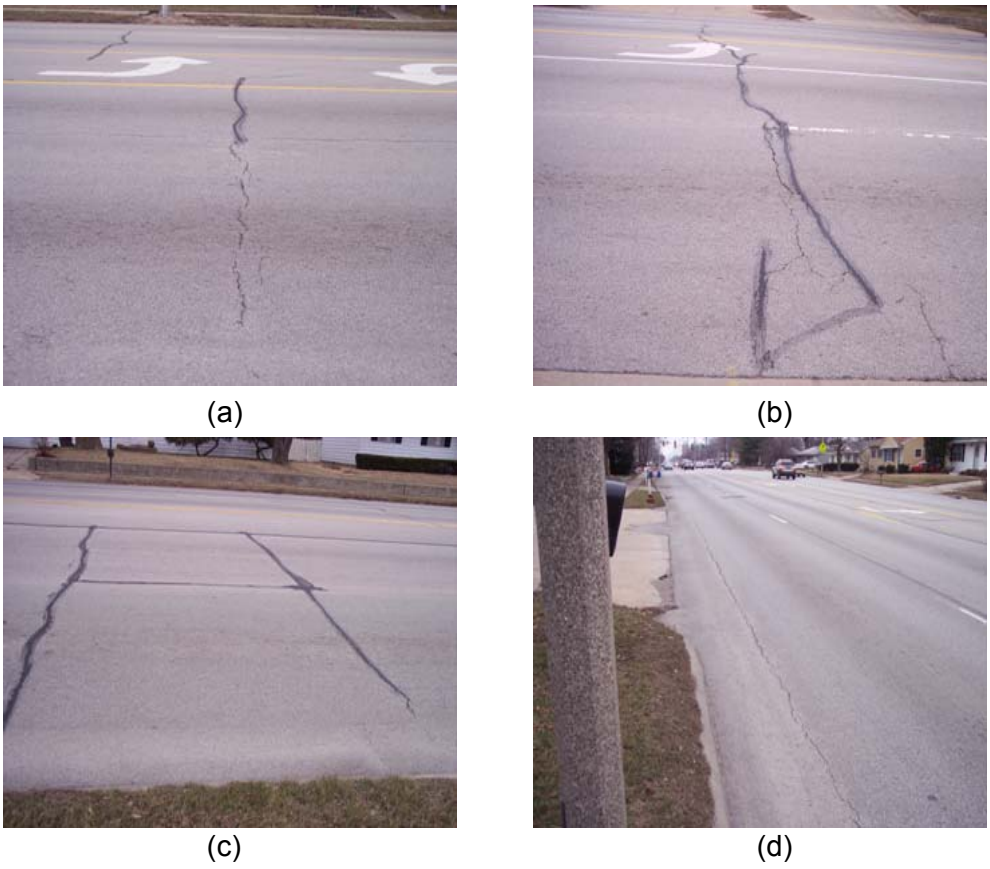

Figure A.17.3. Typical reflective cracks in this section: (a) sealed and unsealed low-severity-level crack; (b) medium- (upper) and high- (lower) severity-level crack; (c) patch-associated crack; and (d) longitudinal crack.

A.17.2.2 Coring

Cores with 4-in and 6-in diameter were obtained from the evaluated sections (Figure A.17.4). Construction information, crack mapping, and GPR survey results were used to locate pavement joints and treatment locations. Table A.17.1 presents the number of cores and locations. Cores on top of reflective crack, in both wheel-path (WP) and between wheel-paths (BWP) were obtained. Cores for bulk testing were obtained from WP intact surface; while cores for interface shear testing were obtained from both WP and BWP over treated locations. Since interface between PCC and HMA with interlayer systems was debonded during coring, samples could not be obtained for interface bond strength tests.

(a)

(b)

Figure A.17.4. Field coring work: (a) coring truck (b) coring locations on a transverse crack.

Table A.17.1. Coring Details

Project	Section	Core Type	# of cores
Mattis Ave.	PavePrep	Permeability	8
		Bulk	6
		Interface Shear	0

A.17.3 DATA ANALYSIS

A.17.3.1 Crack Analysis

For data analysis of this section, extent and severity of reflective cracking is utilized to compute uniform, R_{RCA}, and weight, R_{RCAW}, reflective cracking appearance rates. Excluding other unidentified transverse cracking, only reflective cracking is examined accordingly to strip locations (10 strips of System A, 102 strips of System B, 485 strips of System D, and 39 joints in the control section). Table A.17.2 summarizes the crack survey results for the past seven years.

In order to investigate the effect of the interlayers on crack severity as well as extent, R_{RCAW} variations over overlay age are demonstrated in Figure A.17.5. Four R_{RCAW} curves show a good linear relationship with respect to overlay age except the first year in the control section. In the control section, since low- and medium-severity-level reflective cracks were already developed within one year, the R_{RCAW} increased suddenly compared to the treated sections. Thus, the three interlayer systems delayed the occurrence of reflective cracking during the short term period. However, with the increase of overlay age, the Systems A and B do not show any performance benefit since the R_{RCAW} curves of the Systems A and B are not differentiable from that of the control section. On the other hand, the R_{RCAW} of the System D is always less than that of the control section. Using the linear regression curves shown in the figure, the deterioration rate is obtained: 0.294, 0.294, 0.122, and 0.277 for the System A, B, D, and control section, respectively. Consequently, the performance benefit ratio yields 0.94, 0.94, and 2.77 for the Systems A, B, and D, respectively.

Table A.17.2. Summary of Crack Survey

System A, 10 strips								
Severity	1/0/00	3/20/01	7/6/01	7/3/02	5/5/03	4/30/04	3/2/06	8/11/07
S	0	2	2	1	0	3	0	0
L	0	1	1	4	5	7	5	4
M	0	0	0	0	0	0	5	9
H	0	0	0	0	0	0	0	0
# Crack	0	3	3	5	5	10	10	13
R_{RCA}	0.0	0.3	0.3	0.5	0.5	1.0	1.0	1.0
R_{RCAW}	0.0	0.3	0.3	0.7	0.8	1.3	1.9	2.1
System B, 102 strips								
Severity	1/0/00	3/20/01	7/6/01	7/3/02	5/5/03	4/30/04	3/2/06	8/11/07
S	0	10	9	9	8	7	9	0
L	0	19	19	19	28	62	43	59
M	0	3	5	12	21	15	37	36
H	0	0	0	0	2	2	8	1
# Crack	0	32	33	40	59	86	97	96
R_{RCA}	0.0	0.3	0.3	0.4	0.6	0.9	1.0	0.9
R_{RCAW}	0.0	0.4	0.5	0.6	1.0	1.4	1.8	1.8
System D, 485 strips								
Severity	1/0/00	3/20/01	7/6/01	7/3/02	5/5/03	4/30/04	3/2/06	8/11/07
S	0	3	4	5	44	31	35	11
L	0	3	3	11	53	117	134	185
M	0	0	0	1	4	6	47	45
H	0	0	0	0	0	0	0	3
# Crack	0	6	7	17	101	154	216	244
R_{RCA}	0.0	0.0	0.0	0.0	0.2	0.3	0.5	0.5
R_{RCAW}	0.0	0.0	0.0	0.0	0.3	0.5	0.7	0.9
Control, 39 strips								
Severity	1/0/00	3/20/01	7/6/01	7/3/02	5/5/03	4/30/04	3/2/06	8/11/07
S	0	0	0	0	4	2	5	5
L	0	11	9	4	5	12	22	22
M	0	4	6	12	11	9	11	11
H	0	0	0	0	1	1	1	1
# Crack	0	15	15	16	21	24	39	39
R_{RCA}	0.0	0.4	0.4	0.4	0.5	0.6	1.0	1.0
R_{RCAW}	0.0	0.7	0.7	0.8	1.0	1.1	1.7	1.7

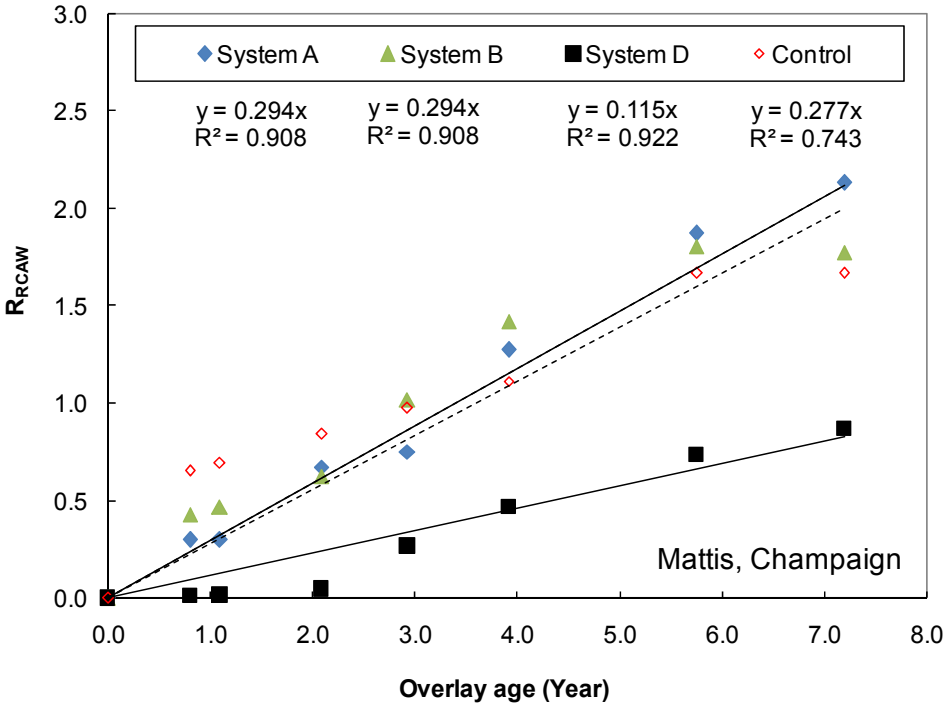

Figure A.17.5. Comparisons of the R_{RCAW} of the treated sections (Systems A, B, and D) and the control section.

A.17.4 SUMMARY OF SECTION EVALUATION

Several tasks were performed in 2006 and 2007 at Mattis Ave., Champaign. Table A.17.3 summarizes the conducted survey, forensic investigation, and analysis.

Table A.17.3. Summary for Mattis Ave.

Year	2006	2007
Survey	Visual crack survey Video crack survey GPR survey	Visual crack survey
Forensic investigation	Coring Laboratory tests	
Analysis	Reflective Crack GPR	Reflective Crack

From the Mattis section, the interlayer system evaluations and findings are presented as follows:

- Compared to the control section, the System D performs better to abate reflective cracking and extend the service life of the HMA overlay; the Systems A and B does not show better performance.
- The performance benefit ratio of the System D to the control section is 2.77; that of the Systems A and B are 0.94.

A.18 IL 130 PHILO; CONTRACT NO. 70235

A.18.1 SECTION DESCRIPTION

This project, IL 130 Philo (Contract No. 70235), was completed in October 2003. The project is located at Philo (Champaign County, District 5), Illinois, as shown in Figure A.18.1. The evaluated section is between Philo and Winsor Rd. (STA. 100+19 to 369+78). It has one lane in each direction: northbound and southbound. The pavement system consists of JRCP and multiple HMA overlays. The existing JRCP is 8-in thick. The joints are spaced at 100 ft. The overlay is 2.25 in. HMA: 1.5in wearing surface and 0.75 in. level binder. Out of 5.0-mile-long section, ten 500-ft-long segments are selected for this evaluation (Figure A.13.2). The treatment used in this project is System E, IL 4.75 N50 level binder so called “Sand mix” which was placed southbound instead of conventional level binder (IL 9.5 mix). Traffic volume at the time of overlay construction in 2003 was reported as 7400 AADT and in 2008 was reported as the same 7400 AADT (450 ADTT and 166 MU) according to traffic map on IDOT.

Figure A.18.1 Section location.

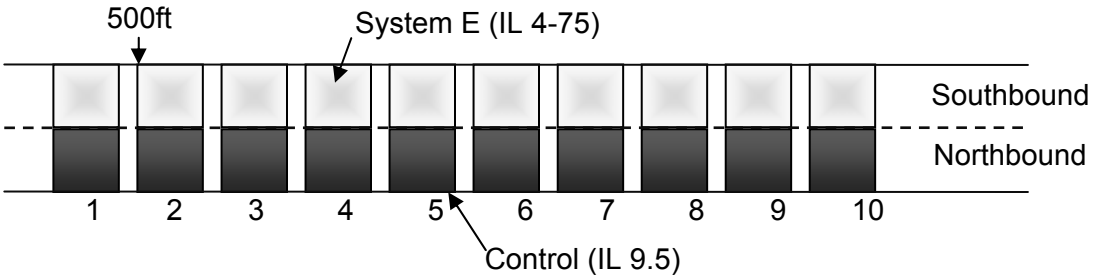

Section 1: 135+00 to 140+00
Section 2: 160+00 to 165+00
Section 3: 185+00 to 190+00
Section 4: 210+00 to 215+00
Section 5: 240+00 to 235+00
Section 6: 250+00 to 255+00
Section 7: 270+00 to 275+00
Section 8: 295+00 to 300+00
Section 9: 320+00 to 325+00
Section 10: 340+00 to 355+00

Figure A.18.2. Section layout.

A.18.2 FIELD EVALUATION

The UIUC research team conducted a visual, video, and GPR surveys. The visual and video surveys quantified surface cracking; while the GPR surveys predicted pavement layer thicknesses and located interface systems. The video and GPR surveys were conducted at highway speed. Specimens were obtained through coring from the field for forensic investigation as well as laboratory testing. This task was conducted on July 24, 2006, and coordinated with IDOT researchers and District 5 (traffic control and coring crews).

A.18.2.1 Survey

Two lanes of 6000-ft-long section were surveyed. The crack severity of this section has been monitored since 2003 by IDOT. The same surveying criteria were used in this evaluation. The severity and extent of transverse cracks were reported. Figure A.18.3 shows typical reflective cracks found in this section. When a crack is sealed, the severity of the crack is evaluated differently, i.e., when no additional crack is developed around the sealed crack, its level goes down to low level in most cases regardless of previous crack severity. For example, two sealed cracks have different severity: low severity (Figure A.18.3(a)) and medium to high severity (Figure A.18.3(b)). Other distress types were also reported. The video and GPR survey was conducted at highway speed without moving traffic control.

(a) (b)

Figure A.18.3 Severity of sealed crack: (a) low and (b) medium (up) to high (down) level.

A.18.2.2 Coring

Twelve cores with 4-in diameter and 11 cores with 6-in. diameter were obtained from the evaluated sections (Figure A.18.4). Construction information, crack mapping, and GPR survey results were used to locate pavement joints. Cores on top of reflective crack, in both wheel-path (WP) and between wheel-paths (BWP) were obtained. Cores for bulk testing were obtained from WP intact surface; while cores for interface shear testing were obtained from both WP and BWP over treated locations.

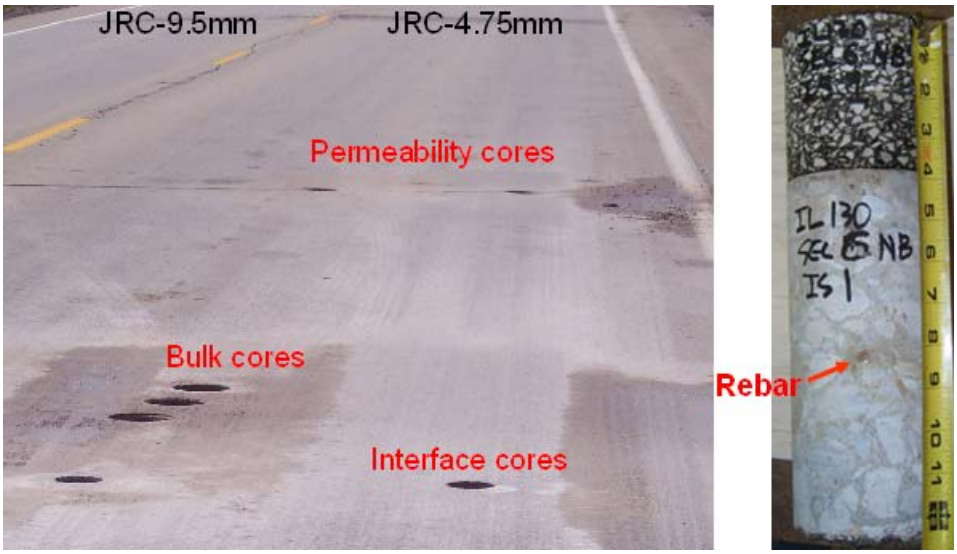

(a) (b)

Figure A.18.3 Field coring work: (a) Coring locations and (b) sample core from JRCP in the section 6.

A.18.3 DATA ANALYSIS

A.18.3.1 Video Survey

The quality of the video image recorded on July 24, 2006, was not good enough to use for data analysis because the video recorder was not set correctly to receive fast images at highway speed. Therefore, a couple of trials were performed in 2006 summer. Finally, fine-tuned video data were good enough to count the number of transverse cracks and distinguish crack severity. Figure A.18.4 shows the comparison of visual and video crack survey data. Through the video crack survey, total 165 transverse cracks were detected out of 195 (84.2%) transverse cracks were observed via visual crack survey. Among missed cracks, 18.8% is cracks less severe than low level due to relatively lower resolution of the video camera and/or the unstable mount system. Also, severity of cracks is shifted from high to medium levels since it was hard to specify sealed crack severity accurately. When R_{TCAW} is calculated with those visual and video crack survey results, the difference of R_{TCAW} between the control and treated section is 25.0% and 20.7%, respectively. 20% of performance error indicates that this video crack survey is neither good nor bad as a trial approach to quantify the performance evaluation. Since the video survey can provide much safer and fast applications in field than the visual survey, it may be an affordable method as a substitute of the visual survey.

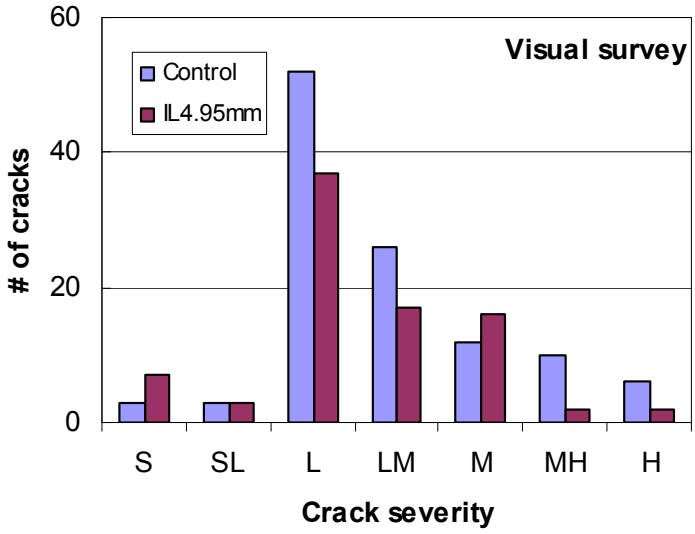

(a)

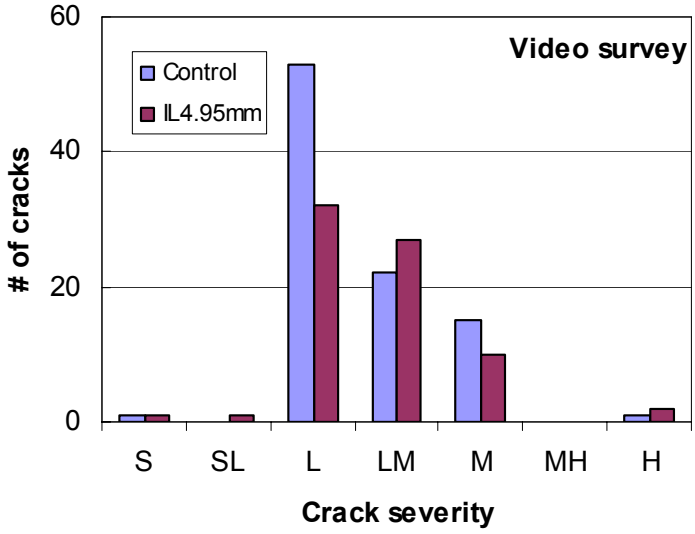

(b)

Figure A.18.4 Crack severity distribution: (a) visual survey and (b) video survey.

A.18.3.2 GPR Survey

The possibility of GPR testing was examined to detect interlayer systems and joints. A 1.0 GHz air-couple antenna was selected to collect data at highway speed while video crack surveys were being conducted. Figure A.18.5 shows the GPR data in the section 1 northbound. A scan rate of 1scan/ft of the GPR data was used to collect GPR data. Three distinct GPR data patterns were found regarding substructure of the overlay (Figure A.18.5): joint with a dowel bar, HMA patch, and PCC patch. Multiple strong reflections are observed in the middle of the concrete pavement, which resulted from that when electromagnetic (EM) wave meets an obstacle which has very high dielectric property. In this overlay pavement, dowel bars made of steel are the most feasible obstacles to produce the multiple reflections. The multiple reflections are spaced in 100ft which is identical to the joint spacing of the existing concrete pavement. On the other

hand, a finite length of strip is found in the middle of HMA overlay and/or in the middle of PCC. Those strips are reflected from an HMH/PCC interface. Based on this overlay pavement structure, those two strip reflection patterns can be identified as either an HMA or PCC patch. When a strip reflection occurs in the middle of HMA overlay, there exists a PCC patch; when a strip reflection is located in the middle of PCC pavement, it indicates the existence of an HMA patch. Thus, using the GPR data, the location of joints and/or patches can be estimated. Consequently, reflective cracking can be identified when joint/patch locations are specified. Figure A.18.6 shows GPR data and joint/patch identification for the all sections northbound.

Figure A.18.5 GPR data obtained in section1 northbound.

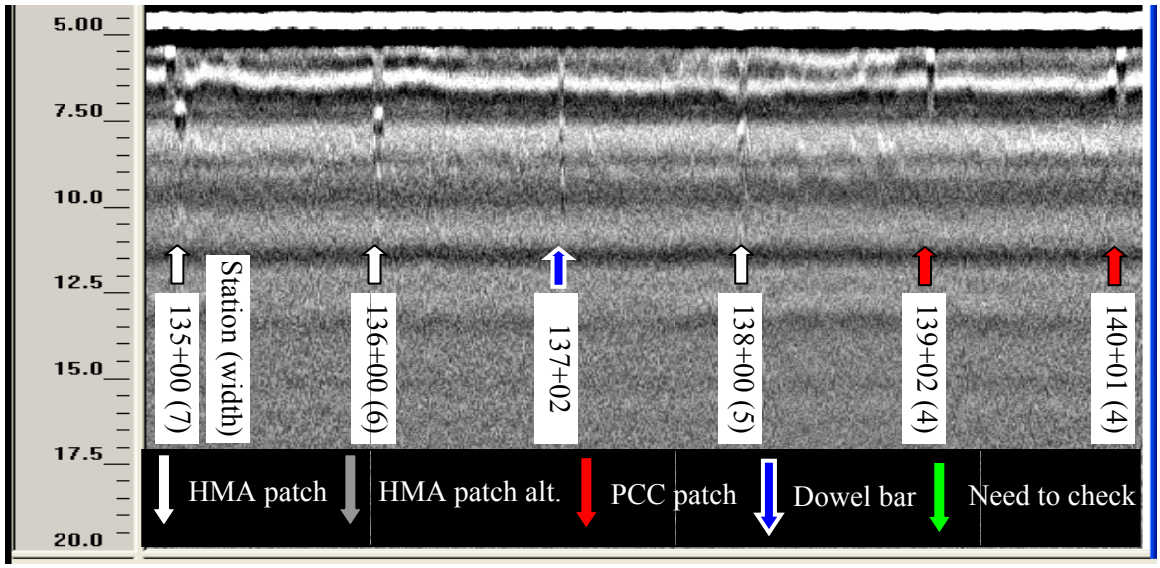

(a) Section1 northbound

Figure A.18.6 GPR data in all sections northbound

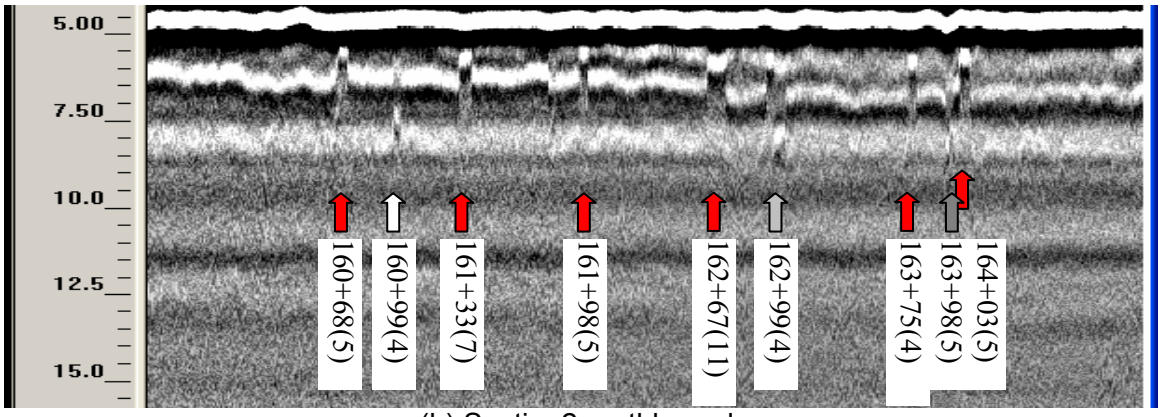

(b) Section2 northbound

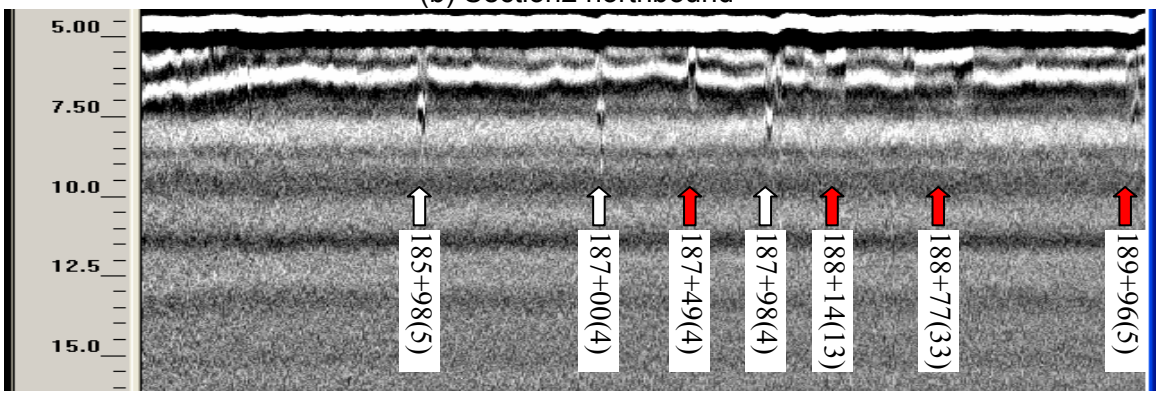

(c) Section3 northbound

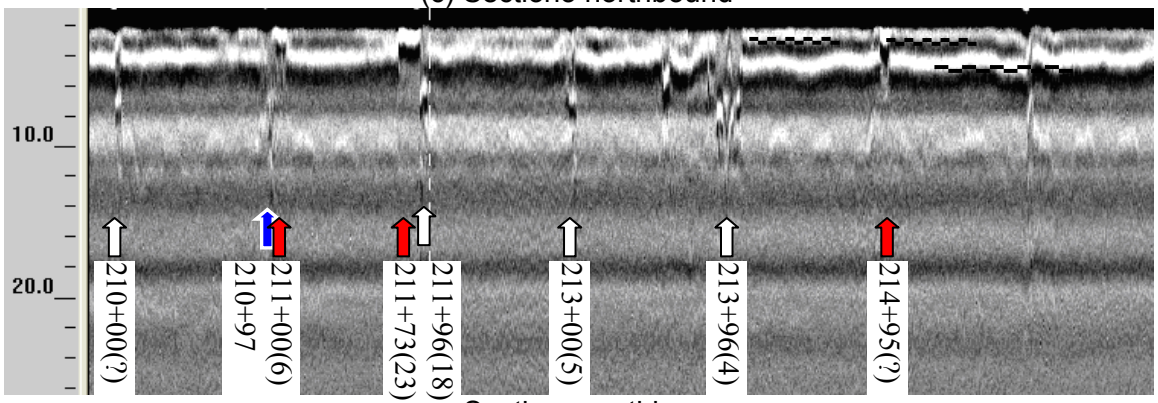

(d) Section4 northbound

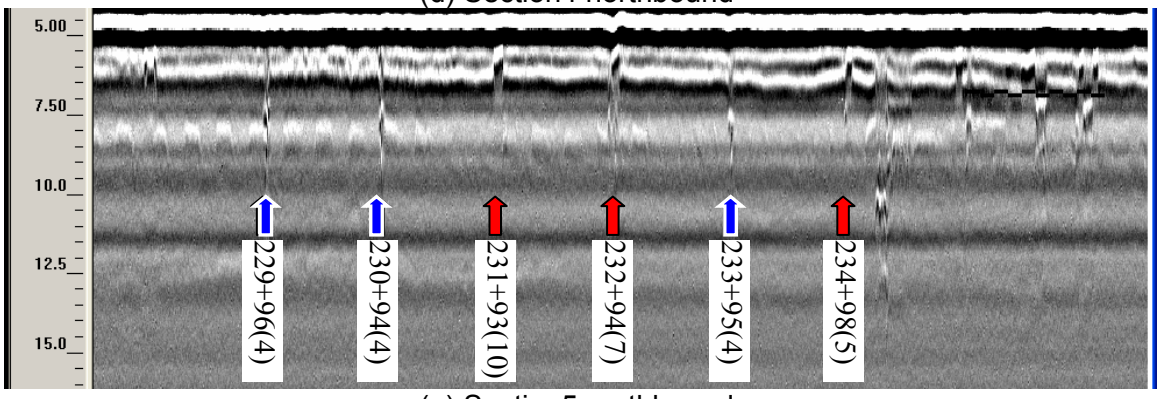

(e) Section5 northbound

Figure A.18.6 (Continued) GPR data in all sections northbound

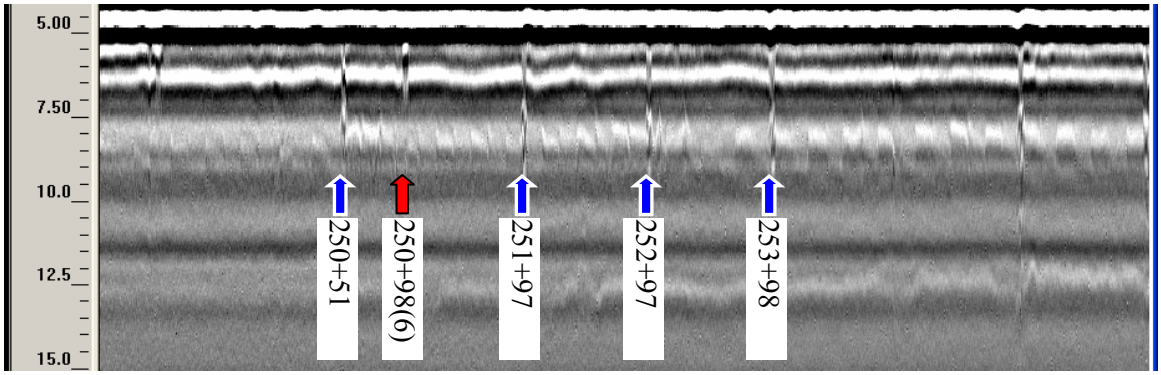

(f) Section6 northbound

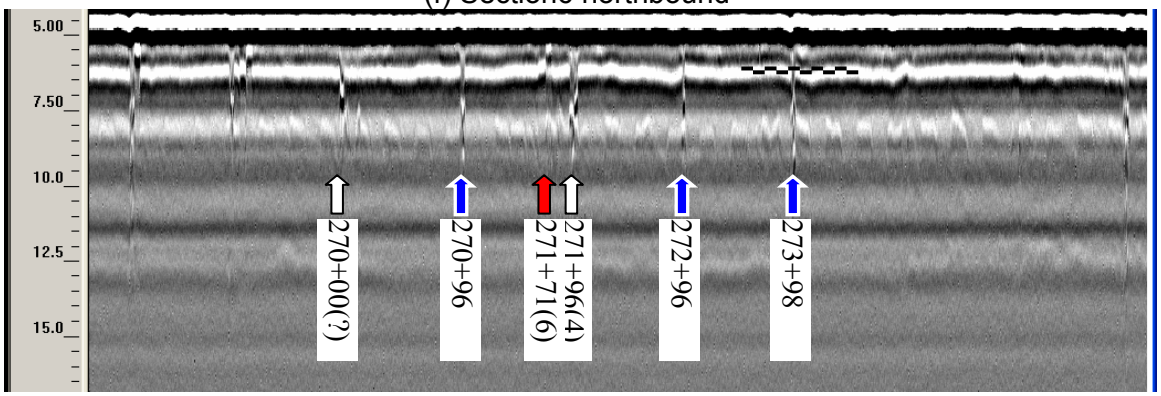

(g) Section7 northbound

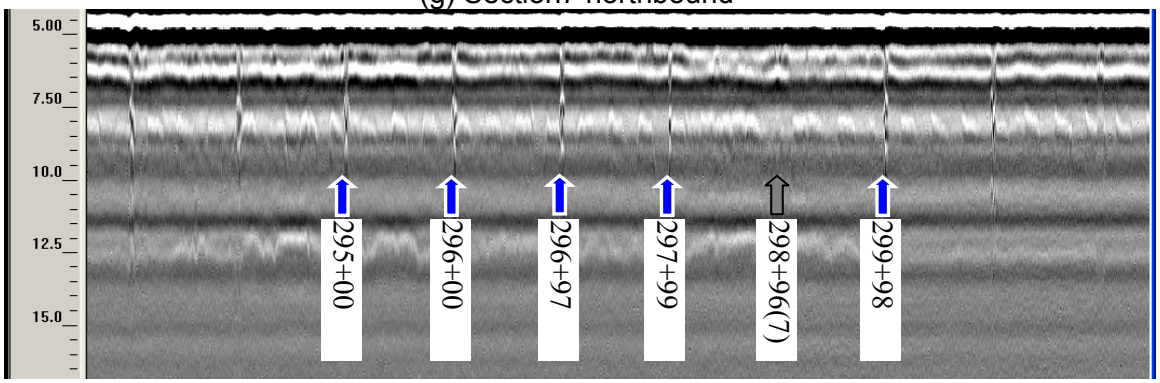

(h) Section8 northbound

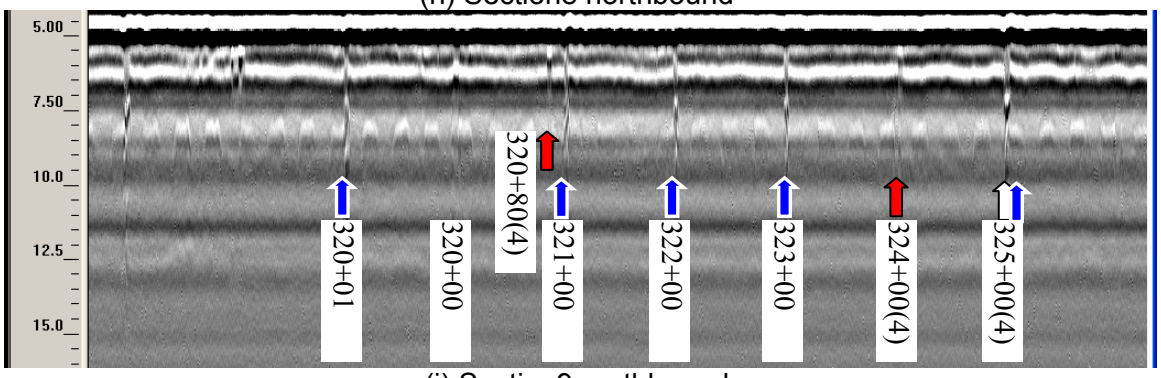

(i) Section9 northbound

Figure A.18.6 (Continued) GPR data in all sections northbound

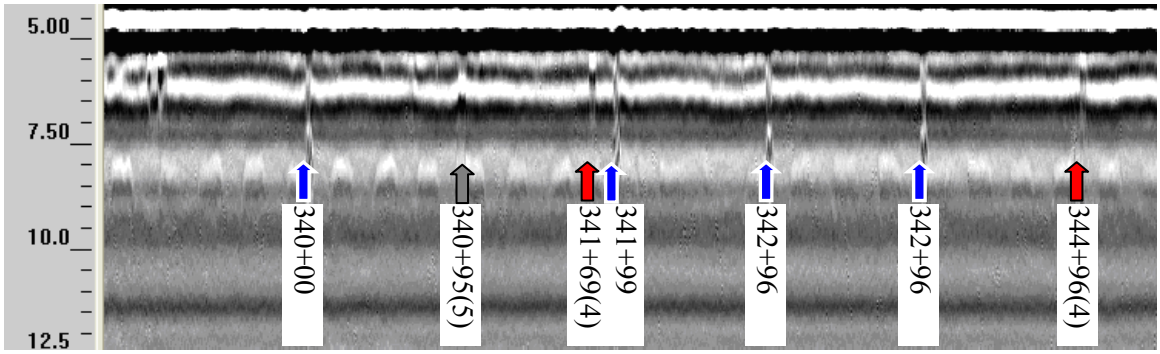

(j) Section10 northbound

Figure A.18.6 (Continued) GPR data in all sections northbound

A.18.3.3 Crack Analysis

For data analysis of this section, extent and severity of reflective cracking is utilized to compute uniform, R_{TCA}, and weight, R_{TCAW}, transverse cracking appearance rates. All transverse cracks are included for the evaluation. Table A.18.1 summarizes the crack survey results for the control and treated sections for the past three years. In both sections, majority of the transverse cracks belongs to low-severity level. For the control section, a couple of medium-severity-level cracks appeared in 2004 and three times more medium-severity-level cracks were developed in 2006 compared to the System E section. Regarding all transverse cracks, 21% less cracks were developed in the System E section three years after the overlay construction.

Table A.18.1. Summary of Crack Survey

	Control section (5000 ft)			
Severity	6/1/03	8/13/04	8/17/05	7/24/06
S	0	3	1	4
L	0	28	59	58
M	0	3	4	19
H	0	0	0	0
# Crack	0	34	64	81
R_{TCA}	0.0	0.7	1.3	1.6
R_{TCAW}	0.0	1.0	2.0	2.7
	System E section (5000 ft)			
Severity	6/1/03	8/13/04	8/17/05	7/24/06
S	0	3	0	2
L	0	31	54	56
M	0	0	0	6
H	0	0	0	0
# Crack	0	34	54	64
R_{TCA}	0.0	0.7	1.1	1.3
R_{TCAW}	0.0	1.0	1.6	2.0

In order to investigate the effect of the interlayers on crack severity as well as extent, R_{TCA} and R_{TCAW} are compared with respect to overlay age in Figure A.18.7. In both sections, R_{TCA} and R_{TCAW} increase linearly. Thus, rather than crack severity, crack extent influences the crack evaluation. The deterioration rate, a slope of the linear regression, of the control and System E section is 0.873 and 0.689. Then, the performance benefit ratio of the System E becomes 1.27.

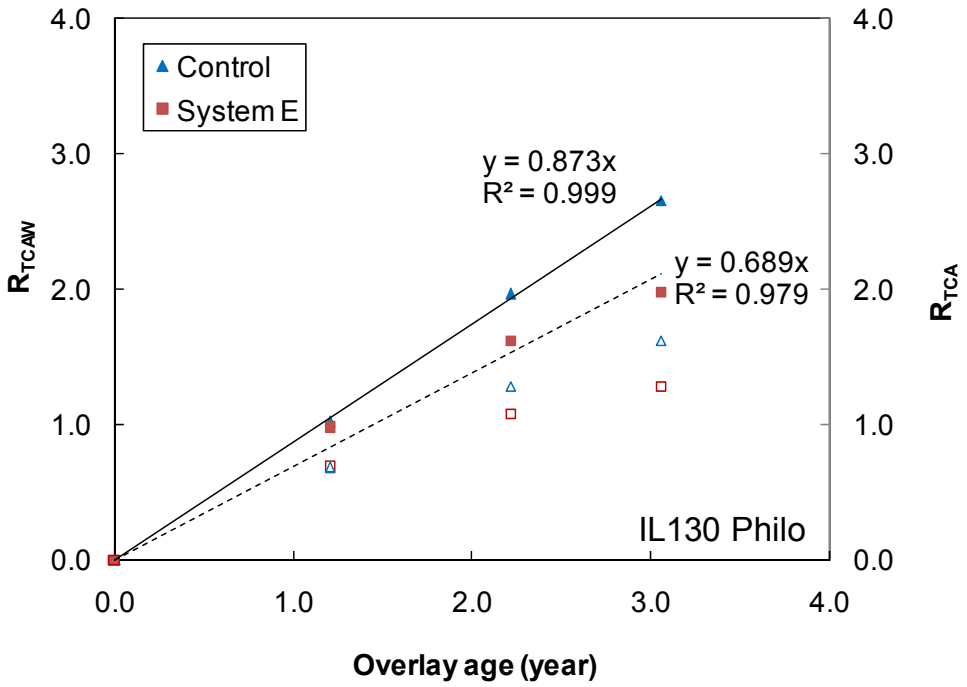

Figure A.18.7. Comparisons of deterioration rate, ΔR_{TCAW} per year on the control and treated sections with System E.

A.18.4 SUMMARY OF SECTION EVALUATION

A couple of tasks were performed in 2006 and in 2007 at IL 130 Philo. Table A.18.2 summarizes the conducted survey and analysis.

Table A.18.2. Summary for IL 130 at Philo

Year	2006	2007
Survey	Visual crack survey Video crack survey GPR survey	Visual crack survey
Forensic investigation	Coring Laboratory test	
Analysis	Crack GPR	Crack

From the IL 130 Philo section, the interlayer system evaluation and findings are presented as follows:

- Compared to the control section, the System E performs better to abate reflective cracking than the control section.
- In the System E section, 21% of cracks were retarded at overlay age three.
- The performance benefit ratio of the System E is 1.27.
- Video crack survey method was shown to be affordable in that safer and fast crack survey can be achieved, but 20% of measurement error needs to be improved.
- Using GPR survey, joints (or dowel bar) and patches (HMA or PCC) were detected successfully.
- Integrating video and GPR survey, reflective cracking could be identified.

A.19 US 136 E. SAN JOSE; CONTRACT NO. 72080

A.19.1 SECTION DESCRIPTION

This project, US 136 E. San Jose (Contract No. 72080), was completed in October 1999 and additional overlays were partially placed in 2003 and 2005 with milling. The project is located east of San Jose (Logan County, District 6), Illinois, as shown in Figure A.19.1. The evaluated sections is between east San Jose to west of I-155 (STA. 11+550 and 12+165, metric). It has one lane in each direction: eastbound and westbound. The pavement system consists of JCP with multiple HMA overlays. The existing JCP has varied 9-6-9 thickness. The joints are spaced at 30 ft. The HMA overlay is 2.25 in. (1.5 in. wearing surface and 0.75 in. binder level). Type 2 mix D with 12% RAP with AC-20 binder was used for asphalt mixture. The treatments used in this project are the following (Figure A.19.2): area-type of System A (Petromat) in westbound, System D (ISAC) in westbound close to I-55, and System E (sand anti-fracture (SAF)) in eastbound. This evaluation considered both two lanes. Traffic volume at the time of overlay construction in 1998 was reported as 2350 AADT (650 ADTT and 500 MU) in the previous report and in 2008 was reported as 2450 AADT (700 ADTT and 600 MU) according to traffic map on IDOT.

Figure A.19.1 US 136 E. San Jose Section Location

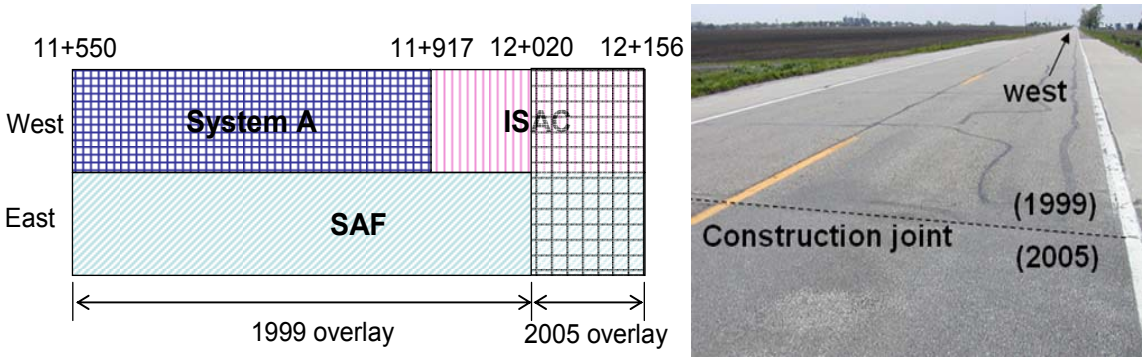

Figure A.19.2 Section layout

A.19.2 FIELD EVALUATION

The UIUC research team conducted a visual, video, and GPR surveys. The visual and video surveys quantified surface cracking; while the GPR surveys predicted pavement layer thicknesses and located interface systems. The video and GPR surveys were

conducted at highway speed. Specimens were obtained through coring from the field for forensic investigation as well as laboratory testing. Crack surveys were conducted on April 27, 2006. Coring work was executed on Sep. 26, 2007 which was coordinated with IDOT researchers and District 6 (traffic control and coring crews).

A.19.2.1 Survey

A 4000-ft-long section was surveyed (2000-ft-long in each direction). The crack severity of this section had been monitored since 2000 by IDOT. The same surveying criteria were used in this reflective cracking evaluation. The severity and extent of transverse cracks were reported. Figure A.19.3 shows four severity levels of unsealed reflective cracking found in this section. Other distress types, such as block cracking shown in Figure A.19.3 (d), were also reported. During coring work, a video crack survey and GPR survey were conducted with a moving traffic control.

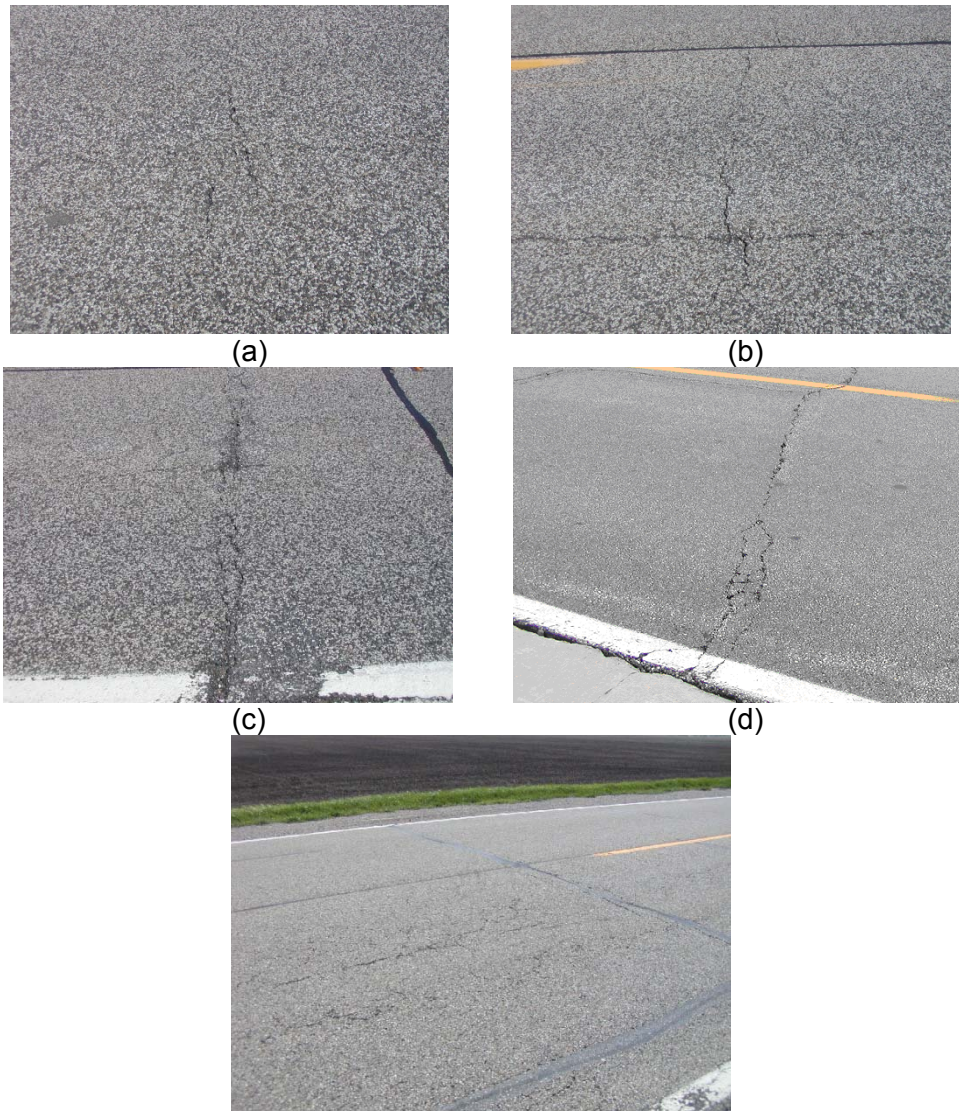

Figure A.19.3 Four severity of cracks: (a) staring, (b) low, (c) medium, and (d) high; and (e) block cracking

A.19.2.2 Coring

Seven 4-in diameter cores and 18 6-in. diameter cores were obtained from the evaluated sections (Figure A.19.4). Construction information, crack mapping, and GPR survey results were used to locate pavement joints and treatment locations. Cores on top of reflective crack, in both wheel-path (WP) and between wheel-paths (BWP) were obtained. Cores for bulk testing were obtained from WP intact surface; while cores for interface shear testing were obtained from both WP and BWP over treated locations. Based on several cores at the System A section, no fabric was found while a part of fabric was discovered at STA. 11+639 (Figure A.19.4 (b)).

(a) (b)

Figure A.19.4 Field coring work: (a) coring truck and (b) System A treatment on the edge of overlay

A.19.3 DATA ANALYSIS

A.19.3.1 GPR Survey

The possibility of GPR testing was examined to detect interlayer systems and joints with a 1.0G Hz air-couple antenna and 1.5G Hz ground-couple antenna. A scan rate of 1scan/ft of the air-couple GPR data is too fast to detect joints (or dowel bars), and the interlayer systems are too thin to be detected. However, ISAC was captured by using ground antenna. Figure A.19.5 shows the GPR data obtained from the 1.5 GHz antenna. Based on GPR tests, dowel bars are detected in the middle of PCC pavement with 30ft of interval so that joint spacing is confirmed as 30 ft. Under the overlays, two 3-ft-long ISAC strips were found over the joint in which reflective cracking exists.

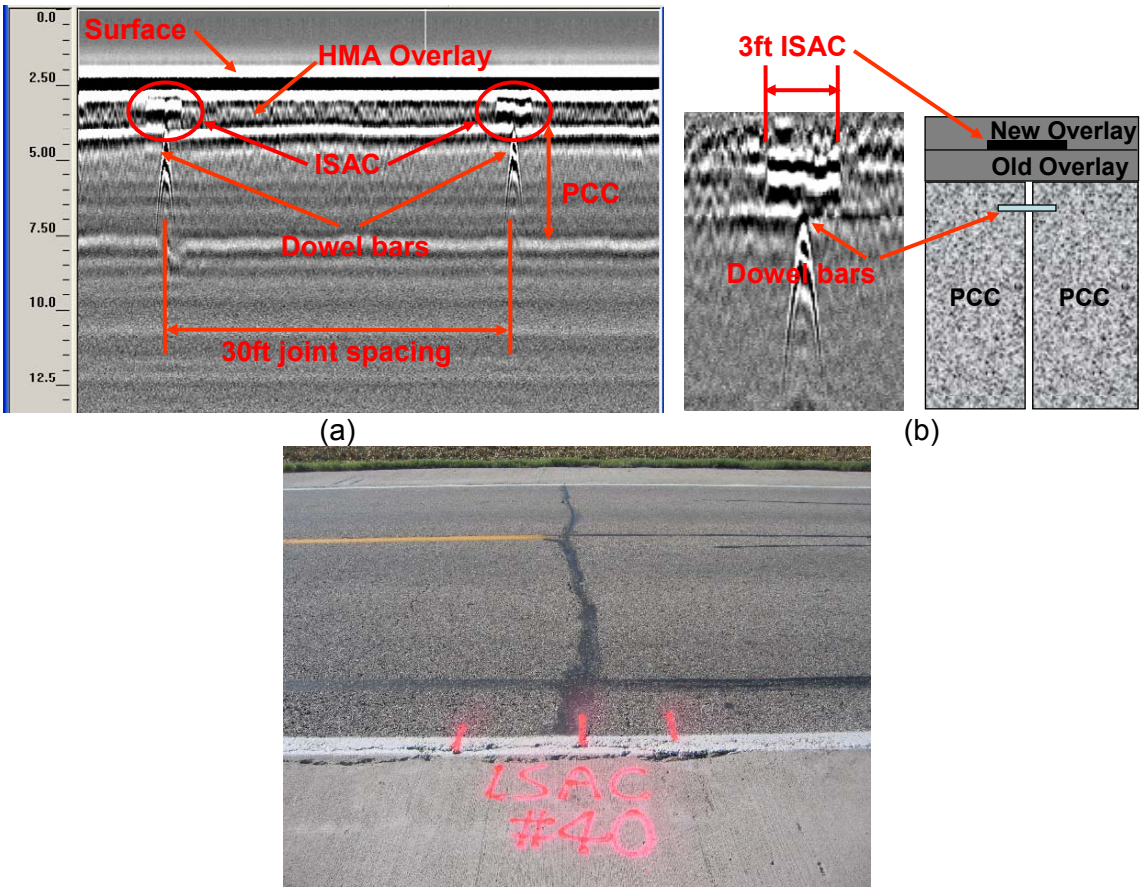

Figure A.19.5 GPR data analysis: (a) layer configuration in depth, (b) ISAC location and width, and (c) transverse reflective cracking over ISAC

A.19.3.2 Crack Analysis

For data analysis of this section, extent and severity of reflective cracking is utilized to compute uniform, R_{RCA}, and weight, R_{RCAW}, reflective cracking appearance rates. Excluding other unidentified transverse cracking, only reflective cracking is examined accordingly to strip locations for the Systems D and E. Table A.19.1 summarizes the crack survey results of R_{RCA} and R_{RCAW} for the past six years. In both sections, low-severity-level cracks have been majority cracks until 2005. After that, those cracks deteriorated to the medium-severity level in 2006. Regarding all severity levels of reflective cracking, 10% more reflective cracks appeared in the System E than in the System D.

In addition, uniform R_{TCA}, and weight, R_{TCAW}, transverse cracking appearance rates are computed to include all transverse cracks for the control section and Systems A and E. Table A.19.2 summarizes the crack survey results of R_{TCA} and R_{TCAW} during the same period of six years. In the three sections, low-severity-level cracks have been majority cracks until 2005. After that, those cracks deteriorated to the medium-severity level in 2006. Including all severity levels of reflective cracking, 27% and 41% less transverse cracks appeared in the System A and the System E section than in the control section.

Table A.19.1. Summary of Crack Survey for the Systems D and E sections

System D, 25 strips							
Severity	3/26/01	8/17/01	7/24/02	4/16/03	6/2/04	10/4/05	4/27/06
S	2	3	11	3	2	2	0
L	2	2	3	17	20	15	5
M	0	0	0	0	0	5	16
H	0	0	0	0	0	0	0
# Crack	4	5	14	20	22	22	21
R_{RCA}	0.2	0.2	0.6	0.8	0.9	0.9	0.8
R_{RCAW}	0.2	0.2	0.5	1.1	1.3	1.4	1.7
System E, 25 joints							
Severity	3/26/01	8/17/01	7/24/02	4/16/03	6/2/04	10/4/05	4/27/06
S	1	3	4	1	0	0	0
L	13	9	18	23	25	13	7
M	0	0	0	0	0	12	16
H	0	0	0	0	0	0	0
# Crack	14	12	22	24	25	25	23
R_{RCA}	0.6	0.5	0.9	1.0	1.0	1.0	0.9
R_{RCAW}	0.8	0.6	1.2	1.4	1.5	1.9	1.9

Table A.19.2. Summary of Crack Survey for the Systems A and E and control section

Control, 827ft							
Severity	3/26/01	8/17/01	7/24/02	4/16/03	6/2/04	10/4/05	4/27/06
S	2	6	5	1	0	0	0
L	39	43	59	84	73	46	22
M	1	1	3	3	18	43	64
H	0	0	0	0	0	3	5
# Crack	42	50	67	88	91	92	91
R_{TCA}	5.1	6.0	8.1	10.6	11.0	11.1	11.0
R_{TCAW}	7.5	8.6	12.0	16.1	18.1	21.1	23.2
System A, 286ft							
Severity	3/26/01	8/17/01	7/24/02	4/16/03	6/2/04	10/4/05	4/27/06
S	1	3	4	1	0	0	0
L	12	8	17	22	24	12	8
M	0	0	0	0	0	12	15
H	0	0	0	0	0	0	0
# Crack	13	11	21	23	24	24	23
R_{TCA}	4.5	3.8	7.3	8.0	8.4	8.4	8.0
R_{TCAW}	6.6	5.0	10.0	11.8	12.6	15.7	16.0
System E, 1526ft							
Severity	3/26/01	8/17/01	7/24/02	4/16/03	6/2/04	10/4/05	4/27/06
S	4	5	6	2	1	1	0
L	47	43	60	88	91	71	48
M	0	1	4	4	6	25	49
H	0	0	0	0	0	1	2
# Crack	51	49	70	94	98	98	99
R_{TCA}	3.3	3.2	4.6	6.2	6.4	6.4	6.5
R_{TCAW}	4.8	4.6	6.8	9.3	9.9	10.9	12.3

In order to investigate the effect of the interlayers on crack severity as well as extent, R_{RCA} and R_{RCAW} of the Systems D and E are compared with respect to overlay age in Figure A.19.6. For the both sections, R_{RCAW} keeps increasing linearly until six years; R_{RCA} increases until four years, but after then, it becomes level-down. This indicates that new cracks are being developed rather than existing cracks becoming further deteriorated until four years. At the next stage, the slope of the R_{RCAW} is higher than that of the R_{RCA}, meaning that the severity of the existing cracks is severed. Compared to the System E, the System D shows better performance to delay the occurrence of reflective cracking at early stage and to mitigate the deterioration of the reflective cracking at late stage. Using the deterioration rate, the performance benefit ratio of the System D to the System E becomes 1.27.

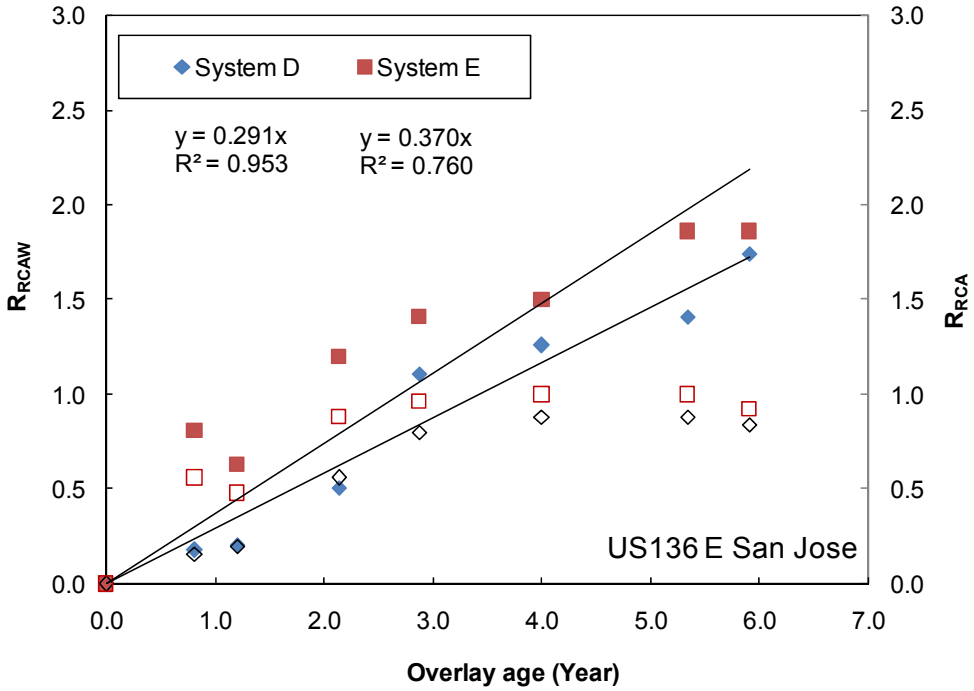

Figure A.19.6. Comparisons of the R_{RCAW} and R_{RCA} of the System D and System E sections.

The R_{TCAW} of the control and Systems A and E are compared with respect to overlay age in Figure A.19.7. For the three sections, R_{TCAW} increase linearly until six years. Compared to the control section, the System A and E sections show better performance to retard reflective cracking during the evaluation period. Using the deterioration rate, the performance benefit ratio of the Systems A and E to the control section become 1.39 and 1.85. Combing the performance benefit ratio of the System E to the control section and that of the System D to the System E, the performance benefit ratio of the System D to the control section is indirectly obtained as 2.40 (=1.27x1.85).

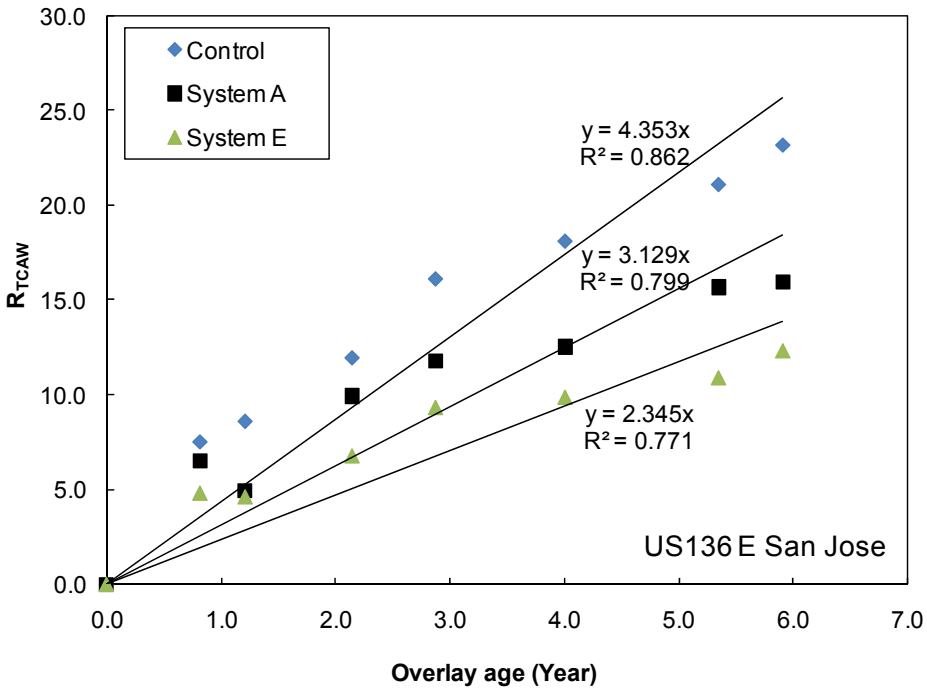

Figure A.19.7. Comparisons of the R_{TCAW} of the control and Systems A and E sections.

A.19.4 SUMMARY OF SECTION EVALUATION

Several tasks were performed in 2006 and 2007 at US 136 E. San Jose. Table A.19.2 summarizes the conducted survey, forensic investigation, and analysis.

Table A.19.2. Summary for US 136 E. San Jose

Year	2006	2007
Survey	Visual crack survey Video crack survey GPR survey	Visual crack survey
Forensic investigation	Coring Laboratory tests	
Analysis	Crack GPR	Crack

From the US 136 E. San Jose section, the interlayer system evaluations and findings are presented as follows:

- Compared to the control section, the Systems A and E perform better to abate reflective cracking.
- Compared to the System E, the System D performs better to abate reflective cracking.
- The performance benefit ratio of the Systems A, D, and E is 1.39, 2.40, and 1.85, respectively.
- From the GPR survey, the System D was detected by the 1.5 ground-couple antenna and moreover, the location and width of the System D was accurately estimated. However, joint locations (or dowel bars) were not identified by using the 1.0 air-couple antenna.

A.20 US66 LINCOLN; CONTRACT NO. 92939

Since this section has been resurfaced between 2005 and 2006, it is excluded from the performance evaluation.

A.21 US136 W. SAN JOSE; CONTRACT NO. 92939

A.21.1 SECTION DESCRIPTION

This project, US 136 W. San Jose (Contract No. 92939), was completed in July 1998. The project is located west of San Jose (Mason County, District 6), Illinois, as shown in Figure A.21.1. The evaluated section is between STA. 26+300 to 26+630 and 34+100 to 34+430, metric. It has one lane in each direction: eastbound and westbound. The pavement system consists of 30 ft JCP with multiple HMA overlays. The thickness of the existing JCP is unknown. The HMA overlay is 2.25 in. (1.5 in. wearing surface and 0.75 in. binder level) which mixture had 10% RAP with AC-20 binder. The treatments used in this project are the following (Figure A.21.2): area-type of System A (Petromat) in westbound, and System E (SAF) in eastbound. This evaluation considered both two lanes. Traffic volume at the time of overlay construction in 1998 was reported as 1500 AADT in the previous report and in 2008 was reported as 1650 AADT (700 ADTT and 553 MU) according to traffic map on IDOT.

Figure A.21.1 Section location

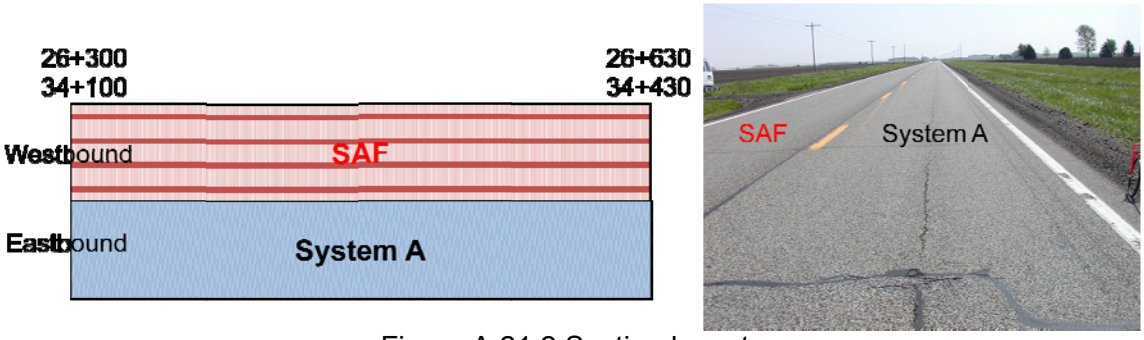

Figure A.21.2 Section layout

A.21.2 FIELD EVALUATION

A.21.2.1 Survey

The UIUC research team conducted a visual and video survey. The visual and video surveys quantified surface cracking. Crack surveys were conducted on May 22, 2006. A 4000-ft-long section was surveyed (2000-ft-long in each direction). The crack severity of this section had been monitored since 2003 by IDOT. The same surveying criteria were used in this reflective cracking evaluation. The severity and extent of transverse cracks were reported. Figure A.21.3 shows typical cracks found in this section. Longitudinal

cracks were found in the middle of a lane. Parts of transverse were sealed. Other distress types were also reported.

(a) (b)

Figure A.21.3 Typical cracks: (a) longitudinal crack and (b) joint-associated sealed reflective cracking.

A.21.3 DATA ANALYSIS

A.21.3.1 Crack Analysis

For data analysis of this section, extent and severity of reflective cracking is utilized to compute uniform, R_{TCA}, and weight, R_{TCAW}, transverse cracking appearance rates to include all transverse cracks for the Systems A and E. Table A.21.1 summarizes the crack survey results of R_{TCA} and R_{TCAW} for four years. In both sections, the R_{TCA} and T_{TCAW} increase linearly, but they have conflict behavior. Compared to the System A, the R_{TCA} of the System E is always lower, but the R_{TCAW} of the System E is always higher. It indicates that more cracks occurred in the System A, but the severity of those cracks was lower than that in the System E. Herein, it may not be simple to analyze the effect of the interlayer systems on those cracks due to the following limitations. These indices include all transverse cracks, not only reflective cracking. Also, no information was available to examine the existing pavement condition prior to the last overlay so that total number of discontinuities under the overlay is unknown. The joint spacing of this section is 30ft, which means 3.3 joints are included in those indices, but too many cracks already occurred four years after the last overlay construction. Consequently, it means that many of the transverse cracks counted are not reflective cracking. Therefore, it may not be accurate to evaluate the performance of interlayer systems through those indices. However, the overall quality of the section could be evaluated rather than specific reflective cracking. As Figure A.21.4 shows, the linearity of the R_{TCAW} is good enough. The deterioration rate of the sections is 1.037 and 1.124 for the Systems A and E, respectively. The performance benefit ratio of the System A to the System E becomes 1.08. So, relatively speaking, the performance of the System A to reduce transverse cracks is slightly better (8%) than that of the System E.

Table A.21.1. Summary of Crack Survey

System A (Petromat), 2000 ft				
Severity	8/15/03	11/10/04	10/5/05	5/22/06
S	5	5	6	9
L	72	76	79	67
M	1	5	10	21
H	0	1	1	2
# Cracks	78	87	96	99
R_{RCA}	3.9	4.4	4.8	5.0
R_{RCAW}	5.7	6.6	7.4	8.0
System E (SAF), 2000 ft				
Severity	8/15/03	11/10/04	10/5/05	5/22/06
S	2	3	1	18
L	51	49	51	38
M	7	10	12	18
H	10	16	17	22
# Cracks	70	78	81	96
R_{RCA}	3.5	3.9	4.1	4.8
R_{RCAW}	6.2	7.3	7.8	8.9

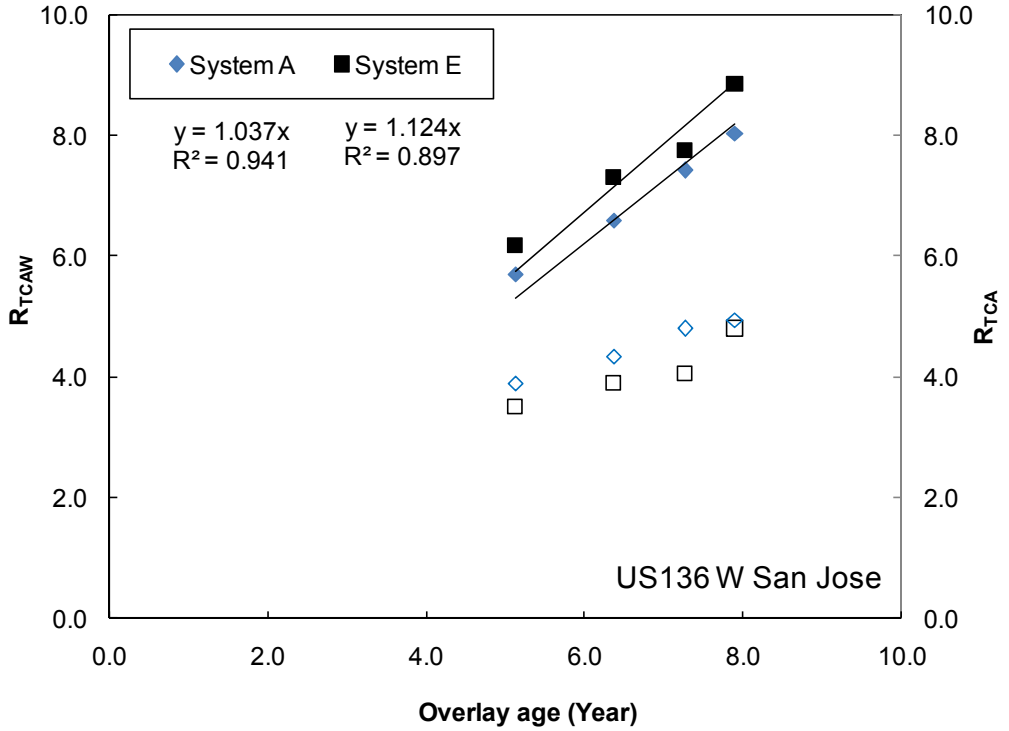

Figure A.21.4. Comparisons of the R_{TCAW} of the control and Systems A and E sections.

A.21.4 SUMMARY OF SECTION EVALUATION

Several tasks were performed in 2006 and 2007 at US 136 W. San Jose. Table A.21.2 summarizes the conducted survey analysis.

Table A.21.2. Summary for US 136 W. San Jose

Year	2006	2007
Survey	Visual crack survey Video crack survey	Visual crack survey
Forensic investigation Analysis	Crack	Crack

From the US 136 W. San Jose section, the interlayer system evaluations and findings are presented as follows:

- Compared to the System E, the Systems A performs slightly better to abate transverse cracking.
- The performance benefit ratio of the Systems A to the System E is 1.08.

A.22 IL 111 PONTOON BEACH; CONTRACT NO. 96539

A.22.1 SECTION DESCRIPTION

This project, IL 111 at Pontoon Beach (Contract No. 96539), was completed in 1994. The project is located at Pontoon Beach (Madison County, District 8), Illinois, as shown in Figure A.22.1. It has two lanes in each direction: northbound and southbound. Existing pavement system consists of JCP constructed in and HMA overlays. The JCP had 10-8-10 varied thickness. New overlay was directly on the JCP. The treatment used in this project was area-type System A. There are two sections which have a 500-ft-long treated section and 1000-ft-long control section (Figure A.22.2). This evaluation considered only southbound two lanes. Traffic volume in 1998 was reported as 15100 AADT. In 2008, it has 13800 AADT (1300 ADTT and 600 MU) according to traffic map on IDOT.

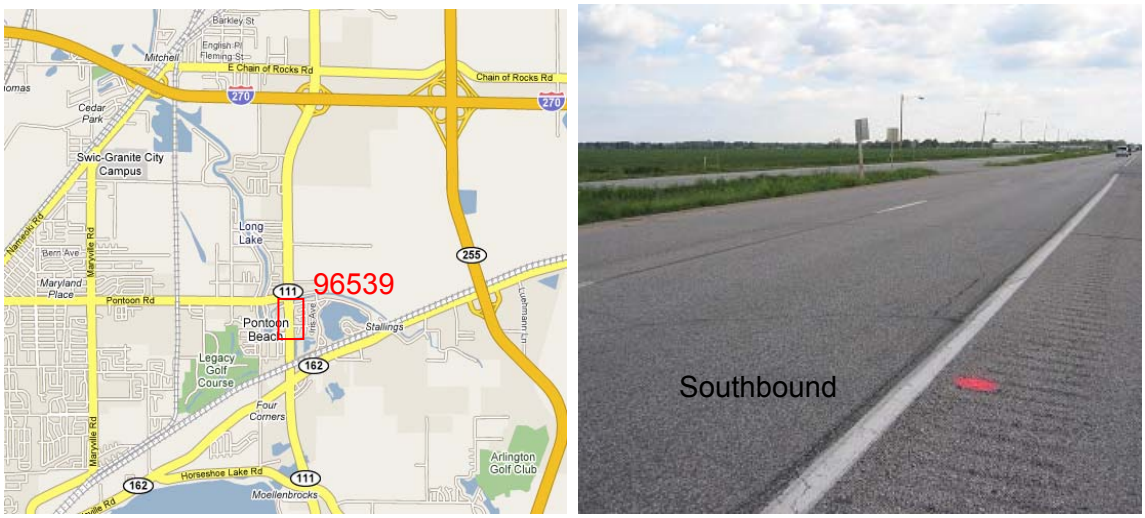

Figure A.22.1 Section location.

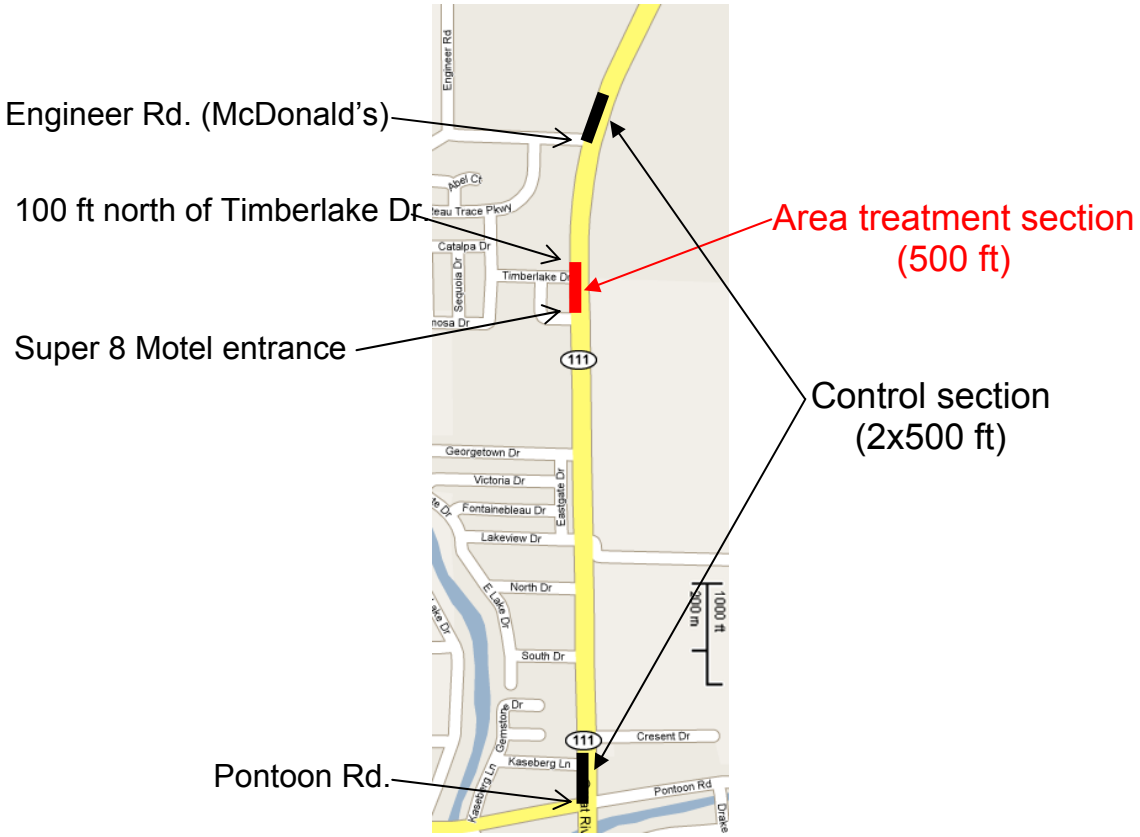

Figure A.22.2. Section layout.

A.22.2 FIELD EVALUATION

A.22.2.1 Survey

The UIUC research team conducted visual and video survey to quantify surface cracking on, 2006. A 3000-ft-long section was surveyed (500 ft + 1000 ft southbound two lanes). The crack severity of this section was conducted in 1998. The same surveying criteria were used in this evaluation. The severity and extent of transverse cracks were reported. Figure A.22.3 demonstrates distresses found in this section.

(a) (b)

Figure A.22.3. (a) Medium-severity-level transverse crack and (b) bleeding and rutting.

A.22.3 DATA ANALYSIS

A.22.3.1 Crack Analysis

For data analysis of this section, extent and severity of reflective cracking is utilized to compute uniform, R_{TCA}, and weight, R_{TCAW}, transverse cracking appearance rates. All transverse cracks are included for the evaluation. Table A.22.1 summarizes the crack survey results for the control and treated sections for the past 12 years. In both sections, low-severity-level cracks are still major cracks even 12 years after the overlay construction. Especially, no medium- and high-severity-level crack exists on the treated section. So, this section might have major and/or minor rehabilitations and/or maintenances between 1998 and 2006. The performance benefit ratio of this section was obtained from R_{TCAW} ratio of the System A to the control section in 2006, not from the deterioration rate due to no apparent changes of R_{TCAW} in 1998 and 2006. So, the performance benefit ratio of the area-type System A becomes 1.0.

Table A.22.1. Summary of Crack Survey

	Control1 section (1000 ft)		System A (area) section (2000 ft)	
Severity	6/24/98	9/2/06	6/24/98	9/2/06
S	1	1	0	0
L	10	93	22	50
M	11	7	8	0
H	0	0	0	0
# Crack	75	105	42	53
R_{TCA}	3.8	5.3	4.2	5.3
R_{TCAW}	7.0	8.2	7.4	8.1

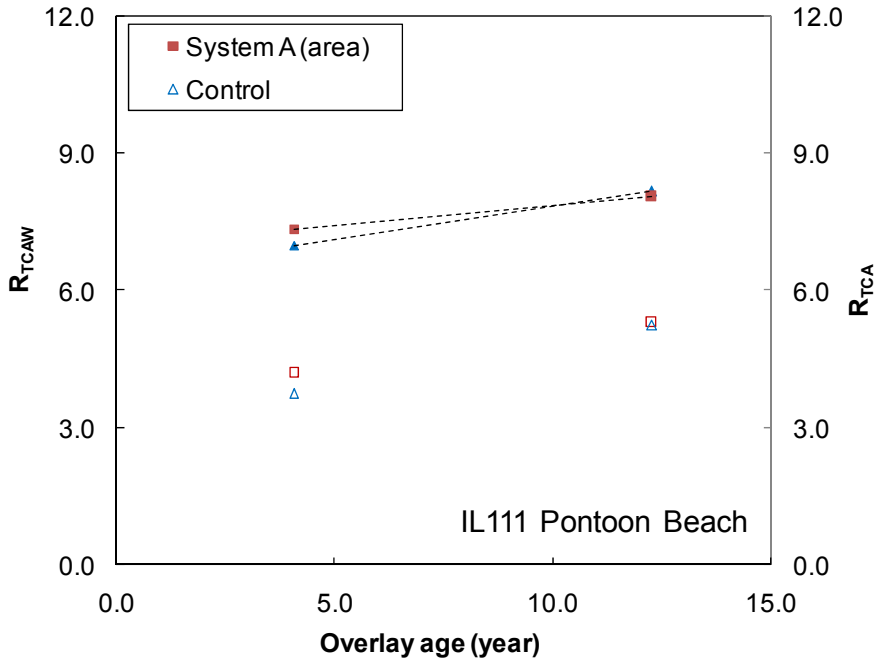

Figure A.22.4. Comparisons of the R_{RCAW} and R_{RCA} of the System A (area) and control sections.

A.22.4 SUMMARY OF SECTION EVALUATION

One task was performed in 2006 at IL 111 Pontoon Beach. Table A.22.2 summarizes the conducted survey and analysis.

Table A.22.2. Summary for IL 111 Pontoon Beach

Year	2006	2007
Survey	Visual crack survey Video crack survey	N/A
Forensic investigation Analysis	Crack	

From the IL 111 Pontoon Beach section, the interlayer system evaluation and findings are presented as follows:

- Regarding reflective cracking, mixture type of level binder affects more than that of surface mixture.
- Compared to the control section, the System E performs better to abate reflective cracking than the control section.
- The performance benefit ratio of the System E is dependent on traffic volume: the better performance the System E can achieve, the lower traffic volume HMA overlay has.
- The performance benefit ratio of the System E to the control section is 1.09 at 7800AADT and 1.90 at 3050AADT.

A.23 IL 267 GREENFIELD; CONTRACT NO. 76140

A.23.1 SECTION DESCRIPTION

This project, IL 267 Greenfield (Contract No. 76140), was completed in October 1998. The project is located north of Greenfield (Jersey County, District 8), Illinois, as shown in Figure A.23.1. The evaluated section is between STA. 0+000 to 2+550. It has one lane in each direction: northbound and southbound. The pavement system consists of JCP with HMA overlay. The existing JCP had varied thickness of 9-6-9. The joints are spaced at 30 ft. The overlay is 2.25 in. HMA: 1.5 in. wearing surface and 0.75 in. binder level. There are two sections for a control section (STA. 1+640 to 2+550) and for a treated section (STA. 0+000 to 1+640). The treatments used in this project are the System D (60 ISAC strips). This evaluation considered both lanes. Twenty four control measurements were conducted at selected cracks/ joints without treatment. Traffic volume at the time of overlay construction in 1998 was reported as 2400 AADT (500 ADTT and 350 MU) in the previous report and in 2008 was reported as 2150 AADT (425 ADTT and 325 MU) according to traffic map on IDOT.

Figure A.23.4. Section location and layout.

A.23.2 FIELD EVALUATION

A.23.2.1 Survey

The UIUC research team conducted visual and video surveys to quantify surface cracking. This task was conducted on Sep. 12, 2006. A 3.2-mi-long section was surveyed (1.6-mi-long in each direction). The crack severity of this section had been monitored since 2000 by IDOT. The same surveying criteria were used in this reflective cracking evaluation. The severity and extent of transverse cracks were reported. Figure A.23.2 shows typical reflective cracks found in this section. Both cracks are double reflective cracking with crack sealing; the left one is low-severity level and the right one is medium-severity level. The severity of sealed crack is mainly dependent on current crack condition such as how many associated cracks exist, not how much a crack was sealed. Thus, while the left crack received lots of crack sealing, current crack condition is sound. On the other hand, the right one got additional adjacent cracks after sealed so that current crack condition is worse than the left one. Thus, a certain level of maintenance was already applied in this section after the overlay.

(a) (b)

Figure A.23.2. Sealed transverse reflective cracking: (a) low-level and (b) medium-level.

A.23.3 DATA ANALYSIS

A.23.3.1 Crack Analysis

For data analysis of this section, extent and severity of reflective cracking is utilized to compute uniform, R_{RCA}, and weight, R_{RCAW}, reflective cracking appearance rates. Excluding other unidentified transverse cracking, only reflective cracking is examined accordingly to strip locations. Table A.23.1 summarizes the crack survey results for the control and treated sections for the past six years. In the control section, 100% of reflective cracking occurred in 2001 (1.0 of R_{RCA}) which is only 2.5 years after the overlay construction. Then, those reflective cracks have got deteriorated, but it was not severe (R_{RCAW} of 1.4 in 2001 to 1.7 in 2006). Thus, in control section, reflective cracking appears suddenly and it is deteriorated gradually by time. Especially, when proper maintenance is applied on the reflective cracking, the deterioration rate can be retarded. On the other hand, in the treated section, the reflective cracking occurred gradually and the severity of the reflective cracking remained in low level until 2004. The number of reflective cracking increased suddenly during 2003 winter which is almost five years after the overlay construction (R_{RCA} of 0.4 in 2003 and R_{RCA} of 0.9 in 2004) and almost reached to the maximum of R_{RCA} of 1.0.

Table A.23.1. Summary of Crack Survey

Control section, 50 untreated joint/crack						
Severity	2/16/00	3/27/01	7/5/02	4/23/03	6/4/04	9/12/06
S	0	7	0	0	0	0
L	0	43	45	38	36	43
M	0	0	5	8	10	7
H	0	0	0	4	4	0
# Crack	0	50	50	50	50	50
R_{RCA}	0.0	1.0	1.0	1.0	1.0	1.0
R_{RCAW}	0.0	1.4	1.6	1.7	1.8	1.7
System D, 101 strips						
Severity	2/16/00	3/27/01	7/5/02	4/23/03	6/4/04	9/12/06
S	0	1	4	10	6	2
L	0	12	23	30	82	89
M	0	0	0	1	1	4
H	0	0	0	0	0	0
# Crack	0	13	27	41	89	95
R_{RCA}	0.0	0.1	0.3	0.4	0.9	0.9
R_{RCAW}	0.0	0.2	0.4	0.5	1.3	1.4

In order to investigate the effect of the interlayers on crack severity as well as extent, R_{RCA} and R_{RCAW} are compared with respect to overlay age in Figure A.23.3. For the control section, both R_{RCA} and R_{RCAW} suddenly increase at overlay age two; R_{RCA} keeps stable R_{RCAW} increases slowly. On the other hand, for the System D section, they increase gradually. Therefore, deterioration rate, a slope of linear regression curve, can represent the increase of the R_{RCAW} as well as R_{RCA} for the System D section (R^2 of 0.802), but not for the control section (R^2 of 0.371). Thus, in this particular project, it may not be ideal to compute the performance benefit ratio from the deterioration ratio.

Figure A.23.4 shows the difference of R_{RCAW} and R_{RCAW} between the control and treated section at each year (ΔR_{RCAW} and ΔR_{RCAW}). The performance differences obtained from R_{RCA} and R_{RCAW} decrease as a similar rate with the increase of overlay age. It means that the main contribution of those performance differences results from the reduction of the number of reflective cracking by the System E, not from crack severity. Also, as the overlay age increases, the effectiveness of the System E on delaying the occurrence of reflective cracking is diminished. Thus, the performance benefit is a function of overlay age and an average value during the use life is regarded as the performance benefit ratio. The obtained performance benefit ratio becomes 2.17.

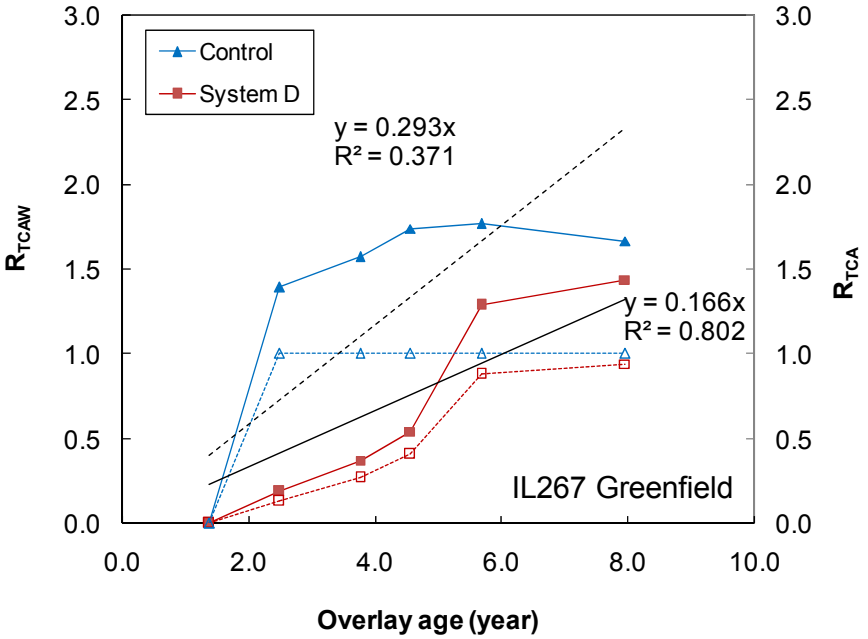

Figure A.23.3. Comparisons of the R_{RCAW} and R_{RCA} of the system B and system D interlayer systems.

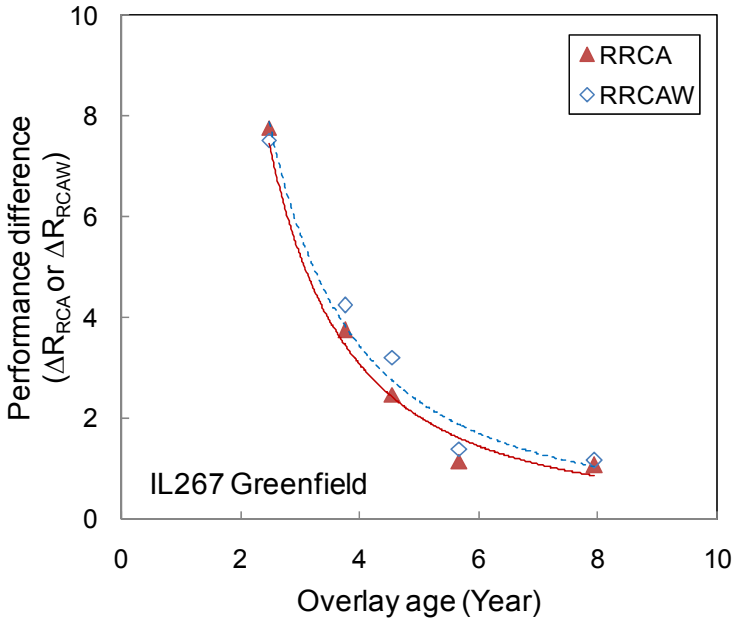

Figure A.23.4 Performance differences between the control and System E section.

A.23.4 SUMMARY OF SECTION EVALUATION

One task was performed in 2006 at IL 267 Greenfield. Table A.23.2 summarizes the conducted survey analysis.

Table A.23.2. Summary for IL 267 Greenfield

Year	2006	2007
Survey	Visual crack survey Video crack survey	N/A
Forensic investigation Analysis	Reflective Crack	

From the IL 267 Greenfield, the interlayer system evaluations and findings are presented as follows:

- Compared to the control section, the System D (ISAC, strip) performs better to abate reflective cracking and extend the service life of the HMA overlay.
- The performance effectiveness of the System D varies over overlay age.
- The performance benefit ratio of the System D is 2.17

A.24 IL 148 CHRISTOPHER; CONTRACT NO. 98511

A.24.1 SECTION DESCRIPTION

This project, IL 148 Christopher (Contract No.98511), was completed in 1998. The project is located at south end of Christopher (Franklin County, District 9), Illinois, as shown in Figure A.24.1. It has one lane in each direction: northbound and southbound. Existing pavement system consists of JCP. The thickness and joint spacing of the JCP is unknown. New MHA overlay was placed directly on the JCP. The treatment used in this project was area-type System A made of Petromat. There are a control section (STA. 11+319 to 11+519) and a treated section (STA. 11+000 to 11+319) as shown in Figure A.24.2. This evaluation considered two lanes in both directions. Traffic volume in 1998 was reported as 5500 AADT. Also, in 2008, AADT is 5800 (335 ADTT and 335 MU) according to traffic map on IDOT.

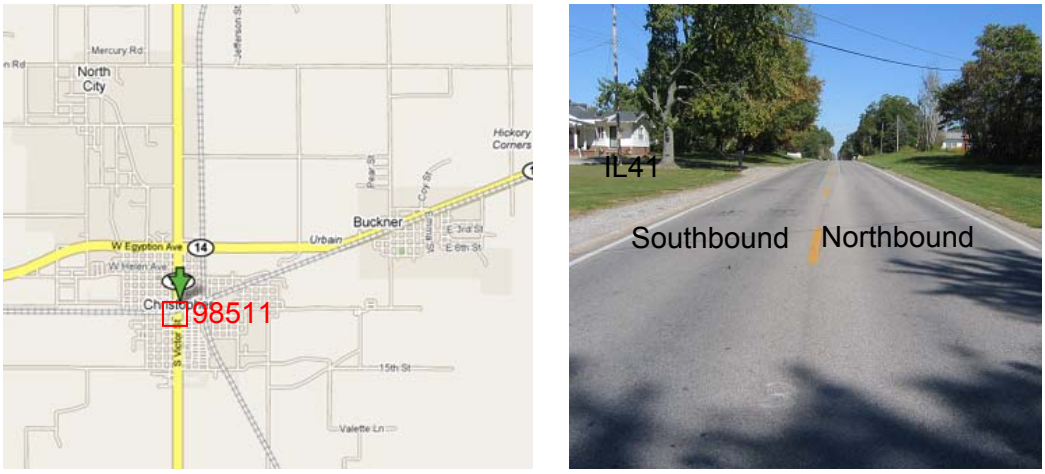

Figure A.24.1 Section location.

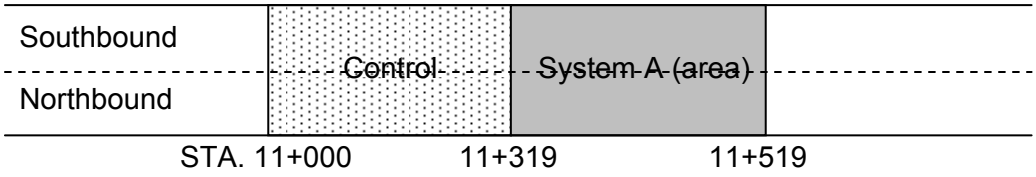

Figure A.24.2. Section layout.

A.23.2 FIELD EVALUATION

A.24.2.1 Survey

The UIUC research team conducted visual survey to quantify surface cracking on Oct. 1, 2006. A 3300-ft-long section was surveyed (663 ft for the control section and 991 ft for the treated section in both lanes). The crack severity of this section has been monitored since 2003. The same surveying criteria were used in this evaluation. The severity and extent of transverse cracks were reported. Figure A.24.3 shows double reflective cracking found in this section. The left one belongs to medium to high severity level and the right one belongs to high severity. However, those cracks were not sealed.

Figure A.24.3. Highly deteriorated double reflective cracks

A.24.3 DATA ANALYSIS

A.24.3.1 Crack Analysis

For data analysis of this section, extent and severity of reflective cracking is utilized to compute uniform, R_{TCA}, and weight, R_{TCAW}, transverse cracking appearance rates. All transverse cracks are included for the evaluation. Table A.24.1 summarizes the crack survey results for the control and treated sections. In both sections, the number of cracks increases gradually and crack severity becomes also worse. In 2006, using the R_{TCA}, 42% less transverse cracks per unit length occurred in the treated section than in the control section. When crack severity is included, the difference of R_{TCAW} between the treated and control section becomes 25%. Thus, when only number of cracks is considered in this evaluation, the performance of the System A can be overestimated.

Table A.24.1. Summary of Crack Survey

	Control section (1326 ft)			
Severity	4/18/03	10/6/04	11/3/05	10/1/06
S	15	17	21	17
L	16	21	16	40
M	0	0	8	3
H	0	0	0	0
# Crack	31	38	45	61
R_{TCA}	2.3	2.9	3.4	4.6
R_{TCAW}	2.7	3.3	4.4	6.1
	System A (area) section (1982 ft)			
Severity	4/18/03	10/6/04	11/3/05	10/1/06
S	9	18	24	7
L	9	12	9	27
M	7	5	6	7
H	1	4	6	7
# Crack	26	39	45	53
R_{TCA}	1.3	2.0	2.3	2.7
R_{TCAW}	2.0	2.8	3.2	4.6

In order to obtain the performance benefit ratio, linear regression curves of the system A and control sections were obtained using the R_{TCAW}. Figure A.24.4 shows the

R_{TCAW} variations with respect to overlay age. The deterioration rate, the change of R_{TCAW} per year, of the System A and control section is 0.495 and 0.654, respectively. Using those deterioration rates, the performance benefit ratio of the System A is calculated as 1.32.

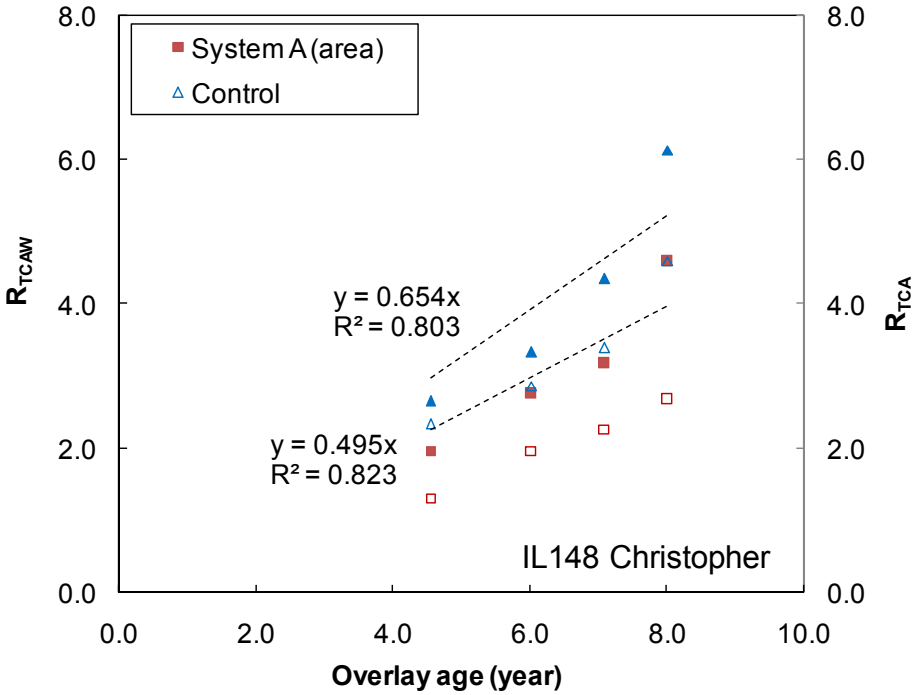

Figure A.24.4. Comparisons of the number of R_{TCAW} and R_{TCA} on the area-type System A and control sections.

A.24.4 SUMMARY OF SECTION EVALUATION

One task was performed in 2006 at IL 148 Christopher. Table A.24.2 summarizes the conducted survey and analysis.

Table A.24.2. Summary for IL 148 Christopher

Year	2006	2007
Survey	Visual crack survey Video crack survey	N/A
Forensic investigation Analysis	Transverse crack	

From the IL 148 Christopher section, the interlayer system evaluation and finding are presented as follows:

- Compared to the control section, the area-type System A shows better performance to retard reflective cracking.
- The performance benefit ratio of the system A is 1.32.

APPENDIX B LABORATORY TEST DATA AND ANALYSIS DETAIL

B.1 IDT Creep Test Results

B.2 IDT Complex Modulus Test Results

B.3 Details of Overlay and Interlayer Mixture Ranking System

B.1 IDT Creep Test Results

T	Loading	IL29CC		IL29MO		IL29CH		IL130SN	
(^{o}C)	Time	D(t)	S(t)	D(t)	S(t)	D(t)	S(t)	D(t)	S(t)
0	1	0.08437	11.85	0.12906	7.75	0.06442	15.52	0.07060	14.17
	2	0.09440	10.59	0.14764	6.77	0.08255	12.11	0.07909	12.64
	5	0.10795	9.26	0.18073	5.53	0.10425	9.59	0.09320	10.73
	10	0.12347	8.10	0.21509	4.65	0.13036	7.67	0.10802	9.26
	20	0.14187	7.05	0.25793	3.88	0.16134	6.20	0.12510	7.99
	50	0.16910	5.91	0.33832	2.96	0.22005	4.54	0.15466	6.47
	100	0.20071	4.98	0.42000	2.38	0.28808	3.47	0.18582	5.38
-10	1	0.06485	15.42	0.08383	11.93	0.05031	19.88	0.04934	20.27
	2	0.07003	14.28	0.09212	10.86	0.05207	19.20	0.05172	19.33
	5	0.07824	12.78	0.10709	9.34	0.05786	17.28	0.05680	17.61
	10	0.08805	11.36	0.11822	8.46	0.06437	15.54	0.06146	16.27
	20	0.09744	10.26	0.13304	7.52	0.07100	14.08	0.06578	15.20
	50	0.11383	8.79	0.15997	6.25	0.08128	12.30	0.07454	13.42
	100	0.13031	7.67	0.18689	5.35	0.09088	11.00	0.08256	12.11
-20	1	0.03935	25.42	0.04451	22.47	0.04255	23.50	0.04183	23.91
	2	0.04105	24.36	0.04684	21.35	0.04357	22.95	0.04329	23.10
	5	0.04462	22.41	0.04977	20.09	0.04674	21.39	0.04565	21.91
	10	0.04681	21.36	0.05354	18.68	0.04954	20.19	0.04759	21.01
	20	0.04972	20.11	0.05732	17.45	0.05165	19.36	0.04996	20.02
	50	0.05360	18.66	0.06524	15.33	0.05595	17.87	0.05411	18.48
	100	0.05739	17.42	0.07408	13.50	0.05852	17.09	0.05788	17.28

T	Loading	IL130SI		IL130NI		US136EW		US136EI	
(^{o}C)	Time	D(t)	S(t)	D(t)	S(t)	D(t)	S(t)	D(t)	S(t)
0	1	0.10945	9.14	0.07151	13.98	0.06346	15.76	0.29650	3.37
	2	0.12735	7.85	0.07919	12.63	0.06941	14.41	0.37862	2.64
	5	0.15832	6.32	0.09610	10.41	0.07921	12.62	0.54455	1.84
	10	0.19432	5.15	0.11202	8.93	0.08921	11.21	0.72838	1.37
	20	0.24252	4.12	0.12797	7.81	0.09938	10.06	0.96035	1.04
	50	0.32950	3.03	0.16627	6.01	0.11882	8.42	1.34655	0.74
	100	0.41416	2.41	0.21061	4.75	0.13873	7.21	1.70656	0.59
-10	1	0.06889	14.52	0.05760	17.36	0.04597	21.75	0.09590	10.43
	2	0.07543	13.26	0.06090	16.42	0.04899	20.41	0.11241	8.90
	5	0.08701	11.49	0.06817	14.67	0.05328	18.77	0.14084	7.10
	10	0.09769	10.24	0.07528	13.28	0.05721	17.48	0.17072	5.86
	20	0.10982	9.11	0.08302	12.04	0.06183	16.17	0.20893	4.79
	50	0.13205	7.57	0.09784	10.22	0.06893	14.51	0.28338	3.53
	100	0.15565	6.42	0.11228	8.91	0.07611	13.14	0.35941	2.78
-20	1	0.05482	18.24	0.04462	22.41	0.03736	26.76	0.05637	17.74
	2	0.05819	17.18	0.04632	21.59	0.03839	26.05	0.06170	16.21
	5	0.06296	15.88	0.04773	20.95	0.04044	24.73	0.07070	14.14
	10	0.06803	14.70	0.05051	19.80	0.04208	23.77	0.07882	12.69
	20	0.07322	13.66	0.05340	18.73	0.04439	22.53	0.08842	11.31
	50	0.08295	12.06	0.05812	17.20	0.04679	21.37	0.10454	9.57
	100	0.09185	10.89	0.06174	16.20	0.04951	20.20	0.12061	8.29

T (°C)	Loading Time	US136WI		MatBD	
		D(t)	S(t)	D(t)	S(t)
0	1	0.08221	12.16	0.12802	7.81
	2	0.09166	10.91	0.14287	7.00
	5	0.10908	9.17	0.17356	5.76
	10	0.12499	8.00	0.19729	5.07
	20	0.14503	6.89	0.23315	4.29
	50	0.18419	5.43	0.29409	3.40
	100	0.22264	4.49	0.35866	2.79
-10	1	0.05941	16.83	0.06514	15.35
	2	0.06429	15.55	0.06989	14.31
	5	0.06994	14.30	0.07719	12.96
	10	0.07654	13.06	0.08378	11.94
	20	0.08412	11.89	0.09120	10.97
	50	0.09649	10.36	0.10368	9.65
	100	0.10653	9.39	0.11662	8.58
-20	1	0.04311	23.20	0.04954	20.19
	2	0.04520	22.13	0.05210	19.19
	5	0.04751	21.05	0.05540	18.05
	10	0.04989	20.04	0.05854	17.08
	20	0.05262	19.00	0.06196	16.14
	50	0.05673	17.63	0.06749	14.82
	100	0.06008	16.64	0.07225	13.84

B.2 IDT COMPLEX MODULUS TEST RESULTS

T	*f*	IL29CC		IL29MO		IL29CH		IL130SN	
(°C)	*(Hz)*	δ (◦)	E* (MPa)	δ (◦)	E* (MPa)	δ (◦)	E* (MPa)	δ (◦)	E* (MPa)
-20	10	3.2	14,921	4.5	18,924	2.2	17,789	1.88	14,145
	1	5.9	13,782	6.2	18,787	4.6	16,787	4.61	13,398
	0.1	6.8	12,346	7.2	16,601	5.3	15,278	5.28	12,235
	0.01	8.1	10,659	8.3	14,116	6.4	13,539	6.12	10,924
-10	10	4.0	11,924	5.3	12,275	4.9	16,428	5.58	12,783
	1	8.5	10,764	10.6	9,871	7.9	14,544	7.40	11,145
	0.1	10.9	8,068	12.2	7,594	10.0	12,074	9.55	9,255
	0.01	12.6	6,377	14.5	5,810	12.9	9,323	11.20	7,298
0	10	7.9	8,297	10.9	6,785	9.1	12,232	7.72	10,702
	1	11.3	6,733	13.7	5,220	14.3	8,881	11.78	8,448
	0.1	12.5	5,204	16.5	3,816	18.9	6,106	15.46	6,392
	0.01	15.4	3,900	20.6	2,397	25.4	3,694	17.15	4,325

T	*f*	IL130SI		IL130NI		US136EW		US136EI	
(°C)	*(Hz)*	δ (◦)	E* (MPa)	δ (◦)	E* (MPa)	δ (◦)	E* (MPa)	δ (◦)	E* (MPa)
-20	10	2.68	11,714	2.60	11,776	2.25	14,096	6.31	10,132
	1	4.04	11,661	3.24	11,666	4.22	13,234	8.49	8,665
	0.1	7.33	10,595	4.91	10,980	5.19	12,205	11.68	6,985
	0.01	8.47	9,096	6.61	10,164	5.87	11,064	14.70	5,279
-10	10	9.75	7,663	6.83	9,102	3.64	11,709	10.45	6,674
	1	6.55	9,723	2.05	9,684	7.20	10,543	16.58	5,095
	0.1	9.29	9,739	5.18	9,504	8.13	9,224	21.51	3,424
	0.01	10.69	7,672	7.62	8,505	9.62	7,791	28.03	2,012
0	10	13.44	5,813	10.06	7,259	8.55	9,736	20.10	4,068
	1	16.56	4,039	11.92	5,943	10.79	8,046	27.51	2,489
	0.1	11.02	6,266	10.61	9,235	12.54	6,392	33.92	1,252
	0.01	11.85	6,026	9.15	8,648	16.09	4,814	38.91	581

T	*f*	US136WI		MatBD	
(°C)	*(Hz)*	δ (◦)	E* (MPa)	δ (◦)	E* (MPa)
-20	10	3.23	11,586	3.86	11,433
	1	5.08	10,782	5.27	10,761
	0.1	6.27	9,783	6.18	9,767
	0.01	7.56	8,686	6.24	8,650
-10	10	8.02	9,889	5.54	9,885
	1	8.28	8,888	9.02	8,666
	0.1	9.87	7,629	9.66	7,167
	0.01	11.44	6,288	10.26	5,682
0	10	8.98	8,094	7.64	6,359
	1	12.21	6,453	11.57	4,890
	0.1	15.16	4,898	14.25	3,540
	0.01	19.85	3,416	17.36	2,325

B.3 DETAILS OF OVERLAY AND INTERLAYER MIXTURE RANKING SYSTEM

Comparisons and differentiations of the overlay mixture based on the master curve plots presented looked not so clear. Thus, to make this 'ranking' task easier, a simple scoring system was developed. This scoring system and the resulting ranking are discussed here.

B.3.1 Scoring System

First, scoring of the mixtures are only based on the 0 ^{o}C actual test data, not on the fitted or extrapolated data at the reference temperature of 0 ^{o}C. Second, test data are evaluated at four loading time or frequencies. Specifically, the creep stiffness data were evaluated at 1, 10, 50, and 100 seconds of loading and the E* and phase angle data were evaluated at 0.01, 0.1, 1, and 10 Hz of loading frequency. Thus, there are four sets of ordered and accordingly scored lists of mixtures at each of the four loading time or frequency. Example of these four ranked lists is in Table B.3.1. Individual mixtures on the lists are scored according to their rank in a list. Mixtures with lower stiffness values will get higher scores. Likewise, mixtures with lower E* values will get higher scores. On the other hand, mixtures with higher phase angle values will get higher scores since the phase angle is related to the damping ratio of materials, which plays an important role on dissipating energy applied by loading. The higher damping ratio a material has, the more energy the material will dissipate and the less energy will be stored in the material as a form of residual strain, which will be accumulated and eventually reach the maximum limit to crack. The four scores mixtures earned from each of four lists are summed up, and then the mixtures are ranked again on the basis of high scores. Individual rankings determined by individual ranking parameters (i.e. creep stiffness, E*, and phase angle) are submitted to calculate the averaged overall ranking points, and then finally the mixtures are ranked as the lowest average ranking points as the winner of overall combined ranking.

B.3.2 Individual Rankings

Table B.3.1 Creep stiffness scoring at four loading times

Score	S(t) @1 sec		S(t) @10 sec		S(t) @50 sec		S(t) @100 sec	
10	US136EI	3.37	US136EI	1.37	US136EI	0.74	US136EI	0.59
9	IL29MO	7.75	IL29MO	4.65	IL29MO	2.96	IL29MO	2.38
8	MatBD	7.81	MatBD	5.07	IL130SI	3.03	IL130SI	2.41
7	IL130SI	9.14	IL130SI	5.15	MatBD	3.40	MatBD	2.79
6	IL29CC	11.85	IL29CH	7.67	IL29CH	4.54	IL29CH	3.47
5	US136WI	12.16	US136WI	8.00	US136WI	5.43	US136WI	4.49
4	IL130NI	13.98	IL29CC	8.10	IL29CC	5.91	IL130NI	4.75
3	IL130SN	14.17	IL130NI	8.93	IL130NI	6.01	IL29CC	4.98
2	IL29CH	15.52	IL130SN	9.26	IL130SN	6.47	IL130SN	5.38
1	US136EW	15.76	US136EW	11.21	US136EW	8.42	US136EW	7.21

Table B.3.2 Ranking by total creep stiffness score

Rank	Name	Ranking Score @				Total score
		1	10	50	100	
1	US136EI	10	10	10	10	40
2	IL29MO	9	9	9	9	36
3	IL130SI	7	7	8	8	30
4	MatBD	8	8	7	7	30
5	IL29CH	2	6	6	6	20
6	US136WI	5	5	5	5	20
7	IL29CC	6	4	4	3	17
8	IL130NI	4	3	3	4	14
9	IL130SN	3	2	2	2	9
10	US136EW	1	1	1	1	4

Table B.3.3 Ranking by total E* score

Rank	Name	Ranking Score @				Total score
		0.01	0.1	1	10	
1	US136EI	10	10	10	10	40
2	MatBD	9	9	8	8	34
3	IL29MO	8	8	7	7	30
4	IL130SI	2	4	9	9	24
5	US136WI	7	7	5	5	24
6	IL29CC	5	6	4	4	19
7	IL130NI	1	1	6	6	14
8	IL29CH	6	5	1	1	13
9	US136EW	3	3	3	3	12
10	IL130SN	4	2	2	2	10

Table B.3.4 Ranking by total phase angle score

Rank	Name	Ranking Score @				Total score
		0.01	0.1	1	10	
1	US136EI	10	10	10	10	40
2	IL29CH	6	8	9	9	32
3	IL29MO	8	7	8	8	31
4	US136WI	5	6	6	7	24
5	IL130SI	9	9	2	2	22
6	IL130SN	2	4	7	5	18
7	MatBD	1	3	5	6	15
8	IL130NI	7	5	1	1	14
9	US136EW	4	1	4	4	13
10	IL29CC	3	2	3	3	11

According to the scoring system explained in the previous section, all of 10 mixtures are ordered by their creep stiffness at each of given four loading times and scored accordingly. For example, US136EI earned 10 points for each ordered list since it showed the lowest stiffness values at all four loading times. On the other hand, US136EW only earned 1 point per each list because of the highest stiffness it exhibited. Scores these mixtures earned at each list are all summed together and the total score for the creep stiffness are calculated as shown in Table B.3.2.

Table B.3.3 and Table B.3.4 show the total scores and the individual ranking of these mixtures based on the E* and phase angle, respectively. These three individual rankings are finally used to calculate the average ranking score and the overall ranking based on the bulk material properties of overlay mixture.

B.3.3 Overall Combined Ranking

Table B.3.5 finally summarize the overall ranking of these 10 overlay mixtures based on the bulk material properties measured at 0C. Also, the rough stiffness category discussed earlier in section 4.1 and a ranking by the fracture energy discussed in section 4.3 are presented for a comparison to the simplified ranking system results.

Table3.3.5 Overall bulk material property ranking – compared with fracture ranking

Overall Ranking	Name	Individual Ranking			Average Ranking	Category	Fracture Ranking	Name
		S(t)	E*	δ				
1	US136EI	1	1	1	1.0	LS	1	US136EI
2	IL29MO	2	3	3	2.7	IS	2	IL130SI
3	IL130SI	3	4	5	4.0	IS	3	IL29CH
4	MatBD	4	2	7	4.3	IS	4	MatBD
5	US136WI	6	5	4	5.0	HS	5	IL29MO
5	IL29CH	5	8	2	5.0	HS	6	IL130SN
7	IL29CC	7	6	10	7.7	HS	7	US136WI
7	IL130NI	8	7	8	7.7	HS	8	IL29CC
9	IL130SN	9	10	6	8.3	HS	9	US136EW
10	US136EW	10	9	9	9.3	HS	10	IL130NI


Illinois Department
of Transportation


ILLINOIS
UNIVERSITY OF ILLINOIS AT URBANA-CHAMPAIGN